



University
of Glasgow

Robinson, Hollie Christine (2014) *Investigation of the role of microRNA-143 and microRNA-145 in acute vascular injury*. PhD thesis.

<http://theses.gla.ac.uk/5221/>

Copyright and moral rights for this thesis are retained by the author

A copy can be downloaded for personal non-commercial research or study, without prior permission or charge

This thesis cannot be reproduced or quoted extensively from without first obtaining permission in writing from the Author

The content must not be changed in any way or sold commercially in any format or medium without the formal permission of the Author

When referring to this work, full bibliographic details including the author, title, awarding institution and date of the thesis must be given

Investigation of the role of microRNA-143 and microRNA- 145 in acute vascular injury

**Hollie Christine Robinson
B.Sc (Hons), MRes**

Submitted in the fulfilment of the requirements of the
degree of Doctor of Philosophy in the College of Medical,
Veterinary and Life Sciences, University of Glasgow

British Heart Foundation Glasgow Cardiovascular Research
Centre, Institute of Cardiovascular and Medical Sciences,
College of Medical, Veterinary and Life Sciences, University
of Glasgow

May 2014

© H.C. Robinson 2014

Author's Declaration

I declare that this thesis has been written entirely by myself and is a record of work performed by myself with the exception of adenovirus cloning (Dr R.A. McDonald). This thesis has not been submitted previously for a higher degree. The research was carried out in the Institute of Cardiovascular and Medical Sciences, University of Glasgow, under the supervision of Prof. A.H. Baker.

Hollie C. Robinson

May 2014

Acknowledgements

Firstly, I would like to thank my supervisor Prof. Andrew H. Baker for his advice and guidance throughout my studies and the opportunities afforded to me throughout the duration. I would also like to thank the British Heart Foundation for their support and funding of this work.

I would like to say a special thank you to Dr Gillian Douglas, for kindly teaching me the stent surgery and resin cutting techniques and for her advice on all matters stent-related. Thank you to Dr Paul Coats who allowed me to use his resin cutting equipment and to Dr Crawford Halliday who built the electrolysis equipment used in this study.

Thank you to Dr Robert McDonald for all his help and advice. I would also like to thank Dr Ruifang Lui for her advice on all things RNA related and Nicola Britton and Gregor Aitchison for teaching me the basics and for all their help throughout.

A massive thank you to my good friends Jenny, Clare, Lesley, Erin, Jen and Liz and Hannah (you can't sit with us) for providing so much hilarity and always making me smile! Thanks for listening on those stressful days and always having a youtube video on hand to remind me not to take life too seriously! I had so much fun with you girls on all of our escapades, nights out, dinners, parties and award winning Halloween costumes ("I'm a mouse, duh!"). There were lots of truly memorable moments and I'll miss you all!

Thank you to Andy for all the laughs, encouragement and for listening to my boring work chat and even pretending to be interested! Thanks to my brother Steven for his support and "inspirational" emails.

Most importantly thank you to my amazing mum and dad, for all their love and support and for always being there for me. I couldn't have done it without you!

Table of Contents

Author's Declaration	2
Acknowledgements	3
List of Tables	7
List of Figures	8
List of Publications	10
List of Abbreviations/Definitions	11
Summary	18
1 Introduction	20
1.1 Cardiovascular Disease	21
1.1.1 Pathogenesis of atherosclerosis	21
1.1.2 Treatments of atherosclerosis	25
1.1.3 In-stent restenosis	27
1.2 Vascular smooth muscle cells	29
1.2.1 Regulation of VSMC phenotype	31
1.3 MicroRNAs	37
1.3.1 MiRNA Biogenesis	37
1.3.2 Function of miRNAs	40
1.3.3 Importance of miRNAs during development	42
1.3.4 Dysregulation of miRNAs in disease	44
1.3.5 Importance of miRNAs in VSMCs	45
1.3.6 Importance of miRNAs in ECs	47
1.3.7 MiR-143 and miR-145 are enriched in VSMCs	48
1.3.8 Control of the miR-143/145 gene by serum response factor	49
1.3.9 MiR-143 and miR-145 influence VSMC phenotype <i>in vitro</i>	50
1.3.10 MiR-143 and miR-145 expression after vascular injury	50
1.3.11 Identifying miRNA targets	52
1.3.12 Targets of miR-143 and miR-145	53
1.3.13 Signalling pathways involving miR-143 and miR-145	57
1.3.14 Studies in miR-143 and miR-145 KO mice	60
1.3.15 Potential role of miR-143 and miR-145 in stenting	64
1.4 Aims	65
2 Materials and Methods	66
2.1 Materials	67
2.2 General cell culture techniques	67
2.3 Production of miRNA expressing adenovirus	67

2.3.1	Cloning of pre-miRNA sequences into pAdEasy-1	67
2.3.2	Production of adenovirus stocks.....	70
2.3.3	Adenovirus purification	70
2.3.4	Virus titration by end-point dilution assay.....	71
2.3.5	Viral particle titre	72
2.4	Primary cell culture	73
2.4.1	Isolation of primary vascular endothelial cells from the human saphenous vein	73
2.4.2	Isolation of primary vascular smooth muscle cells from the human saphenous vein	74
2.5	Adenoviral transduction of cultured cells.....	74
2.6	Transfections with premiRs and antimiRs.....	75
2.7	Extraction of RNA from cells and tissues.....	76
2.8	Reverse transcription polymerase chain reaction (RT-PCR).....	78
2.9	Taqman quantitative real-time PCR (qRT-PCR)	79
2.10	X-gal staining	80
2.11	Northern blotting.....	81
2.12	Protein isolation and western blotting.....	83
2.12.1	Protein isolation.....	83
2.12.2	Western blots	83
2.13	Migration assays	84
2.14	Cell proliferation assays.....	85
2.15	Exosome isolation	85
2.16	<i>In vivo</i> models	86
2.16.1	MicroRNA knockout mice.....	86
2.16.2	AntimiR dosing schedule	87
2.16.3	Mouse model of in-stent stenosis	87
2.16.4	Tissue harvesting	89
2.16.5	Resin embedding	89
2.16.6	Sectioning of resin embedded vessels.....	90
2.16.7	Electrolysis	90
2.16.8	Histology.....	91
2.16.9	Haematoxylin and eosin staining	92
2.16.10	Elastin staining	93
2.16.11	Immunohistochemistry	93
2.16.12	Morphometric analysis and injury scoring	96
2.16.13	Measurement of heart weights	98
2.17	Statistical analysis	98
3	The role of miR-143 and miR-145 in human primary vascular cells	99

3.1	Introduction	100
3.1.1	Aims	102
3.2	Results	103
3.2.1	Adenovirus-mediated modulation of miRNA expression	103
3.2.2	PremiR and antimiR modulation of miRNA expression	111
3.2.3	Functional studies in human primary cells with modulated miRNA expression	115
3.2.4	Analysis of miR-143 and miR-145 target expression	120
3.3	Discussion	123
4	Analysis of neointimal formation in a mouse model of in-stent stenosis ...	130
4.1	Introduction	131
4.2	Aims	134
4.3	Results	135
4.3.1	Vessel morphology following stent electrolysis	135
4.3.2	Neointimal formation in C57BL/6 mice 28 day post-stenting	137
4.3.3	Composition of neointima in 28 day stented C57BL/6 mice	138
4.4	Discussion	143
5	Analysis of neointimal formation following stenting in miR-143 and miR-145 knockout mice	148
5.1	Introduction	149
5.2	Aims	150
5.3	Results	151
5.3.1	MiRNA expression in miR-143 and miR-145 KO mice	151
5.3.2	Neointimal formation in miRNA KO mice	152
5.3.3	MiR-143 and miR-145 target expression in miRNA KO mice	156
5.4	Discussion	160
6	Neointimal formation following AntimiR-mediated knockdown of miR-143 in mice	165
6.1	Introduction	166
6.2	Aim	169
6.3	Results	170
6.3.1	MiRNA expression levels in tissues of antimiR treated mice	170
6.3.2	Analysis of neointimal formation in antimiR treated mice	173
6.3.3	Composition of the 28 day neointima in antimiR treated mice	176
6.3.4	Target gene expression in tissues from antimiR treated mice	180
6.4	Discussion	184
7	General discussion	190
7.1	General discussion	191
	List of References	201

List of Tables

Table 2.1. MiRNA reverse transcription primers.	78
Table 2.2. Tissue processing for paraffin embedding.	92
Table 2.3. Primary antibodies used in immunohistochemistry.	95
Table 2.4. Secondary antibodies used in immunohistochemistry.	95
Table 2.5. Definition of morphometric measurements.	96
Table 2.6. Definition of injury scores.	98
Table 4.1. Neointimal measurements from 28 day stented C57BL/6 mice.	137
Table 5.1. Body weights and injury scores of miRNA KO and WT mice.	152
Table 6.1. Body weights and injury scores of anti-miR treated mice.	173

List of Figures

Figure 1.1. The normal and the atherosclerotic artery.	25
Figure 1.2. Problems associated with stenting.	28
Figure 1.3. The contractile and synthetic VSMC.	36
Figure 1.4. Biogenesis of miR-143 and miR-145.	42
Figure 1.5. Overview of miR-143/145 transcription.	60
Figure 2.1. Overview of pre-miRNA cloning procedure.	69
Figure 2.2. Overview of surgery to produce mouse model of in-stent stenosis. .	89
Figure 2.3. Overview of equipment used in stent electrolysis.	91
Figure 2.4. Diagram of morphometric measurements.	97
Figure 3.1. MiRNA expression in HeLa cells transduced with AdmiR-143 and AdmiR-145.	104
Figure 3.2. X-gal expression in HSV SMCs transduced with Ad5CMVlacZ.	106
Figure 3.3. MiRNA expression in Ad-miR-143 and AdmiR-145 transduced HSV SMCs.	107
Figure 3.4. Migration of HSV SMCs transduced with AdmiR-143 and AdmiR-145.	108
Figure 3.5. MiRNA expression in AdmiR-143 and AdmiR-145 transduced HSV ECs.	109
Figure 3.6. Migration of HSV ECs transduced with AdmiR-143 and AdmiR-145. .	110
Figure 3.7. Gene expression in HSV SMCs transduced with AdmiR-143 and AdmiR-145.	111
Figure 3.8. Cy3 fluorescence in HSV SMCs transfected with antimiR-Cy3.	112
Figure 3.9. MiR-143 expression in transfected HSV SMCs.	113
Figure 3.10. MiR-145 expression in transfected HSV SMCs.	114
Figure 3.11. MiR-143 and miR-145 expression in premiR transfected HSV ECs. .	115
Figure 3.12. Migration of HSV SMCs transfected with premiRs.	116
Figure 3.13. Migration of HSV SMCs transfected with antimiRs.	117
Figure 3.14. Migration of HSV ECs transfected with premiRs.	118
Figure 3.15. Proliferation in primary cells with modulated miR-143 and miR-145 levels.	119
Figure 3.16. MiR-143 and miR-145 expression in HSV EC exosomes.	120
Figure 3.17. Target mRNA expression in HSV SMCs transfected with antimiRs. .	121
Figure 3.18. Target mRNA expression in HSV SMCs transfected with premiRs ..	122
Figure 4.1. Morphology of electrolysed vessels from C57BL/6 mice stained with H&E.	136
Figure 4.2. EVG staining of electrolysed vessels from C57BL/6 mice.	139
Figure 4.3. α -SMA expression in electrolysed vessels from 28 day stented C57BL/6 mice.	140
Figure 4.4. MAC-2 and PCNA expression in vessels from 28 day stented C57BL/6 mice	141
Figure 4.5. CD31 expression in vessels from 28 day stented C57BL/6 mice.	142
Figure 5.1. MiR-143 and miR-145 expression in mouse aortas.	151
Figure 5.2. H&E staining of 28 day stented vessels from miRNA KO and WT mice.	153
Figure 5.3. Analysis of neointimal formation in 28 day stented miRNA KO and WT mice.	154
Figure 5.4. Analysis of medial morphometry in control miRNA KO and WT mice.	155
Figure 5.5. α -SMA expression in stented vessels from miRNA KO and WT mice. .	156

Figure 5.6. MiRNA target expression in the aorta of miR-143 KO, miR-145 KO and WT mice.	157
Figure 5.7. MiRNA target expression in the heart of miR-143 KO, miR-145 KO and WT mice.	158
Figure 5.8. Analysis of heart weight indices in miRNA KO and WT mice.	159
Figure 6.1. AntimiR mediated inhibition of miRNA.	168
Figure 6.2. AntimiR study dosing schedule.	168
Figure 6.3. Tissue expression of miR-143 following dosing with antimiRs.	171
Figure 6.4. Tissue expression of miR-145 following dosing with antimiRs.	172
Figure 6.5. H&E staining of stented vessels from antimiR treated mice.	174
Figure 6.6. Quantification of vessel morphometry in 28 day stented antimiR treated mice.	175
Figure 6.7. EVG staining of 28 day stented vessels from antimiR treated mice.	177
Figure 6.8. CD31 expression in 28 day stented vessels from antimiR treated mice.	178
Figure 6.9. α -SMA expression in 28 day stented vessels from antimiR treated mice.	179
Figure 6.10. PCNA expression in 28 day stented vessels from antimiR treated mice.	180
Figure 6.11. Expression of miR-143 target mRNA in the tissues of antimiR treated mice.	181
Figure 6.12. Analysis of miRNA and target mRNA expression in the recipient heart.	182
Figure 6.13. Western blot of KLF5 expression in hearts of antimiR treated mice.	183

List of Publications

Robinson HC, Baker AH. How do microRNAs affect vascular smooth muscle cell biology? *Current opinion in lipidology*. 2012;23(5):405-11.

Abstracts:

British Society for Gene and Cell Therapy (BSGCT)

Royal Holloway, University of London, 2013.

Genetic ablation of microRNA-143 leads to reduced neointimal formation in mouse model of in-stent stenosis. **H.C. Robinson**, G. Douglas, R.A. McDonald, K.M. Channon, A.H. Baker.

(Poster communication)

International Union of Physiological Sciences (IUPS)

Birmingham, 2013.

MicroRNA-143 and microRNA-145 knockout mice show reduced neointimal formation in model of in-stent stenosis*. **H.C. Robinson**, G. Douglas, R.A. McDonald, K.M. Channon, A.H. Baker.

(Poster communication)

*Awarded a European Society for Microcirculation (ESM) and the European Vascular Biology Organisation (EVBO) Poster Abstract Prize, 2013.

List of Abbreviations/Definitions

α -SMA	Alpha smooth muscle actin
ACE	Angiotensin converting enzyme
Ad	Adenovirus
ADAR	Adenosine deaminase acting upon RNA
Ago	Argonaute
Ang II	Angiotensin II
ANOVA	Analysis of variance
ApoE	Apolipoprotein E
B-gal	Beta galactosidase
bFGF	Basic fibroblast growth factor
BMP4	Bone morphogenetic protein 4
BMS	Bare metal stent
bp	Base pair
BrdU	5-bromo-2-deoxyuridine
<i>C. elegans</i>	<i>Caenorhabditis elegans</i>
CABG	Coronary artery bypass graft
caMKII δ	Calcium/calmodulin-dependent protein kinase II delta
CAR	Coxsackievirus and adenovirus receptor

cDNA	Complementary deoxyribonucleic acid
CHD	Coronary heart disease
CMV	Cytomegalovirus
C _T	Cycle threshold
CTGF	Connective tissue growth factor
CVD	Cardiovascular disease
DAB	3, 3'-diaminobenzidine
DAB2	Disabled protein 2
DEPC	Diethylpyrocarbonate
DES	Drug-eluting stent
DGCR8	DiGeorge critical region 8
DMEM	Dulbecco's Modified Eagle's Medium
DNA	Deoxyribonucleic acid
dsRBD	double-stranded RNA binding domain
E	Embryonic day
EC	Endothelial cell
ECM	Extracellular matrix
EDTA	Ethylenediamine tetra-acetic acid
EGTA	Ethylene glycol tetra-acetic acid

eNOS	Endothelial nitric oxide synthase
EPC	Endothelial progenitor cell
ER	Endoplasmic reticulum
ESC	Stem cell
EVG	Elastin van gieson
FCS	Foetal calf serum
FSCN1	Fascin homologue 1
GTP	Guanosine triphosphate
h	Hour
H&E	Haematoxylin and eosin
HDL	High density lipoprotein
HEK	Human embryonic kidney
HMG-CoA	Hydroxymethylglutaryl-CoA
HSV EC	Human saphenous vein endothelial cell
HSV SMC	Human saphenous vein smooth muscle cell
HUVECS	Human umbilical vein endothelial cells
ICD	Intracellular domain
IFN- γ	Interferon gamma
IL	Interleukin

IP	Intraperitoneal
ITGBL1	Integrin beta-like 1
IV	Intravenous
Kb	Kilobase
KLF	Kruppel-like factor
KO	Knockout
LDL	Low density lipoprotein
LNA	Locked nucleic acid
MCP-1	Monocyte chemoattractant protein 1
MEM	Minimum essential medium
MI	Myocardial infarction
min	Minute
MiRNA	MicroRNA
MMPs	Matrix metalloproteinases
mRNA	Messenger ribonucleic acid
MRTF	Myocardin-related transcription factor
NO	Nitric oxide
nt	Nucleotide
oxLDL	Oxidised low density lipoprotein

p38MAPK	p38 mitogen activated protein kinase
PACT	Protein activator of PKR
PAZ	PIWI/Argonaute/Zwille
PBS	Phosphate buffered saline
PCI	Percutaneous coronary intervention
PCNA	Proliferating cell nuclear antigen
PDGF	Platelet-derived growth factor
PFA	Paraformaldehyde
PFU	Plaque forming unit
PIWI	p element-induced wimpy testes
PKC- ϵ	Protein kinase C ϵ
Pre-miRNA	Precursor microRNA
Pri-miRNA	Primary microRNA
qRT-PCR	Quantitative real-time polymerase chain reaction
RISC	RNA induced silencing complex
RNA	Ribonucleic acid
RNase	Ribonuclease
RT	Room temperature
RT-PCR	Reverse transcription polymerase chain reaction

SBE	Smad-binding element
SC	Subcutaneous
SCs	Stem cells
SDS	Sodium dodecyl sulphate
sec	Seconds
SEM	Standard error of the mean
SiRNA	Small interfering RNA
SM22 α	Smooth muscle 22 alpha
SMemb	Embryonic smooth muscle myosin heavy chain
SM-MHC	Smooth muscle myosin heavy chain
Sp-1	Stimulating-protein 1
SRF	Serum response factor
TBS-T	Tris-buffered saline plus tween-20
TCE	Transforming growth factor beta control element
TGF- β	Transforming growth factor beta
TGF- β RII	TGF- β receptor II
T_m	Melting temperature
TNF- α	Tumour necrosis factor alpha
TRBP	TAR RNA binding protein

UTR	Untranslated region
VCAM-1	Vascular cell adhesion molecule 1
VEGF	Vascular endothelial growth factor
VLDL	Very low density lipoprotein
VP	Viral particle
VSMC	Vascular smooth muscle cell
v/v	Volume/volume
WT	Wildtype
w/v	Weight/volume

Summary

Vascular smooth muscle cell (VSMC) activation leading to proliferation, migration and extracellular matrix (ECM) production is a major cause of neointimal formation after stenting and coronary artery bypass grafting. Drug-eluting stents have reduced clinical incidence of in-stent restenosis by inhibiting this proliferative response but they can also delay vessel re-endothelialisation after injury leading to an increased thrombotic risk. MicroRNAs (miRNAs) are short (~22 nt) non-protein-coding RNAs which act as regulators of gene expression largely through binding to the 3' untranslated region of target genes and causing degradation or repression of expression. MiR-143 and miR-145 are a miRNA family that are enriched in VSMCs and have been previously shown to influence VSMC phenotype through regulation of their gene targets. Consequently, the aim of this study was to investigate the role that miR-143 and miR-145 play in the neointimal response to stenting.

Initial experiments investigated whether modulation of miR-143 or miR-145 expression was capable of significantly altering VSMC phenotype. It was found that modulation of miRNA levels in human saphenous vein (HSV) SMC or endothelial cells (EC) using adenoviruses was not ideal due to transduction and toxicity issues. Use of anti-miR miRNA inhibitors and premiR miRNA mimics revealed that modulation of miR-143 or miR-145 levels alone was not sufficient to alter proliferation or migration of HSV SMCs *in vitro*. Knockdown of miR-143 expression in cells resulted in de-repression of target genes kruppel-like factor 4 (KLF4) and KLF5 but expression levels of other previously identified target genes were unaltered by miRNA modulation.

Pre-clinical stenting studies are largely performed in porcine models due to similarities in vessel structure and neointimal formation, however large animal models are not ideal for early investigative studies. In order to examine the role of miR-143 and miR-145 in stent-induced vascular injury we utilised a mouse model where a bare metal stent is deployed in the thoracic aorta of a donor mouse and interposition grafted into the carotid artery of a recipient. This model resulted in the development of a defined neointima over 28 days which consisted largely of VSMCs and ECM, similar to that of the human in-stent restenosis.

Vessel expression of miR-143 and miR-145 has been previously shown to be reduced following vascular injury and furthermore overexpression of these miRNA can reduce neointimal formation. MiR-143 and miR-145 knockout (KO) mice have previously been shown to have abnormal VSMC phenotype in their vessel walls including perturbed stress fiber formation, increased presence synthetic machinery and an increased number of synthetic versus contractile VSMCs. MiR-143 and miR-145 KO mice were found to develop significantly less neointimal formation in response to stenting than WT mice indicating that these miRNA are essential for normal vessel response to injury.

The reduced neointimal formation following genetic ablation of miR-143 or miR-145 led to the investigation of whether pharmacological knockdown of these miRNA was able to mimic this effect. An antimiR consisting of DNA and locked nucleic acid bases targeted against mature miR-143 expression was used to knockdown miR-143 expression in mice prior to stenting. AntimiR-143-mediated knockdown of miR-143 expression did not significantly alter the degree of neointimal formation seen 28 days following stent deployment when compared to mice that received a control non-targeted antimiR (antimiR-ctl). The neointima of both antimiR-143 and antimiR-ctl mice were comparable and consisted largely of VSMCs and ECM. Re-endothelialisation had occurred by day 28 post-injury in antimiR-143 and antimiR-ctl treated mice indicating that knockdown of miR-143 did not significantly delay EC repopulation in this model.

Expression of miRNA and mRNA after vascular injury can be both spatial and temporal. Target de-repression was not detected in the aorta or heart of miRNA KO or antimiR-143 treated mice. This is likely to reflect the complex nature of miRNA gene regulation *in vivo* which is governed by many different factors including the relative expression of the miRNA and its target, cell stress, and transcriptional activation or inhibition by growth and transcription factors.

In summary, the influence of miR-143 and miR-145 on VSMC biology was investigated *in vitro* using a range of molecular biology techniques and *in vivo* in a mouse model of in-stent stenosis. Results have extended current knowledge of the degree of influence these miRNA exert over VSMC phenotype and identified that miR-143 and miR-145 are involved in neointimal formation after stenting.

1 Introduction

1.1 Cardiovascular Disease

Cardiovascular disease (CVD) is the primary cause of morbidity and mortality worldwide, with an estimated 17.3 million deaths from CVD in 2008 alone (World Health Organization, 2013). Advances in the treatment of CVD have been successful in pushing mortality rates into decline however CVD is still responsible for around 50,000 premature deaths in the UK each year (British Heart Foundation, 2012). With global annual mortality predicted to reach 25 million by 2030 (World Health Organization, 2013) there is a need to develop more specialised treatments for CVD to improve patient survival.

Coronary heart disease (CHD) is the most prominent form of CVD and is responsible for around 45% of the deaths from CVD each year in the UK (British Heart Foundation, 2012). The two main consequences of CHD are angina, due to impaired blood flow and inadequate oxygen delivery to the heart, and myocardial infarction (MI) which occurs when a coronary artery becomes occluded by a thrombus. Angina and MI are a direct result of the presence or rupture of lipid rich atherosclerotic plaques within the wall of the coronary vessels.

1.1.1 Pathogenesis of atherosclerosis

1.1.1.1 Endothelial dysfunction

The endothelium forms the tunica intima of the artery, a monolayer of endothelial cells (ECs) that forms the interface with the blood (Figure 1.1). Surrounding the tunica intima is the internal elastic lamina, which forms the inner surface of tunica media. The media is comprised of layers of vascular smooth muscle cells (VSMCs), elastin fibers and extracellular matrix (ECM) surrounded by the external elastic lamina. The outermost layer of the artery is the tunica adventitia which consists of connective tissue comprised largely of collagen.

The initiation of an atherosclerotic plaque is believed to occur due to an insult to the vascular endothelium lining the coronary arteries and is most likely to occur in areas of low shear stress, for example, near curvatures or bifurcations (Cunningham and Gotlieb, 2005). Risk factors include tobacco use, hypertension,

high circulating cholesterol, sedentary lifestyle and obesity (British Heart Foundation, 2012, Ross, 1999). The endothelium plays an essential role in the vasculature, providing an antithrombotic, antiplatelet and anticoagulant interface with the blood through expression of several molecules including nitric oxide (NO), prostacyclin, thrombomodulin, tissue plasminogen activator and endothelium derived hyperpolarizing factor (Davignon and Ganz, 2004). The endothelium also controls vessel tone by release of a variety of vasoactive substances including NO, endothelin and angiotensin II (Ang II) (Davignon and Ganz, 2004).

One of the key signalling molecules secreted by the endothelium is NO which is produced by endothelial NO synthase (eNOS) (Furchgott and Zawadzki, 1980, Palmer et al., 1987, Ignarro et al., 1987). NO is an essential mediator of the endothelium which inhibits platelet activation and aggregation as well as having anti-inflammatory effects via inhibition of inflammatory cell adhesion and migration. NO is a potent vasodilator which diffuses to underlying medial VSMCs and promotes VSMC relaxation and inhibition of proliferation (Deanfield et al., 2007). Damage to the vascular endothelium results in impaired production of NO by eNOS and increased production of reactive oxygen species including superoxide, which reduces NO bioavailability in the vessel wall, resulting in a loss of endothelial-dependent vasorelaxation (Deanfield et al., 2007, Davignon and Ganz, 2004, Ludmer et al., 1986). This phenomenon of 'endothelial dysfunction' was first discovered when atherosclerotic arteries were found to constrict rather than dilate in the presence of acetylcholine (Ludmer et al., 1986).

1.1.1.2 Inflammation and plaque formation

Endothelial dysfunction results in a shift to a pro-inflammatory state whereby adhesion molecule expression and vascular permeability are increased allowing leukocyte and platelet adhesion. These changes are accompanied by the release of inflammatory cytokines, macrophage recruitment and stimulation of VSMC proliferation and migration (Ross, 1999). Increased permeability of the vascular endothelium leads to uptake of low density lipoprotein (LDL) from the circulation into the intima of the vessel wall where it becomes trapped and accumulates (Steinberg, 1997). Trapped LDL becomes oxidised within the vessel

wall forming oxidised LDL (oxLDL) which promotes inflammation through monocyte recruitment from the blood and increased expression of inflammatory genes. This early atherosclerotic plaque is termed a 'fatty streak'.

Monocytes recruited from the blood differentiate into macrophages in the vessel wall and engulf oxLDL to form foam cells, a characteristic cell type of the atherosclerotic plaque (Steinberg, 1997). A necrotic core that contains leukocytes, foam cells, cell debris and lipid is eventually formed. Macrophages and T Cells within the plaque secrete cytokines which stimulate VSMC proliferation and migration from the medial layer into the lesion where they produce ECM proteins, including collagen, that form a fibrous cap which contains the necrotic core (Ross, 1999).

Vessels with developing atherosclerotic plaques can undergo outward 'positive' remodelling, where the external elastic lamina expands, or inward 'negative' remodelling where the external elastic lamina shrinks at the site of the plaque (Figure 1.1)(Hermiller et al., 1993, Nishioka et al., 1996). Reduction in lumen area is higher in negatively remodelled vessels than positively remodelled vessels (Nishioka et al., 1996, Pasterkamp et al., 1995). Conversely, atherosclerotic plaques with positive remodelling have been shown to contain larger lipid and macrophage content (Varnava et al., 2002). It has been shown that negative remodelling is associated with stable whereas positive remodelling tends to be associated with unstable angina (Schoenhagen et al., 2000).

An atherosclerotic plaque is thought to be less likely to rupture when it displays a thick fibrous cap which contains a high proportion of VSMCs and collagen and low lipid and macrophage content (van der Wal and Becker, 1999, Davies et al., 1993). Larger lipid and inflammatory cell content is often seen in unstable atherosclerotic plaques which are associated with increased incidence of coronary thrombosis (Falk, 1989, van der Wal et al., 1996, Arbustini et al., 1995). However, plaques from clinically stable angina can be histologically unstable (van der Wal et al., 1996). Several studies have reported the association between inflammatory cells and plaque rupture with macrophage, T cell and mast cell density high at the site of fibrous cap erosion and rupture (van der Wal et al., 1994, Lendon et al., 1991, Kovanen et al., 1995). It was later shown that activated matrix metalloproteinases (MMPs), which are produced by

both macrophages and VSMCs, are enriched in atherosclerotic plaques and are responsible for collagen breakdown and weakening of the fibrous cap which can lead to plaque rupture (Shah et al., 1995, Galis et al., 1994). VSMC apoptosis is also thought to contribute to plaque instability and rupture (Isner et al., 1995, Geng and Libby, 1995). VSMC apoptosis can be stimulated by growth factors and cytokines released from cells which are present in atherosclerotic plaques including T Cell derived interferon gamma (IFN- γ) and macrophage derived tumour necrosis factor alpha (TNF- α) and interleukin-1 β (IL-1 β) (Geng et al., 1996). Increased apoptosis was seen in cultured human VSMCs isolated from atherosclerotic plaques (Bennett et al., 1995). Furthermore, the pathology of lesions following VSMC apoptosis in atherosclerotic apolipoprotein E (ApoE) knockout (KO) mice shared many features with human unstable plaques (Clarke et al., 2006). This included fibrous cap thinning, loss of ECM proteins, increased lipid core and increased inflammation, seen by greater expression of monocyte chemoattractant protein 1 (MCP-1) and influx of macrophages (Clarke et al., 2006).

Atherosclerotic plaques can undergo cycles of rupture and repair which are clinically silent (Davies and Thomas, 1985). Sites of prior plaque rupture show increased presence of VSMCs which proliferate and migrate to the site and synthesize ECM components to heal the rupture (Mann and Davies, 1999). Cycles of plaque rupture and repair has been shown to result in greater vessel stenosis (Mann and Davies, 1999) and were also shown to be associated with sudden cardiac death (Burke et al., 2001). Rupture of an atherosclerotic plaque leads to exposure of the blood to the thrombogenic plaque core, resulting in activation of the coagulation cascade, platelet activation and accumulation and formation of a thrombus (Falk, 1991, Zaman et al., 2000). Whether a thrombus remains silent and is repaired or progresses to fully occlude the vessel leading to clinical presentation seems to depend on several factors including degree of plaque disruption, blood flow, thrombotic versus thrombolytic activity of the blood and composition of the exposed plaque (Falk, 1991). Plaque rupture and thrombus formation is the major cause of MI and sudden cardiac death (Davies and Thomas, 1985).

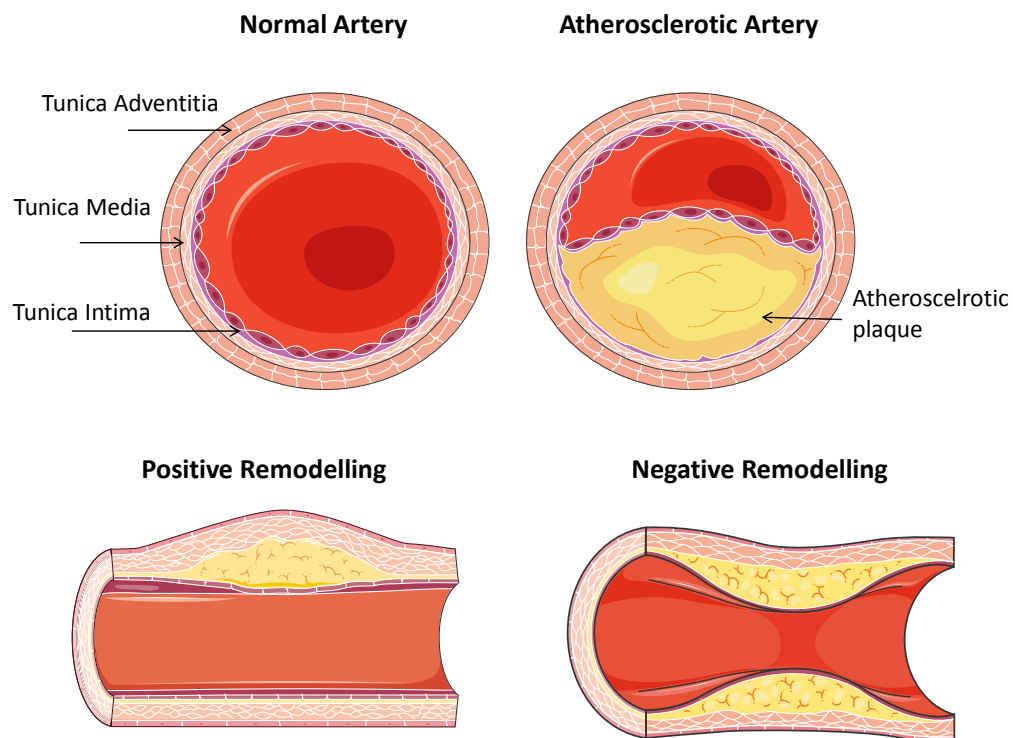


Figure 1.1. The normal and the atherosclerotic artery.

The artery is made up of 3 distinct layers (top left), the tunica intima, comprising of ECs, the VSMC-containing tunica media and the tunica adventitia which is composed of connective tissues. Cross section of the atherosclerotic artery (top right) showing an atherosclerotic plaque which impinges on the lumen. Longitudinal view of positive remodelling, (bottom left), where the external elastic lamina remodels outwards, and negative remodelling (bottom right) where shrinkage of the external elastic lamina at the site of the atherosclerotic plaque contributes to luminal narrowing. Adapted from Servier Medical Art.

1.1.2 Treatments of atherosclerosis

The main pharmacological intervention used to treat atherosclerosis is inhibition of Hydroxymethylglutaryl-CoA (HMG-CoA) reductase (Go et al., 2013), a key enzyme involved in the production of cholesterol in the liver. HMG-CoA reductase inhibitors are widely known as statins. Statins significantly lower cholesterol content in the liver hepatocytes which results in the upregulation of LDL receptors that act to clear LDL from the blood, significantly lowering circulating levels (Vaughan et al., 2000, Maron et al., 2000). This allows statins to significantly reduce plaque progression and even promote regression of plaque size (Vaughan et al., 2000). Statins are hugely successful clinically and reduce the incidence of major cardiac events by approximately 30% (Maron et al., 2000).

When an atherosclerotic plaque causes narrowing of the lumen to a degree in which blood flow through the coronary artery is significantly impaired a coronary artery bypass graft (CABG) or percutaneous coronary intervention (PCI) may be performed to re-vascularise the myocardium. PCI is the most common revascularisation procedure performed in the UK with around 80,000 operations performed per annum compared to approximately 25,000 CABG procedures (British Heart Foundation, 2012). CABG is generally regarded as preferential to PCI for patients with triple vessel or left main coronary-artery disease as it has been shown in randomised trials to reduce incidence of major cardiac events in this patient group (Serruys et al., 2009, Mohr et al., 2013).

The CABG procedure involves harvesting of a vein or artery from the patient which is then grafted into the heart to allow blood to bypass the narrowed coronary artery. Arterial conduits such as the internal mammary artery have more successful long term patency than the saphenous vein, with 10 year patency rates of around 85% vs. 61% respectively (Goldman et al., 2004). However, the saphenous vein is still commonly used for CABG due to the need to bypass multiple vessels (Goldman et al., 2004). The failure of around 40% of vein grafts within 10 years is due to the remodelling of the vein under the high pressures of the arterial circulation which occurs largely via endothelial dysfunction, VSMC proliferation and migration and ECM production, eventually followed by the development of atherosclerosis within the grafted vein (Cox et al., 1991).

PCI involves a balloon angioplasty of the narrowed vessel often accompanied by placement of a metal scaffold known as a 'stent'. During the balloon angioplasty procedure a balloon angioplasty catheter is fed through the vasculature to the narrowed coronary artery where it is then inflated to a certain pressure in order to compress the atherosclerotic plaque against the vessel wall, leading to revascularisation of the lumen. The balloon angioplasty procedure is initially very successful in restoring blood flow but is hampered by high rates of restenosis (Serruys et al., 1994, Fischman et al., 1994). The introduction of bare-metal stents (BMS) in 1994 significantly reduced restenosis rates associated with balloon angioplasty alone (Fischman et al., 1994, Serruys et al., 1994). However, target vessel revascularisation is still required in around 15%-17% of

vessels with BMS by 5 years due to in-stent restenosis (Kiemeneij et al., 2001, Rubartelli et al., 2003).

1.1.3 In-stent restenosis

The PCI procedure results in denudation of the endothelium lining of the vessel as well as mechanical stretch to the underlying medial layer of VSMCs. Endothelial denudation provides a surface favoured for thrombus formation, platelet aggregation and influx of inflammatory molecules such as macrophages (Libby et al., 1992). This triggers inflammatory signalling whereby growth factors and cytokines are released and promote cell VSMC migration, proliferation and ECM deposition resulting in neointimal formation and restenosis of the vessel (Figure 1.2) (Libby et al., 1992, Clowes and Schwartz, 1985, Clowes and Clowes, 1985). It has been shown that degree of mechanical stretch and injury to the vessel wall during stent deployment directly relates to amount of neointimal formation that occurs (Schwartz et al., 1992). Neointimal formation is thought to be largely due to activation of resident VSMCs which proliferate and migrate from the media (Clowes and Schwartz, 1985, Clowes and Clowes, 1985, Schwartz et al., 1975). However, there is also evidence to suggest that a proportion of the neointimal VSMCs are derived from the bone marrow (Han et al., 2001, Sata et al., 2002).

Inhibition of VSMC migration and proliferation is therefore a major clinical goal to prevent restenosis. This led to the development of drug-eluting stents (DES), which elute cell cycle inhibitory drugs such as Sirolimus and Paclitaxel (Schampaert et al., 2006, Caixeta et al., 2009, Stone et al., 2009). DES are coated with polymers that allow drugs to be loaded and released over a certain time period (usually within 4-6 weeks) to lessen the initial proliferative response evoked following stent deployment (Htay and Liu, 2005). DES have been highly successful clinically in further reducing incidence of in-stent restenosis confirming that inhibition of cell proliferation is a viable strategy (Schampaert et al., 2006, Caixeta et al., 2009, Stone et al., 2009).

However, DES are inhibitors of cell cycle in all cells exposed to them and thus are non-specific and target both ECs and VSMCs. This can lead to delayed or incomplete re-endothelialisation following stent deployment (Joner et al.,

2006). This delayed re-endothelialisation leads to increased risk of fatal late in-stent thrombosis in patients with DES versus BMS (Figure 1.2) (Joner et al., 2006, Finn et al., 2007). Discontinuation of antiplatelet therapy is a risk factor for late in-stent thrombosis (Pfisterer et al., 2006, McFadden et al., 2004).

DES have proved extremely successful in improving the patency rates of stented vessels. However the risks associated with delayed and incomplete re-endothelialisation indicate that there is a substantial need for new therapies which specifically target the VSMCs.

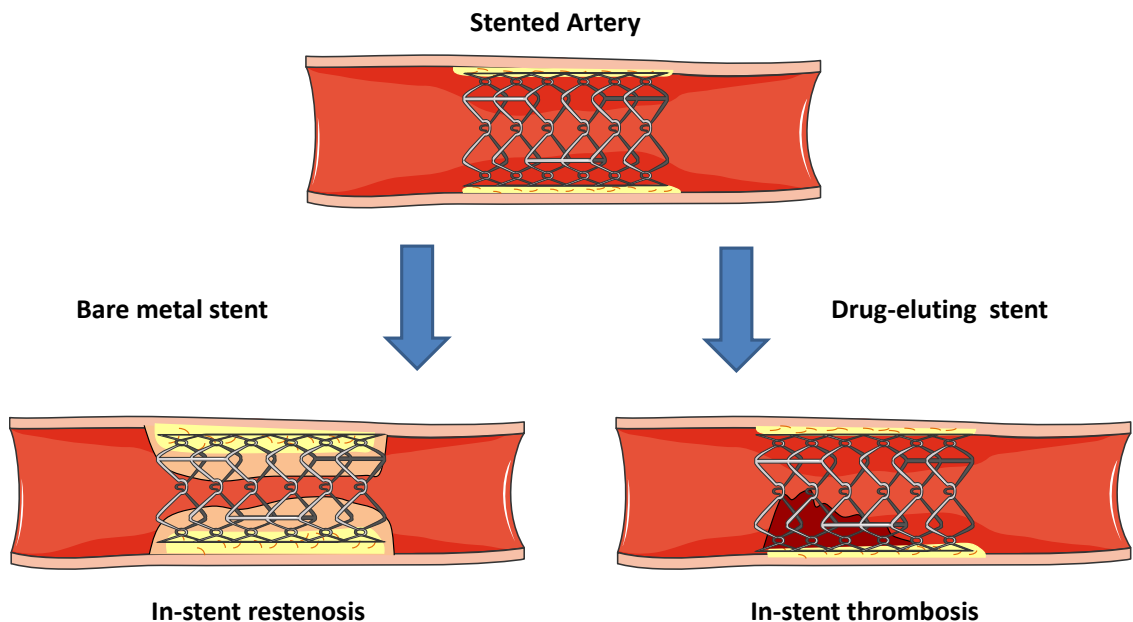


Figure 1.2. Problems associated with stenting.

During the stent procedure a balloon catheter is inflated to compress the atherosclerotic plaque against the vessel wall and a metal stent is deployed to acts as a scaffold to maintain the newly revascularised lumen. Stenting causes endothelial denudation and mechanical injury to the vessel which results in activation of VSMC proliferation and migration which leads to in-stent restenosis, a common side-effect of BMS. DES inhibit VSMC proliferation thereby reducing incidence of in-stent restenosis. However DES also inhibit EC proliferation which can lead to delayed re-endothelialisation of the vessel and increased risk of in-stent thrombosis. Adapted from Servier Medical Art.

1.2 Vascular smooth muscle cells

VSMCs are not terminally differentiated and can undergo phenotypic modulation from a differentiated 'contractile' to a dedifferentiated 'synthetic' state in response to environmental cues (Owens et al., 2004). VSMCs are a major structural component of the vessel wall which express a unique set of proteins including components of the actin cytoskeleton and contractile response e.g. alpha smooth muscle actin (α -SMA); smooth muscle myosin heavy chain (SM-MHC) and calponin, termed 'contractile proteins' (Shanahan and Weissberg, 1998). These contractile proteins, together with other proteins including ion channels and receptors, act together to maintain vascular tone (Owens et al., 2004). In healthy adult vessels there is high expression of contractile proteins and very low (or no) expression of synthetic proteins, for example embryonic SM-MHC (SMemb), which is expressed in the VSMCs of the developing embryo prior to them reaching full differentiation (Kuro-o et al., 1991, Shanahan and Weissberg, 1998). Adult VSMCs show virtually no migration and very low proliferation rates (Owens et al., 2004). Injury to the vessel wall as occurs in revascularisation procedures triggers a signalling cascade by release of cytokines and growth factors from cells of the vessel wall, platelets and inflammatory cells (Libby et al., 1992). Cytokine and growth factor signalling after vascular injury leads to a phenotypic modulation of VSMCs from a contractile to a synthetic state which results in proliferation, migration and neointimal formation (Kocher et al., 1991, Orlandi et al., 1994).

Fully synthetic VSMCS display an epithelioid morphology which is easily distinguished from the long spindle-like shape of contractile VSMCs (Figure 1.3) (Walker et al., 1986). The change in cell morphology following vascular injury is accompanied by decreased expression of contractile marker proteins including α -SMA and SM-MHC (Kuro-o et al., 1991, Kocher et al., 1991). Increased expression of dedifferentiation markers such as embryonic SMemb accompanies the decrease in contractile gene expression, indicating that the VSMCs are transitioning towards a dedifferentiated phenotype (Kuro-o et al., 1991). α -SMA comprises around 40% of all protein in contractile VSMCs and together with myosin forms highly organised contractile filaments which govern VSMC contraction (Fatigati and Murphy, 1984). Reduced α -SMA expression seen in synthetic intimal VSMCs is accompanied by a significant reduction in the number

of actin stress fibers within these cells and thus a major rearrangement of the actin cytoskeleton (Manderson et al., 1989, Kocher et al., 1991, Kocher et al., 1984). Synthetic VSMCs also produce large amounts of ECM proteins, which comprise largely of collagen, elastin and proteoglycans. They also contain increased numbers of the protein synthesis apparatus- rough endoplasmic reticulum (ER), free ribosomes and golgi apparatus (Chamley-Campbell et al., 1979). DNA synthesis and cell proliferation along with cell migration is also increased in synthetic VSMCs when compared with contractile VSMCs (Clowes and Schwartz, 1985). It should be noted that decrease in VSMC contractile proteins does not always result in increased proliferation and migration and vice versa, instead there appears to be a scale of dedifferentiation between a fully contractile to fully synthetic phenotype (Shanahan and Weissberg, 1998). The consequence of this shift to a more synthetic state following vascular injury is migration and proliferation of the VSMCs from the media to the intima resulting in the formation of neointima and vessel stenosis (Clowes and Schwartz, 1985).

It has been reported that a small population of SM-MHC-negative cells (~10%) exist in the media that are multipotent and can differentiate into neural cells and mesenchymal SC-like cells (Tang et al., 2012). A lineage tracing experiment, in which SM-MHC-positive cells were labelled with EGFP, revealed that following isolation of medial cells by enzymatic digestion SM-MHC-positive cells were the dominant cell type (>92%) in culture. However, after culture for 10 days only SM-MHC-negative multipotent vascular SCs remained, indicating that these cells appear to have a greater proliferative capacity *in vitro* than VSMCs. Culture of multipotent vascular SCs resulted in differentiation into mesenchymal SC-like cells which further differentiated into SM-MHC-positive VSMCs following 8 weeks in culture, indicating that accumulation of VSMCs following vascular injury could be partly due to proliferation and differentiation of multipotent vascular SCs (Tang et al., 2012). Significantly, following carotid artery injury in mice which express EGFP-labelled SM-MHC, expression of the proliferation marker Ki67 was restricted to EGFP-negative cells which expressed the multipotent vascular SC marker S100B. The authors further investigated this in a rat EC denudation model and found that Ki67 expression in multipotent vascular SCs was decreased from 32% at day 15 to around 1% at day 30 post-injury. Furthermore, at day 30 post-injury the majority of cells positive for S100B were also positive for SM-

MHC, suggesting that multipotent vascular SCs may have started to differentiate into VSMCs (Tang et al., 2012). The results of this study certainly suggest that proliferation of multipotent vascular SCs and not de-differentiation of adult VSMCs may be the causative factor behind neointimal formation.

Nemenoff and colleagues (Nemenoff et al., 2011) utilised a mouse model in which SM-MHC-positive cells were labelled with β -gal to show that accumulations of β -gal-positive VSMCs were present in the neointima 7 days post wire-injury of the femoral artery, indicating that migration of differentiated VSMCs to the intima plays a role in neointimal formation. Furthermore the authors showed that 3 weeks post-injury the majority of proliferating cells in the media and neointima were SM-MHC expressing β -gal-positive cells, indicating the presence of proliferating VSMCs (Nemenoff et al., 2011). These results are in contrast to Tang and colleagues who found that 5 days after wire-injury the majority of medial cells expressed multipotent vascular SC marker S100B and lost expression of SM-MHC (Tang et al., 2012). It was suggested that the discrepancies between these two studies may be due in part to a greater degree of VSMC death in the media following a more severe vascular injury in the study by Tang and colleagues, which may have resulted in the lack of contribution to neointimal formation by VSMCs (Tang et al., 2012). These studies highlight that neointimal formation after vascular injury may have contributions from both multipotent vascular SCs and VSMCs.

1.2.1 Regulation of VSMC phenotype

1.2.1.1 Serum response factor

The transcription factor serum response factor (SRF) is a major signalling molecule which governs VSMC phenotype. SRF binds to CC(A/T)₆GG sequences known as a CArG elements/boxes which are present in the promoter and enhancer regions of target genes (Mack and Owens, 1999, Li et al., 1997, Manabe and Owens, 2001). CArG elements have been found in the promoters and enhancers of virtually all contractile genes and mutation of these elements can abolish expression of these genes *in vivo* including α -SMA, SM-MHC and smooth muscle 22 alpha (SM22 α) (Mack and Owens, 1999, Li et al., 1997, Manabe and Owens, 2001). SRF targets include not only contractile genes but also a

significant number of components of the actin cytoskeleton (Miano et al., 2007). SRF target genes include proteins involved in actin cytoskeleton arrangement, cell migration, calcium handling, and contraction (Miano et al., 2007). Myocardin is an SRF cofactor which acts as a powerful promoter of VSMC differentiation when bound to SRF, increasing contractile gene expression within VSMCs and also activating the expression of contractile genes in pluripotent embryonic stem cells (ESCs) (Chen et al., 2002, Du et al., 2003, Yoshida et al., 2003). Furthermore, myocardin KO mice die *in utero* with complete absence of SMC differentiation (Li et al., 2003). Significantly, myocardin gene expression is downregulated following vascular injury (Hendrix et al., 2005), suggesting that this loss of myocardin may be a causative factor for the loss of contractile gene expression seen following vascular injury. Myocardin-related transcription factors (MRTF-A, MRTF-B) have also been identified which act as coactivators of SRF (Wang et al., 2002). The induction of contractile gene expression by MRTF-A, MRTF-B and myocardin in ESCs was shown to be entirely dependent on SRF expression (Wang et al., 2002). The importance of myocardin in VSMC contractile gene expression was further shown when it was described how the ETS domain-containing protein ELK-1 competes with and can displace myocardin from its binding site on SRF, resulting in the suppression of a contractile gene expression (Wang et al., 2004). Functional studies have identified that myocardin acts an inhibitor of cell proliferation consistent with the promotion of a differentiated cell state (Tang et al., 2008, Long et al., 2008).

1.2.1.2 Growth factor and cytokine regulation of VSMCs

Many growth factors are major regulators of VSMCs and are released by resident or infiltrating cells in the vessel wall including ECs, VSMCs, macrophages and platelets (Raines and Ross, 1993). Increased expression levels of several cytokines and growth factors including platelet-derived growth factor (PDGF), transforming growth factor beta (TGF- β), IL-1, and basic fibroblast growth factor (bFGF), have been detected in atherosclerotic plaques and after vessel injury (Ross et al., 1990, Hughes et al., 1993, Arbustini et al., 1995, Majesky et al., 1991). Stimulation by these agents is thought to be the driving force behind VSMC chemotaxis, proliferation and migration into the plaque and ECM deposition to form the fibrous cap which helps to increase plaque stability (Raines and Ross, 1993). Similarly, growth factors released after vascular injury

promote a synthetic VSMC phenotype which leads to formation of neointima (Libby et al., 1992). Some of the most influential regulators of VSMC phenotype are discussed below.

1.2.1.3 Platelet-derived growth factor

PDGF is a potent promoter of VSMC proliferation, migration, chemotaxis and ECM production (Amento et al., 1991, Deguchi et al., 1999). PDGF production is high in VSMCs in early post-natal rats but much lower in VSMCs isolated from adults (Seifert et al., 1984). Similarly, synthetic VSMCs isolated from the intima of injured rat carotids produce more PDGF than those from the media exhibiting a contractile phenotype, indicating that PDGF is important synthetic VSMC signalling (Walker et al., 1986). *In vitro*, exposure of aortic VSMCs to PDGF results in cell proliferation and downregulation of VSMC marker genes including α -SMA and SM-MHC (Blank and Owens, 1990, Holycross et al., 1992). PDGF can be released from several cell types including ECs, VSMCs, macrophages and platelets and PDGF-B has been shown to be expressed with macrophages throughout all stages of atherosclerosis (Ross et al., 1990). Furthermore, expression of the PDGF receptor β subunit is also increased in atherosclerosis (Ross et al., 1990). This suggests that PDGF may play a role in triggering VSMC proliferation and migration from the intima to promote and fibrous cap formation in atherosclerosis.

PDGF is elevated in the human coronary circulation after angioplasty as is the mitogenicity of isolated serum (Caplice et al., 1997). Inhibition of PDGF and bFGF significantly reduced proliferation of cultured VSMCs induced by mitogenic serum suggesting that these growth factors may promote VSMC activation after injury (Caplice et al., 1997). PDGF and bFGF expression is upregulated in the atherosclerotic plaque and further upregulated in vessels with restenosis, indicating that these growth factors may be important activators of VSMCs after injury (Arbustini et al., 1995). Neutralisation of bFGF using an antibody has been shown to significantly reduce VSMC proliferation in the medial layer of the balloon-injured rat carotid but did not result in decreased neointimal formation (Lindner and Reidy, 1991). This result is consistent with another study which showed that bFGF inhibition does not affect intimal SMC proliferation or neointimal formation (Olson et al., 1992).

In vivo studies have confirmed the importance of PDGF in VSMC phenotypic switching. Infusion of PDGF-BB into rats following carotid artery endothelial denudation resulted in small increases (2-3 fold) in medial VSMC proliferation and large increases (approximately 20-fold) in VSMC migration to the intima, resulting in increased neointimal formation (Jawien et al., 1992). Furthermore, inhibition of either the PDGF-A chain or PDGF-B chain significantly reduced neointimal formation following balloon catheter injury of the carotid artery (Deguchi et al., 1999, Kotani et al., 2003). This appears to occur both through decreased proliferation and decreased chemotaxis of VSMCs to the intima following PDGF inhibition (Deguchi et al., 1999, Ferns et al., 1991).

1.2.1.4 Transforming growth factor beta

TGF- β is released from cells including macrophages and VSMCs and expression has been shown to be upregulated in atherosclerotic plaques, after vascular injury and in vessels with restenosis (Rappolee et al., 1988, Majesky et al., 1991, Nikol et al., 1992). TGF- β is a potent agonist of ECM production which stimulates production of collagens I and II by VSMCs (Amento et al., 1991). TGF- β control elements (TCE) exist in the promoter regions of contractile genes and along with the CARG box are essential for TGF- β mediated control of the contractile genes α -SMA, SM-MHC and SM22 α (Adam et al., 2000, Hautmann et al., 1997). It has been shown that TGF- β promotes binding of kruppel-like factor (KLF) 5 to the TCE which enhances transcription of contractile genes through an SRF-CARG box dependent mechanism (Hautmann et al., 1997, Adam et al., 2000). TGF- β also inhibits the expression of KLF4, which competes at the TCE with KLF5 to decrease contractile gene expression (Adam et al., 2000). TGF- β has been shown to inhibit human VSMC proliferation and migration *in vitro* and can inhibit PDGF-induced migration (Mii et al., 1993, Reddy and Howe, 1993). Interestingly, despite the inhibitory effect TGF- β exerts on PDGF induced migration TGF- β can promote VSMC migration in a dose dependent manner (Koyama et al., 1990). Others have reported that TGF- β stimulates VSMC proliferation via activation of PDGF-AA secretion by VSMCs in a dose dependent manner and also potentiates growth responses to bFGF, PDGF -BB and epidermal growth factor *in vitro* (Stouffer and Owens, 1994, Battegay et al., 1990). Conversely high doses of TGF- β inhibit VSMC proliferation and decrease PDGF receptor alpha subunit expression (Battegay et al., 1990).

Injury to the rat carotid artery has been reported to result in significantly increased expression of several TGF- β isoforms with TGF- β 1 showing the greatest upregulation of expression, whilst infusion of TGF- β 1 promoted proliferation of the neointima (Majesky et al., 1991, Smith et al., 1999). Delivery of a TGF- β 1 expression plasmid to porcine arteries resulted in neointimal hyperplasia and ECM synthesis (Nabel et al., 1993). Furthermore inhibition of TGF- β 1 by a neutralising antibody significantly reduced neointimal formation and expression of ECM proteins fibronectin and versican after vascular injury (Wolf et al., 1994).

Similarly, delivery of soluble TGF- β receptor II (TGF- β RII) was shown to lead to a significant reduction in neointimal lesion formation (Smith et al., 1999). The expression of the TGF- β RII is reduced in VSMCs isolated from human atherosclerotic plaques and in proliferating intimal VSMCs following vascular injury (Smith et al., 1999, McCaffrey et al., 1995). TGF- β 1 was shown to exert an antiproliferative response on in VSMCs derived from normal arteries but this effect was absent in VSMCs derived from atherosclerotic arteries where TGF- β 1 strongly promoted synthesis of ECM (McCaffrey et al., 1995). Delivery of TGF- β RII to atherosclerotic VSMCs resulted in an antiproliferative response to TGF- β 1, indicating that the promotion of neointimal formation by TGF- β *in vivo* following injury may be partly due to decreased expression of TGF- β RII (McCaffrey et al., 1995). Taken together these studies indicate that the role of TGF- β in governing VSMC phenotype is largely context dependent, however, following vascular injury TGF- β signalling appears to promote neointimal formation by activation of VSMCs.

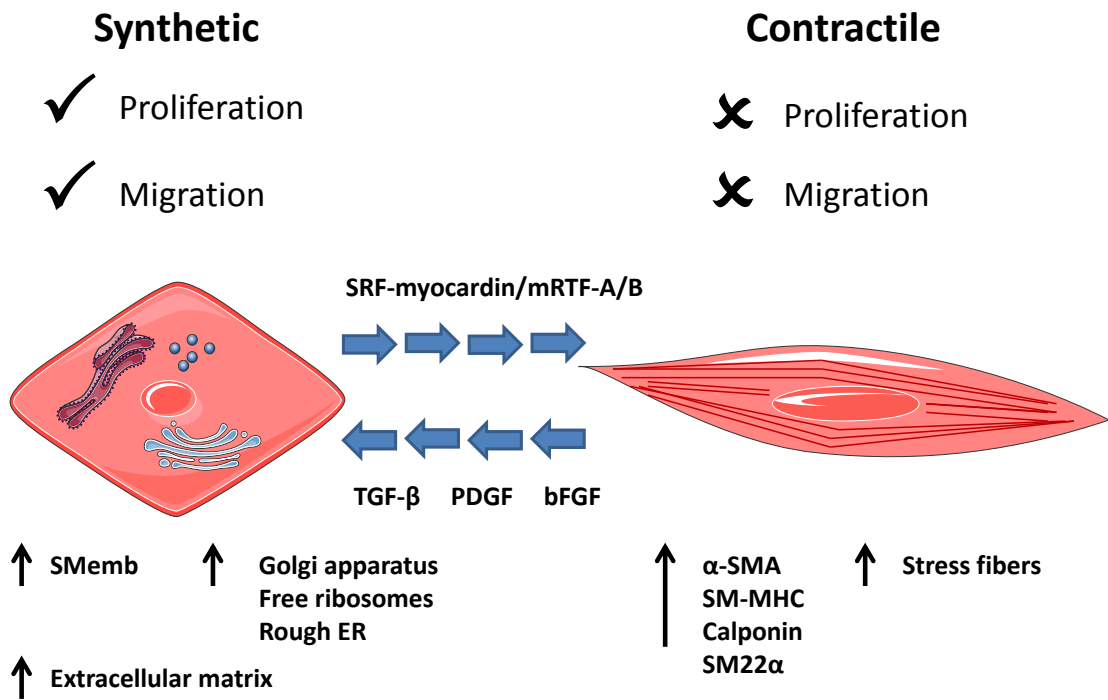


Figure 1.3. The contractile and synthetic VSMC.

Serum response factor (SRF) in combination with its cofactor myocardin, myocardin related transcription factor A (MRTF-A) or MRTF-B promotes a contractile phenotype. Fully contractile VSMCs have an elongated shape with an abundance of highly organised actin stress fibers and contractile proteins including alpha smooth muscle actin (α -SMA), smooth muscle myosin heavy chain (SM-MHC), calponin and smooth muscle 22 alpha (SM22 α). Contractile VSMCs are largely non-proliferative and non-migratory. Synthetic VSMC phenotype is promoted by signalling of growth factors such as platelet-derived growth factor (PDGF) and transforming growth factor beta (TGF- β). Fully synthetic VSMCs have an epithelioid shape and display less contractile gene expression and increased expression of synthetic genes such as SMemb. Stress fiber numbers are decreased in synthetic VSMCs whereas there is increased expression of the protein synthesis machinery- golgi apparatus, rough endoplasmic reticulum and free ribosomes. Synthetic VSMCs produce large amounts of ECM and are proliferative and migratory. Adapted from Servier Medical Art.

1.3 MicroRNAs

The human genome contains approximately 20,000 - 25,000 protein coding genes, surprisingly only around 30-fold more than that of a nematode worm (IHGSC, 2004). Protein coding genes make up less than 2% of the human genome whereas the remainder is made up of non-protein coding deoxyribonucleic acid (DNA) (IHGSC, 2004). Non-coding DNA was originally thought of as 'junk' DNA with no purpose but it was later shown that approximately 75% of the human genome is in fact transcribed indicating that non-coding ribonucleic acid (RNA) accounts for a large proportion of transcriptional output (Djebali et al., 2012). Non-coding RNAs include well described RNAs including transfer RNA and ribosomal RNA which have functions in protein synthesis as well as the more recently discovered long non-coding RNAs, small interfering RNAs (siRNAs) and microRNAs (miRNAs) (Mercer et al., 2009, Zeng et al., 2003). MiRNAs were first discovered by the Ambros lab in 1993 when a small non-protein coding RNA was shown to control developmental timing through gene regulation in *Caenorhabditis elegans* (*C. elegans*) (Lee et al., 1993). Decades on and hundreds of miRNAs have now been discovered and are believed to regulate a large proportion of the human genome (van Rooij, 2011).

1.3.1 MiRNA Biogenesis

MiRNAs are ~20-25 nucleotide (nt) non coding RNA molecules which regulate gene expression typically through binding to the 3' untranslated region (UTR) of messenger RNA (mRNA) transcripts and preventing translation via RNA interference (Lee et al., 1993, Wightman et al., 1993, Lau et al., 2001, Lagos-Quintana et al., 2001). MiRNAs can be encoded within the introns of coding genes or in intergenic regions (Ramalingam et al., 2014, Saini et al., 2007, Monteys et al., 2010). MiRNAs encoded within introns can share a common transcriptional unit with the host gene and may therefore show concordant expression with the host gene (Baskerville and Bartel, 2005). However, other intron encoded miRNAs show differential expression patterns to the host gene and have been found to be transcribed from separate transcriptional units (Ramalingam et al., 2014, Monteys et al., 2010). A miRNA may exist alone or clustered alongside other miRNAs on the genome giving rise to 'families' of

miRNA, which have been commonly found to work to within in similar pathways (Baskerville and Bartel, 2005, Gregory et al., 2008).

MiRNA biogenesis begins in the nucleus with transcription by RNA polymerase II or RNA polymerase III to form a long transcript, often more than 1 kilobase (kb) in length, known as a primary miRNA (pri-miRNA) (Figure 1.4) (Lee et al., 2004, Borchert et al., 2006, Lee et al., 2002). For miRNAs clustered on the genome a single pri-miRNA may be produced which encodes several miRNAs (Lee et al., 2002). It has also been shown that pri-miRNA transcripts containing single miRNAs can be produced from miRNA clusters through separate transcriptional unit or alternative splicing on the host gene (Ramalingam et al., 2014). Post-transcriptional modification of pri-miRNAs by adenosine deaminases acting upon RNA (ADARs) has been described for several miRNAs (Luciano et al., 2004). ADARs act upon the pri-miRNA to change adenosine to inosine, which can lead to alterations in base-pairing, structure, processing and target recognition (Yang et al., 2006). Typically, pri-miRNAs contain a double stranded hairpin stem around 33 base pairs (bp) in length, with terminal loop and two single stranded flanking regions located at the 5' and 3' ends of the transcript with a 5' 7-methyl guanosine cap and a 3' poly-A tail (Cai et al., 2004, Lee et al., 2004). It is this general structure, that allows the pri-miRNA to be distinguished from other hairpin RNAs and be recognised by the miRNA 'microprocessor complex' Drosha and DiGeorge critical region 8 (DGCR8) (Lee et al., 2003, Gregory et al., 2004, Han et al., 2006). Drosha is a class II ribonuclease (RNase) III enzyme, which contains two RNase III domains and one double-stranded RNA binding domain (dsRBD) (Han et al., 2004). The two RNase III domains of Drosha form an intramolecular dimer which cleaves the pri-miRNA at the 5' and 3' strand leaving an overhang of around 2 bp in the 3' strand (Han et al., 2004). DGCR8 contains two dsRBD and has been shown to be an essential component of the microprocessor complex (Gregory et al., 2004, Denli et al., 2004, Landthaler et al., 2004). The current model predicts that DGCR8 acts as an anchor by binding to the pri-miRNA at the junction where the single stranded flanking regions meet the double stranded hairpin stem (Han et al., 2006). DGCR8 anchoring to the pri-miRNA appears essential in aiding Drosha to identify the correct position for cleavage of the pri-miRNA (Han et al., 2006). This position is believed to be approximately 11 bp from the junction where the single stranded flanking arm

meets the double stranded stem of the pri-miRNA (Han et al., 2006). In intronic miRNAs which share a transcriptional unit with the host gene, Drosha cleavage has been shown to occur prior to the completion of intron splicing (Kim and Kim, 2007). The result of cleavage by Drosha is a double-stranded stem-loop precursor miRNA (pre-miRNA) around 60 - 100 nt long.

The pre-miRNA, along with its 3' overhang created during cleavage by Drosha, is recognised by Exportin 5, which in the presence of its cofactor Ran-guanosine triphosphate (GTP) allows for the nuclear export of the pre-miRNA to the cytoplasm (Figure 1.4) (Yi et al., 2003, Bohnsack et al., 2004). Once in the cytoplasm the pre-miRNA is acted upon by the RNA induced silencing complex (RISC)-loading complex comprised of Argonaute (Ago) 2, the class III RNase III enzyme Dicer and the cofactors TAR RNA binding protein (TRBP) and protein activator of PKR (PACT) (Hutvagner et al., 2001, Lee et al., 2006, MacRae et al., 2008, Chendrimada et al., 2005). Dicer contains two RNase III domains, one dsRBD and a long N terminus containing a PIWI/Argonaute/Zwille (PAZ) domain which recognises the 2 nt 3' overhang (Ma et al., 2004) and cleaves the pre-miRNA via its RNase III domains around 22-25 nt from the 3' terminus (Macrae et al., 2006, Zhang et al., 2002). TRBP and PACT are double stranded RNA binding proteins which form a complex with Dicer that is not essential for but helps facilitate Dicer's cleavage of the pre-miRNA (Haase et al., 2005, Lee et al., 2006, Chendrimada et al., 2005). Interestingly, biogenesis of miR-451, a miRNA abundantly expressed in red blood cells, has been shown to be processed by a Dicer-independent mechanism that requires Ago2-dependent cleavage to form mature miR-451 (Yang et al., 2010, Cifuentes et al., 2010). Dicer cleavage removes the loop region of the pre-miRNA to form an intermediate RNA duplex around 22 nt long with 2 nt 3' overhangs on each strand. Once Dicer cleavage has occurred the RNA duplex associates with Ago2 and is unwound, a phenomenon that has recently been shown to be dependent upon the N domain of Ago2 (Kwak and Tomari, 2012). The strand with the least stable hydrogen bonds in its 5' region is usually preferentially chosen to become the 'guide strand' and is loaded onto Ago2 to form the RISC, whereas the remaining passenger strand is predominantly degraded (Schwarz et al., 2003, Khvorova et al., 2003). However, it has been shown that in some tissues a miRNA may undergo passenger strand degradation whereas in other tissues both strands of

the same miRNA are retained suggesting that the passenger strand may have a functional role (Ro et al., 2007).

1.3.2 Function of miRNAs

The miRNA guides the RISC to mRNA targets which it recognises via complementary base pairing to the 3' UTR of target mRNAs. Complementarity to the highly evolutionary conserved 'seed sequence', nucleotides 2 to 7 in the 5' region of the miRNA and corresponding 3' region of its target mRNA is needed for target recognition, although additional binding to further sites in the 3' UTR is thought to aid recognition (Wightman et al., 1993, Lewis et al., 2003, Grimson et al., 2007). The degree of complementarity between the miRNA and its mRNA target in the 3'UTR appears important in determining whether mRNA degradation or repression occurs (Zeng et al., 2003). Full complementarity of a miRNA within the 3'UTR can result in target mRNA cleavage as is seen in siRNAs, however this appears to be much more common in plants and rarer in animal miRNAs (Rhoades et al., 2002, Davis et al., 2005). Ago proteins are an essential component of the RISC with Ago2 shown to be vital for RISC cleavage of mRNA (Liu et al., 2004, Meister et al., 2004). Structural studies have revealed that the Ago2 p element-induced wimpy testes (PIWI) domain is highly similar in structure to the endonuclease RNase H, which cleaves mRNA to form a 5' phosphate and 3' hydroxyl groups products (Liu et al., 2004, Song et al., 2004). Site-directed mutagenesis studies have revealed that it is this RNase-H-like PIWI domain within Ago2 that is responsible for cleavage activity (Liu et al., 2004). Ago2 proteins also contain a PAZ domain, which binds the 3' region of the guide strand and a middle domain which anchors the 5' region (Song et al., 2003, Frank et al., 2010).

MiRNAs which do not have full complementarity to mRNA target 3' UTR, but are complementary to the seed sequence may trigger repression rather than cleavage of the mRNA (Figure 1.4) (Zeng et al., 2003). This has been found to occur through inhibition of the initiation of translation (Humphreys et al., 2005, Pillai et al., 2005) and also following the initiation of translation (Olsen and Ambros, 1999, Petersen et al., 2006, Nottrott et al., 2006). However, several studies looking into the abundance of miRNAs and their target mRNAs have shown that target mRNA levels largely inversely correlate with miRNA levels

suggesting that mRNA degradation may be the more common form of gene silencing than translational repression (Lim et al., 2005, Baek et al., 2008, Guo et al., 2010, Hendrickson et al., 2009). MiRNAs which pair imperfectly to target mRNA 3'UTR have been shown to regulate expression by directing targets to mRNA degradation pathways (Figure 1.4). This has been shown to occur through decapping and deadenylation of the mRNA which leads to its degradation (Rehwinkel et al., 2005, Wu et al., 2006, Eulalio et al., 2009, Piao et al., 2010). These studies indicate that a miRNA-RISC complex can regulate target expression through a variety of mechanisms and are likely to depend on the miRNA itself and its complementarity to each individual target gene 3'UTR.

Importantly, activity of miRNA passenger strands which are not degraded by the cell has now been demonstrated for several miRNAs, indicating that these strands can be incorporated into the RISC and functionally inhibit target expression (Zhang et al., 2013, Yang et al., 2013). For example both miR-126 and its passenger strand miR-126* were shown to inhibit the expression of target gene SDF-1 α , which promotes tumour angiogenesis (Zhang et al., 2013). This resulted in reduced recruitment of mesenchymal SCs and inflammatory cells to the primary tumour site and reduced incidence of lung metastasis in mice (Zhang et al., 2013).

An overview of miRNA biogenesis is shown in figure 1.4 with miR-143 and miR-145 used as an example for the biogenesis of clustered miRNAs.

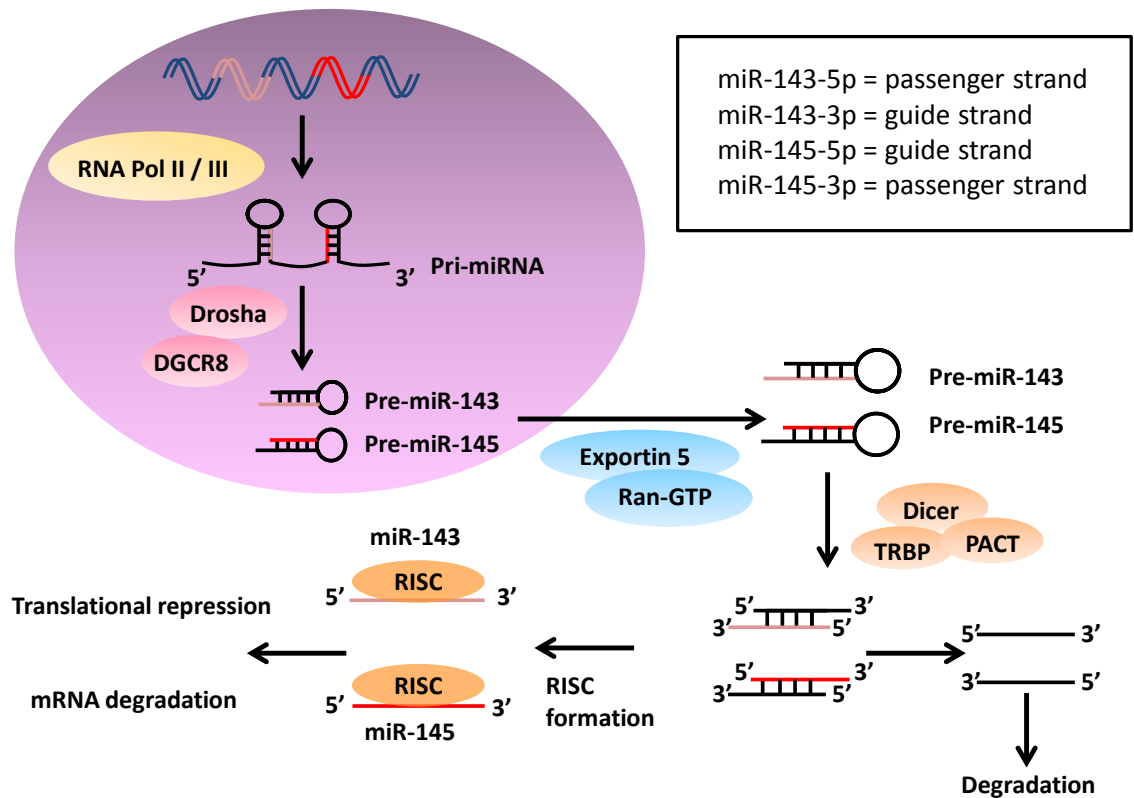


Figure 1.4. Biogenesis of miR-143 and miR-145.

MiR-143 and miR-145 are transcribed by RNA Polymerase II or III (RNA Pol II/III) from a common bicistronic gene in the nucleus to form a large pri-miRNA transcript which contains both miRNAs. The pri-miRNA is cleaved by Drosha and its cofactor DiGeorge critical region 8 (DGCR8) to form the individual pre-miR-143 and pre-miR-145. Pre-miR-143 and pre-miR-145 are transported to the cytoplasm by Exportin 5 and its cofactor ran-guanosine triphosphate (Ran-GTP) where they are then acted upon by Dicer and its cofactors tar binding protein (TRBP) and protein activator of PKR (PACT) which cleave the stem loop to form double stranded intermediates. One strand is chosen and loaded onto the RISC complex composed of argonaute proteins to act as a 'guide' where it directs the RISC to target mRNA recognised by complementary based pairing to the 3' region of the mRNA, triggering mRNA degradation or translational repression.

1.3.3 Importance of miRNAs during development

MiRNAs are essential during development where the expression profiles of individual miRNAs are modulated, according to developmental stage (Wienholds et al., 2005, Mineno et al., 2006). By increasing miRNAs profiles the expression of certain genes can essentially be 'switched off' by miRNA repression or alternatively absent or decreased miRNA expression levels may permit translation and gene expression. Studies in vertebrates have shown that certain miRNAs are important in the critical maternal to zygotic transition stage of

embryogenesis where they act to degrade maternal mRNAs to allow development to continue under the control of the zygotic genome (Giraldez et al., 2006, Lund et al., 2009). ESCs are pluripotent cells that are isolated from the inner cell mass of the blastocyst (4-5 days post-fertilisation in humans), which can differentiate to form all cells within the 3 major germ layers: ectoderm, endoderm and mesoderm (Evans and Kaufman, 1981, Martin, 1981). ESCs have been shown to express a unique set of miRNAs, including the miR-302 family consisting of 5 clustered miRNAs, which appear to be ESC-specific and are not detectable at later stages of development or in adult tissues (Houbaviy et al., 2003, Suh et al., 2004). It is thought that these miRNAs may play an essential role in maintaining pluripotency and aiding differentiation of ESCs (Houbaviy et al., 2003, Suh et al., 2004). Conditional KO of Dicer, an enzyme responsible for miRNA maturation, has been shown to reduce differentiation and proliferation of ESCs (Murchison et al., 2005, Kanellopoulou et al., 2005).

The first study to show the importance of miRNAs during development came at their very discovery, when *lin-4* was shown to negatively regulate the expression of *lin-14* in *C. elegans* (Lee et al., 1993, Wightman et al., 1993). *Lin-14* is a heterochronic gene whose protein is expressed in a temporal gradient that controls the timing of developmental events in larvae (Ambros and Horvitz, 1987, Ruvkun and Giusto, 1989). By post-transcriptionally repressing *lin-14* expression, *lin-4* was shown to create this temporal gradient of *lin-14* expression, thus controlling developmental timing in *C.elegans* (Lee et al., 1993). The use of profiling techniques, such as miRNA arrays, has allowed the expression of large numbers of miRNAs to be studied during vertebrate and mammalian embryogenesis and development where temporal patterns of miRNA expression, similar to those seen in *C. elegans*, are observed (Wienholds et al., 2005, Mineno et al., 2006, Cao et al., 2012, Krichevsky et al., 2003).

Further evidence for the importance of miRNAs in development comes from KO mouse studies where global KO of Dicer, an essential component of the miRNA biogenesis pathway, was shown to be embryonically lethal (Bernstein et al., 2003). Importantly, Dicer is also essential for the development of the cardiovascular system. A cre recombinase mediated cardiac-specific Dicer KO, which under the control of the *Nkx2.5* promoter directs Dicer KO in cardiac progenitor cells by embryonic day (E) 8.5, was shown to be embryonic lethal in

mice by E12.5 due to gross abnormalities in cardiac development (Zhao et al., 2007). Cardiovascular specific Dicer KO has also been performed using cre recombinase under the control the alpha myosin heavy chain promoter, where miRNA level began to decrease in the heart at E14.5. The loss of Dicer expression at this later time point resulted in postnatal lethality within 4 days of birth due to dilated cardiomyopathy and heart failure (Chen et al., 2008). Similarly, cardiomyocyte specific KO of DGCR8, an essential cofactor of Drosha mediated cleavage of pri-miRNAs, was shown to result in lethality within 2 months of birth in mice, due to dilated cardiomyopathy and heart failure (Rao et al., 2009).

Individual miRNAs that are tissue specific or are enriched within a certain tissue type can also be particularly important for development. This has been demonstrated for the skeletal and cardiac muscle-specific bicistronic miRNAs miR-1 and miR-133a, which are essential for normal cardiac development. KO of miR-1-2 resulted in 50% lethality in mice occurring from E15.5 to a few days postnatally, which was attributed to the presence of ventricular septal defect and pericardial oedema (Zhao et al., 2007). Furthermore surviving miR-1-2 KO mice displayed abnormalities in cardiac electrical conductance including prolonged ventricular depolarisation (Zhao et al., 2007). Conversely, overexpression of miR-1 in the developing heart also led to embryonic lethality by E13.5 due to thin ventricular walls and heart failure (Zhao et al., 2005). Similar to its cotranscribed miR-1, KO of both miR-133a-1 and miR-133a-2 led to around 50% embryonic lethality due to ventricular septal defect, whereas surviving mice went on to develop dilated cardiomyopathy and heart failure (Liu et al., 2008).

1.3.4 Dysregulation of miRNAs in disease

Currently more than 1000 human microRNAs have been identified which are thought to regulate approximately 60% of genes (van Rooij, 2011). When considering the importance of miRNAs in regulating normal cellular homeostasis in health, it is perhaps unsurprising that aberrant expression of these regulators has been reported in a broad range of human diseases including heart disease (Sucharov et al., 2008, Naga Prasad et al., 2009) and cancer (Lu et al., 2005, Blenkiron et al., 2007, Zhang et al., 2007). Differential expression patterns of

miRNAs are also reflected in animal models of disease and alteration of miRNA levels can provide a therapeutic benefit (Fiedler et al., 2011, van Rooij et al., 2006, Kumar et al., 2008). The therapeutic benefit of altering miRNA expression is now being investigated in humans with the first miRNA-targeted drug Miravirsen, currently in phase II clinical trials (Lindow and Kauppinen, 2012). Miravirsen is a locked nucleic acid (LNA) antisense oligonucleotide which binds to miR-122 inhibiting its expression. MiR-122 is an abundantly expressed liver miRNA which promotes the expression of hepatitis C viral RNA in infected cells through binding to sites in the viral 5' terminus and protecting it from nucleolytic degradation (Jopling et al., 2005, Machlin et al., 2011). In non-human primates inhibition of miR-122 provides an antiviral effect, significantly reducing hepatitis C viral titre (Lanford et al., 2010). Although the action of miR-122 on hepatitis C viral RNA is somewhat unconventional in that it increases RNA levels rather than degrading or repressing them, these studies provide strong support that drugs targeting miRNAs may be useful clinically.

1.3.5 Importance of miRNAs in VSMCs

The global importance miRNA expression for VSMC development was highlighted in a study by Albinsson and colleagues (Albinsson et al., 2010) who showed that KO of Dicer within the VSMCs resulted in late embryonic death between E16 to E17 due to haemorrhaging. VSMC-Dicer KO embryos displayed reduced SMC proliferation, thin aortic walls and reduced vessel contractility as well as reduced levels of VSMC differentiation markers SM-MHC, SM22 α and calponin (Albinsson et al., 2010). Albinsson and colleagues went on to generate adult VSMC-Dicer KO mice by a tamoxifen-dependent cre recombinase under the control of SM-MHC promoter (Albinsson et al., 2011). Blood pressure measurements performed 6-8 weeks post-tamoxifen treatment revealed that adult VSMC Dicer-KO mice had substantial reductions in both systolic and diastolic blood pressure. VSMC-Dicer KO mice also displayed significantly blunted contractile responses to phenylephrine and reduced expression of contractile proteins calponin, α -SMA and SM-MHC (Albinsson et al., 2011). Together these studies highlight the fundamental role of miRNAs in the development and maintenance of VSMCs phenotype. Some of the individual miRNAs identified as important regulators of VSMC phenotype are discussed in more detail below.

MiR-21 has been identified as a potent regulator of VSMC phenotype and its expression has been shown to induce proliferation and decreases apoptosis of cultured VSMCs (Ji et al., 2007). MiR-21 expression is upregulated in the vessel wall following balloon catheter injury of the rat carotid artery and knockdown of miR-21 using an antagomiR significantly reduces neointimal formation (Ji et al., 2007). Furthermore knockdown of miR-21 resulted in around 50% increase in apoptosis and decrease in proliferation in the neointima detected 7 days post balloon injury (Ji et al., 2007).

The expression of miR-221 and miR-222 is also increased in the vessel wall following injury and was localised to VSMCs (Liu et al., 2009). Expression of these miRNA is increased in VSMCs following PDGF or serum-induced proliferation and knockdown of miR-221 or miR-222 reduces proliferation. This has been shown to occur partly through repression of their targets p27(Kip1) and p57(Kip2) (Liu et al., 2009). Furthermore, p27(Kip1) and p57(Kip2) were downregulated in the vascular wall following injury and upregulated following miR-221 and miR-222 inhibition, suggesting that they are targeted by these miRNA *in vivo*. Inhibition of both miRNA reduced neointimal formation after balloon catheter injury of the carotid artery by around 40% (Liu et al., 2009).

PDGF has been previously shown to repress VSMC contractile gene expression by activating the expression of stimulating protein-1 (Sp-1), which binds to sites in the KLF4 promoter to activate transcription and promote the inhibitory action of KLF4 on myocardin (Deaton et al., 2009). MiR-133 expression is decreased in proliferating and migrating VSMCs and PDGF has been shown to repress the expression of this miRNA through a mechanism involving the ERK1/2-dependent pathway (Torella et al., 2011). Overexpression of miR-133 inhibited both VSMC proliferation and PDGF induction of Sp-1 and KLF4 which prevented myocardin downregulation and the downregulation of VSMC markers α -SMA and SM-MHC (Torella et al., 2011). Adenoviral overexpression of miR-133 in the balloon-injured rat carotid artery reduced neointimal formation by around 60% which was concurrent with decreased proliferation and reduced Sp-1 induction. Furthermore, delivery of an antimiR against miR-133 significantly increased neointimal formation and proliferation (Torella et al., 2011).

MiR-146a is a promoter of VSMC proliferation and knockdown of miR-146a *in vivo* using an anti-miR significantly reduced neointimal formation and proliferation in the injured rat carotid artery (Sun et al., 2011). MiR-146a represses the expression of its target KLF4, which in turn competes with KLF5 for a common binding site in the miR-146a promoter. KLF4 and KLF5 were shown to exert opposing effects on the miR-146a promoter activity with KLF4 decreasing miR-146a expression in VSMCs and KLF5 increasing expression respectively (Sun et al., 2011). Therefore miRNAs can act in feedback loops with transcription factors in VSMCs.

1.3.6 Importance of miRNAs in ECs

ECs have high expression of many miRNAs including members of the let-7 family, miR-126, miR-221, miR-222 and miR-21 (Kuehbacher et al., 2007). ECs are usually quiescent in adult vessels but can become activated following vascular injury or during ischemia. Angiogenesis, the formation of new capillaries from existing vessels, primarily involves ECs which are stimulated to proliferate and migrate outwards from the vessel whilst organising into vessel like structures (Auerbach and Auerbach, 1994). Angiogenesis occurs following MI where it helps to revascularise the ischaemic tissue and also during cancer where vascularisation of the tumour has been shown to promote progression and metastasis (Auerbach and Auerbach, 1994).

Knockdown of Dicer using siRNAs *in vitro* significantly reduces FGF-induced EC capillary sprouting, formation of capillary-like structures on matrigel and migration and proliferation (Kuehbacher et al., 2007, Suarez et al., 2007). Furthermore Dicer-deficient ECs showed significantly impaired formation of capillary-like structures in matrigel plugs *in vivo* in nude mice, indicating the global importance of miRNAs in angiogenesis (Kuehbacher et al., 2007). Further studies identified many EC miRNAs which are regulators of angiogenesis. MiR-126, an EC-specific miRNA, has been shown to enhance vascular endothelial growth factor (VEGF) and FGF activation of MAP kinase signalling by repressing the expression of its target Spred-1 (Wang et al., 2008b). MiR-126 promotes EC proliferation, migration and angiogenesis and miR-126 KO mice show impaired ability to form vessel-like structures in matrigel plugs in response to FGF-2 *in vivo* (Wang et al., 2008b). MiR-126 KO mice were associated with around 50%

lethality due to severe oedema and blood vessel rupture and haemorrhage (Wang et al., 2008b). Induction of MI resulted in death in approximately 30% of wildtype (WT) mice compared with 80% of miR-126 KO mice, which were found to have extensive fibrosis and ventricular dilatation and significantly abrogated vascularization of the injured myocardium compared to WT mice (Wang et al., 2008b). Together these studies suggest that miR-126 is an important promoter of angiogenesis. Other pro-angiogenic miRNAs include the let-7 cluster (Kuehbacher et al., 2007) and miR-17-92 cluster, which contains miRNAs with both pro- and anti-angiogenic effects (Dews et al., 2006, Bonauer et al., 2009, Doebele et al., 2010, Suarez et al., 2008). Overexpression of miR-221 and miR-222 has been shown to be anti-angiogenic by reducing the ability of stem cell factor to promote EC migration and formation of capillary-like structures on matrigel (Poliseno et al., 2006). This is thought to occur partly through inhibition of its receptor c-Kit (Poliseno et al., 2006). MiR-21 expression is reduced during angiogenesis and overexpression of this miRNA reduced EC migration and capillary-like tube formation in matrigel (Sabatel et al., 2011). This effect was mimicked by siRNA knockdown of miR-21 target RhoB, which has been shown to stimulate actin stress fiber formation, indicating a possible mechanism (Sabatel et al., 2011). The process of endothelial-to-mesenchymal transition, where ECs change to fibroblasts, occurs during cardiac fibrosis and has been shown to be mediated in part through TGF- β stimulation of miR-21 (Kumarswamy et al., 2012).

MiR-126 directly represses the expression of vascular cell adhesion molecule 1 (VCAM-1) which is upregulated during vascular inflammation, indicating the miR-126 may act to reduce leukocyte adhesion *in vivo* (Harris et al., 2008). MiR-155 represses the expression of the Ang II type 1 receptor and overexpression of this miRNA can reduce Ang II stimulated T cell adhesion and migration of ECs (Zhu et al., 2011). Together these studies indicate that miRNAs play an important role in the regulation of ECs including influencing proliferation, migration, angiogenesis and inflammation.

1.3.7 MiR-143 and miR-145 are enriched in VSMCs

Two miRNAs which have been identified as particularly important for normal VSMC development and function are the bicistronic miRNAs miR-143 and miR-145

(Figure 1.4). MiR-143 and miR-145 are highly conserved, 21 nt and 23 nt long miRNAs, which are clustered on human chromosome 5 and mouse chromosome 18 where they are co-transcribed from the same transcriptional unit (Cordes et al., 2009). Studies of mouse embryonic development revealed that miR-143 and miR-145 are highly expressed in multipotent cardiac progenitor cells which are capable of differentiating into cardiomyocytes, SMCs and ECs (Cordes et al., 2009). The expression of both miR-143 and miR-145 remains high during heart development but decreases during later cardiogenesis. Postnatally, expression is mostly observed in VSMCs and SMCs lining organs, including the lung, bladder and organs of the gastrointestinal tract (Cordes et al., 2009, Boettger et al., 2009, Xin et al., 2009). In adults miR-143 and miR-145 are the most abundantly expressed miRNAs in the artery wall where expression is enriched and largely confined to VSMCs, although low expression can be detected in ECs (Ji et al., 2007, Cheng et al., 2009, Hergenreider et al., 2012). It is generally thought that the differential expression of miRNAs in different lineages is reflective of the importance of different miRNAs in different cell types, for example the high expression miR-126 in ECs (Wang et al., 2008b). The enrichment of miR-143 and miR-145 in VSMCs suggests that miR-143 and miR-145 may predominately act to regulate these cells.

1.3.8 Control of the miR-143/145 gene by serum response factor

SRF, a major regulator of the actin cytoskeleton, regulates migration, contraction, and in combination with its cofactor myocardin, differentiation of VSMCs via the transcriptional regulation of numerous genes (see section 1.2.1.1) (Miano et al., 2007, Du et al., 2003). Strong evidence of the importance of miR-143 and miR-145 in the maintenance of VSMC phenotype comes from studies which show that the miR-143/145 cluster is transcriptionally activated by SRF in combination with its cofactor myocardin or MRTF-A (Cordes et al., 2009, Xin et al., 2009). SRF in combination with myocardin or MRTF-A was found to bind to an evolutionary conserved CARG box within cis regulatory elements in the miR-143/145 enhancer region and activate transcription. Studies revealed that disruption of the CARG box binding site by mutagenesis abolished the expression of miR-143/145 reporter genes within the SMCs and heart of developing embryos (Xin et al., 2009, Cordes et al., 2009).

1.3.9 MiR-143 and miR-145 influence VSMC phenotype *in vitro*

The evidence that miR-143 and miR-145 are both enriched within VSMCs and activated by SRF/myocardin signalling pathways prompted many groups to investigate whether these miRNAs are important in maintaining VSMC phenotype. *In vitro* studies have revealed that miR-143 and miR-145 expression is significantly reduced in VSMCs exposed to PDGF, which promotes SMC proliferation and migration (Cheng et al., 2009, Quintavalle et al., 2010). Furthermore, PDGF-induced VSMC proliferation and concurrent downregulation of markers of VSMC differentiation - calponin, SM-MHC and α -SMA - is inhibited by overexpression of miR-145 (Cheng et al., 2009, Cordes et al., 2009). Inhibition of miR-143 expression has been shown to increase the proliferation rate of VSMCs (Cordes et al., 2009). MiR-145 expression is necessary for myocardin reprogramming of fibroblasts into VSMCs (Cordes et al., 2009). In addition, exposure of multipotent neural crest SCs to miR-145 was found to be sufficient to guide 75% to VSMC fate (Cordes et al., 2009). Together these studies suggest that miR-143 and miR-145 may have a regulatory role in VSMC phenotype.

1.3.10 MiR-143 and miR-145 expression after vascular injury

In vivo studies have revealed that vessel wall expression of miR-143 and miR-145 is reduced in vascular injury models characterised by VSMC proliferation and migration. Elia and colleagues demonstrated that following transverse aortic constriction in the rat miR-143 and miR-145 expression is decreased by around 70% in the areas surrounding the constricted site (Elia et al., 2009). Mice deficient of ApoE, a glycoprotein important for cholesterol clearance, have elevated blood cholesterol and develop spontaneous atherosclerotic lesions within their vessels, a phenomenon which is exacerbated by high fat feeding (Piedrahita et al., 1992, Plump et al., 1992). Basal expression of miR-143 and miR-145 in the vessels of ApoE KO is approximately 50% less than that of WT mice and is further decreased upon high fat feeding (Elia et al., 2009). Furthermore, expression of miR-145 is significantly reduced in human carotid atherosclerotic plaques when compared to adjacent plaque-free sites (Lovren et al., 2012). A substantial loss of miR-143 and miR-145 also occurs following carotid artery ligation in the mouse and coincides with decreased expression of SMC contractile gene α -SMA (Cordes et al., 2009). Cheng and colleagues

demonstrated that following carotid balloon-injury in the rat miR-145 is downregulated by around 80% at 7 days and is concordant with decreased expression of α -SMA, calponin and SM-MHC and that recovery of expression of these genes over 28 days was closely associated with recovery of miR-145 expression (Cheng et al., 2009). MiR-145 expression has also been reported to be decreased in human aortic biopsies from patients presenting with aortic aneurysms (Elia et al., 2009). These studies provide evidence that the adoption of a synthetic phenotype by VSMCs occurs in concordance with a loss of miR-143 and miR-145 expression *in vivo*.

In order to determine whether downregulation of miR-143 or miR-145 in vascular injury directly affects VSMC phenotype several groups used overexpression strategies. Local delivery of adenovirus overexpressing either miR-143 or miR-145 was capable of reducing neointimal formation in the rat carotid balloon-injury model (Elia et al., 2009, Cheng et al., 2009). Furthermore, lentiviral-mediated overexpression of miR-145 in the ligated carotid artery of mice was sufficient to increase the expression of contractile genes α -SMA and calponin as well as myocardin (Cordes et al., 2009).

Systemic delivery of a miR-145-expressing lentivirus with a SM22 α promoter was shown to increase miR-145 expression in the VSMCs of ApoE KO mice (Lovren et al., 2012). Atherosclerotic lesion area following 12 weeks of western diet was reduced by up to 60% in lentiviral-miR-145 treated ApoE KO mice, which showed sustained increases (approximately 2.5 fold) in miR-145 expression over the course of the study (Lovren et al., 2012). Reduced plaque area was concurrent with increased expression of markers of plaque stability including reduced lipid and macrophage content, increased fibrous cap area, increased plaque collagen content and increased expression of VSMC differentiation markers α -SMA and calponin (Lovren et al., 2012).

The evidence that miR-143 and miR-145 are downregulated following vascular injury and that restoring expression of these miRNAs reduces neointimal formation supports *in vitro* studies which indicate the possible role of these miRNAs in inhibiting VSMC proliferation and migration.

1.3.11 Identifying miRNA targets

A widely used method to identify potential miRNA targets are bioinformatics websites (e.g. TargetScan, PicTar). This software identifies possible mRNA targets based on the complementarity between the 3'UTR of an mRNA and the miRNA of interest. They usually take into account areas of the 3'UTR which show strong evolutionary conservation which increases the likelihood of regulation occurring and reduces the incidence of false positives (Bartel, 2009). A 7 nt match to the seed sequence, nt 2-7, plus nt 1 or 8 in the 5' region of the miRNA is effective at predicting target mRNA (Bartel, 2009). The number of predicted binding sites for the miRNA within a 3'UTR are also usually considered. Some software requires strict seed pairing whereas others allow slight mismatch in the seed sequence which may allow for prediction of valid targets that would otherwise be missed. It has been shown that pairing to further complementary regions outside the seed sequence in the 3' UTR, termed 'compensatory' regions, can result in target repression even in the case of a base mismatch in the seed sequence (Yekta et al., 2004). Continuous 'supplementary' pairing to nucleotides 13-16 of the 3'UTR has been shown to associate with increased incidence of target repression (Grimson et al., 2007). Bioinformatics websites predict potential targets and list them in order of preference based on properties described above.

Proteomic approaches such as stable isotope labelling with amino acids in cell culture (SILAC) are high-throughput methods which have been utilised to assess the expression of large numbers of proteins in response to alterations in miRNA levels by introduction of miRNA mimics or inhibitors (Baek et al., 2008). Microarrays are another high-throughput approach which can be used to identify mRNAs which are dysregulated in cells following overexpression or knockdown of the miRNA of interest (Guo et al., 2010). Several studies have reported that the vast majority of miRNA targets are dysregulated at both the protein and mRNA level indicating that identifying targets at the mRNA level is a valid method (Guo et al., 2010, Baek et al., 2008, Selbach et al., 2008). Microarrays are particularly useful when used together with bioinformatics software to help identify mRNAs which contain complementarity regions to the miRNA suggesting that direct regulation may occur. Quantitative real-time polymerase chain reaction (qRT-PCR) can be used to confirm the dysregulation of an mRNA in response to a

miRNA in overexpression or knockdown studies to help remove the risk of false positives.

To test direct binding of a miRNA to a target mRNA luciferase constructs are often used. This involves cloning of the 3'UTR of the potential mRNA target into a luciferase reporter which is then either transfected into cells which express the miRNA of interest or transfected into cells along with a miRNA mimic of the miRNA of interest. Decreased luciferase activity suggests that target repression is occurring (van Rooij, 2011). Mutations are often made in the 3'UTR as a control to ensure that target repression does not occur when binding sites are disrupted.

1.3.12 Targets of miR-143 and miR-145

Several target mRNA have been identified for miR-143 and miR-145, with many of them encoding proteins involved in cell proliferation, migration and SMC gene expression. For example, miR-145 negatively regulates the expression of calcium/calmodulin-dependent protein kinase II delta (caMKII δ), which is induced in VSMCs and fibroblasts following injury and promotes proliferation, migration and neointimal formation (Cordes et al., 2009, House and Singer, 2008). MiR-145 regulates the expression of angiotensin converting enzyme (ACE) which converts Ang I into its active form Ang II, a well-studied regulator of VSMC contraction and proliferation (Boettger et al., 2009, Daemen et al., 1991). MiR-143 and miR-145 are both downregulated in glioma tumours, a phenomenon that is associated with poor prognosis (Lee et al., 2013). Conversely overexpression of miR-145 reduces glioma cell migration and invasion via downregulation of its target connective tissue growth factor (CTGF), suggesting that miR-145 is important in preventing tumour invasion into surrounding tissue (Lee et al., 2013). MiR-145 expression is also significantly downregulated in bladder cancer whereas the expression of its target, actin-binding protein fascin homologue 1 (FSCN1) is upregulated (Chiyomaru et al., 2010). Knockdown of FSCN1 is capable of reducing invasion and migration in bladder cancer cell lines (Chiyomaru et al., 2010). MiR-145 has also been shown to target FSCN1 and reduce proliferation and invasion in oesophageal squamous cell carcinoma cell lines (Kano et al., 2010). Together these studies indicate that miR-145 may function as a tumour suppressor. Disabled protein 2 (DAB2) acts as an inhibitor of wnt signalling

pathways and has been identified as a target of miR-145 in mesenchymal SCs and pulmonary SMCs (Mayorga and Penn, 2012, Caruso et al., 2012). Interestingly, Wnt signalling promotes cell proliferation (Mayorga and Penn, 2012) so by repressing the expression of DAB2 miR-145 may be predicted to induce proliferation, however further studies are required to determine whether this occurs. In human pulmonary artery SMCs the expression of Intergrin beta-like 1 (ITGBL1) and TGF- β 2 are downregulated by overexpression of miR-145 whereas knockdown with anti-miR-145 upregulated their expression suggesting these mRNA may also be targets of miR-145 (Caruso et al., 2012).

Some miR-143 and miR-145 targets that have been studied in more detail are discussed below.

1.3.12.1 Kruppel-like factor 5

MiR-143 and miR-145 have both been shown to bind to luciferase constructs containing the 3' UTR of KLF5 resulting in reduced luciferase activity (Cheng et al., 2009, Xin et al., 2009). This phenomenon was further investigated for miR-145 where it was shown that miR-145 downregulation of luciferase activity was inhibited by mutations in the predicted miR-145 binding site in the KLF5 3'UTR (Cheng et al., 2009). In cultured VSMCs KLF5 expression is upregulated by miR-145 knockdown and downregulated by miR-145 overexpression. Furthermore, adenovirus-mediated overexpression of miR-145 is capable of preventing the increase in KLF5 levels that occurs following balloon injury to the rat carotid artery (Cheng et al., 2009). Together this evidence supports that KLF5 is a direct target of miR-145.

KLF5 is a member of the KLF family of zinc-finger proteins and is associated with a synthetic VSMC phenotype. SM-MHC isoforms SM-1 and SM-2 are the predominantly expressed forms of SM-MHC in adult vessels (Kuro-o et al., 1991). Following vessel injury SM-2 expression is absent in the developing neointima and SMemb expression appears (Kuro-o et al., 1991). KLF5 is abundantly expressed in SMCs of the vessel walls during fetal development but is markedly reduced in adult vessels (Hoshino et al., 2000). However, following balloon-injury to the rat aorta, KLF5 expression is induced in the developing neointima (Watanabe et al., 1999). KLF5 has been shown to bind to a cis-regulatory

element to promote transcription of SMemb within the neointima, a phenomenon associated with the de-differentiation of VSMCs (Watanabe et al., 1999, Kuro-o et al., 1991). Interestingly, KLF5 can also promote transcriptional activation of contractile gene SM22 α suggesting that KLF5 may have variable roles depending on the context of expression (Adam et al., 2000). Homozygous KLF5 KO results in embryonic lethality, however mice that are heterozygous for KLF5 KO have thin vessel walls and display significantly less neointima formation following femoral cuff placement (Shindo et al., 2002). Conversely, adenoviral overexpression of KLF5 following vascular injury results in increased neointima formation and cell proliferation (Suzuki et al., 2009). This was further dissected *in vitro* where it was shown that KLF5 expression in cultured VSMCs increases the number of cells in the S phase whereas reduction in KLF5 expression reduces S phase transition (Suzuki et al., 2009). KLF5 transcriptional activation of cyclin D1, a key regulator of cell-cycle progression, may be responsible at least in part, for the increased proliferation seen with KLF5 expression (Suzuki et al., 2009). KLF5 has also been shown to transcriptionally activate PDGF-A and TGF- β expression in response to Ang II stimulation, indicating that KLF5 is involved in a number of signalling pathways known to influence cell proliferation and migration (Shindo et al., 2002). In patient coronary atherectomy samples high KLF5 expression is associated with restenosis (Sakamoto et al., 2003, Hoshino et al., 2000). Together these studies provide strong evidence for the role KLF5 in promoting cell proliferation, migration and neointimal formation. The negative regulation of KLF5 by miR-143 and miR-145 indicates that downregulation of these miRNA following vascular injury may influence VSMC phenotype in part via de-repression of KLF5.

1.3.12.2 ELK-1 and myocardin

Luciferase reporter assays have revealed that miR-143 binds the 3' UTR of the ETS-domain transcription factor, Elk-1, *in vitro* and reduces luciferase expression (Cordes et al., 2009). Overexpression of miR-143 in VSMCs reduces ELK-1 protein expression but not mRNA, suggesting that miR-143 represses rather than degrades Elk-1 at the mRNA level (Cordes et al., 2009). Elk-1 has been shown to play an important role in the SRF signalling pathway by opposing the SRF-myocardin interaction and promoting a synthetic VSMC phenotype (Wang et al., 2004). SRF promotes a contractile VSMC phenotype when in association with

its cofactor myocardin (see section 1.2.1.1). However, upon PDGF stimulation, Elk-1 was shown to inhibit the myocardin-SRF interaction by binding competitively to the docking site myocardin utilises for SRF-binding (Wang et al., 2004). This was demonstrated at the promoter region of the contractile genes SM22 and α -SMA genes which contain ternary complex factor binding sites, utilised by ELK-1, adjacent to SRF binding site. The Elk-1-SRF interaction resulted in repressed SMC contractile gene expression, thought to occur due to the disruption in myocardin binding (Wang et al., 2004).

Interestingly, miR-145 was shown to directly bind to the 3'UTR and enhance the expression of myocardin (Cordes et al., 2009). Myocardin in combination with SRF is known to promote the transcription of miR-143/145 therefore suggesting that miR-145 and myocardin mutually promote expression of one another (Cordes et al., 2009). By repressing Elk-1 and promoting myocardin expression miR-143 and miR-145 promote the SRF-myocardin interaction which will not only promote the expression of contractile genes but may also promote miR-143/145 transcription.

1.3.12.3 Kruppel-like factor 4

KLF4 has been shown to be a miR-143 and miR-145 target through 3'UTR luciferase and knockdown studies (Cordes et al., 2009, Xin et al., 2009, Davis-Dusenbery et al., 2011). KLF4 expression has also been shown to be upregulated in human atherosclerotic plaques which show concurrent downregulation of miR-145 expression (Lovren et al., 2012). KLF4, along with the transcription factors; Oct3/4, c-Myc and Sox2, is capable of producing induced pluripotent cells from adult human fibroblasts, indicating that KLF4 is important in producing a de-differentiated phenotype (Takahashi et al., 2007). Expression of KLF4 is low in adult vessels but is upregulated following vascular injury (Liu et al., 2005). KLF4 has been shown repress both expression of myocardin itself and myocardin-SRF activation of the α -SMA gene by binding to SRF at the same domain utilised by myocardin. Interaction of KLF4 with SRF prevented SRF from binding to the CARG box in the α -SMA promoter and thus prevented activation of α -SMA transcription (Liu et al., 2005). KLF4 is recruited to a TCE, located adjacent to the SRF CARG binding site in the promoter region of contractile genes (e.g. α -SMA, SM-MHC and SM22 α) following vascular injury, which allows the interaction between SRF and

KLF4 (Adam et al., 2000, Liu et al., 2005, Yoshida et al., 2008). In ApoE KO mice restoration of miR-145 expression to VSMCs was shown to decrease KLF4 expression and increase myocardin expression (Lovren et al., 2012). PDGF-BB activates KLF4 expression and was shown also shown to inhibit interaction of SRF with the CArG binding domain in α -SMA an action that could be partially blocked by inhibition of KLF4 expression (Liu et al., 2005). KLF4 has also been shown to suppress activation of SM22 α via a TCE in its promoter (Adam et al., 2000). Conversely, others have reported that KLF4 is required for the upregulation of SMC contractile gene expression by all-trans-retinoic acid (Wang et al., 2008a). The expression of SM22 α and α -SMA is reduced following vascular injury; however in mice with conditional KLF4 KO the downregulation of these SMC contractile genes is delayed suggesting that KLF4 may be crucial in the initial suppression of contractile gene expression (Yoshida et al., 2008). Interestingly, despite KLF4 expression being increased following vascular injury, KO of KLF4 resulted in greater neointimal formation following carotid ligation. It was found the KLF4 directly represses SMC proliferation via a synergistic interaction with p53 at the cyclin-dependent kinase inhibitor p21^{waf1/cip1} promoter region (Yoshida et al., 2008). Other studies have also reported that KLF4 inhibits cell proliferation *in vitro* (Wassmann et al., 2007). The conflicting evidence suggests the role of KLF4 in maintaining SMC phenotype is extremely complex and it may have differential effects depending on the context. MiR-145 regulation of KLF4 expression may result in different outcomes depending upon the context and the actions of other signalling molecules involved.

1.3.13 Signalling pathways involving miR-143 and miR-145

The de-regulation of miR-143 and miR-145 in migrating and proliferating VSMCs *in vitro* and *in vivo* has prompted many studies into what signalling pathways control miR-143/143 expression.

1.3.13.1 Communication between ECs and VSMCs by miR-143/miR-145

Despite miR-143 and miR-145 expression being relatively SMC enriched, the expression of these miRNAs is detectable in ECs albeit at much lower levels. However, although low basal expression of a miRNA within a cell type suggests minimal regulation may occur, miRNAs can be upregulated within a cell by stress

and have a functional effect. The relevance of miR-143/145 expression in ECs was investigated in a recent study where it was shown that high shear stress results in a significant increase in miR-143/145 expression within ECs (Hergenreider et al., 2012). High shear stress is protective against the formation of atherosclerotic lesions, which most commonly form at areas of low shear stress such as bifurcations (Cunningham and Gotlieb, 2005). Laminar flow induces expression of KLF2, which was shown to directly bind to a putative KLF2 binding site in the miR-143/145 promoter region, activating transcription in human umbilical vein ECs (HUVECs) (Hergenreider et al., 2012). This resulted in an approximately 30-fold enrichment of miR-143 and miR-145 in extracellular exosomes, significantly greater than the 10-fold increase observed in the HUVECs. The authors went on to show that co-culture of KLF2-overexpressing HUVECs with VSMCs resulted in exosomal transfer to VSMCs resulting in increased expression of miR-143 and miR-145 in VSMCs and decreased expression of targets mRNA ELK-1 and KLF4 (Figure 1.5) (Hergenreider et al., 2012). Furthermore, injection of the miR-143/145 enriched exosomes into fat fed ApoE KO mice significantly reduced aortic atherosclerotic lesion area, showing that this 'miRNA transfer' can function *in vivo* (Hergenreider et al., 2012).

1.3.13.2 Alteration of the SRF cofactor expression by TGF- β and BMP4

Bone morphogenetic protein 4 (BMP4) is a major signalling molecule known to promote a contractile VSMC phenotype and has been shown to promote miR-143/145 transcription in pulmonary artery SMCs (Figure 1.5). This was shown to occur via stimulation of the nuclear translocation of SRF cofactor MRTF-A, thereby promoting the SRF-MRTF-A interaction with the CArG box and transcriptionally activating miR-143/145 (Davis-Dusenbery et al., 2011). Interestingly, another major regulator of VSMC phenotype, TGF- β , was shown to promote miR-143/145 transcription via activation of SRF cofactor myocardin in pulmonary and human coronary artery SMCs (Long and Miano, 2011). Furthermore, activation of miR-143/145 by TGF- β or BMP4 was essential for the downregulation of KLF4 by these signalling molecules (Long and Miano, 2011, Davis-Dusenbery et al., 2011).

Induction of myocardin expression and activation of miR-143/145 expression by TGF- β occurs through binding of SMAD2/3 and SMAD4 to SMAD-binding elements

(SBEs) in the myocardin promoter and activating transcription (Davis-Dusenbery et al., 2011). Activation of myocardin transcription and increased miR-143/145 expression has also been shown to occur through a p38 mitogen activated protein kinase (p38MAPK) dependent pathway (Long and Miano, 2011). TGF- β -induced SMAD signalling was also shown to directly activate miR-143/145 transcription by promoting SMAD3 and SMAD4 binding to a SBE in the miR-143/145 promoter (Figure 1.5) (Long and Miano, 2011). Significantly, both the SBE and CArG sequence were essential for TGF- β activation of miR-143/145 transcription, which promoted increased expression of contractile genes CNN1 and ACTA2, suggesting that miR-143/145 is an essential downstream mediator of TGF- β signalling (Long and Miano, 2011).

1.3.13.3 SRF-independent regulation of MiR-143/145

MiR-143/145 expression can also be regulated by SRF-independent mechanisms. It has been shown that Jagged-1 activation of Notch receptors leads to nuclear translocation of the Notch intracellular domain (ICD) and formation of a complex with transcription factor CBF1 (Figure 1.5) (Boucher et al., 2011). This occurred in concurrence with an increased expression of contractile genes including α -SMA and SM22 α , which could be inhibited by inhibition of miR-143 or miR-145 expression. Upon further investigation a CBF1 binding domain was shown to exist in the miR-145/145 promoter which could be activated upon binding of the Notch ICD/CBF1 complex (Boucher et al., 2011).

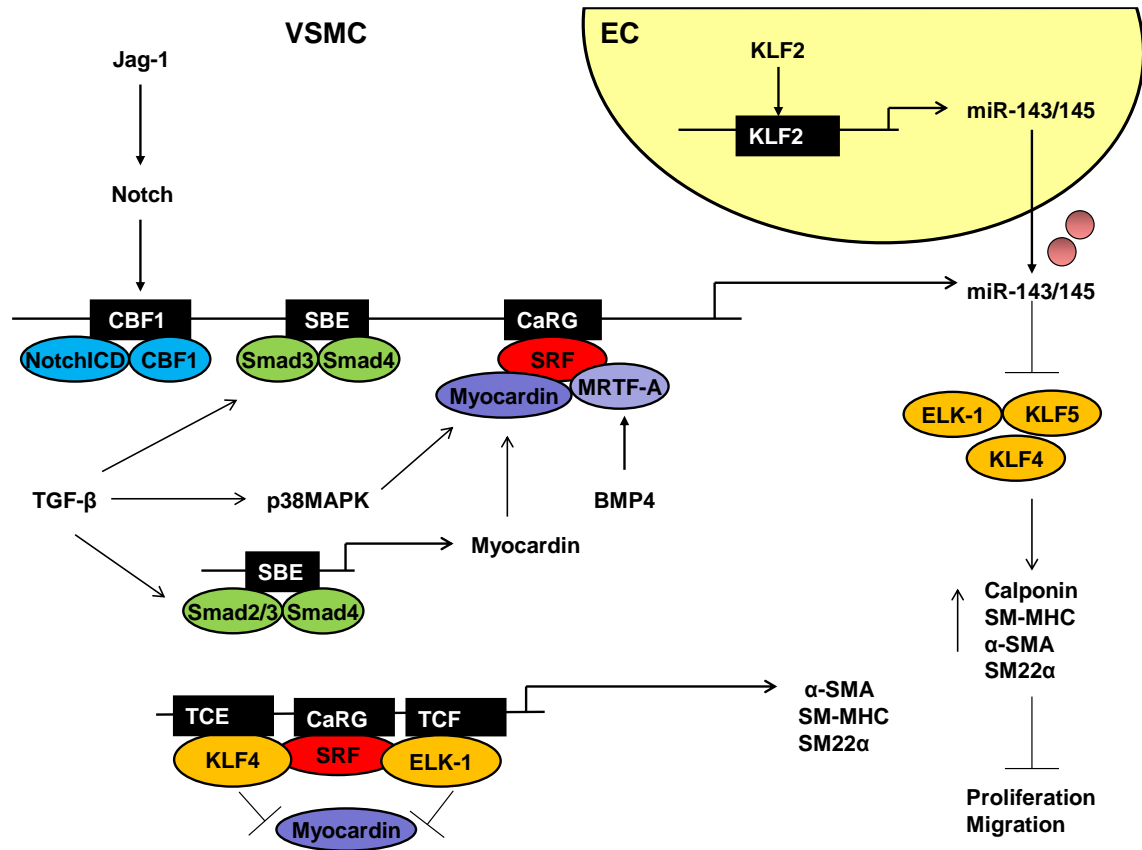


Figure 1.5. Overview of miR-143/145 transcription.

Jagged-1 (Jag-1) signalling promotes nuclear translocation of the Notch intracellular domain (Notch1CD) which forms a complex with CBF1 to activates miR-143/145 transcription via a CBF1 binding site. Transforming growth factor beta (TGF- β) promotes SMAD binding to SMAD binding elements (SBE) leading to transcriptional activation of miR-143/145 via the SBE in the miR-143/145 and myocardin promoter. TGF- β also promotes myocardin expression via the p38MAPK pathway. SRF in combination with its cofactor myocardin or MRTF-A promotes transcription of miR-143/145 via a CaRG box in the miR-143/145 regulatory region. The nuclear translocation of MRTF-A is stimulated by bone morphogenetic protein 4 (BMP4) resulting in increased SRF/MRTF-A binding and miR-143/145 transcription. A kruppel-like factor 2 (KLF2) binding site in the miR-143/145 promoter activates transcription of miR-143/145 in ECs which are transferred to VSMCs via exosomes. MiR-143 and miR-145 promote a contractile phenotype by negatively regulating the expression of targets involved in proliferation and migration including including ELK-1, KLF4 and KLF5. KLF4 and ELK-1 compete with myocardin at the SRF binding site to prevent myocardin/SRF interaction and reduce SRF mediated activation of contractile genes alpha smooth muscle actin (α -SMA), smooth muscle myosin heavy chain (SM-MHC) and smooth muscle 22 alpha (SM22 α).

1.3.14 Studies in miR-143 and miR-145 KO mice

In vitro and *in vivo* evidence that miR-143 and miR-145 regulate VSMC phenotype prompted several groups to further investigate the importance of these miRNA in the vasculature, by use of KO mice (Boettger et al., 2009, Elia et al., 2009, Xin et al., 2009, Quintavalle et al., 2010).

1.3.14.1 Abnormalities in the vessels of miR-143/145 KO mice

Mice that have had the entire genomic pre-miRNA sequence of both miR-143 and miR-145 removed (miR-143/145 KO) are reported to have abnormal vessels when compared to WT mice (Elia et al., 2009, Boettger et al., 2009, Xin et al., 2009). The arteries of miR-143/145 KO mice are thinner than those of WT mice with the femoral wall approximately half the thickness of WT mice and the aortic wall reduced by around a third (Elia et al., 2009, Boettger et al., 2009). This was found to be due to a reduction in VSMC size but not number (Boettger et al., 2009, Xin et al., 2009, Elia et al., 2009). Xin and colleagues dissected this further by producing individual miR-143 KO and miR-145 KO mice and showed that miR-145 KO but not miR-143 KO resulted in reduced vessel wall thickness (Xin et al., 2009). Electron microscopy studies revealed that miR-143/145 KO mice have reduced numbers of contractile and increased numbers of synthetic VSMCs within their vessel walls, with no change in proliferation or apoptosis rates (Boettger et al., 2009, Elia et al., 2009). It is believed that that the shift in the number of elongated contractile vs. epithelioid shaped synthetic VSMCs may be responsible for the overall reduction in VSMC size and thus vessel wall thickness (Boettger et al., 2009). Another study reported the presence of small groups of synthetic VSMCs within the intima region of the vessel walls, potentially from migration from the media (Elia et al., 2009). *In vitro* analysis of VSMCs isolated from miR-143/145 KO mice revealed these cells exhibit greater migration towards PDGF than cells isolated from WT mice (Elia et al., 2009).

Organised actin stress fibers are essential for SMC contraction and are a feature of a differentiated VSMC phenotype. Interestingly, miR-143/145 KO and miR-145 KO mice showed reduced numbers and disorganisation of actin stress fibers within their VSMCs both *in vivo* and *in vitro* indicating these miRNAs are important for the arrangement of the actin cytoskeleton (Xin et al., 2009). VSMCs of miR-143/145, miR-143 and miR-145 KO mice also had increased numbers of rough ER which were reported to be dilated, characteristics of synthetic SMCs (Elia et al., 2009, Xin et al., 2009, Boettger et al., 2009). It has been reported that a thick ECM surrounds the VSMCs in the aorta of miR-143/145 and miR-145 KO mice however other have reported areas of ECM degradation (Xin et al., 2009, Elia et al., 2009). The expression of VSMC marker genes including calponin, α -SMA and SM-MHC were decreased in the vessels of miR-143/145 KO

mice in some studies (Elia et al., 2009, Boettger et al., 2009) but this was not seen by others (Xin et al., 2009). Many miR-143 and miR-145 targets, including KLF4 and KLF5 are also upregulated in carotid arteries of miR-143/145 KO mice (Xin et al., 2009).

1.3.14.2 Vascular tone in miR-143/145 KO mice

MiR-143/145 KO and MiR-145 KO mice are reported to have reduced heart weight and left ventricular mass when compared to control mice (Xin et al., 2009, Boettger et al., 2009). The reduction in vessel wall thickness and actin stress fibers within the vessel walls of miR-143/145 KO and miR-145 KO mice prompted investigations into their blood pressure. MiR-143/145 KO and miR-145 KO mice were found to be hypotensive with significant reductions in mean arterial, systolic and diastolic blood pressure (Xin et al., 2009, Boettger et al., 2009). However, others reported no significant difference in basal systolic blood pressure in miR-143/145 KO mice (Elia et al., 2009). This phenomenon is not only due to reduced vascular tone as a result of the thin arterial walls but also due to a reduction in receptor-mediated vasoconstriction (Xin et al., 2009, Boettger et al., 2009). Boettger and colleagues investigated VSMC contraction in arterial rings isolated from miR-143/145 KO mice and showed that they display significantly blunted contractile responses to pressor agents Ang II and phenylephrine (Boettger et al., 2009). MiR-143/145 KO mice were also shown *in vivo* to have a blunted increase in systolic blood pressure in response to Ang II (Elia et al., 2009). This reduction in contractile response was found to be due, in part, to reduced calcium sensitivity of synthetic VSMCs within the miR-143/145 KO vessels and also reduced receptor mediated contraction by VSMCs (Boettger et al., 2009). This was further dissected *in vivo* where it was shown that miR-143/145 KO mice have increased local Ang II signalling within their VSMCs which may result in VSMCs desensitisation and thus blunted contractile response to Ang II. ACE, the enzyme which converts Ang I to Ang II was upregulated in the VSMCs of miR-143/145 KO mice and is a target of miR-145 (Boettger et al., 2009). Inhibition of ACE or the Ang type I receptor was capable of partially rescuing the blunted contractile responses to Ang II, phenylephrine and calcium in miR-143/145 KO mice (Boettger et al., 2009). This was thought to occur in part due to decreased Ang II signalling but also the normalisation of expression of many hundreds of transcripts that differed between WT and miR-143/145 KO mice,

many of which are known to be involved in VSMC contraction (Boettger et al., 2009).

1.3.14.3 Neointimal lesions in aged miR-143/145 KO mice

Boettger and colleagues went on to investigate the long term consequence of miR-143/145 KO and reported the presence of neointimal lesions in the femoral arteries of 18 month miR-143/145 KO mice (Boettger et al., 2009). The composition of these lesions varied from accumulation of VSMCs in the intima at earlier time points, to the addition of macrophages and collagen I in more advanced lesions, however no accumulation of lipids was observed (Boettger et al., 2009). These results suggest that the increase in synthetic VSMCs and global dysregulation of targets brought about by loss of miR-143/145 promotes a signalling process that over time leads to neointimal formation.

1.3.14.4 Podosome formation in miR-143/145 KO mice

It has been reported that the aortas of miR-143/145 KO mice contain a significant presence of podosomes (Quintavalle et al., 2010). Podosomes are actin rich membrane structures which are found in migrating cells, including VSMCs, and are involved in cell adhesion and ECM degradation (Gimona et al., 2003, Linder and Aepfelbacher, 2003). Podosome formation was shown to be under the control of PDGF which stimulates a Src tyrosine kinase-mediated decrease in miR-143/145 expression that promotes podosome formation (Quintavalle et al., 2010). This was further investigated and it was shown that Src inhibition of the p53 tumour suppressor protein was essential for miR-143/145 inhibition and podosome formation (Quintavalle et al., 2010). Response elements for p53 repressor were discovered in the miR-143/145 promoter which allowed p53 regulation of miR-143/145, with inhibition of p53 shown to reduce miR-143/145 transcription (Quintavalle et al., 2010). Protein kinase C ϵ (PKC- ϵ) and PDGF receptor alpha were shown to be targets of miR-143 and FSCN1 a target of miR-145 and these targets were upregulated in miR-143/145 KO VSMCs. Knockdown of PKC- ϵ or FSCN1 *in vitro* in miR-143/145 KO VSMCs reduced podosome formation and migration indicating that repression of these targets by miR-143 and miR-145 may reduce the formation of podosomes (Quintavalle et al., 2010).

1.3.14.5 Reduced neointimal formation in miR-143/145 KO mice

Interestingly, neointimal formation in response to coronary artery ligation was significantly reduced by 60% in miR-143 KO mice and almost ablated in miR-145 and miR-143/145 KO mice (Xin et al., 2009). Furthermore, carotid artery ligation resulted in premature death in 50% of miR-143/145 KO and miR-145 KO mice, which displayed severe neurological abnormalities, including loss of coordination, seizures and circling behaviour (Xin et al., 2009). The authors postulated that this may have been due to failure of the circle of willis to supply the left hemisphere of the brain following carotid artery ligation, resulting in ischemia and cell death in the left hemisphere (Xin et al., 2009). The reduced neointimal formation in miR-143 and miR-145 KO mice is in contrast to several studies that have reported that restoration of miR-145 levels in WT models of neointimal formation resulted in reduced neointimal formation (Elia et al., 2009, Cheng et al., 2009). Furthermore overexpression studies revealed increased expression of contractile VSMC marker genes including α -SMA and SM-MHC (Cordes et al., 2009). The differential effects seen following overexpression and genetic KO may be due to developmental differences or differences in the ability for VSMCs to change phenotype. Both overexpression and KO studies indicate that miR-143 and miR-145 are important for VSMC fate.

1.3.15 Potential role of miR-143 and miR-145 in stenting

The results of the studies discussed above have suggested that miR-143 and miR-145 are important for the development and maintenance of a contractile VSMC phenotype. The expression of these miRNA promotes contractile and reduces synthetic gene expression and is capable of reducing neointimal formation in animal models. However, genetic loss of these miRNA reduces neointimal formation which raises uncertainties about the exact role of these miRNA in VSMC phenotype. MiR-143/145 transcription is under the control of several important regulators of VSMC phenotype including TGF- β , BMP4 and SRF-myocardin/MRTF which utilise these miRNA as downstream effectors of gene expression. MiR-143 and miR-145 are the most abundantly expressed miRNA in VSMCs. The low expression of these miRNA in ECs and preferential transfer of these miRNAs from ECs to VSMCs following shear stress suggests that these miRNA may act as relatively specific regulators of VSMCs. Therefore, we propose

that miR-143 and miR-145 are promising candidate miRNA that could have therapeutic benefit in preventing in-stent restenosis.

1.4 Aims

In-stent restenosis is a major clinical problem that is characterised by VSMC proliferation and migration from the media to the intima resulting in neointimal formation. MiR-143 and miR-145 are important regulators of VSMC contractile phenotype which can reduce neointimal formation in animal models. Therefore it is the aim of this thesis to investigate the role of miR-143 and miR-145 in stent-induced vascular injury.

The specific aims of the study are:

1. To investigate the role that miR-143/145 play in human VSMC and EC biology.
2. To reproduce a relevant small animal model of stenting.
3. To compare the response of miR-143 and miR-145 KO and WT mice to a model of in-stent stenosis.
4. To determine the effect of pharmacologically modulating miR-143/145 levels on stenosis in WT mice.

2 Materials and Methods

2.1 Materials

All chemicals unless otherwise stated were purchased from Sigma-Aldrich (Poole, UK). All cell culture reagents were purchased from Gibco (Paisley, UK) unless otherwise stated. Magnesium- and calcium-free Dulbecco's phosphate-buffered saline (PBS) was used for all cell culture experiments.

2.2 General cell culture techniques

Cell culture was performed in class II biological safety vertical laminar flow cabinets under sterile conditions. All cells were cultured as a monolayer in 25 cm², 75 cm² or 150 cm² vented-cap cell culture flasks (Corning, Poole, UK) and maintained in incubators at 37°C in 5% CO₂. Cell culture medium was replenished on cells every 2-3 days and cells were passaged when approximately 80% confluent to prevent overgrowth.

To passage cells media was removed and cells were washed twice with PBS before incubation with 0.05% trypsin 0.02% (w/v) ethylenediamine tetra-acetic acid (trypsin-EDTA) solution at 37°C for 5 minutes (min). When the majority of cells had detached from the bottom of the flask, an equal volume of the appropriate complete cell culture medium was added to neutralise the reaction. Cells were pelleted by centrifugation at 1500 x g for 5 min before being resuspended in medium and passaged. Cells were counted using a haemocytometer prior to plating for experiments where a known seeding density was required.

2.3 Production of miRNA expressing adenovirus

2.3.1 Cloning of pre-miRNA sequences into pAdEasy-1

Prior to the commencement of this PhD, the full human pre-miR-143 and pre-miR-145 sequences were cloned in house into the adenovirus serotype 5 (Ad5) based vector pAdEasy-1 (Agilent Technologies Ltd, Cambridge, UK). Double stranded DNA constructs of hsa-pre-miR-143 and hsa-pre-miR-145 were designed in house and produced by GeneArt® (Invitrogen, Paisley, UK). To ensure expression of the pre-miRNA a Kozak sequence (ACCATGG) was included at the 5' end immediately prior to the start of each pre-miRNA. A stop codon (TAG) and

poly(A) tail sequence (TTTTTT) were included at the 3' end of the constructs to ensure miRNA production and nuclear export following transcription. The full cloned sequence of hsa-pre-miR-143 and hsa-pre-miR-145 including start/stop codons and poly(A) tail are shown below for the 5' strand, the mature miRNA sequence is underlined.

hsa-pre-miR-143

5'ACCATGGGCGCAGCGCCCTGTCTCCCAGCCTGAGGTGCAGTGCTGCATCTCTGGTCA
GTTGGGAGTCTGAGATGAAGCACTGTAGCTCAGGAAGAGAGAAGTTGTTCTGCAGCTAG
TTTTTT 3'

hsa-pre-miR-145

5'ACCATGGCACCTTGTCCTCACGGTCCAGTTTTCCAGGAATCCCTTAGATGCTAAGAT
GGGATTCTGGAAATACTGTTCTTGAGGTCATGGTTTAGTTTTTT 3'

Pre-miRNAs were initially cloned into the shuttle vector pShuttle-CMV, which contains right and left arms which are homologous to the pAdEasy-1. The pShuttle-CMV vector containing pre-miRNA was then cloned into the pAd-Easy-1 vector by homologous recombination in accordance with the AdEasy™ Adenoviral Vector System (Agilent Technologies Ltd). The pAdEasy-1 vector is deleted of the E1 and E3 regions of the Ad5 genome, which render it replication incompetent. Transcription of the pre-miRNA was driven by the cytomegalovirus (CMV) promoter. An overview of the cloning system is shown below in Figure 2.1.

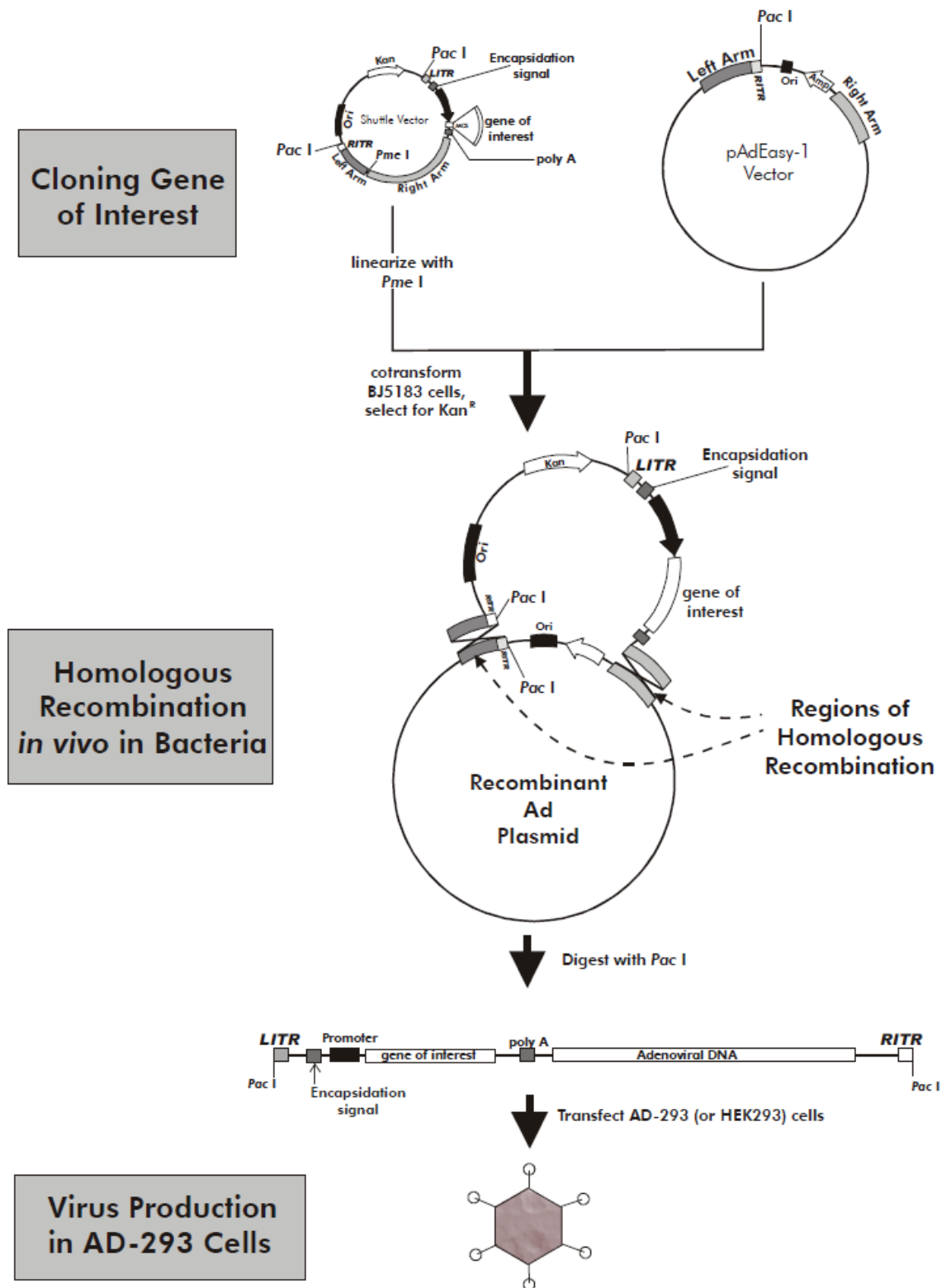


Figure 2.1. Overview of pre-miRNA cloning procedure.

The miRNA constructs were first cloned into the pShuttle-CMV vector which contains right and left arms which are homologous to the right and left arms of the larger pAdEasy-1 plasmid. pShuttle-CMV was linearized by restriction digest with *Pme* I and transformed into BJ5183-AD-1 bacteria cells, which are pre-transformed with pAdEasy-1. This allows recombination to occur between the arms of homology. Recombinant plasmids were identified by kanamycin resistance followed by restriction digest with *Pac* I. Linearized recombinants were transfected into Ad-293 or HEK-293 cells to prepare a primary viral stock. Adapted from the 'AdEasy™ Adenoviral Vector System' instruction manual (Agilent technologies Ltd).

2.3.2 Production of adenovirus stocks

All Ad production from this stage forward was carried out by me. From here on in the cloned viruses will be referred to as AdmiR-143 and AdmiR-145, representing the pAdEasy-1 vector expressing hsa-pre-miR-143 and hsa-pre-miR-145, respectively.

Human Embryonic Kidney (HEK) 293 cells express the E1 region of the Ad5 genome that is absent in pAdEasy-1. Transduction of HEK 293 cells with E1 deficient Ads allows viral replication to occur resulting in propagation of the virus. Briefly, 50 µl of crude AdmiR-143 or AdmiR-145 was added to one bottle of normal growth medium [minimum essential medium (MEM) supplemented with 10% (v/v) foetal calf serum (FCS), 100 IU/ml penicillin, 100 µg/ml streptomycin, 2 mM L-glutamine and 111 µg/ml sodium pyruvate]. Ad-containing medium (22-25 ml) was added to 70-80% confluent HEK 293 cells cultured in 150 cm² vented cap cell culture flasks and maintained at 37°C in 5% (v/v) CO₂. Media was refreshed every 3 days and cells were left until a cytopathic effect became apparent (cells round up and begin to detach from bottom of flask). Media was collected and centrifuged at 2000 x g for 10 min. Cell pellets were resuspended in 5 ml of PBS. An equal volume of Arklone P (trichlorofluoroethane) was added to cells to extract the virus and mixed thoroughly by inverting the several times prior to centrifugation at 3000 x g for 10 min. The aqueous top layer containing crude Ad was removed and stored at -80°C until purification.

2.3.3 Adenovirus purification

Ad purification was performed using caesium chloride (CsCl) gradients. Briefly, 2.5 ml of both 1.40 g/ml and 1.25 g/ml CsCl were layered in a sterilised ultra-clear centrifuge tube (Beckman Coulter Ltd, Buckinghamshire, UK). The crude Ad was gently dripped on top of the gradient and the tube filled with PBS. Tubes were centrifuged using the Beckman Optima L-80 ultracentrifuge and Beckman SW40Ti swing out bucket rotor at 25,000 rpm for 1.5 hour (h) at 4°C. A white band containing the Ad was visualised between the two CsCl layers. A 21 gauge needle was used to pierce the ultra-centrifuge tube directly below the band and the Ad was isolated by gently pulling back on the syringe. A second CsCl gradient

was created by adding the Ad on top of 5 ml of 1.34 g/ml CsCl and centrifuging at 25,000 rpm for 18 h at 4°C. The Ad band was removed as described above.

Dialysis of Ads was performed using Pierce Slide-A-Lyzer Dialysis Cassettes with a molecular weight cut off of 10,000 Da (Thermo Scientific, Leicestershire, UK). Briefly, Ads were added to hydrated dialysis cassettes using a 21 gauge needle and incubated in 1 X Tris-EDTA dialysis buffer [10X stock contains: 10 mM Tris-HCL and 1 mM EDTA, pH 8] for 2 h. Dialysis buffer was then replaced and supplemented with 10% (v/v) glycerol and dialysis was continued overnight. Purified Ad was removed from dialysis cassettes, aliquoted and stored -80°C.

2.3.4 Virus titration by end-point dilution assay

The plaque forming unit (PFU) titre of AdmiR-143 and AdmiR-145 was determined by end-point dilution assay. Briefly, HEK 293 cells were seeded in 96 well cell culture plates and grown to 50-60% confluence. Purified Ad stocks were serially diluted in normal growth medium to the following dilutions: 1×10^{-4} , 1×10^{-6} , 1×10^{-7} , 1×10^{-8} , 1×10^{-9} , 1×10^{-10} and 1×10^{-11} . Media was refreshed on the bottom row of cells with 100 µl of virus-free media added to each well to form a row of 10 control wells. Media from the remaining wells was replaced with the Ad dilutions so that each dilution formed one row of the titre plate. The most concentrated virus (1×10^{-4}) formed the top row and the most dilute virus (1×10^{-11}) formed the row directly above the control row. Cells were maintained at 37°C in 5% CO₂. Media was replaced after 18-24 h and then every second day until the end of the assay. At day 8 titre plates were analysed under a 10X microscope for a cytopathic effect and positive wells containing viral plaques (holes in the cell layer surrounded by cells which are 'rounded up') were noted. PFU titre was determined by the following calculation (Lowenstein, 1996):

Proportionate Distance= (% positive wells above 50%- 50%) / (% positive wells above 50% - % positive wells below 50%)

Log ID₅₀ (infectivity dose) = log dilution above 50% + (proportionate distance X dilution factor) = -X

$$ID_{50} = 10^{-X}$$

$$TCID_{50} \text{ (Tissue culture infectivity dose 50)} = 1/10^{-X}$$

$$TCID_{50}/100 \mu\text{l} = 10^X$$

$$TCID_{50}/\text{ml} = 10^X \times \text{dilution factor [10]}$$

$$1 \text{ TCID}_{50} = 0.7 \text{ PFU}$$

$$\text{PFU}/\text{ml} = \text{TCID}_{50}/\text{ml} \times 0.7$$

In order to ensure no replication competent Ad was contaminating the AdmiR-143 and AdmiR-145 stocks the end-point dilution assay was also carried out in HeLa cells. HeLa cells are an immortalised cell line derived from human cervical cancer cells which do not contain regions of the Ad5 genome, they are therefore non-permissive to viral replication using replication-incompetent Ads. If no cytopathic effect was found at the end of the end point dilution assay in HeLa cells it was assumed that the Ads were essentially replication incompetent.

2.3.5 Viral particle titre

The viral particle (VP) titre of AdmiR-143 and AdmiR-145 was calculated using the MicroBCA Protein Assay Kit (Thermo Scientific). Briefly, albumin standards from 0.5 µg/ml to 200 µg/ml were prepared in accordance with the manufacturer's instructions. Viral stocks were diluted 1:30, 1:50 and 1:150 in PBS and standards and samples were added in duplicate to a clear, flat-bottomed 96-well plate. 150 µl of BCA working reagent was added to the standards and samples and the plate was incubated for 2 h at 37°C. Absorbance was read at 570 nm using the Wallac VICTOR2 plate reader (Wallac, Turku, Finland). Background absorbance was subtracted from the samples and standards and the total amount of protein contained within each virus was

calculated from the standard curve. VP titre was determined using the formula described by Von Seggern and colleagues (Von Seggern et al., 1998) whereby 1 µg of protein is equal to 1×10^9 VP.

2.4 Primary cell culture

Excess human saphenous vein from patients undergoing CABG procedures was obtained with ethical approval and patient consent by the surgical team at the Golden Jubilee Hospital Clydebank and stored in sterile saline for collection. Non-varicose portions of saphenous vein from patients undergoing varicose vein removal were isolated by the surgical team at New Stobhill Hospital Glasgow and stored in sterile saline. All primary cell isolations were performed in class II biological safety cabinets under sterile conditions.

2.4.1 Isolation of primary vascular endothelial cells from the human saphenous vein

Primary human saphenous vein endothelial cells (HSV ECs) were isolated on the day of surgery by collagenase digestion, based on the method previously described by Jaffe and colleagues (Jaffe et al., 1973). Briefly, the lumen was flushed with wash medium [Dulbecco's Modified Eagle's Medium (DMEM), supplemented with 100 IU/ml penicillin, 100 µg/ml streptomycin and 2 mM L-glutamine]. The lumen was filled with 2 µg/ml collagenase solution diluted in wash medium and incubated at 37°C in 5% CO₂ for 15 min. The lumen was then flushed with wash medium to obtain HSV ECs in suspension. This process was repeated with collagenase digestion time reduced to 10 min. The wash medium/HSV EC suspension was centrifuged at 2000 x g for 15 min and pelleted HSV ECs were resuspended in EC growth medium [Large Vessel Endothelial Basal Cell Medium (TCS Cellworks Ltd, Bucks, UK), supplemented with 20% (v/v) FCS, 100 IU/ml penicillin, 100 µg/ml streptomycin and 2 mM L-glutamine]. Cells were plated in 25 cm² vented cap cell culture flasks and maintained in a 37°C, 5% CO₂ incubator for 24 h to ensure cell adhesion before media was refreshed.

2.4.2 Isolation of primary vascular smooth muscle cells from the human saphenous vein

Primary human saphenous vein smooth muscle cells (HSV SMCs) were isolated within 48 h of surgery by an explant technique originally described by Southgate and Newby (Southgate and Newby, 1990). Briefly, the lumen was flushed with wash medium before the vein was cut longitudinally and the 4 corners pinned out with the lumen en face. HSV ECs cells were removed by gently running a rubber policeman over the lumen surface. Vessels were scored with a scalpel blade and the SMC layer peeled back from the adventitia with forceps. The SMC tissue was cut into small pieces (~1 mm²) using the McIlwain tissue chopper. SMC tissue was washed twice with wash medium and once in SMC growth medium [Smooth Muscle Cell Growth Medium 2 (Contains: 0.5 ng/ml epidermal growth factor, 2 ng/ml basic fibroblast growth factor and 5 µg/ml insulin) (PromoCell, Heidelberg, Germany) supplemented with 15% FCS, 100 IU/ml penicillin and 100 µg/ml streptomycin]. SMC tissue was plated in 25 cm² vented cap cell culture flasks and maintained in a 37°C 5% CO₂ incubator. All excess SMC growth medium was removed to allow HSV SMCs to adhere to the flask before SMC growth medium was replaced 24 h later.

2.5 Adenoviral transduction of cultured cells

2.5.1.1 HeLa cells

HeLa cells were plated in 6 well cell culture plates at a seeding density of 3X10⁵ cells/well in normal growth medium and incubated overnight at 37°C in 5% CO₂. AdmiR-143 and AdmiR-145 were diluted in normal growth medium to a final PFU of 10, 50 or 100 PFU/Cell. RAd60, a replication incompetent Ad5 based vector, was used as a control Ad. RAd60 contains no transgene and is thus thought of as an ‘empty’ vector (George et al., 2011). Cells were incubated with AdmiR-143, AdmiR-145, RAd60 or medium only (control) for 24 h at 37°C at 5% CO₂ before medium was replaced with virus-free normal growth medium and incubated for a further 24 h. Cells were lysed for RNA extraction and qRT-PCR analysis as described in sections 2.7 - 2.9.

2.5.1.2 Human primary cells

HSV ECs and HSV SMCs were seeded at 3×10^5 cells/well in 6 well plates in the appropriate growth medium and incubated overnight at 37°C in 5% CO₂. Cells were then incubated for 24 h in growth medium alone or containing AdmiR-143 or AdmiR-145 diluted to a final VP of 5000 - 50,000 VP/Cell. Ad5CMVlacZ, an Ad5 vector made in-house using the pAdEasy-1 system and containing the lacZ transgene, was used as a control. The following day medium was replaced with 0.1% (v/v) FCS EC growth medium or 0.1%, 2% or 15% (v/v) SMC growth medium and cells were incubated for a further 24 h (HSV EC) or 48h (HSV SMC). Cells were then used for migration assays, lysed for RNA extraction and qRT-PCR analysis or fixed and stained for X-gal expression.

2.6 Transfections with premiRs and antimiRs

Modulation of endogenous miR-143 and miR-145 expression in human primary cells was achieved by use of miRNA mimics and AntimiRs. Ambion Pre-miR miRNA precursor molecules (Life Technologies, Paisley, UK) premiR-143, premiR-145, premiR-negative control (will be referred to as premiR-scr) are double-stranded RNA molecules which mimic the mature form of the miRNA. These premiRs are chemically modified to ensure the correct strand is incorporated into the RISC complex and are used to increase mature miRNA expression levels within cells. AntimiR-143, antimiR-145 and antimiR-ctl were provided by MiRagen Therapeutics (Colorado, USA). AntimiRs are 16 nt in length with phosphorothioate backbones and consist of a mixture of LNA and DNA bases complimentary to the 5' end of mature miR-143 (antimiR-143) or miR-145 (antimiR-145) respectively. An antimiR which was targeted against a *C. elegans* specific miRNA (antimiR-ctl) was used as a control. AntimiRs bind tightly to mature miRNA to prevent the miRNA from binding to its mRNA targets. AntimiRs can therefore be used to investigate effects of reducing endogenous miRNA expression.

HSV EC and HSV SMC transfection with premiRs (premiR-143, premiR-145 and premiR-scr) or antimiRs (antimiR-143, antimiR-145 and antimiR-ctl) was performed using siPORT NeoFX Transfection Agent (Life Technologies) in accordance with the manufacturer's instructions. Briefly, Siport NeoFX

Transfection Agent was diluted in Opti-MEM® reduced serum medium (Invitrogen) at a ratio of 1 µl to 24 µl for 24 well plates or 5 µl to 95 µl for 6 well plates and incubated at room temperature (RT) for 10 min. PremiRs and anti-miRs were diluted in a total volume of 25 µl (24 well plate) or 100 µl (6 well plate) Opti-MEM® medium to a final concentration of 10 nM, 25 nM or 50 nM. Siport NeoFX/OptiMEM® and diluted premiRs/anti-miRs were combined and incubated for a further 10 min to allow transfection complexes to form before being dispensed into cell culture plates. HSV ECs or HSV SMCs were seeded in the appropriate growth medium at density of 4×10^4 or 3×10^5 cells/well for 24 well and 6 well plates, respectively. The final volumes were 500 µl for 24 well plates and 2.5 ml for 6 well plates. A 'Mock' control containing cells incubated with Siport NeoFX/Opti-MEM® and medium alone, and a control of cells incubated with Opti-MEM® and medium alone was included in each experiment. Cells were incubated with transfection complexes overnight. The following day media was removed and cells were incubated in 0.1% (v/v) FCS EC or SMC medium for a further 24 h (HSV EC) or 48 h (HSV SMC) to achieve cell quiescence. Cells were then lysed for RNA analysis or used in migration or proliferation experiments.

Transfection efficiency was initially investigated in HSV SMCs using an AntimiR labelled with the fluorophore Cy3 (AntimiR-Cy3). Cy3 acts as a fluorescent reporter allowing visualisation of cells which have been transfected with the AntimiR. Transfections were carried out in 8 well chamber slides following the instructions for 24 well plates described above. Cells were washed in PBS and fixed in 2% (w/v) paraformaldehyde (PFA) for 10 min before mounted with coverslips using Prolong Gold Antifade Reagent with DAPI (Life Technologies). Slides were kept in the dark overnight and photographed at 40X using Olympus IX70 fluorescent microscope.

2.7 Extraction of RNA from cells and tissues

Isolation of cells for RNA extraction was performed as described. Culture medium was removed and cells washed twice with PBS prior to the addition of 700 µl QIAzol® Lysis Reagent (Qiagen, Crawley, UK) to each well. Cells were homogenised by pipetting up and down and transferred to 1.5 ml microcentrifuge tubes for storage at -80°C until processing.

Tissues were snap frozen in liquid nitrogen at sacrifice and stored at -80°C until processing. Tissue disruption was achieved as follows. A stainless-steel bead (5 mm) and 700 µl QIAzol® were added to each sample and tissue disrupted using the TissueLyser System (Qiagen) at 25 Hz for 1-2 min until full tissue disruption occurred.

Total RNA including miRNA was extracted from isolated cells and tissues using the miRNeasy Mini Kit (Qiagen) in accordance with the manufacturer's instructions. Briefly, the cell/tissue homogenate was mixed thoroughly with 140 µl chloroform and incubated for 3 min at RT. Samples were centrifuged at 12,000 x g for 15 min at 4°C to separate the sample into 3 distinct layers, a top aqueous phase containing the RNA and miRNA, an interphase containing DNA and proteins and an organic phase containing proteins. The aqueous phase was collected, added to 1.5 volumes of 100% ethanol and mixed thoroughly. Samples (700 µl) were transferred into RNeasy mini spin columns and centrifuged at 8000 x g for 15 seconds (sec) at RT to allow binding of RNA to the spin column membrane, flow-through was discarded. Buffer RWT (350 µl) was added spin columns and centrifuged at 8000 x g for 15 sec.

At this stage on-column DNase digestion was performed in order to remove contaminating genomic DNA from the samples. Briefly, DNase was prepared by according to the RNase-Free DNase Set (Qiagen) and diluted 1:8 (v/v) in buffer RDD. The DNase/RDD mixture (80 µl) was added to the spin columns and incubated for 15 min at RT.

Spin columns were then washed with the following: 350 µl buffer RWT, 8000 x g for 15 sec; 500µl buffer RPE, 8000 x g for 15 sec and 500µl buffer RPE, 8000 x g for 2 min. Spin columns were placed in a fresh collection tubes and centrifuged at 12,000 x g for 1 min to remove any remaining buffer RPE contaminants. Spin columns were transferred into 1.5 ml microcentrifuge tubes and 30-50 µl RNase-free H₂O added to each tube. RNA was eluted by centrifugation at 8000 x g for 1 min. The eluted RNA was collected and re-eluted through the spin column to increase RNA yield.

The quantity of RNA in each sample was determined using the NanoDrop 1000 Spectrophotometer (Thermo Scientific). This method determines the

concentration of nucleic acid in sample by determining its absorbance at 260 nm. A 260 nm / 280 nm ratio of ~2.0 is generally considered to denote RNA free from protein or phenol contaminants which absorb nearer 280 nm.

2.8 Reverse transcription polymerase chain reaction (RT-PCR)

Reverse transcription complementary DNA (cDNA) synthesis of miRNAs was performed using the Taqman® MicroRNA Reverse Transcription Kit (Applied Biosystems, Warrington, UK) according to the manufacturer's instructions. Reactions contained 2.5 µl of 2 ng/µl sample RNA, 0.25 mM of each dNTP, 3.33 U/µl Multiscribe reverse transcriptase, 1X reverse transcriptase buffer, 0.25 U/µl RNase inhibitor and 2.08 µl RNase-free water. Reaction mixtures also contain 1X vol. of Taqman® miRNA Reverse Transcription Primers (Applied Biosystems) for the mature sequence of the miRNA of interest, shown in Table 2.1. Reverse transcription of an endogenous control (Table 2.1) was also performed for each sample in order to normalise changes in miRNA expression.

Table 2.1. MiRNA reverse transcription primers.

miRNA/Control	Sequence	Species
hsa-miR-143 3p	5' UGAGAUGAAGCACUGUAGCUC 3'	Human/mouse
hsa-miR-145 5p	5' GUCCAGUUUCCAGGAAUCCCU 3'	Human/mouse
RNU48	5'GATGACCCCAGGTA ACTCTGAGTGTGTCGCTGATGCCA TCA CCGCAGCGCTCTGACC 3'	Human
U6	5'GTGCTCGCTTCGGCAGCACATATACTAAAATTGGAACG ATACAGAGAAGATTAGCATGGCCCCTGCGCAAGGATGA CACGCAA TTCGTGAAGCGTTCCATATTTT 3'	Mouse

Synthesis of cDNA was performed by incubating at 16°C for 30 min to facilitate primer binding, 42°C for 30 min for reverse transcription to take place and finally 85°C for 5 min to inactivate the reverse transcriptase enzyme.

Reverse transcription of RNA was performed using Taqman® Reverse Transcription Reagents (Applied Biosystems). Each reaction contained 200-1000 ng RNA, (concentration consistent within experiments) and the following reagents: 1X reverse transcriptase buffer, 5.5 mM MgCl₂, 0.5 mM of each dNTP, 2.5 µM random hexamers, 0.4 U/µl RNase inhibitor and 1.25 U/µl Multiscribe reverse transcriptase. RNase-free water was added to give a final reaction volume of 20 µl per well.

Synthesis of cDNA for RNA samples was performed by incubating at 25°C for 10 min to allow annealing of primers, 48°C for 30 min for reverse transcription and 95°C for 5 min to inactivate reverse transcriptase.

A non-template control, where RNA was replaced with H₂O was included in each experiment. Samples were then stored at 4°C for short term or -20°C for longer term storage.

2.9 Taqman quantitative real-time PCR (qRT-PCR)

QRT-PCR is a method of quantifying the abundance of an RNA within a sample. Taqman® qRT-PCR Assays are 5' labelled with a fluorescent reporter dye e.g. FAM and 3' labelled with a quencher dye that inhibits the 5' dye fluorescence by fluorescence resonance energy transfer (FRET). When the probe anneals to its target it is cleaved by Taq DNA polymerase and the fluorescent reporter signal is emitted proportional to the amount of RNA product present within each cycle and can be measured and quantified. The number of cycles a product takes to reach a fixed threshold is known as the threshold cycle (C_T), with lower C_T values indicating higher expression and higher C_T values indicating lower expression of the product respectively. A housekeeping gene, which is stably expressed, is used as an endogenous control to allow corrections due to RNA concentration to be made. C_T values were normalised to the appropriate endogenous control and fold changes calculated by the $2^{-\Delta\Delta C_T}$ method (Schmittgen and Livak, 2008).

MiRNA qRT-PCR was performed using Taqman® miRNA Assay RT-PCR Probes and Taqman® Universal Mastermix II (Applied Biosystems) in accordance with the manufacturer's instructions. Briefly, mastermixes were set up to contain 1X (v/v) Taqman® Mastermix, 1X (v/v) Taqman® miRNA Assay of interest and H₂O

to a total volume of 9.33 μl per sample. CDNA was pipetted in duplex into a 384 well plate 0.67 μl per well and the mastermix added to each well to give a total reaction volume of 10 μl . Human RNU48 or mouse U6 were used as an endogenous control.

QRT-PCR for RNA samples was performed using Taqman® Gene Expression Assays (Applied Biosystems) and Taqman® Universal Mastermix II in accordance with the manufacturer's instructions. Mastermixes contained 1X (v/v) Taqman® Mastermix, 1X (v/v) Taqman® gene expression probe and H₂O to a total volume of 8.5 μl were added to a 384 well plate. CDNA was added in duplex to the 384 well plate (1.5 μl /well) to give a total reaction volume of 10 μl . The endogenous control human 18s or mouse GAPDH was probed for in each sample in order to normalise changes in gene expression.

MiRNA and RNA expression was measured using the ABI Prism Applied Biosystems 7900HT sequence detection system. Cycling conditions for miRNA and RNA qRT-PCR where: denaturing at 95°C for 10 min, followed by 40 cycles of denaturing at 95°C for 15 sec and primer and probe binding and primer extension at 60°C for 60 sec.

2.10 X-gal staining

Ad5CMVlacZ expresses a lacZ transgene which encodes β -galactosidase (β -gal), an enzyme which hydrolyses β -galactoside bonds within its substrates to yield monosaccharides. X-gal (5-bromo-4-chloro-3-indolyl- β -D-galactopyranoside) is cleaved by β -gal to form galactose and 5-bromo-4-chloro-3-hydroxyindole, which dimerises and is oxidised into 5,5'-dibromo-4,4'-dichloro-indigo, which is seen by its intense blue colour.

HSV SMCs were incubated with Ads as described in section 2.5.1.2. After 24 h in Ad containing medium cells were incubated in 0.1%, 2% or 15% (v/v) FCS SMC growth medium for a further 48 h. Cells were washed twice in PBS and fixed for 10 min in 2% PFA and washed a further 2 times in PBS. X-gal stain [100 mM sodium phosphate, pH 7.3, 1.3 mM magnesium chloride, 3 mM potassium ferricyanide, 3 mM potassium ferrocyanide, 1 mg/ml X-gal] was applied onto fixed cells and incubated at 37°C overnight. Cells were imaged the following day

using a Nikon Eclipse TS1000 microscope and QICAM Fast1394 camera (QImaging, Maidenhead, UK) and the percentage of cells expressing X-gal was determined by cell counting.

2.11 Northern blotting

Northern blotting was performed to probe for mature miR-143 and miR-145. All solutions used in this process were made using dH₂O which had been treated with 0.1% diethylpyrocarbonate (DEPC), which inactivates RNase enzymes, for 24 h before autoclaving for 30 min/L to remove traces of DEPC. All equipment and surfaces used were treated with RNaseZap® (Life Technologies) to inhibit RNase enzymes. Briefly, 3-5 µg of RNA was mixed with RNA sample loading buffer (without ethidium bromide) (Sigma) and denatured at 95°C for 5 min along with RNA Marker Low Easy (Abnova, Heidelberg, Germany) then placed on ice. RNA samples were loaded into Novex® 15% TBE-Urea gels (Invitrogen) and ran at 150 V in 1X Tris-EDTA until the dye front reached the bottom of the gel. Gels were stained in ethidium bromide in Tris-EDTA for 5 min and imaged under ultraviolet light using the Molecular Imager Chemidoc XRS+ System to visualise RNA bands. Gels were transferred onto Amersham Hybond-NX Membranes (GE Life sciences, Buckinghamshire, UK) by blotting at 20 V for 1.5 h using the Trans-Blot Semi-Dry Transfer System (Biorad, Hertfordshire, UK). Gels were re-imaged under UV light to ensure RNA transfer to the membranes had been successful.

Membranes were transferred to N-Ethyl-N'-(3-dimethylaminopropyl)carbodiimide hydrochloride (EDC) cross-linking solution [2 mM EDC, 1% (v/v) 1-Methylimidazole] in order to crosslink RNA molecules to the nylon membrane. Cross-linking was carried out for 1 h at 60°C before membranes were washed twice in DEPC H₂O.

Membranes were pre-hybridised in hybridisation buffer [50% (v/v) formamide, 5X SSPE Buffer, 5X Denharts solution, 0.02 mg/ml boiled herring sperm DNA, 0.5% (v/v) sodium dodecyl sulphate (SDS), made to a final volume with DEPC H₂O]. Pre-hybridisation was carried out at hybridisation temperature: 55°C miR-143, 45°C miR-145 for 1 h. MiRCURY LNA miRNA 5' DIG labelled detection probes (Exiqon, Vedbaek, Denmark) hsa-miR-143 (GAGCTACAGTGCTTCATCTCA), hsa-miR-145 (AGGGATTCCTGGGAAAAGTGGAC) were diluted 1:10,000 in hybridisation

buffer and hybridisation carried out overnight at hybridisation temperature. Hybridisation temperature was initially tested based on RNA melting temperature (T_m) (hsa-miR-143, RNA- T_m 85°C; hsa-miR-145, RNA- T_m 84°C) minus 30°C. The hybridisation temperatures used in all experiments were then determined by a number of experiments where the temperature was altered slightly each time in order to reduce background staining while still effectively labelling the miRNA.

Membranes were washed for at 50°C in NorthernMax® Low Stringency and High Stringency Buffer (Life Technologies) each for 30 min then transferred to wash buffer [0.1 M Maleic acid, 0.15 M NaCl, 0.3% (v/v) Tween-20, pH 7.5] for a further 10 min. Membranes were then incubated in Anti-Digoxigenin-alkaline phosphatase (AP), Fab fragments (Roche Diagnostics Ltd, Burgess Hill, UK), which bind DIG-labelled probes with high affinity, diluted 1:10,000 in 1X Blocking Reagent (Roche Diagnostics Ltd) for 1 h at RT on a shaker.

Membranes were washed twice in wash buffer for 15 min and then incubated with detection buffer [0.1M Tris-HCL, pH 7.5] for 5 min. CDP-Star® Chemiluminescent Substrate was applied to membranes for 5 min. Films were exposed to membranes for varying lengths of time (usually between 1-5 min) and films developed using the Kodak X-Omat developer.

In order to reprobe for the U6 loading control, membranes were stripped in 1% (v/v) SDS by boiling in the microwave for 6-8 min and left to cool for 15 min. Membranes were rinsed in DEPC H₂O before being probed overnight at 60°C with control U6 miRCURY LNA™ miRNA 5' DIG labelled detection probe (CACGAATTTGCGTGTCATCCTT) (Exiqon) diluted 1:10,000 in hybridisation buffer. The original protocol was then followed from this point forward.

Intensity of miRNA bands was measured by densitometry on the Molecular Imager Chemidoc XRS+ System using Quantity One software. Bands were normalised to U6 loading control.

2.12 Protein isolation and western blotting

2.12.1 Protein isolation

Protein lysis buffer was prepared on ice containing the following reagents: 20 mM Tris pH 7.5, 150 mM NaCl, 1 mM EDTA, 1 mM Ethylene glycol tetra-acetic acid (EGTA), 2.5 mM Na pyrophosphate, 1 mM β -glycerophosphate, 1 mM Na_3VO_4 , 0.5% (w/v) sodium deoxycholate, 1 mM phenylmethylsulfonylfluoride (PMSF), 2 mM NaF, 1 $\mu\text{g}/\text{ml}$ leupeptin, 1X Roche Complete Mini Protease Inhibitor cocktail tablets (made up in H_2O) (Roche Diagnostics). Protein lysis was performed on snap frozen tissues. Briefly, 200 μl ice cold protein lysis buffer was added to eppendorfs containing 25 mg frozen tissue and tissue was disrupted using the Qiagen TissueLyser System as described in section 2.7. The eppendorfs containing the tissue/lysis buffer were shaken on a shaker for 1 h at 4°C and then centrifuged at 12,000 rpm at 4°C for 40 min. The protein supernatant was removed and stored at -80°C. Protein concentration was determined using the Pierce BCA Protein Assay Kit (Thermo Scientific) in accordance with the manufacturer's instructions and read at 570 nm using the Wallac VICTOR2 plate reader (Wallac). Protein concentrations were worked out from the standard curve produced by the protein standards.

2.12.2 Western blots

Protein samples were diluted to equal concentrations (10-20 μg) in PBS, mixed with NUPAGE® 4X LDS Sample Buffer (Life Technologies) and denatured by heating at 95°C for 10 min. Samples were loaded in Mini-Protean® TGX 10% polyacrylamide gels (Biorad) along with the reference ladder Full-Range Rainbow Molecular Weight Ladder (GE Life sciences). Electrophoresis was performed at 80-120 V in running buffer [25mM Tris, 0.2M glycine, 1% (w/v) SDS] until the dye reached the bottom of the gel.

Gels were transferred onto Amersham Hybond P nitrocellulose membranes (GE Life Sciences) in transfer buffer [Running buffer plus 20% (v/v) methanol]. Membranes were blocked for 1 h at RT on a shaker in 10% (w/v) fat-free milk powder in Tris buffered saline plus tween (TBS-T) [150 mM NaCl, 2 mM KCl, 25 mM Tris and 1% (v/v) Tween-20]. Membranes were incubated with rabbit polyclonal

anti-KLF5 (ab137676; Abcam, Cambridge, UK) diluted 1:1000 in 5% milk in TBS-T overnight at 4°C on shaker.

The following day membranes were washed in 3 X 10 min changes of 10% milk TBS-T before being incubated with the secondary antibody: polyclonal swine anti-rabbit immunoglobulins/horseradish peroxidase (HRP) (P0217, Dako, Cambridgeshire, UK), diluted 1:1000 in 5% milk TBS-T for 1 h at RT. Membranes were washed in 4 changes of 5% milk TBS-T and 4 changes of TBS-T each for 15 min on shaker.

Proteins were visualised using Amersham Enhanced Chemiluminescence (ECL) Prime Western Detection Reagent (GE Life Sciences) according to the manufacturer's instructions. Films were exposed for varying lengths of time and developed using the Kodak X-Omat developer.

Membranes were stripped in 3 X 10 min washes in stripping buffer [0.2M glycine, 0.1% (w/v) SDS, 1% (v/v) Tween-20] followed by 3 X 10 min washes in TBS-T. Membranes were then blocked in 10% milk TBS-T and protocol repeated to probe for rabbit monoclonal GAPDH (14C10, Cell signalling Technology, Hertfordshire, UK) diluted 1:1000 in 5% milk-TBS-T, for protein normalisation.

Intensity of protein bands was measured by densitometry on the Molecular Imager Chemidoc XRS+ System using Quantity One software. Bands were normalised to GAPDH loading control.

2.13 Migration assays

Cell migration was assessed using a scratch wound assay previously described by Liang and colleagues (Liang et al., 2007). Briefly, cells were seeded at a density of 3×10^5 cells/well in 6 well plates and incubated with AdmiR-143, AdmiR-145 or Ad5CVlacZ as described in section 2.5 or transfected with premiRs or antimiRs as described in section 2.6. A horizontal line was drawn on the underside of each well to act as a reference. A 200 μ l pipette tip was used to produce 3 vertical scratches per well and dead cells removed by gently washing with PBS. Media was replaced with 0.1% or 5% (v/v) FCS containing EC or SMC medium and the scratches were photographed immediately above the reference line under a 10X

lens using the Nikon Eclipse TS1000 microscope and QICAM Fast1394 camera (QImaging) to give the 0 h images. Cells were maintained at 37°C at 5% CO₂ throughout the assay and photographed at further time points between 0 and 24 h. The scratch in the cell monolayer produces a wound which the bordering cells migrate into, giving an *in vitro* model of wound healing. Migration of cells into the scratch was determined by measuring the scratch width using Image J software. To ensure measurements were unbiased a grid of 12 horizontal lines was overlaid on each image and measurement lines were drawn directly on these guidelines. Results are displayed as the distance migrated in 24 h.

2.14 Cell proliferation assays

Cell proliferation was assessed using the CellTiter96® Aqueous One Solution Cell Proliferation Assay (Promega, Southampton, UK). The assay consists of a solution containing both MTS [3-(4,5-dimethylthiazol-2-yl)-5-(3-carboxymethoxyphenyl)-2-(4-sulfophenyl)-2H-tetrazolium] and the electron coupling reagent phenazine ethosulfate (PES). The MTS solution is bio-reduced by living cells to form a soluble formazan product of which absorbance at 490 nm is directly proportional to the number of viable cells.

HSV ECs or HSV SMCs were transfected, plated and serum starved in 24 well cell culture plates as described in section 2.6. Following serum starving for 24 h (HSV ECs) or 48 h (HSV SMC) proliferation was induced by incubating cells for 72 h with culture medium containing 0.1-5% (v/v) FCS. Cells were incubated with MTS/PES solution at a ratio of 100 µl culture medium to 20 µl MTS/PES solution for 3 h at 37°C. Absorbance was read at 490 nm on the Wallac 1420 Victor2 plate reader (Wallac).

2.15 Exosome isolation

Exosomes are small vesicles released by cells which contain RNA and protein which allow paracrine communication to occur between different cell types. It has been shown that ECs are capable of producing exosomes enriched in miRNAs.

In order to assess whether increased expression of miRNAs within HSV ECs results in transfer to exosomes HSV ECs were transfected in suspension with 10 nM

premiR-scr, premiR-143 or premiR-145 using SiPORT NeoFX Transfection Reagent (Invitrogen) and seeded at 3×10^5 cells/well in 6 well cell culture plates. Culture medium was replaced with 0.1% (v/v) FCS EC medium and cells were incubated at 37°C for 96 h. HSV ECs were incubated in 0.1% FCS due to the naturally high levels of exosomes within FCS which would interfere with the results.

Cell culture medium was collected for each sample and centrifuged at 2000 x g for 30 min in order to pellet any cell debris. The supernatant containing the exosomes was transferred to a fresh falcon tube. Exosome isolation was then performed using the Total Exosome Isolation (from cell culture media) Reagent (Invitrogen) according to the manufacturer's instructions. Briefly, 0.5 vol. of Total Exosome Isolation Reagent was added to the medium and mixed by vortexing before being incubated at 4°C overnight. The following day samples were centrifuged at 10,000 x g at 4°C for 1 h. The supernatant was discarded and the pelleted exosomes were resuspended with 1 ml PBS. RNA was then extracted from exosomes by following the protocol for RNA extraction from cells described in section 2.7.

2.16 *In vivo* models

All *in vivo* experiments were performed in accordance with the United Kingdom Animals Scientific Procedures Act of 1986 under the project license 60/4429 held by Professor Andrew Baker. C57BL/6 mice were purchased from Charles River (Kent, UK). Mice were maintained on a 12 h cycles of light and dark at ambient temperature and fed a normal chow diet with free access to food and water. Mice were aged to 18 weeks prior to surgery.

2.16.1 MicroRNA knockout mice

MiR-143, miR-145 and WT mice were kindly gifted by Professor Eric Olson of the University of Texas SouthWestern and bred in-house. MiRNA KO mice were generated by Professor Olson's groups as described by Xin and colleagues (Xin et al., 2009).

Briefly, targeting vectors were generated using the pGKNEO-F2DTA vector, which contains a neomycin resistance gene driven by the pGK promoter, flanked

by loxP sites, and a diphtheria toxin gene cassette. Targeting vectors for the pre-miR-143 or pre-miR-145 sequence were generated using 3.5 kb fragment upstream and a 4.5 - 5 kb fragment downstream of the respective pre-miRNA sequence to form the 5' and 3' targeting arms respectively. These targeting vectors were designed to replace the entire pre-miRNA sequence of miR-143 or miR-145 with the neomycin resistance cassette flanked by loxP sites.

Following linearization and electroporation of the targeting vectors into 129SvEv-derived ESCs, southern blotting was performed to identify cell clones which were positive for homologous recombination. Positive clones were injected into E3.5 C57BL/6 blastocysts and male chimeric offspring bred with female C57BL/6 mice. This cross produced a number of heterozygous offspring that contained 1 allele for the neomycin resistance cassette flanked by loxP sites and 1 allele for the normal pre-miRNA. Cre recombinase is an enzyme which catalyses recombination events between loxP sites and results in deletion of DNA when loxP sites are located in the same direction on a chromosome (Sauer, 1998). In order to remove the neomycin resistance cassette heterozygous mice were bred with Cre-transgenic mice producing mice heterozygous for miR-143 KO or miR-145 KO. Finally, miRNA homozygous KO mice were produced by breeding heterozygous KO mice.

2.16.2 AntimiR dosing schedule

AntimiR-ctl and antimiR-143 for were kindly provided by MiRagen Therapeutics (see section 2.6 for details). AntimiRs were reconstituted in sterile PBS and filter-sterilised before being aliquoted and frozen at -20°C for storage until use. AntimiRs were administered at 10 mg/kg by subcutaneous (SC) injection to donor and recipient 15 week old C57BL/6 mice at 1 week intervals for a total of 3 doses for donor mice and 7 doses for recipient mice. AntimiRs were administered between 21 days prior to the stent surgery and 21 days post-operative.

2.16.3 Mouse model of in-stent stenosis

A mouse model of in-stent stenosis was used incorporating the technique developed by Ali and colleagues (Ali et al., 2007). An overview of the surgical technique is shown in Figure 2.2. Briefly, a 2.5 X 0.6 mm stainless-steel stent

(Cambus Medical, Galway, Ireland) was hand crimped onto a 1.2 X 8 mm coronary dilatation catheter (Abbott, Berkshire, UK) by applying equal pressure to all surfaces of the stent with the fore finger and thumb. The stent and catheter were then sterilised in Actril® cold sterilant (Guardline Technologies ltd, Norfolk, UK) followed by 2 washes in sterile saline. The donor (female) mouse was euthanized by intraperitoneal (IP) injection with 150 mg/kg sodium pentobarbital and the abdomen opened and rib cage deflected. A small incision was made in the right atrium and the vessels perfused with 100 IU/ml heparin in saline via cardiac puncture of the left ventricle. This process was continued periodically throughout the procedure to ensure vessels remained moist. The thoracic aorta was isolated from the aortic arch to the diaphragm and the layer of fat lining the anterior aorta was removed by dissection along the connecting fascia. A small incision was made at the distal end of the thoracic aorta close to the diaphragmatic outlet. The balloon catheter was inserted and positioned in the descending aorta. The stent was deployed by inflating the balloon catheter to 10 atmospheres pressure for 30 sec, to produce a final stent diameter of 1.25 mm and a stent to vessel ratio of 1.5:1. The stented aorta was isolated by cauterisation of the intercostal vessels and stored in heparinised saline.

Recipient (male) mice of identical genotype were anaesthetised using 1-3% vaporised Isoflurane (Abbott) and under a dissection microscope the right common carotid artery was isolated and ligated with 2, 7-0 sutures (Ethicon, Edinburgh, UK) distal to the bifurcation. The carotid was dissected between the sutures and each end was passed through a 0.65 mm outer diameter nylon cuff (Smiths Medical, Kent, UK) and secured with a microhemostatic clamp. Sutures were removed and each free end of the carotid was everted over its corresponding cuff and secured with an 8-0 silk suture (Ethicon). The donor stented aorta was then sleeved over the everted ends of the carotid and secured in place with sutures. Microhemostatic clamps were removed to restore blood flow and the skin closed with a continuous 5-0 suture. An overview of the surgery is shown in Figure 2.2.

Recipient mice received approximately 10 mg/kg/day aspirin in their drinking water, 7 days pre- and 28 days post-surgery to help prevent in-stent thrombosis. Peri-operatively recipient mice received 0.5 ml SC saline to prevent dehydration

and 0.05 mg/kg of the analgesic, Buprenorphine. Following surgery mice were transferred to a 37°C heated chamber for recovery.

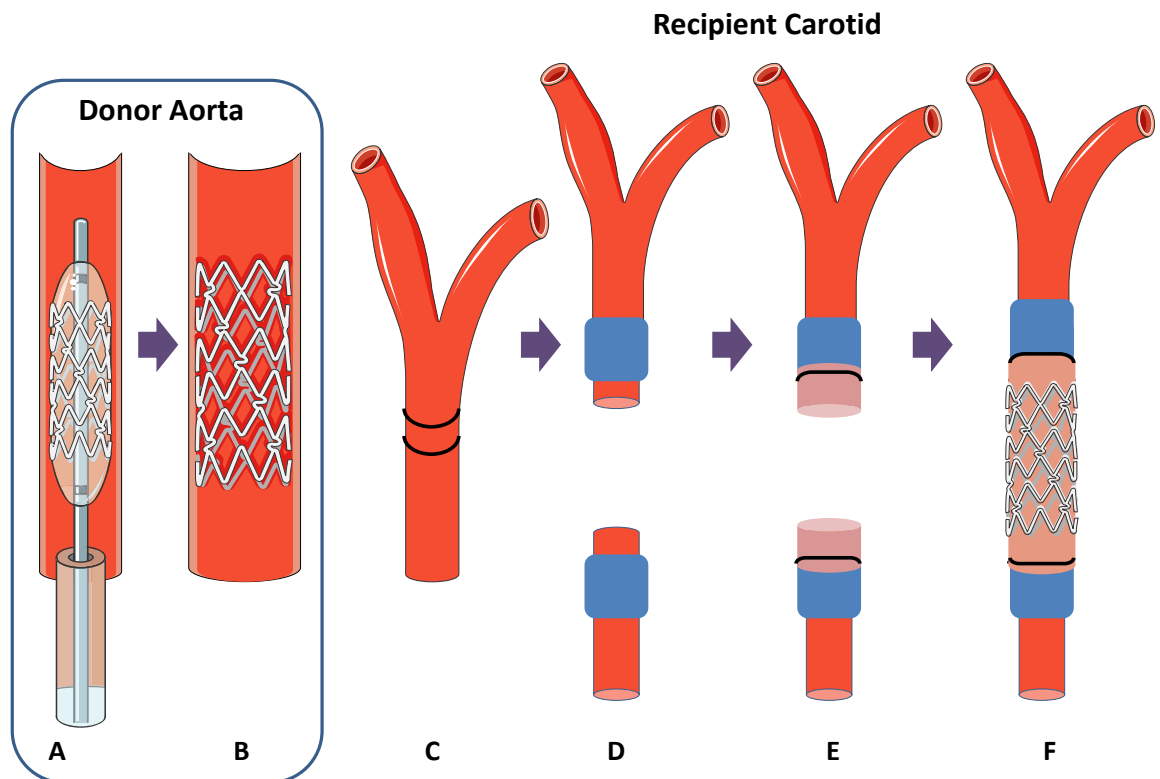


Figure 2.2. Overview of surgery to produce mouse model of in-stent stenosis.

The thoracic aorta of the donor mouse was isolated and a 2.5 X 0.6 mm stainless-steel stent hand-crimped onto a 1.20 mm balloon angioplasty catheter was advanced into the aorta and deployed by inflating to 10 atmospheres pressure (A and B) to give a final internal diameter of 1.25 mm. The right common carotid was isolated in the genetically identical recipient mouse and ligated with 2 sutures distal to the bifurcation (C). The carotid was dissected between the sutures and each end was passed through a plastic cuff and secured with microhemostatic clamps (D). The sutures were removed and each free end of the carotid was everted over its corresponding cuff and secured with a suture (E). The donor stented aorta was then sleeved over the everted ends of the carotid and secured in place with sutures (F). Microhemostatic clamps were removed to restore blood flow.

2.16.4 Tissue harvesting

Mice were euthanized 28 days post-operative by anaesthetic overdose followed by excision of the heart. Tissues were perfused with saline prior to fixation in 10% (v/v) formalin for 24 h followed by transfer to 70% (v/v) ethanol for storage.

2.16.5 Resin embedding

Formalin fixed vessels were embedded in Technovit 8100 resin (TAAB, Berkshire, UK), a methyl methacrylate resin, in accordance with the manufacturer's

instructions. Vessels were placed in 0.5 ml embedding capsules (Electron Microscopy Sciences, Hatfield, UK) and dehydrated in 100% acetone for 1 h at 4°C. Dehydrated vessels were then placed in infiltration solution [0.6% (w/v) Hardener 1 in Basic Solution] overnight at 4°C. Finally, vessels were positioned in the correct orientation and covered in polymerisation solution [0.5 ml Hardener 2 in 15 ml infiltration solution] and left to set overnight at 4°C.

2.16.6 Sectioning of resin embedded vessels

Resin embedded vessels were glued to microscope slides and sectioned using the Isomet 1000® precision saw (Buehler, Düsseldorf, Germany). Sections were ground to approximately 7-10 µm using the Metaserv® 2000 Grinder Polisher (Buehler) using P1200 grit paper (Buehler) and placing the sample on the paper intermittently at 1 sec intervals for approximately 30-40 sec. Slides were then polished using P2500 grit paper holding the sample against the paper for 10 sec.

2.16.7 Electrolysis

Electrolysis was performed in order to remove the stent from the vessel prior to paraffin embedding. This process was developed from a method previously described by Bradshaw and colleagues (Bradshaw et al., 2009) based on the theory that if two metal objects are placed in a weak acid/salt solution and a differential voltage applied, then the object attached to the positive voltage will form complexes in solution i.e. dissolve. Briefly, under a dissection microscope a small incision was made in the stented vessel to expose the top of a stent strut. The stent strut was hooked onto a stainless-steel expansion spring attached to a stainless-steel wire and positioned in a 5 ml universal tube. Through a small hole in the lid of the universal, a solution containing 5% (w/v) citric acid and 5% (w/v) NaCl was added to the tube until the distal stent struts were touching the liquid. An electrode connected to the positive terminal of a power supply was attached to stainless-steel wire. The negative electrode was connected to a copper wire which was submerged in the citric acid/NaCl solution at the distal end of the universal. The power supply was turned on to 5 V and small bubbles could be seen rising from the copper electrode. Stent struts began to dissolve after around 3-5 min. This process was repeated until all stent struts

were dissolved. A diagrammatic overview of the experimental setup is shown in Figure 2.3.

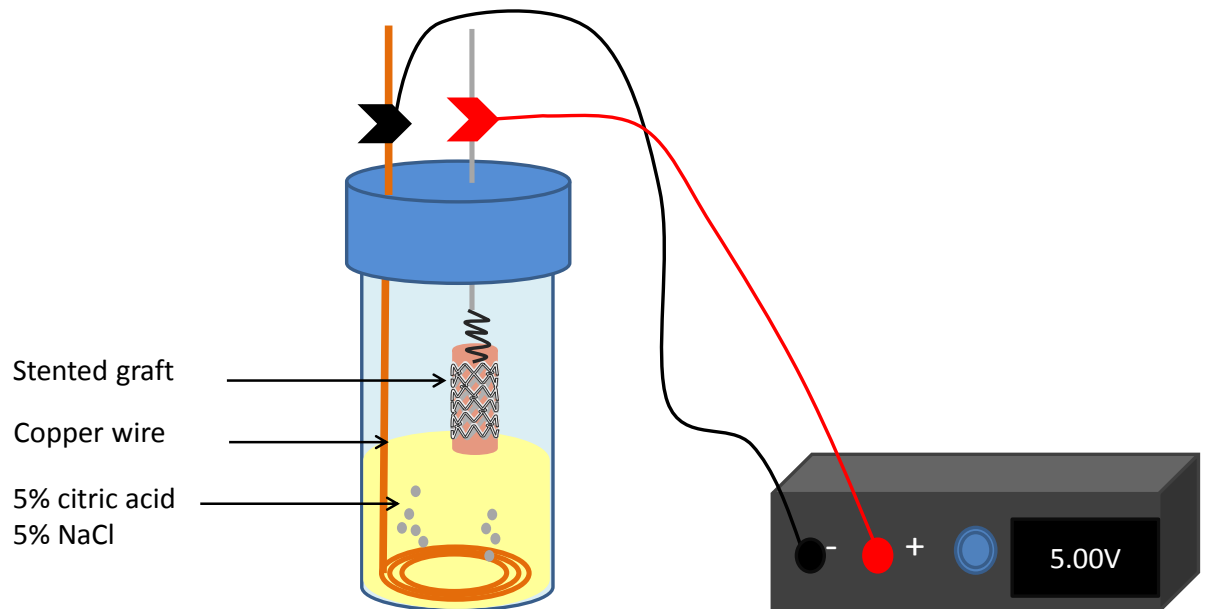


Figure 2.3. Overview of equipment used in stent electrolysis.

2.16.8 Histology

Vessel samples to be embedded in paraffin wax were first dehydrated through an ethanol gradient to xylene and finally to 62°C paraffin wax using the Shandon Excelsior tissue processor (Thermo Scientific) an overview of this process is shown in Table 2.2.

Table 2.2. Tissue processing for paraffin embedding.

Solution	Incubation Period
70% Ethanol	30 min
95% Ethanol	30 min
100% Ethanol	30 min
100% Ethanol	30 min
100% Ethanol	45 min
100% Ethanol	45 min
100% Ethanol	60 min
Xylene	30 min
Xylene	30 min
Xylene	30min
Paraffin wax	30 min
Paraffin wax	45 min
Paraffin wax	45 min

Following the tissue processing sequence, vessels were held in the correct orientation in biopsy cassettes and embedded in paraffin wax using the Shandon Histocenter 3 (ThermoFisher Scientific). Vessels were sectioned at 3-5 μm using the Leica microtome and transferred to a 45°C water bath where they were mounted onto slides and then baked overnight at 60°C in a histology oven.

2.16.9 Haematoxylin and eosin staining

Haematoxylin and eosin (H&E) staining was performed to visualise neointimal formation in stented vessels. Sections were rehydrated by placing in 2 changes of Histo-Clear® (Fisher Scientific Ltd, Leicestershire, UK) followed by 100%, 95%, 70% ethanol and distilled water (dH_2O) each for 7 min. Nuclei were stained with Harris modified haematoxylin (Cell Pathology Ltd, Newtown Powys, UK) before being washed in running tap water for 5 min and transferred to 70% (v/v) ethanol for 1 min. Sections were incubated in eosin Y solution for 2 min to stain cytoplasmic structures before being dehydrated in 2 changes of each of the following: 95% (v/v) ethanol, 100% ethanol and Histo-Clear® each for 5 min. Slides were mounted with glass coverslips using DPX non-aqueous mounting medium (Merck Millipore, Darmstadt, Germany).

2.16.10 Elastin staining

Elastin van gieson (EVG) staining was performed in order to visualise the internal and external elastic lamina in stented vessels. Briefly, sections were rehydrated through the gradient described in 2.15.9. Sections were oxidised by incubating in 0.5% (w/v) potassium permanganate for 10 min, washed in running tap water for 3 min and rinsed in dH₂O for 30 sec. Decolourising of sections was achieved by placing in 1% (w/v) oxalic acid for 10 min, running tap water for 3 min and dH₂O for 30 sec. Sections were incubated overnight with Miller's elastin stain (VWR Chemicals, Leicestershire, UK) which stains elastin fibres black. The following day sections were washed by dipping the slides 7 times in 70% (v/v) ethanol followed by distilled water for 5 min. Sections were counterstained with Van Gieson solution (contains picric acid and 1% acid fuchsin), which stains collagen red. Slides were dried in a histology oven at 60°C for 30 min and then rinsed in 2 changes of 100% ethanol and transferred to 2 changes of Histo-Clear® before being mounted with glass slides using DPX non-aqueous mounting medium.

2.16.11 Immunohistochemistry

10X PBS [80g/L NaCl, 2g/L KCl, 14.4g/L Na₂HPO₄ and 2.4g/L KH₂PO₄ pH 7.4] was diluted to 1X PBS in dH₂O for all washes. Following rehydration of sections (as described in 2.15.9) heat induced antigen retrieval was performed by heating 10 mM citric acid (pH 6.0) to 95-100°C at 5 min intervals for a total of 20 min before allowing sections to cool for 30 min followed by 2 X 5 min washes in PBS. In order to block endogenous peroxidase activity sections were incubated in 3-20% (v/v) H₂O₂ in methanol for 30 min prior to 2 X 5 min washes in PBS. Blocking of tissue sections was performed by incubation with 20% (v/v) of the appropriate serum (Table 2.3), diluted in PBS, for 1 h at RT. Sections were incubated in a humidified chamber with the primary antibody or control IgG antibody, diluted in 2% (v/v) blocking serum for 1 h at RT or 4°C overnight. Details of the primary antibodies used are shown in Table 2.3. Control IgG antibodies were diluted to at equal concentration as that of the primary antibody against the protein of interest. Sections were washed 3 X 5 min in PBS prior to incubation with the biotinylated secondary antibody in PBS for 1 h at RT. A list of the secondary antibodies used in immunohistochemistry experiments is shown in Table 2.4. Sections were washed in 3 X 5 min in PBS prior to incubation with 1:200 (v/v)

ExtrAvidin®-peroxidase (Sigma). ExtrAvidin-peroxidase contains avidin, which contains 4 biotin binding sites and binds to biotin with high affinity. The resultant avidin-biotin peroxidase cleaves its substrate DAB (3, 3'-diaminobenzidine) (Vector Laboratories, Peterborough, UK) to reveal the antigen by producing a dark brown colour. This was performed as described. Sections were washed 3 X 5 min in PBS prior to incubation with DAB peroxidase substrate for 2-5 min or until the dark brown staining was visualised. Sections were washed in H₂O for 5 min prior to dehydration through dH₂O, 70%, 95%, 100% ethanol and 2 changes of Histo-Clear® each for 7 min. Sections were mounted with glass coverslips using DPX non-aqueous mounting medium.

α -SMA staining was performed using the VECTASTAIN® Elite ABC kit (Universal) (Vector Laboratories) in accordance with the manufacturer's instructions. Briefly, following dehydration through the alcohol gradient (see 2.15.9) sections were blocked for 1 h at RT with 1% (v/v) blocking serum (normal horse serum) in PBS. The sections were incubated with primary antibody or primary control IgG antibody (described in Table 2.3) diluted in PBS 2% normal horse serum, for 1 h at RT and washed for 3 X 5 min in PBS. Biotinylated secondary antibody (Table 2.4) diluted in 2% blocking serum was incubated with sections for 30 min at RT. VECTASTAIN® Elite avidin biotinylated enzyme complex (ABC) reagent was prepared by adding 2 drops reagent A and 2 drops reagent B to 5ml PBS prior to incubation for 30 min. Following 3 X 5 min washes in PBS sections were incubated with the ABC reagent for 30 min at RT. The ABC complex binds to the biotin of the secondary antibody, when incubated with DAB peroxidase substrate dark brown staining occurs to reveal the antigenic site. DAB staining was performed as described above.

Table 2.3. Primary antibodies used in immunohistochemistry.

Primary antibody	Conc.	Dilution	IgG Control antibody	Blocking Serum
Rabbit polyclonal anti- α -SMA (Abcam : ab5694)	0.2mg/ml	1:75	Normal rabbit IgG (Invitrogen: 10500C)	Normal horse (Vector)
Rat monoclonal anti-CD31 (Dianova: DIA-310)	0.2mg/ml	1:20	Normal rat IgG (Invitrogen: 10700)	Normal rabbit (Vector)
Rat monoclonal anti-MAC-2 (Cedarlane: CL8942AP)	1mg/ml	1:5000	Normal rat IgG (Invitrogen: 10700)	Normal rabbit (Vector)
Rabbit polyclonal anti- PCNA (Abcam: ab2426)	0.2mg/ml	1:200	Normal rabbit IgG (Invitrogen: 10500C)	Normal goat (Vector)

Table 2.4. Secondary antibodies used in immunohistochemistry.

Primary antibody used	Secondary antibody	Conc.	Dilution
Rabbit polyclonal anti- α -SMA (Abcam: ab5694)	Biotinylated Universal antibody horse anti-rabbit IgG (Vector: BA-1400)	1.05mg/ml	1: 50
Rat monoclonal anti-CD31 (Dianova: DIA-310)	Biotinylated rabbit anti-rat IgG (Vector: BA-4000)	1.5mg/ml	1:200
Rat monoclonal anti-MAC-2 (Cedarlane: CL8942AP)	Biotinylated rabbit anti-rat IgG (Vector: BA-4000)	1.5mg/ml	1:200
Rabbit polyclonal anti- PCNA (Abcam: ab2426)	Biotinylated goat anti-rabbit IgG (Vector: BA-1000)	1.5mg/ml	1:250

2.16.12 Morphometric analysis and injury scoring

In order to assess the morphometry of stented sections, photographs of stained sections were taken using QCapture Pro 6.0 and a series of measurements were performed using Image-Pro® Analyzer 7.0 software (Media Cybernetics, Marlow, UK). Analysis was performed on at least 3 sections/animal, descriptions of each measurement performed are shown in Table 2.5 and a diagrammatic overview is shown in Figure 2.4.

Table 2.5. Definition of morphometric measurements.

Measurement	Definition
Neointimal Thickness	Perpendicular distance between internal elastic lamina and lumen measured between stent struts
Strut Depth	Perpendicular distance between stent struts and lumen
Neointimal Area	Area inside internal elastic lamina minus lumen minus stent struts
Total Vessel Area	Area inside external elastic lamina
Medial Area	Area inside external elastic lamina minus area inside internal elastic lamina
% Stenosis	Neointimal area divided by area inside internal elastic lamina multiplied by 100
Stent Expansion	Area inside polygon connecting the centre of each stent strut

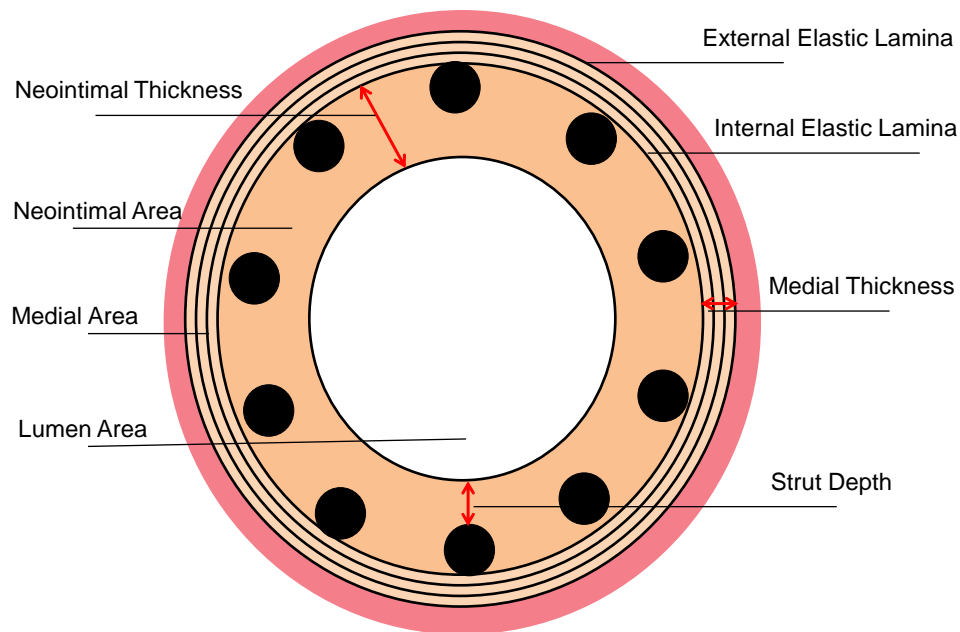


Figure 2.4. Diagram of morphometric measurements.

In order to assess whether the stenting procedure produced a consistent and reproducible injury to the vessel wall between animals, stented sections were given an injury score based on a modified version of the Schwartz method. For each stented section, each individual stent strut (n=10) was given a numeric injury score based on the criteria described in Table 2.6, this process was then repeated for a n=3 sections/animal.

Table 2.6. Definition of injury scores.

Injury Score	Definition
0	Stent struts against internal elastic lamina
1	Perforation of internal elastic lamina
2	Perforation of media
3	Perforation of the external elastic lamina

2.16.13 Measurement of heart weights

Heart weight measurements were performed on formalin fixed hearts. The whole heart, left ventricle plus septum and right ventricle were weighed and weight displayed as a percentage of the body weight at the time of sacrifice.

2.17 Statistical analysis

All results are displayed as mean \pm standard error of the mean (SEM). *In vitro* experiments were performed in biological triplicates and repeated on 3 separate occasions. *In vivo* experiments were performed on n = 7-13 animals per experiment group.

Statistical analysis was performed using Graphpad Prism 4 Software (California, USA) by unpaired Student's t-test when 2 groups were present or by one-way analysis of variance (ANOVA) when more than 2 groups were present. Tukey's post hoc test, which corrects for multiple comparisons, was applied when using ANOVA in order to compare all groups. Significance was determined as a P value of $P < 0.05$.

3 The role of miR-143 and miR-145 in human primary vascular cells

3.1 Introduction

Neointimal formation is a pathological process that occurs following vascular injury and can lead to narrowing of the lumen. A key component of neointimal formation is activation of VSMCs which proliferate and migrate from the media to form the neointima (Schwartz et al., 1992). VSMCs are highly plastic and can modulate their phenotype in response to environmental cues. In normal adult vessels, VSMCs display a differentiated, contractile phenotype with expression of contractile proteins and minimal migration or proliferation (Owens et al., 2004, Shanahan and Weissberg, 1998). In contrast, during development and following vascular injury VSMCs display a synthetic phenotype characterised by lower contractile and higher synthetic protein expression, proliferation and migration (Kuro-o et al., 1991, Kocher et al., 1991).

MiRNAs, miR-143 and miR-145 have been identified as regulators of VSMC contractile phenotype. *In vitro* studies have shown that transcription of miR-143/miR-145 is activated at a CArG box in its regulatory region by SRF and its cofactors myocardin and MRTF (Cordes et al., 2009, Xin et al., 2009). MiR-145 is decreased in cells exposed to PDGF and overexpression of miR-145 prevents PDGF-induced VSMC proliferation and downregulation of contractile genes, including SM-MHC and α -SMA (Cordes et al., 2009, Cheng et al., 2009). Furthermore, identified miR-143 and miR-145 targets include several transcription factors that have been shown to promote a synthetic VSMC phenotype. These include KLF5 (Xin et al., 2009), which promotes cell proliferation and expression of synthetic proteins (Watanabe et al., 1999, Suzuki et al., 2009). Elk-1, a miR-143 target (Cordes et al., 2009), has been shown to competitively inhibit the interaction between SRF and its cofactor myocardin at CArG box binding sites in the promoter regions of contractile genes (Wang et al., 2004). Another identified miR-143/miR-145 target is KLF4 (Xin et al., 2009) which has been shown to inhibit SRF-myocardin interaction at the α -SMA promoter and repress activation of α -SMA (Liu et al., 2005). Together this evidence suggests that expression of miR-143 and miR-145 promotes a contractile VSMC phenotype. Although detectable at low levels in other cell types miR-143 and miR-145 are particularly enriched in SMCs (Cheng et al., 2009). This relatively specific expression of miR-143 and miR-145 in SMCs is potentially beneficial as it may allow a means of targeting VSMC proliferation

and migration whilst having minimal effects on other cell types. One of the main issues associated with DES is delayed re-endothelialisation of the vessel due to inhibition of EC proliferation (Joner et al., 2006). This increases risk of in-stent thrombosis and there is a need to develop more selective therapies to target VSMC without effecting EC proliferation and migration.

The saphenous vein is an extensively used vessel in CABG procedures but is associated with around 40% failure by 10 years, due to vessel remodelling and superimposed atherosclerosis (Goldman et al., 2004). Initial stages of remodelling involve activation of VSMC proliferation and migration following the shift to the high pressure arterial circulation and is eventually followed by the development of atherosclerotic plaques (Cox et al., 1991). In the present study SMCs and ECs isolated from the saphenous vein were used for *in vitro* studies to test the effects of miR-143 and miR-145 modulation, due to their clinical relevance and ability to exhibit proliferative and migratory properties *in vivo*.

Modulation of miRNA levels can be achieved by several different means including transfection with miRNA mimics or inhibitors or vector-mediated delivery (van Rooij, 2011). PremiRs are double-stranded mature miRNA mimics which can be transfected directly into the cell where strand selection and incorporation into the RISC can take place. AntimiRs are complementary to the mature miRNA sequence and contain a mix of DNA and LNA bases. AntimiRs act as miRNA inhibitors by binding tightly to the miRNA and preventing its interaction with targets. Vectors such as Ads and lentiviruses are useful molecular tools as they facilitate transgene delivery to cells both *in vitro* and *in vivo*, without the need for transfection. Ads are 90-100 nm non-enveloped DNA viruses, which comprise of at least 55 known species subdivided into groups A-G (Coughlan et al., 2010). Subgroup C Ads, particularly Ad5 and Ad2, are the most extensively studied serotypes for use as gene therapy vectors and enter cells through binding to the coxsackievirus and adenovirus receptor (CAR) present on the cell membrane (Bergelson et al., 1997). The Ads used in the present study are Ad5 vectors that have their E1 and E3 genes deleted in order to render them replication incompetent and to accommodate transgene insertion, so called “1st generation” Ads. Following cellular transduction via CAR, transgene expression is driven by the CMV promoter which acts as a potent transcriptional enhancer (Boshart et al., 1985).

This chapter was designed to study the effects of modulating miR-143 and miR-145 expression in human primary cells with respect to proliferation, migration and target gene expression in order to investigate the importance of these miRNA in influencing VSMC phenotype *in vitro*.

3.1.1 Aims

- To successfully modulate miR-143 and miR-145 expression within HSV SMC and HSV ECs.
- To carry out functional studies to investigate whether modulation of miR-143 or miR-145 expression effects migration and proliferation of HSV SMCs or HSV ECs.
- To investigate changes in miRNA target expression that could be linked to any detected changes in proliferation and migration.

3.2 Results

3.2.1 Adenovirus-mediated modulation of miRNA expression

AdmiR-143 and AdmiR-145 were produced by cloning the human pre-miR-143 or pre-miR-145 sequence into the replication incompetent Ad5 based vector pAdEasy-1. AdmiR-143 and AdmiR-145 were designed to allow the effect of increased miR-143 or miR-145 expression to be studied. The ability of AdmiR-143 and AdmiR-145 to increase miR-143 and miR-145 expression was first tested in the HeLa cell line. HeLa cells were incubated with media alone (control), or AdmiR-143, AdmiR-145 or RAd-60 at 10-100 PFU/cell for 24 h before being incubated for a further 24 h in normal growth medium. MiRNA analysis was performed on isolated RNA by Taqman® qRT-PCR and northern blotting (Figure 3.1). Incubation of HeLa cells with AdmiR-143 or AdmiR-145 resulted in a significant increase in miR-143 and miR-145 expression seen by qRT-PCR (Figure 3.1). Bands for mature miR-143 and miR-145 were not detectable by northern blotting in control or RAd60 transduced HeLa cells but prominent bands were detected following transduction with the AdmiR-143 and AdmiR-145 (Figure 3.1).

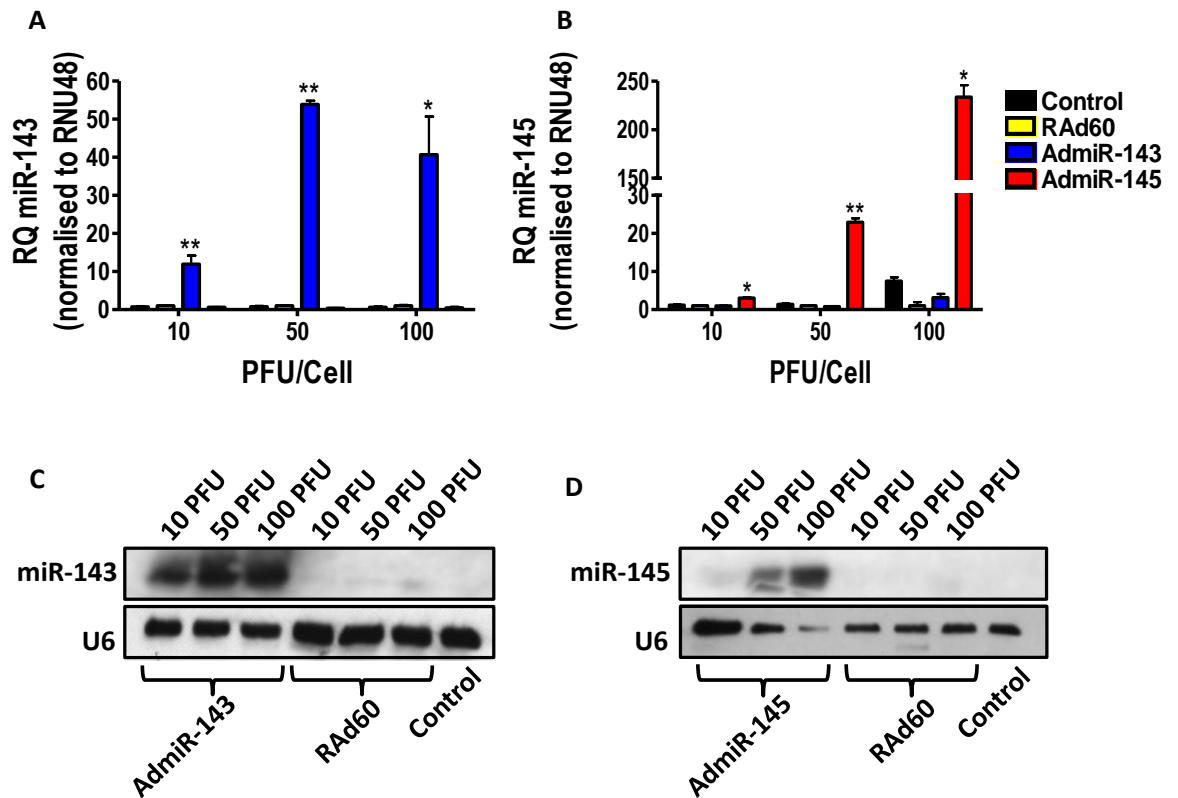


Figure 3.1. MiRNA expression in HeLa cells transduced with AdmiR-143 and AdmiR-145.

HeLa cells were exposed to growth medium alone (control) or containing AdmiR-143, AdmiR-145 or RAd60 at concentrations of 10, 50 and 100 PFU/cell for 24 h. Media was replaced with fresh growth medium and incubated for a further 24 h. A-B. MiRNA expression determined by Taqman® qRT-PCR for miR-143 and miR-145. C-D. Northern blots performed on 3 µg RNA for miR-143, miR-145 and U6. *P<0.05, **P<0.01 vs. RAd60. n = 3.

In contrast to HeLa cells which readily express CAR (Bergelson et al., 1997), HSV SMCs are relatively non-permissive to Ad5 due to their low CAR expression (Havenga et al., 2001) and thus require a higher number of infectious particles per cell in order for adequate transduction to occur. Transduction of HSV SMCs was first tested using Ad5CMVlacZ which expresses the lacZ transgene and produces a blue product when in the presence of its substrate X-gal. VP titre was used for primary cell experiments due to toxicity seen after using PFU/cell in preliminary experiments, presumably due to high VP to PFU ratios and thus an abundance of non-infectious viral particles. HSV SMCs were incubated with 10,000-50,000 VP/cell Ad5CMVlacZ for 24 h before media was replaced with 0.1% FCS medium for 48 h to induce quiescence. Cells were fixed and stained with X-gal and blue staining visualised (Figure 3.2A). Transgene expression could be seen in a small number of cells with the most prominent staining seen in cells treated with 50,000 VP/cell Ad5CMVlacZ ($16.51 \pm 3.63\%$)(Figure 3.2A).

Transgene expression driven by the CMV promoter has previously been shown to be responsive to changes in cell cycle and serum concentrations (Brightwell et al., 1997). In order to determine whether transgene expression was improved in the presence of serum the experiment was repeated with cells being transferred to 2% FCS or maintained in 15% FCS SMC growth medium following 24 h incubation with Ad5CMVlacZ. Transgene expression was greatest in cells treated with 50,000 VP/Cell Ad5CMVlacZ and maintained in 15% FCS ($78.97 \pm 2.40\%$)(Figure 3.2A). Transfer of cells into low serum medium (2% FCS) improved transgene staining seen following transduction with 50,000 VP/Cell ($39.36 \pm 9.15\%$) compared with serum starvation (Figure 3.2A).

Serum starvation was included in the protocol when testing Ad-mediated gene expression in HSV SMCs as it is required to induce quiescence for migration and proliferation assays. In order to determine the proliferative response of HSV SMCs to FCS, HSV SMCs were exposed to different concentrations of FCS-containing SMC growth medium for 48 h and cell proliferation determined by MTS assay (Figure 3.2B). Maintenance of cells in 2% FCS medium did not significantly evoke cell proliferation compared to cells maintained in 0.1% FCS medium (Figure 3.2B). Therefore it was determined that HSV SMCs treated with Ads could be transferred to low serum (2% FCS) medium to reduce cell proliferation prior to functional assays.

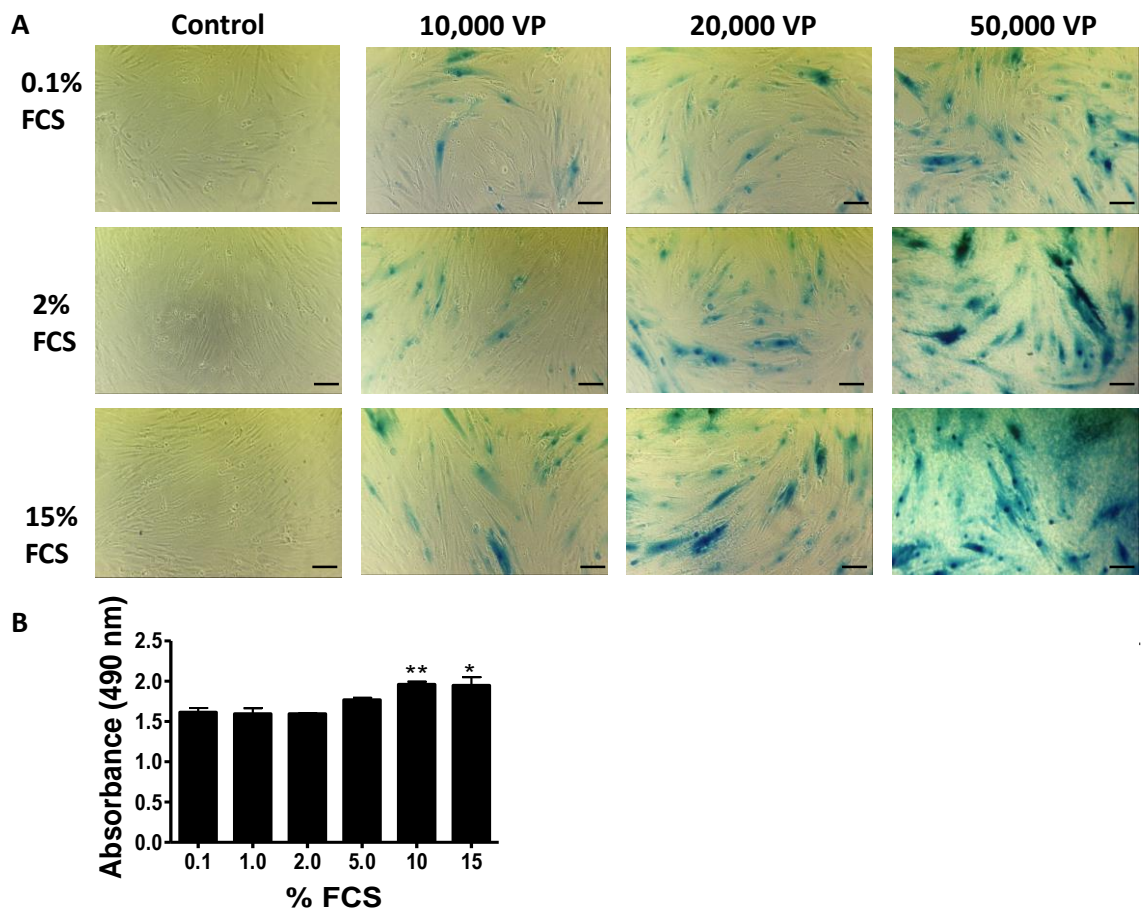


Figure 3.2. X-gal expression in HSV SMCs transduced with Ad5CMVlacZ.

A. X-gal staining of HSV SMCs transduced with 10,000 - 50,000 VP/cell Ad5CMVlacZ prior to 48 h incubation in 0.1%-15% FCS containing media. B. Proliferation of quiescent HSV SMCs exposed to 0.1%-15% serum for 48 h. Proliferation was measured by MTS assay read at 490 nm. 10X magnification. Scale bar = 100 μ m. $P < 0.05$, ** $P < 0.01$ vs. 0.1% FCS. $n = 3$.

In order to confirm the results of our X-gal assay miRNA expression was measured by Taqman® qRT-PCR analysis in HSV SMCs after transduction with AdmiR-143 or AdmiR-145. Results showed a dose dependent increase in miR-143 and miR-145 expression in HSV SMCs maintained in 2% or 15% FCS medium with 3-4-fold increased expression seen in cells transduced with 50,000 VP/cell (Figure 3.3B-C). Conversely, cells maintained in 0.1% FCS medium showed only non-specific changes in miRNA expression (Figure 3.3A).

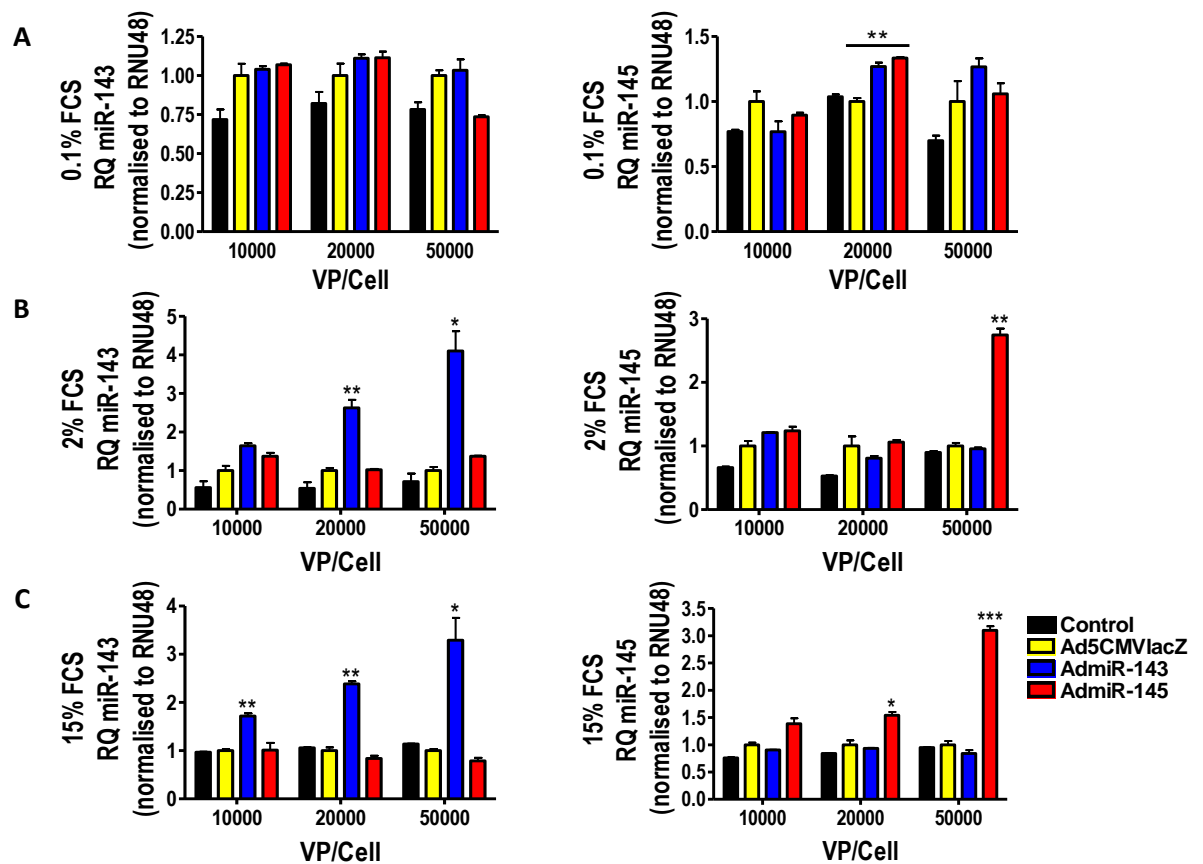


Figure 3.3. MiRNA expression in Ad-miR-143 and AdmiR-145 transduced HSV SMCs.

HSV SMCs cells were incubated for 24 h in normal growth medium alone (control) or containing 10,000-50,000 VP/cell AdmiR-143, AdmiR-145 or Ad5CMVlacZ. Cells were incubated in medium containing 0.1%, 2% or 15% FCS for a further 48 h before being lysed for RNA extraction and analysis. Taqman® qRT-PCR analysis of miR-143 and miR-145 levels in Ad transduced cells incubated in 0.1% (A) 2% (B) or 15% (C) FCS. * $P < 0.05$, ** $P < 0.01$, *** $P < 0.001$ vs. Ad5CMVlacZ. $n = 3$.

The effect of increased miR-143 and miR-145 expression on migration was investigated by a scratch assay. Following transduction with 50,000 VP/cell AdmiR-143, AdmiR-145 or Ad5CMVlacZ and maintenance in low serum (2%) medium for 48 h, scratches were made in the cell monolayer using a 200 μ l pipette tip and medium replaced with fresh 2% FCS medium. Migration into the wound was assessed over 24 h. Migration of HSV SMCs did not significantly differ following transduction with AdmiR-143, AdmiR-145 or Ad5CMVlacZ (Figure 3.4). However, control HSV SMCs migrated significantly further than those transduced with Ad5CMVlacZ (Figure 3.4), indicating that transduction with Ads in general decreased cell migration. The high doses of Ads needed to modulate miRNA expression in HSV SMCs may therefore hinder the ability to detect any effect of miR-143 or miR-145 on migration.

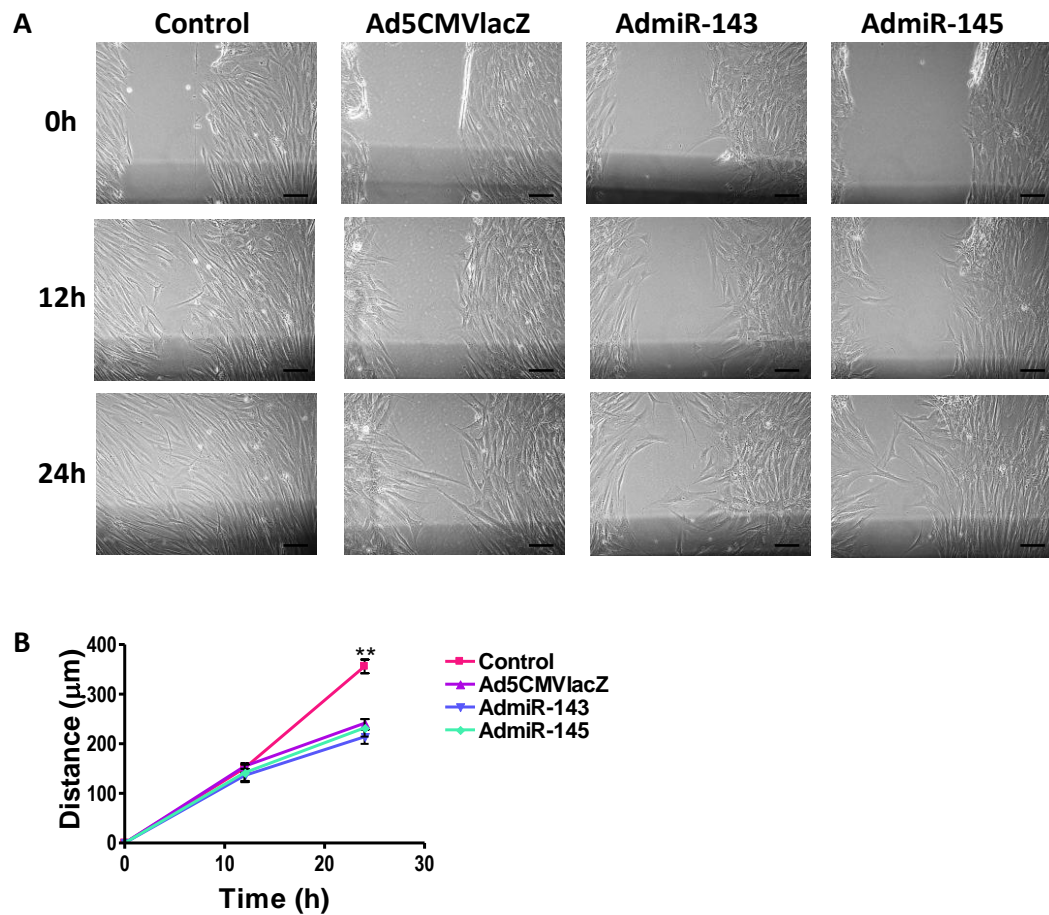


Figure 3.4. Migration of HSV SMCs transduced with AdmiR-143 and AdmiR-145.

HSV SMCs were seeded at 3×10^5 cells/well in 6 well plates and incubated with control (media alone) or 50,000 VP/cell AdmiR-143, AdmiR-145 or Ad5CMVlacZ for 24 h prior to 48 h incubation in 2% FCS media. Vertical scratches were made in the cell monolayer with a 200 µl pipette tip and photographed at 0 h, 12 h and 24 h post scratch to monitor migration into the wound (A). Images were analysed using image J software and distance migration determined over 24h (B). 10X magnification. Scale bar = 100 µm. ** $P < 0.01$ vs. Ad5CMVlacZ. n = 3.

HSV ECs display greater expression of CAR than HSV SMCs making them more readily transduced with Ad5 vectors (Havenga et al., 2001). HSV ECs were incubated with 5000-20,000 VP/cell AdmiR-143, AdmiR-145 or Ad5CMVlacZ for 24 h before being serum starved in 0.1% FCS medium for 24 h. MiR-143 and miR-145 expression, determined by Taqman® qRT-PCR, was significantly increased in a dose dependent manner reaching approximately 20-fold and 7-fold respectively at 20,000 VP/cell (Figure 3.5).

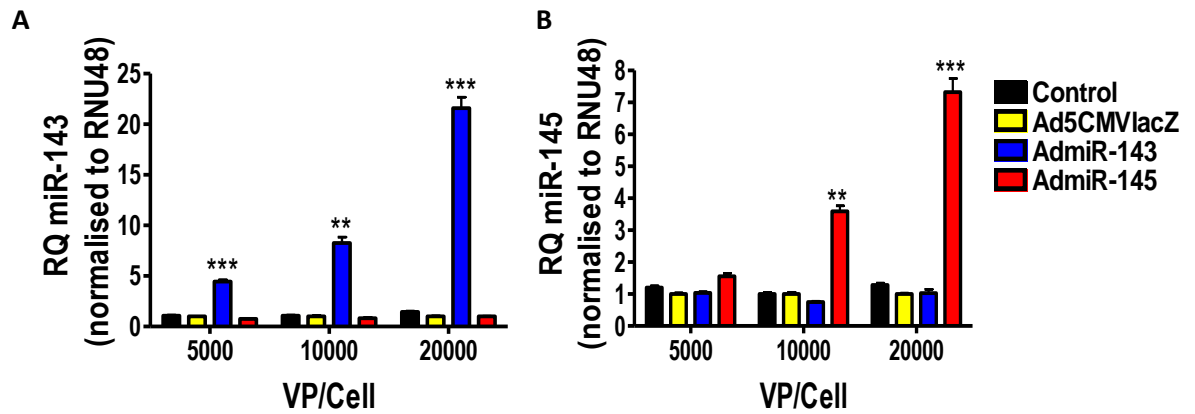


Figure 3.5. MiRNA expression in AdmiR-143 and AdmiR-145 transduced HSV ECs.

HSV ECs cells were incubated for 24 h in normal growth medium alone (control) or containing 5000-20,000 VP/cell AdmiR-143, AdmiR-145 or Ad5CMVlacZ. Cells were incubated in medium containing 0.1% FCS for a further 24 h before being lysed for RNA extraction and analysis. Taqman® qRT-PCR analysis of miR-143 (A) and miR-145 (B) levels in Ad transduced cells incubated in 0.1% FCS. **P<0.01, ***P<0.001 vs. Ad5CMVlacZ. n = 3.

Following a number of optimisation experiments HSV ECs incubated with 20,000 VP/cell Ads displayed significant toxicity during migration assays. This is thought to be due to the combination of high viral transduction and serum starvation. Migration was therefore assessed in HSV ECs transduced with 10,000 VP/cell Ads, which also produced significant increases in miR-143 and miR-145 expression (Figure 3.5) but was not associated with toxicity. Assessment of HSV EC migration over 24 h revealed that transduction with AdmiR-145 produced a significant reduction in migration (Figure 3.6).

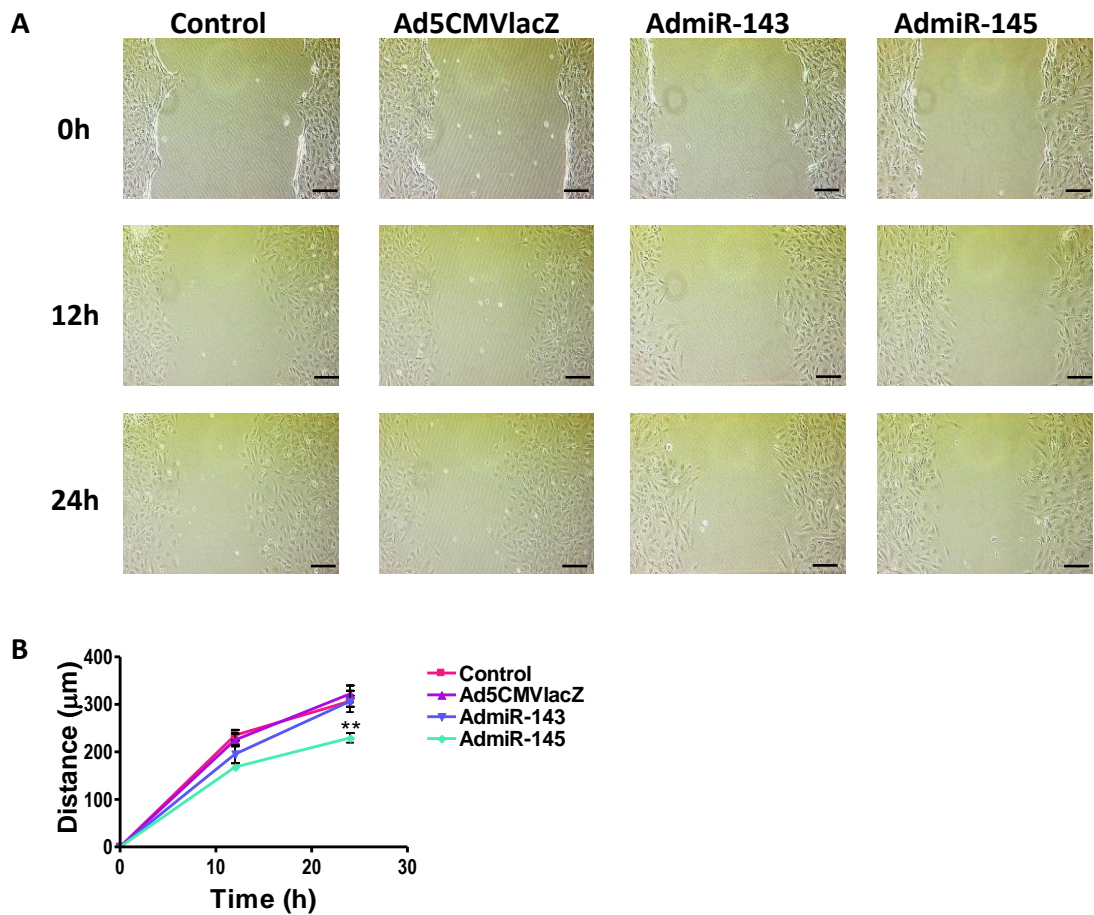


Figure 3.6. Migration of HSV ECs transduced with AdmiR-143 and AdmiR-145.

HSV SMCs were seeded at 3×10^5 cells/well in 6 well plates and incubated with control (media alone) or 10,000 VP/cell AdmiR-143, AdmiR-145 or Ad5CMVlacZ for 24 h prior to 24 h incubation in 0.1% FCS media. Vertical scratches were made in the cell monolayer with a 200 μ l pipette tip and photographed at 0 h, 12 h and 24 h post scratch to monitor migration into the wound (A). Images were analysed using image J software and distance migration determined over 24h (B). 10X magnification. Scale bar = 100 μ m. ** $P < 0.01$ vs. Ad5CMVlacZ. n = 3.

Analysis of expression of miR-143 and miR-145 targets KLF4 and KLF5 in HSV SMCs by Taqman® qRT-PCR did not reveal any significant changes in mRNA expression following transduction with AdmiR-143 or AdmiR-145 (Figure 3.7).

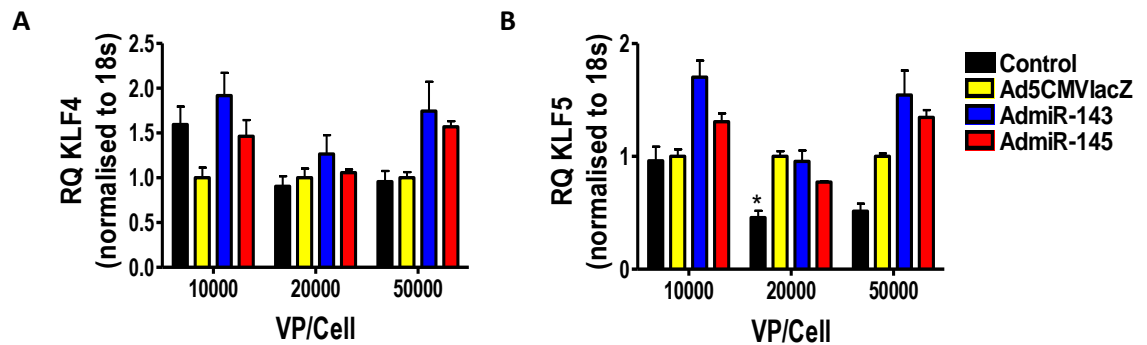


Figure 3.7. Gene expression in HSV SMCs transduced with AdmiR-143 and AdmiR-145.

HSV SMCs were isolated 48 h after incubation with media alone (control) or containing 10,000-50,000 VP/cell AdmiR-143, AdmiR-145 or Ad5CMVlacZ. Taqman® qRT-PCR analysis of KLF4 (A) and KLF5 (B) expression. * $P < 0.05$ vs. Ad5CMVlacZ. $n = 3$.

Whilst optimising Ads as modulators of miRNA expression for functional assays many problems arose including the need to use high VP/cell in order to achieve adequate overexpression, lack of transgene expression following serum starvation, non-specific effects of Ads on cell migration and toxicity. These effects together with the variability in VP to PFU ratios between different Ads (80 and 46 for AdmiR-143 and AdmiR-145, respectively) made their use in functional assays unreliable and as a result a different direction of modulating miRNA expression was pursued through transfection of small molecule mimics and inhibitors.

3.2.2 PremiR and antimiR modulation of miRNA expression

Transfections carried out using SiPORT NeoFX were initially optimised in HSV SMCs using non-targeting antimiR tagged with Cy3 fluorescent reporter. HSV SMCs were plated with antimiR-Cy3 transfection complexes and media changed to 0.1% SMC medium the following day. Cy3 expression was photographed under fluorescent microscope 48 h later. Cy3 was detectable in all cells transfected with 10 nM, 25 nM and 50 nM antimiR-Cy3 (Figure 3.8).

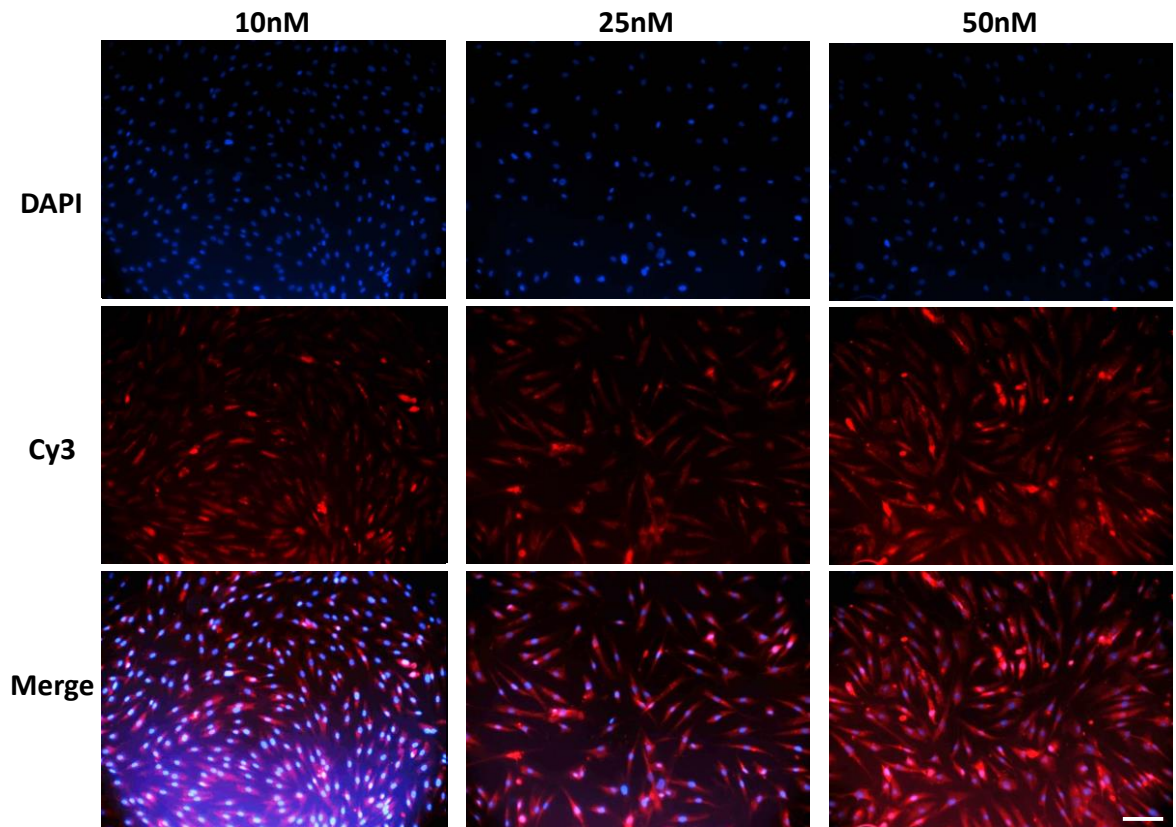


Figure 3.8. Cy3 fluorescence in HSV SMCs transfected with anti-miR-Cy3.

HSV SMCs were transfected with 10 nM - 50 nM anti-miR-Cy3 using SiPORT-NeoFX and seeded at 4×10^4 cells/well in chamber slides. Cells were fixed 48 h later and mounted with Prolong Gold Antifade Reagent with DAPI. Top panel shows blue DAPI nuclear stain. Middle panel shows red Cy3 fluorescence. A merger of both images is shown in the bottom panel. 40X magnification. Scale bar = 20 μ m. n = 3.

Analysis of miRNA expression in HSV SMCs following transfection with premiRs or anti-miRs was carried by Taqman® qRT-PCR and northern blotting. Transfection with premiR-143 and premiR-145 produced significant increases in miR-143 and miR-145 expression compared to premiR-scr with more than 100-fold increases in expression detected at the 10 nM concentration for both miRNA (Figure 3.9A and 3.10A). Northern blots confirmed overexpression with large bands of the respective miRNA detected in RNA isolated from HSV SMCs transfected with premiR-143 and premiR-145 (Figures 3.9C and 3.10C). Anti-miR-143 and anti-miR-145 decreased miR-143 and miR-145 expression by approximately 0.5-0.7-fold detected by qRT-PCR (Figure 3.9B and 3.10B) and expression was undetectable by northern blot compared to anti-miR-ctl (Figure 3.9D and 3.10D). MiR-145 expression was greater in control HSV SMCs when compared to mock and

antimiR-ctl transfected cells suggesting that the transfection process itself may reduce miR-145 levels (Figure 3.10B).

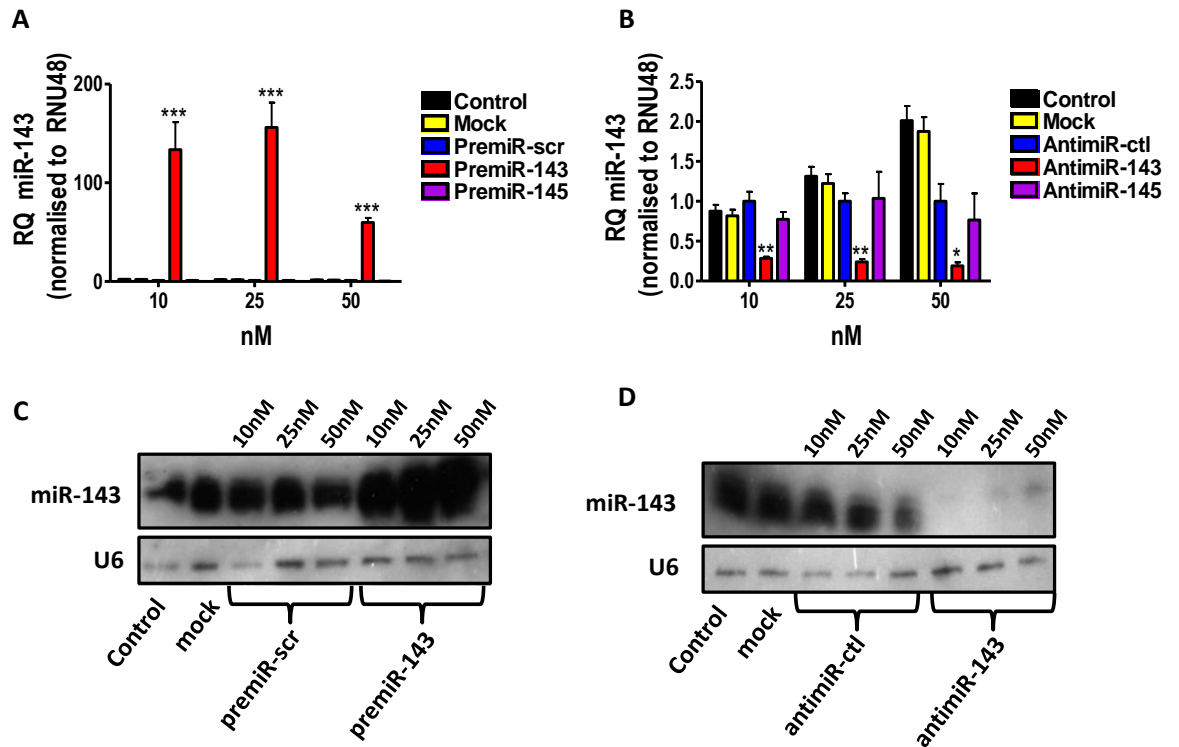


Figure 3.9. MiR-143 expression in transfected HSV SMCs.

HSV SMCs were incubated overnight in medium alone (control), medium + SiPORT NeoFX alone (Mock) or transfected with 10 nM - 50 nM premiR or anti-miR. Cells were quiesced in 0.1% FCS for 48 h. MiR-143 expression was analysed by Taqman® qRT-PCR in HSV SMCs transfected with premiRs (A) and anti-miRs (B). Northern blots of miR-143 and U6 expression in premiR (C) and anti-miR (D) transfected cells. * $P < 0.05$, ** $P < 0.01$, *** $P < 0.001$ vs. premiR-scr or anti-miR-ctl. $n = 3$.

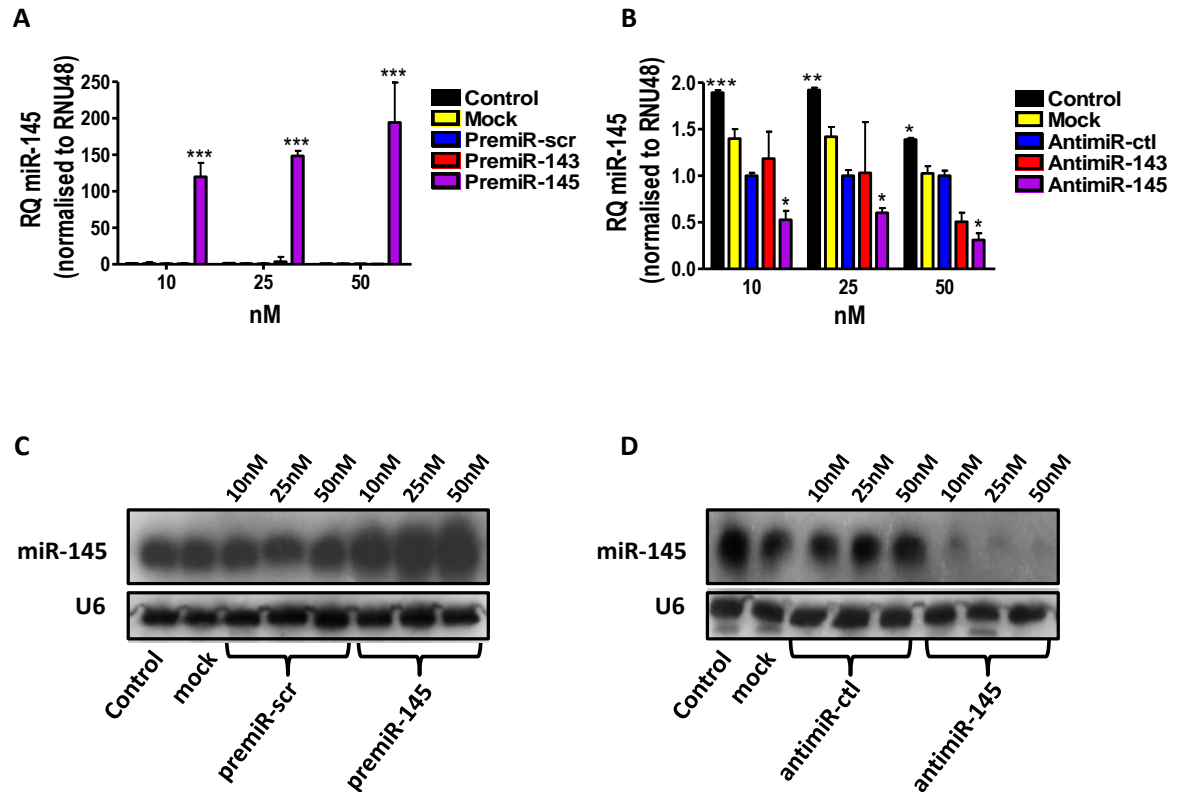


Figure 3.10. MiR-145 expression in transfected HSV SMCs.

HSV SMCs were incubated overnight in medium alone (control), medium + SiPORT NeoFX alone (Mock) or transfected with 10 nM - 50 nM PremiR or antimiR. Cells were then quiesced in 0.1% FCS for 48 h. MiR-145 expression was analysed by Taqman® qRT-PCR in HSV SMCs transfected with premiRs (A) and antimiRs (B). Northern blots of miR-145 and U6 expression in premiR (C) and antimiR (D) transfected cells. * $P < 0.05$, ** $P < 0.01$, *** $P < 0.001$ vs. premiR-scr or antimiR-ctl. $n = 3$.

MiR-143 and miR-145 expression is relatively restricted to SMCs however it is detectable at low levels in other tissues including HSV ECs. Transfection of premiR-145 and premiR-143 into HSV ECs increased miRNA expression, detected by Taqman® qRT-PCR by more than 5000-fold and 10,000-fold for miR-145 and miR-143 respectively (Figure 3.11 A-B). Bands for miR-143 expression were undetectable by northern blot in premiR-scr treated HSV ECs but large bands were present following transfection with premiR-143 (Figure 3.11C). Similarly, northern blots showed that miR-145 bands were considerably larger in HSV ECs transfected with premiR-145 when compared to transfection with premiR-scr at the same concentration (Figure 3.11D).

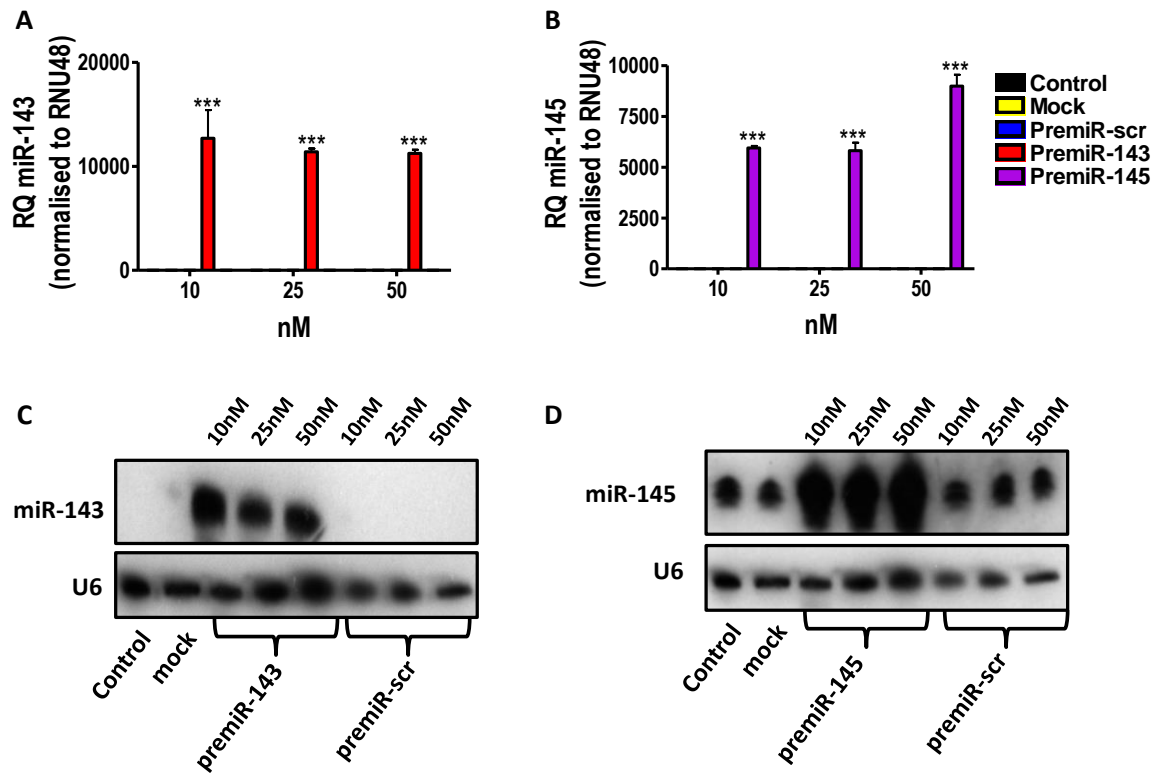


Figure 3.11. MiR-143 and miR-145 expression in premiR transfected HSV ECs.

HSV ECs were incubated overnight with media alone (control) or transfected with medium + SiPORT NeoFX alone (Mock), or 10 nM - 50 nM premiR-143, premiR-145 or premiR-scr. Cells were quiesced in 0.1% FCS for 24 h and isolated for RNA analysis. A-B. Taqman® qRT-PCR of miR-143 and miR-145 expression following transfection with premiRs. C-D. Northern blot analysis of miR-143, miR-145 and U6 expression. *** $P < 0.001$ vs. premiR-scr. $n = 3$.

3.2.3 Functional studies in human primary cells with modulated miRNA expression

In order to ascertain whether modulation of miR-143 or miR-145 expression effects migration of HSV EC or HSV SMCs, scratch assays were performed. Cells were seeded in 6 wells plates and transfected in suspension with SiPORT NeoFX before being serum starved in 0.1% FCS medium for 24h (HSV ECs) or 48 h (HSV SMCs). Vertical scratches were made in the cell monolayer and medium was replaced with either fresh 0.1% FCS or 5% FCS, to determine whether modulation of miR-143 or miR-145 promotes migration in quiescent cells, or alternatively has an inhibitory effect on serum evoked migration. Analysis of migration over 24 h revealed that HSV SMCs maintained in 5% FCS medium migrated approximately

100-150 μm more than those maintained in 0.1% FCS medium (Figure 3.12). However, no significant difference in migration was detectable in HSV SMCs transfected with premiR-143, premiR-145 when compared to premiR-scr (Figure 3.12). Similarly migration of HSV SMCs transfected with antimiR-143 or antimiR-145 was not significantly different from those treated with antimiR-ctl (Figure 3.13). Control HSV SMCs maintained in 5% FCS migrated significantly further than those treated with antimiR-ctl indicating that transfection process may affect migration (Figure 3.13). Increases in miR-143 and miR-145 expression following transfection with premiR-143 and premiR-145 did not result in any significant changes in HSV EC migration (Figure 3.14).

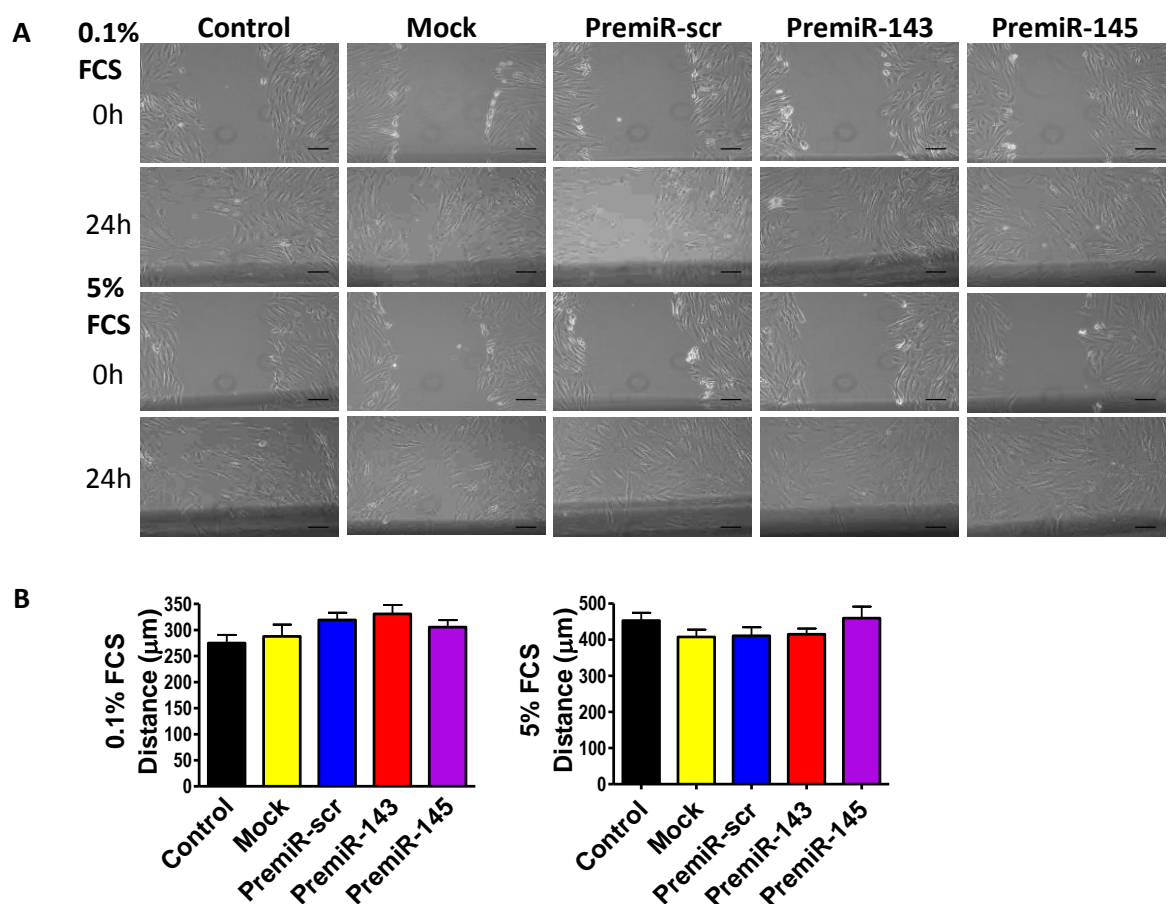


Figure 3.12. Migration of HSV SMCs transfected with premiRs.

HSV SMCs were transfected in 6 well plates at 3×10^5 cells/well with 10 nM PremiRs, medium + SiPORT NeoFX alone (Mock) or medium alone (control) and incubated overnight. Medium was replaced with 0.1% FCS medium and cells were incubated for a further 48 h to promote cell quiescence. Vertical scratches were made in the cell monolayer with a 200 μl pipette tip and media changed to either 0.1% or 5% FCS medium. A. Images taken 0 h and 24 h post scratch to monitor migration into the wound. B. Analysis of Images using ImageJ software showing distance migration over 24h. 10X magnification. Scale bar = 100 μm . n = 3.

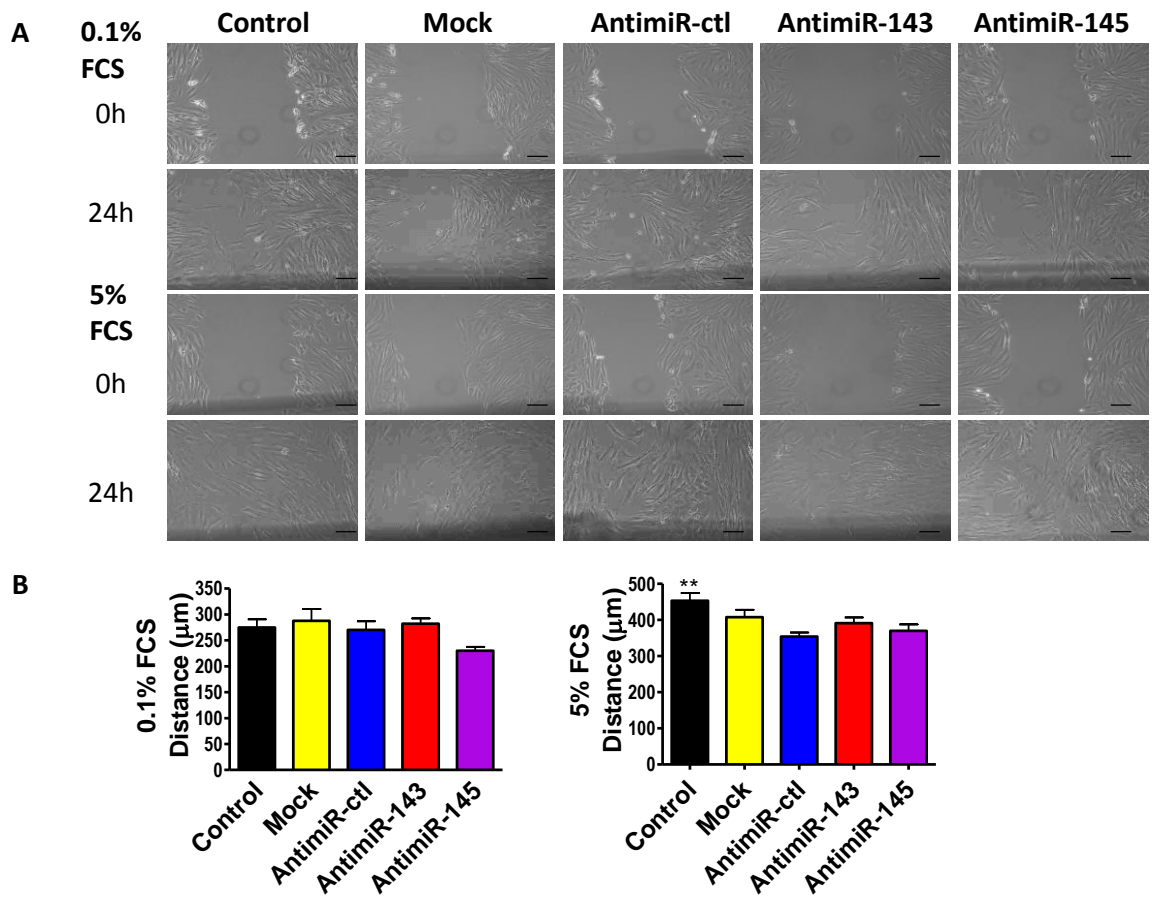


Figure 3.13. Migration of HSV SMCs transfected with anti-miRs.

HSV SMCs were transfected in 6 well plates at 3×10^5 cells/well with 10 nM anti-miRs, medium + SiPORT NeoFX alone (Mock) or media alone (control) and incubated overnight. Cells were quiesced for 48 h in 0.1% FCS medium. Vertical scratches were made in the cell monolayer and medium replaced with 0.1% or 5% FCS medium. A. Images of migration into the wound at 0 h and 24 h post scratch. B. Analysis of Images showing distance migration over 24h. 10X magnification. Scale bar = 100 µm. ** $P < 0.01$ vs. anti-miR-ctl. n = 3.

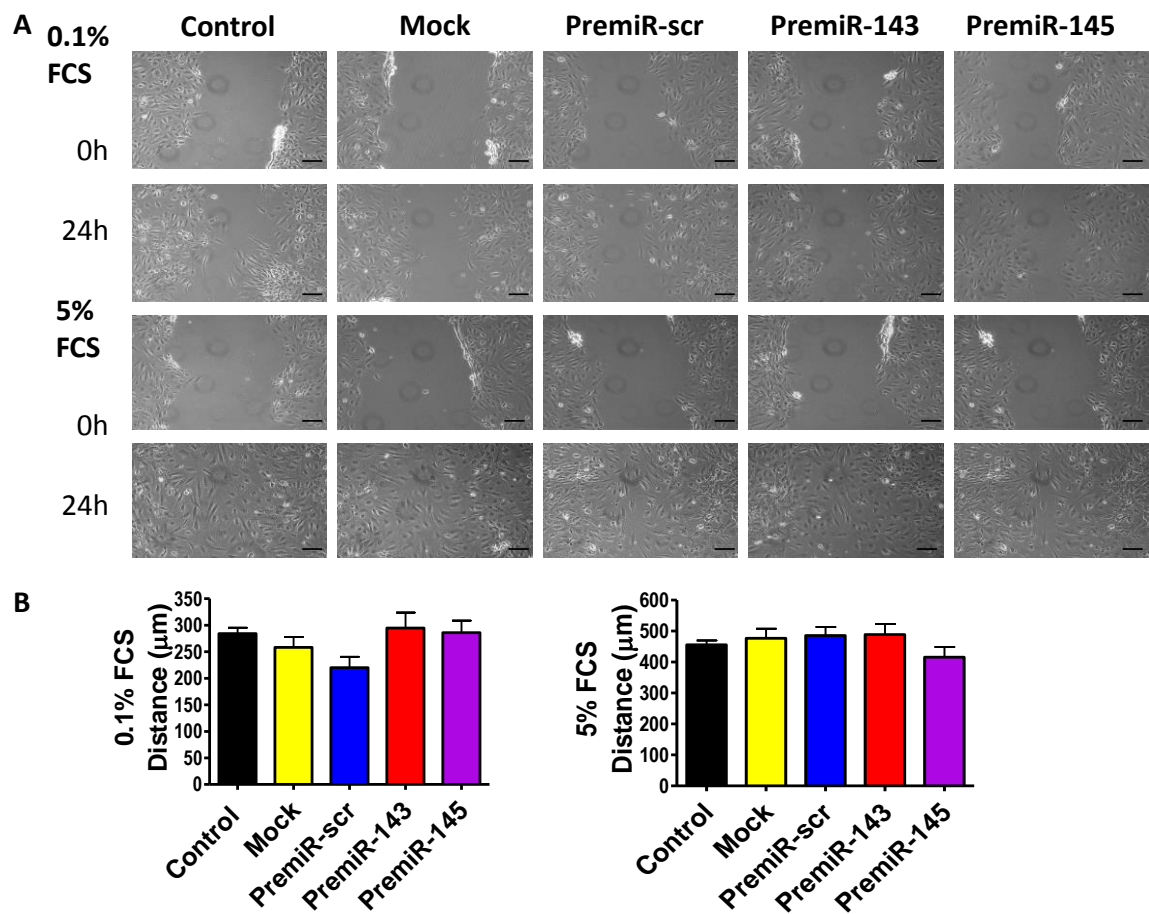


Figure 3.14. Migration of HSV ECs transfected with premiRs.

HSV ECs were transfected in 6 well plates at 3×10^5 cells/well with 10 nM premiRs, medium + SiPORT NeoFX alone (Mock) or medium alone (control) and incubated overnight. Cells were quiesced for 24 h in 0.1% FCS medium before vertical scratches were made in the cell monolayer and media replaced with 0.1% or 5% FCS medium. A. Images of migration into the wound at 0 h and 24 h post scratch. B. Analysis of Images showing distance migration over 24h. 10X magnification. Scale bar = 100 µm. n = 3.

We next assessed the proliferation rates of HSV SMCs and HSV ECs with modulated miR-143 or miR-145 expression. Following transfection with premiRs or antimiRs and serum starvation, cells were immersed in 0.1% or 5% FCS medium for 72 h for proliferation to occur before MTS solution was added and absorbance read at 490 nm. Incubation in 5% medium caused a significant increase in cell proliferation compared to 0.1% medium in both HSV SMCs and HSV ECs (Figure 3.15). No significant difference in proliferation was detectable between HSV SMCs transfected with premiR-143 or premiR-145 compared with premiR-scr (Figure 3.15A). Similarly HSV SMCs transfected with antimiR-143 or antimiR-145 did not show any significant differences in proliferation compared to antimiR-ctl (Figure 3.15B).

Increased cell proliferation was detectable in control (0.1% and 5% FCS) and mock transfected (5% FCS) HSV ECs when compared to premiR-scr (Figure 3.15C). Proliferation of cells transfected with premiR-145 was decreased in cells maintained in 5% but not 0.1% medium (Figure 3.15C).

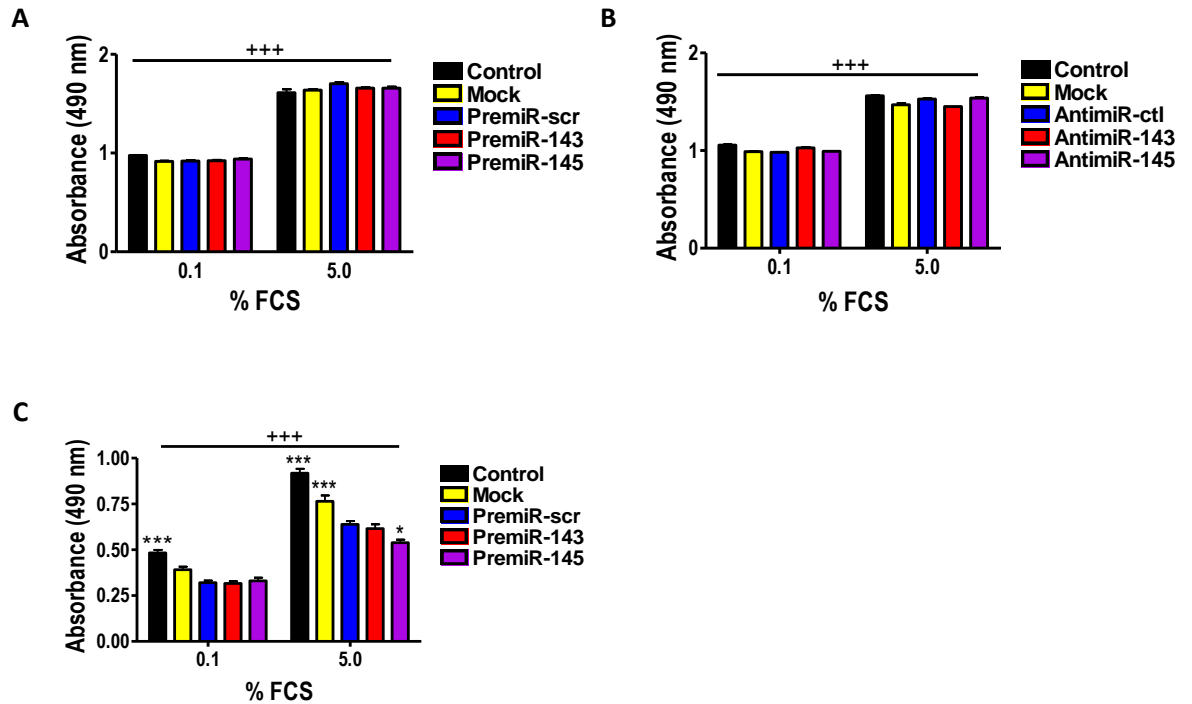


Figure 3.15. Proliferation in primary cells with modulated miR-143 and miR-145 levels.

Cells were transfected in 24 well plates at 4×10^4 cells/well with 10 nM premiRs, medium + SiPORT NeoFX Transfection Agent alone (Mock) or medium alone (control) and incubated overnight. Cells were quiesced for 24 h (HSV ECs) or 48 h (HSV SMCs) in 0.1% FCS medium before transfer to 0.1% or 5% FCS medium for 72 h. Proliferation was measured by MTS assay read at 490 nm. Proliferation of HSV SMCs transfected with premiRs (A) or antimiRs (B). Proliferation of HSV ECs transfected with premiRs (C). +++ $P < 0.001$ vs. 0.1% FCS. * $P < 0.05$, *** $P < 0.001$ vs. premiR-scr. $n = 3$.

To determine whether increasing cellular levels of miR-143 or miR-145 results in increased transfer to exosomes, exosomal RNA was isolated from the media of HSV ECs that had been transfected with premiR-143 or premiR-145 then maintained for 96 h in 0.1% FCS medium. MiR-143 and miR-145 expression in HSV ECs was more than 1000-fold 5 days post-transfection with premiRs (Figure 3.16 A-B). Despite a trend for increased miR-143 and miR-145 expression in exosomes

treated with premiR-143 or premiR-145 this did not reach significance (Figure 3.16 C-D).

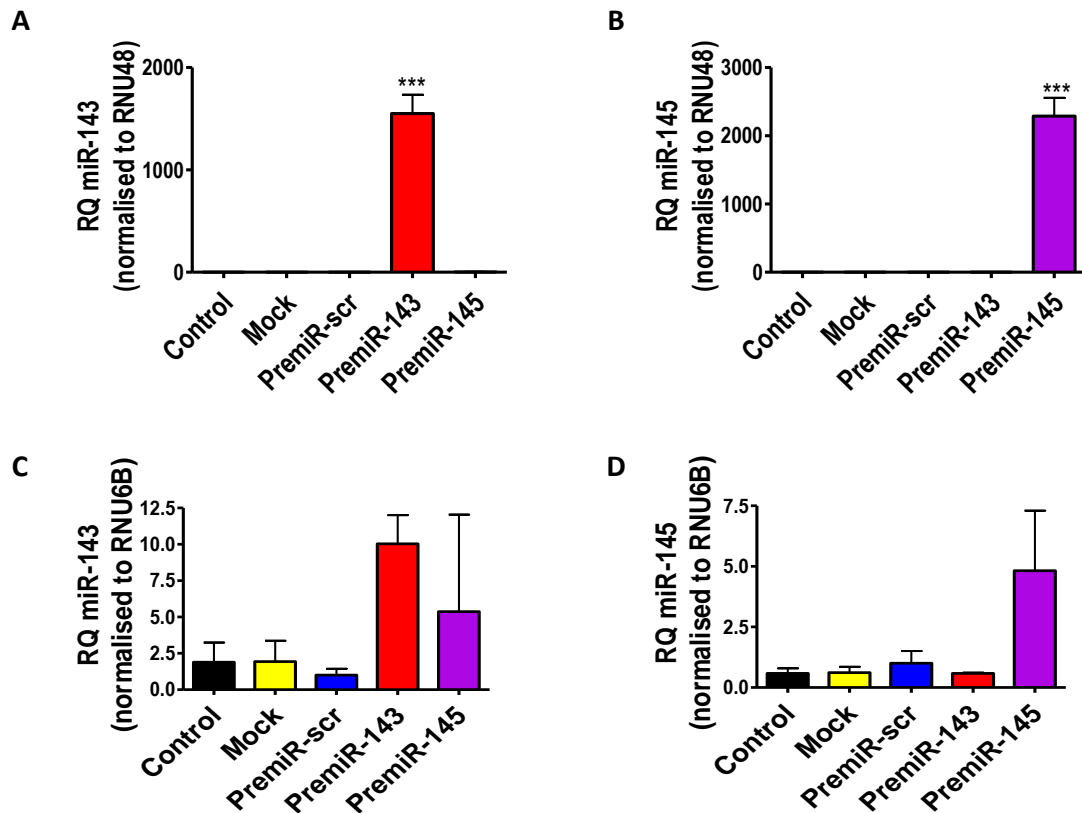


Figure 3.16. MiR-143 and miR-145 expression in HSV EC exosomes.

HSV ECs were transfected in suspension with SiPORT NeoFX with 10 nM premiR-143, premiR-145 or premiR-scr and seeded at 3×10^5 cells/well in 6 well plates. The following day cells were transferred to 0.1% FCS medium and incubated for 96 h. Exosomes were isolated from the cell medium and subjected to Taqman® qRT-PCR analysis. A-B. MiR-143 and miR-145 expression in HSV ECs. C-D. miR-143 and miR-145 expression in HSV EC exosomes. n = 3.

3.2.4 Analysis of miR-143 and miR-145 target expression

MiRNAs act by negatively regulating the expression of target genes by binding to mRNA sequences and preventing translation either through miRNA degradation or inhibition. Decreased expression of a miRNA may therefore lead to increased levels of target mRNA. Likewise, increasing the expression of a miRNA may decrease levels of its target mRNA. Expression of miR-143 and miR-145 targets was analysed in HSV SMCs following transfection with 10 nM premiRs and

antimiRs by Taqman® qRT-PCR. Expression of KLF4 and KLF5 was significantly upregulated by anti-miR-143 compared with anti-miR-ctl (Figure 3.17A-B). However, expression of ACE, ELK-1, ITGBL1 or FSCN1 was not significantly altered (Figure 3.17C-F). In cells transfected with premiRs no significant changes in target mRNA expression were detectable for KLF4, KLF5, ELK-1, ACE, ITGBL1, or TGF β 2 (Figure 3.18).

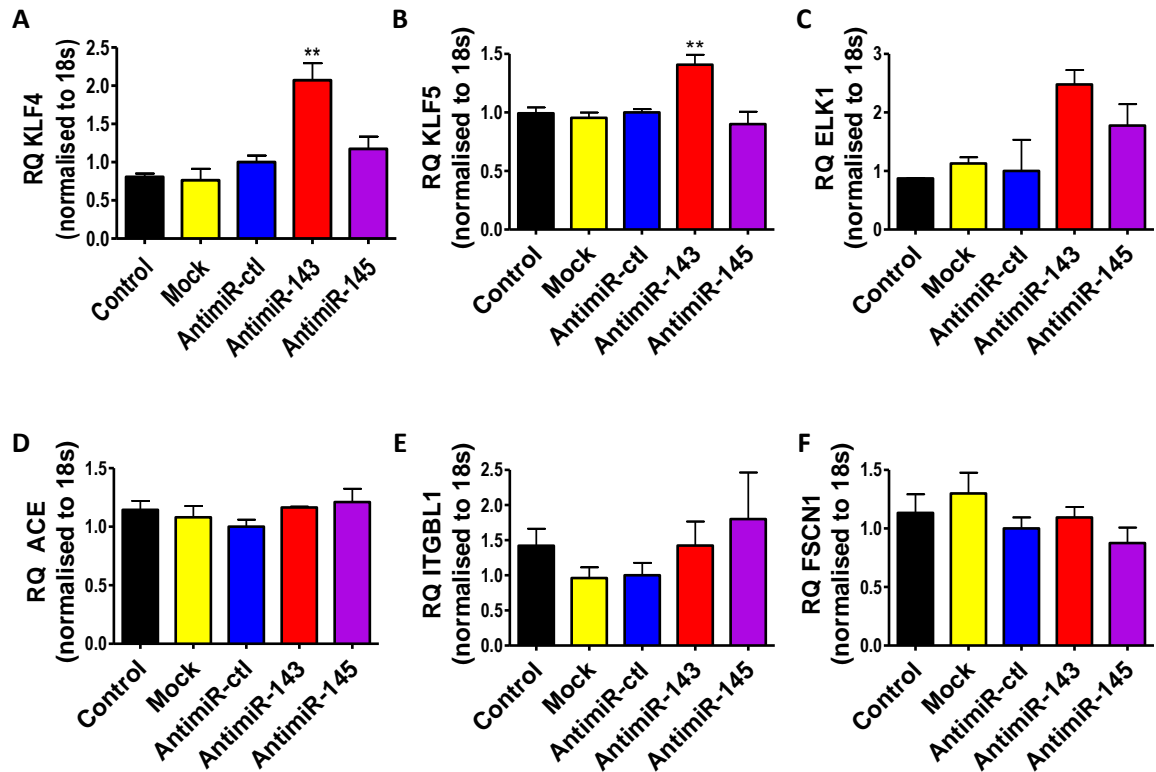


Figure 3.17. Target mRNA expression in HSV SMCs transfected with anti-miRs.

Expression of miR-143 or miR-145 targets KLF4 (A), KLF5 (B) ELK-1 (C) ACE (D) ITGBL1 (E) and FSCN1 (F) was analysed by qRT-PCR in HSV SMCs 48 h post transfection with 10 nM anti-miR-143, anti-miR-145 or anti-miR-ctl. ** $P < 0.01$ vs. anti-miR-ctl. $n = 3$.

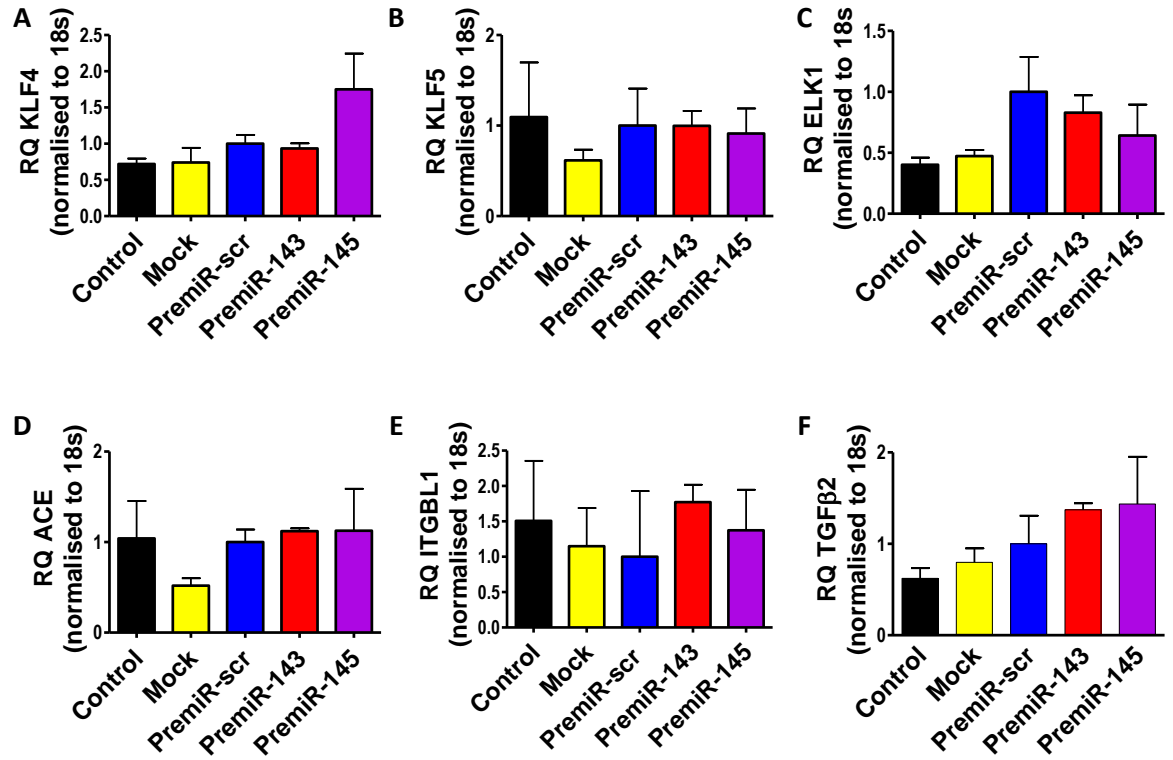


Figure 3.18. Target mRNA expression in HSV SMCs transfected with premiRs

Expression of miR-143 and miR-145 targets KLF4 (A) KLF5 (B) ELK-1 (C) ACE (D) ITGBL1 (E) and TGFβ2 (F) in HSV SMCs 48 h post transfection with premiR-143, premiR-145 or premiR-scr. n = 3.

3.3 Discussion

In summary, it was shown that transduction of human primary cells with Ads that express pre-miR-143 or pre-miR-145 resulted in increased expression of the mature miRNA but was associated with toxicity issues. Modulation of mature miR-143 or miR-145 expression levels using premiR miRNA mimics and anti-miR miRNA inhibitors was found to have no effect on HSV SMC proliferation or migration. Migration of HSV ECs was not affected by premiR overexpression of miRNAs but results of proliferation assays were inconclusive and require further investigation. KLF4 and KLF5 expression levels increased following anti-miR-143 delivery suggesting that target de-repression had occurred. However, the expression of other previously identified targets remained unchanged in response to modulation of miR-143 or miR-145 levels.

AdmiR-143 and AdmiR-145 encode pre-miR-143 and pre-miR-145 which require processing in the cell by Dicer and its cofactors into mature miRNA (Chendrimada et al., 2005). Successful processing on the pre-miRNA transgenes was confirmed by increased expression of mature miR-143 and miR-145 in cells following transduction by AdmiR-143 and AdmiR-145. The degree of miRNA overexpression following incubation with AdmiR-143 or AdmiR-145 was greatest in HeLa cells, which readily express CAR (Bergelson et al., 1997) and lower in HSV ECs and HSV SMCs which have little to no detectable CAR expression respectively (Havenga et al., 2001). CAR is the primary attachment receptor utilised by Ad5 (Bergelson et al., 1997) to enter the cell and thus it is probable that the availability of CAR acted as a rate-limiting step for viral transduction. This was overcome by use of high doses of Ad in primary cells in order to increase transduction.

A previous study showed that activity of the CMV promoter is significantly reduced in cells maintained in the G0/G1 versus the S phase of cell cycle and leads to lower transgene expression (Brightwell et al., 1997). Furthermore, the addition of serum to cells maintained in G0/G1 promotes accelerated transcription and transgene expression by the CMV promoter, which importantly is not associated with any change in the number of cells in the S phase (Brightwell et al., 1997). This serum responsive aspect of CMV activity was evident in AdmiR-143 and AdmiR-145 transduced HSV SMCs, in which increases in

miRNA expression were absent in serum-starved cells but evident in cells maintained in the presence of FCS. Conversely, detectable increases in miR-143 and miR-145 expression were apparent in serum-starved HSV ECs transduced with AdmiR-143 and AdmiR-145. We hypothesise that this superior transduction of HSV ECs by Ads is due to their greater expression of CAR, which would result in a greater fold increase in transgene expression. Reduction in CMV activity by serum starvation would therefore still result in detectable transgene expression in HSV ECs. Other contributing factors may have included the shorter period of serum starvation (24 h vs. 48 h) and lower basal expression of miR-143 and miR-145 in HSV ECs when compared to HSV SMCs.

Ad transduction of HSV SMCs had a negative effect on overall cell migration which was significantly reduced compare to control cells. This was most likely due to toxicity caused by the high doses of Ads required to obtain adequate transduction and miR-143 and miR-145 overexpression. Migration of HSV ECs was significantly reduced following transduction with AdmiR-145 but conversely transfection with premiR-145 was found not to significantly alter HSV EC migration. This may be due to each Ad having a different VP:PFU ratio, which results in variation in the PFU/cell between Ads at a defined VP. Therefore a higher PFU/cell may have resulted in toxicity and reduced migration in HSV ECs transduced with AdmiR-145. Thus Ad5-based vectors were not optimal for functional studies in primary cells.

One method to overcome poor transduction of HSV SMCs by AdmiR-143 and AdmiR-145 would be retargeting the vectors to utilise a receptor more readily expressed on vascular cells. Subgroup B Ads enter cells through a CAR-independent mechanism by binding to the CD46 cellular receptor which is readily expressed on VSMCs (Gaggar et al., 2003, Parker et al., 2013). Transduction of HSV SMCs with Ad35, a subgroup B Ad, is significantly greater than that which occurs with an equivalent dose of Ad5 (Parker et al., 2013). Modification of the Ad5 to contain targeting components of subgroup B Ads, termed 'pseudotyping' is another method being extensively studied to enhance Ad5 transduction of cells with low CAR expression. Transduction of HSV SMCs and vascular ECs is significantly improved when the fiber region of Ad5, which mediates cell binding, is replaced with that of subgroup B Ad16 (Havenga et al., 2001). Delivery of pre-miR-143 and pre-miR-145 to vascular cells using a subgroup B Ad

vector would allow transduction to occur at lower doses and thus potentially avoid toxicity issues associated with the high doses of Ad5 needed to transduce these cells.

Transfection of primary cells with premiRs and antimiRs offered an alternative mechanism of modulating miRNA expression without the need for Ads. PremiRs produced a greater fold increase in miRNA levels when compared with Ads as they were transfected directly into cells and were not limited by CAR expression or activity of the CMV promoter. PremiRs also require less processing within the cell as they exist as mature duplexes.

Previous reports have indicated that miR-143 and miR-145 expression is associated with a non-proliferative phenotype *in vitro* (Cheng et al., 2009, Cordes et al., 2009). Knockdown of miR-143 expression using an antimiR has been shown to double the proliferation rate in the rat A10 VSMC line (Cordes et al., 2009). Furthermore, miR-145 overexpression reduced PDGF-induced proliferation in A10 cells and primary rat VSMCs (Cordes et al., 2009, Cheng et al., 2009). Our study found that proliferation of HSV SMCs was not affected by premiR mediated overexpression or antimiR mediated knockdown of miR-143 or miR-145 levels. These different observations may be due to species differences with the importance of modulating these miRNAs less significant in human VSMCs than rat VSMCs. It also may be indicative of the need for a specific proliferative stimulant such as PDGF in order for the anti-proliferative effects of miR-143 or miR-145 to be observed. PDGF is a potent regulator of VSMC gene expression and proliferation, and has been previously shown to decrease miR-143 and miR-145 expression in cells (Cheng et al., 2009, Quintavalle et al., 2010). FCS also promotes cell proliferation but contains an array of growth factors which are likely to affect cells through a number of signalling pathways, thus modulation of miR-143 or miR-145 alone may be insufficient to affect cell proliferation.

Migration of medial VSMCs to the intima occurs following injury to the vessel wall and is a major contributing factor to neointimal formation (Clowes and Schwartz, 1985). Migration was measured by scratch assay which is a model of wound healing where cells migrate to replace injured or denuded cells (Liang et al., 2007). Neither premiR-mediated increase nor antimiR-mediated decrease in miR-143 or miR-145 expression affected VSMC migration in the presence or

absence of FCS which was used as a non-specific promoter of cell migration. These results indicate that modulation of miR-143 or miR-145 alone is not sufficient to affect HSV SMC migration.

A reduction in HSV ECs proliferation was seen following transfection with premiR-145 which indicates that miR-145 can have functional effects on cell types other than SMCs. However, proliferation of transfected HSV ECs was often less than control or mock transfected HSV ECs. MTS assays are an indirect measure of cell proliferation that measure the bioreduction of MTS by living cells, the absorbance of the product is directly proportional to cell number. This does not take cell viability into account and the transfection process may have reduced viability of HSV ECs which would result in lower absorbance. As such, further studies are now required to ascertain whether premiR-145 affects HSV EC proliferation. One way of doing this would be to perform a 5-bromo-2-deoxyuridine (BrdU) assay. BrdU is a thymidine analogue which is incorporated into DNA in place of thymidine during synthesis in proliferating cells (Porstmann et al., 1985). Incorporated BrdU can then be detected using an immunoassay which produces a colourmetric change that can be detected by spectrophotometer to give an absorbance directly related to cell proliferation. BrdU may be preferable over MTS assays as it is a measure of DNA synthesis and is not affected by cell viability.

KLF4 and KLF5 are previously identified targets of miR-143 and miR-145 (Cordes et al., 2009, Cheng et al., 2009, Xin et al., 2009). HSV SMCs transfected with anti-miR-143 had increased mRNA levels of KLF4 and KLF5 suggesting that target de-repression occurs following knockdown of miR-143 expression. Conversely, premiR-143 did not alter KLF4 or KLF5 mRNA levels. One reason for this may be that KLF5 is maintained at a baseline level by miR-143 in HSV SMCs which cannot be further lowered by increasing miR-143 levels, perhaps due to greater availability of other targets under these conditions. Another reason for this could be that despite the large increases in miRNA expression following transfection with premiRs, incorporation of the guide strand into the RISC may be rate limited and therefore the actual increase in functioning mature miR-143 or miR-145 may be much lower. One way of assessing this would be to use a 'pull-down' assay where a transfected biotinylated miRNA mimic is isolated from cell lysates, first by using an antibody against Ago proteins and then by streptavidin

bead isolation of the bound biotinylated miRNA mimic (Nonne et al., 2010, Beitzinger et al., 2007). This would allow a measure of the amount of functional miRNA mimic following transfection. MiR-145 is a more potent repressor of KLF4 and KLF5 than miR-143 in COS cells and human pulmonary artery SMCs (Xin et al., 2009, Davis-Dusenbery et al., 2011). However, neither premiR-145 nor anti-miR-145 significantly altered KLF4 or KLF5 mRNA levels in HSV SMCs, suggesting that these targets may be preferentially regulated by miR-143 in these cells.

No other previously identified targets investigated in this study were significantly altered by miR-143 or miR-145 knockdown or overexpression in HSV SMCs. We hypothesise that this is due to a number of reasons. Firstly, several of the miR-143 and miR-145 targets investigated in this study were identified as targets by luciferase assays in cells (Xin et al., 2009, Cordes et al., 2009, Cheng et al., 2009). One issue with this is that it involves overexpression of both the miRNA and the 3' UTR target within the cell and therefore it is perhaps unsurprising that target regulation at the complementary site would occur under these circumstances. Although beneficial in identifying whether target regulation can occur, luciferase assays do not necessarily reflect endogenous target regulation, where one target is unlikely to be over-represented at such a level.

Another possible reason why target regulation is not apparent in premiR and anti-miR treated cells may be that target mRNA is being repressed rather than degraded. As a result, target regulation may only be seen at the protein level. This has been observed for ELK-1 and KLF4 following treatment with anti-miR-143 or anti-miR-145 in A10 cells (Cordes et al., 2009). However, others have detected regulation of ELK-1 and KLF4 at the mRNA level following increasing levels of miR-143 and miR-145 in human aortic and pulmonary artery SMCs (Davis-Dusenbery et al., 2011, Hergenreider et al., 2012). Further studies could be carried out to investigate this by performing western blots to look at protein expression of targets following transfection with premiRs and anti-miRs.

Furthermore, modulating miR-143 and miR-145 expression alone may not be sufficient to alter target expression without the influence of certain signalling pathways. MiR-143/miR-145 expression is transcriptionally activated by signalling

molecules including SRF-myocardin/MRTF, TGF- β and BMP4 whereas their expression is repressed by PDGF (Cheng et al., 2009, Cordes et al., 2009, Xin et al., 2009, Davis-Dusenbery et al., 2011, Long and Miano, 2011). MiR-145 expression is essential for downregulation of KLF4 by TGF- β and BMP4 in human pulmonary artery SMCs (Davis-Dusenbery et al., 2011). PDGF-induced increases in KLF5 expression are inhibited by premiR-145 and enhanced by miR-145 inhibition (Cheng et al., 2009). Increased expression of contractile genes, including α -SMA, SM22 α and calponin, by TGF- β , BMP4 and Notch signalling is reduced by miR-145 inhibition (Davis-Dusenbery et al., 2011, Boucher et al., 2011) whereas PDGF-induced downregulation of contractile gene expression is partially rescued by premiR-145 (Cheng et al., 2009). This evidence together suggests that miR-143 and miR-145 are important downstream regulators of several signalling molecules which regulate VSMC phenotype. However, these signalling pathways are likely to affect a whole host of other genes and miRNAs which combine to produce a phenotype. Thus modulation of miR-143 and miR-145 levels alone may not be sufficient to significantly alter target expression.

It has been reported that KLF2 activates transcription of miR-143/145 in HUVECs, resulting in increased expression levels of miR-143 and miR-145 in exosomes (Hergenreider et al., 2012). These exosomes were shown in a co-culture system to mediate functional miR-143 and miR-145 transfer from HUVECs to human aortic SMCs. This paracrine transfer of miRNAs from ECs to SMCs is potentially very significant as it could allow SMC miRNA levels to be altered by delivery of miRNAs to the overlying EC layer of the vessel wall. In our study, treatment with premiR-143 and premiR-145 produced non-significant increases in miR-143 and miR-145 expression in HSV EC exosomes. Interestingly, KLF2 was previously reported to enrich miR-143 and miR-145 in exosomes by around 30-fold compared with around 10-fold increase in HUVECs (Hergenreider et al., 2012). In contrast to this our study found that premiRs increased miR-143 and miR-145 expression in HSV ECs by more than 1000-fold but did not significantly increase expression in exosomes. The discrepancy may be due to the direct increase in mature miRNA with premiRs versus the transcriptional activation of miR-143 and miR-145 by KLF2. KLF2 expression is induced in ECs by sheer stress and has important roles in managing vessel tone through regulation of a host of genes (Dekker et al., 2005). Enrichment of miR-143/145 in exosomes may

require additional signalling which is not activated by premiR transfection. Interestingly transfection of cel-miR-39, a *C. elegans* miRNA which is not expressed in human cells, did result in transfer to vesicles (Hergenreider et al., 2012), suggesting that endogenous miRNA may be under more rigorous regulation.

In summary, it was shown that miR-143 and miR-145 expression can be successfully modulated in human primary cells using Ad5 vectors that express pre-miRNA sequences but that other methods are preferable due to toxicity issues. It was shown that modulation of miR-143 and miR-145 expression is not sufficient to significantly effect *in vitro* migration or proliferation of HSV SMCs and results in altered expression of only a small number of target mRNA. Additional studies or new methods to confirm results were suggested but could not be further investigated due to time constraints.

4 Analysis of neointimal formation in a mouse model of in-stent stenosis

4.1 Introduction

Atherosclerotic plaques that impinge on the lumen can reduce blood and oxygen flow to the heart, causing the symptoms of angina. PCI is the most common procedure carried out to treat this severe narrowing of the arteries (British Heart Foundation, 2012). During the procedure the lumen is re-opened by inflation of a balloon angioplasty catheter which compresses the atherosclerotic plaque against the vessel wall. The most common PCI's performed today involve deployment of a metal stent at the time of inflation, which acts as a scaffold to help maintain the resultant increase in lumen size (Serruys et al., 1994, Sigwart et al., 1987, Fischman et al., 1994).

During deployment, stent expansion causes denudation of the endothelium and stretch and injury to the vessel wall. This triggers a signalling cascade involving the release of cytokines and growth factors from inflammatory cells, injured ECs, VSMCs and platelets which drives inflammation and promotes activation of VSMCs which migrate and proliferate from the media to form the neointima (Libby et al., 1992, Schwartz et al., 2004). Proliferation, migration and ECM production by VSMCs is the major cause of neointimal formation after vascular injury (Clowes and Schwartz, 1985, Clowes and Clowes, 1985).

DES were developed to circumvent the issue of in-stent restenosis. DES are coated with polymers which elute cell cycle inhibitory drugs, for example sirolimus or paclitaxel, over a 4-6 week period to lessen the initial proliferative response to injury following stent deployment (Htay and Liu, 2005). DES have been highly successful at reducing restenosis rates when compared to first generation BMS, confirming that the inhibition of proliferation produces a substantial clinical benefit following stenting (Schampaert et al., 2006, Stone et al., 2009).

However, several studies have reported that DES are associated with an increased risk of late in-stent thrombosis (Bavry et al., 2006, Joner et al., 2006, Luscher et al., 2007), although there are conflicting arguments about the risk (Moreno et al., 2005, Schampaert et al., 2006, Caixeta et al., 2009). DES inhibit not only VSMC but also EC proliferation, which is detrimental as denudation of the EC lining of the artery following stent deployment exposes the blood to a

thrombogenic surface (Joner et al., 2006). DES delay healing of the artery by reducing EC repopulation following stent deployment (Finn et al., 2007). This process has been shown to occur through direct inhibition of EC proliferation by DES and not as a consequence of uncovered stent struts due to reduced VSMC proliferation and migration (Douglas et al., 2012). Therefore new therapies are needed to prevent VSMC proliferation and migration without affecting ECs.

Porcine models of stenting are the gold standard for preclinical studies as the overall action of different therapies in this model have correlated well with human clinical studies (Schwartz et al., 2004). The procedure commonly involves accessing the circulation via cutdown of an artery such as the femoral artery and guiding the catheter through the circulation to one of the coronary arteries where the stent is then deployed (Lowe et al., 2003). This results in the development of a defined neointima over 28 days which is proportional to the degree of damage to the vessel wall (Schwartz et al., 1992). Porcine models of stenting share many of the major characteristics of clinical in-stent restenosis including early mural thrombus formation at the stent struts, inflammation, VSMC proliferation and migration and re-endothelialisation (Schwartz et al., 2004, Lowe et al., 2003). However, large animal models are expensive and not ideal for early investigative studies.

Several small animal models of stenting have now been developed including mouse models, which provide the advantage of being able to utilise genetically altered strains (Rodriguez-Menocal et al., 2010, Chamberlain et al., 2010, Ali et al., 2007). *In situ* stenting of the abdominal aorta has been described by several different methods (Rodriguez-Menocal et al., 2010, Chamberlain et al., 2010). One technique involves feeding a catheter with a spring loaded metal wire through the femoral artery to the aorta where wire deploys to form a spring (Chamberlain et al., 2010). A drawback of this technique is that the coiled shape of the spring means that this model is unlikely to mimic the medial angulation and stretch that occurs clinically following stent deployment and is associated with degree of injury (Schwartz et al., 1992). Direct stenting of the abdominal aorta has also been performed via insertion of a catheter through a direct access point made in the aorta which is then resealed (Rodriguez-Menocal et al., 2010). This produced a modest neointima in ApoE KO mice but very little neointimal formation in C57BL/6 mice (Rodriguez-Menocal et al., 2010) suggesting that this

model would not be ideal to study neointima formation in mice without underlying inflammation or hypercholesterolemia. Furthermore both models were associated with incidence of hind limb paralysis due to damage to the femoral artery and/or thrombosis (Chamberlain et al., 2010, Rodriguez-Menocal et al., 2010).

The mouse model of stenting developed by Ali and colleagues (Ali et al., 2007) involves stenting of the thoracic aorta of a 'donor' mouse which is then isolated and interposition grafted into the carotid artery of a recipient mouse. The model utilises a 2.5 X 0.6 mm stainless steel stent which is expanded to a final diameter of 1.25 mm. The stent was designed to produce comparable vessel stretch, medial angulation, distance between struts and strut coverage to what occurs clinically (Ali et al., 2007). This model was shown to produce a defined neointima over 28 days in C57BL/6 mice indicating that it is a suitable model to investigate the influence of miRNA expression on in-stent stenosis.

Processing of stented tissue for histology is challenging as the presence of a metal stent prohibits traditional paraffin embedding and sectioning. Stented vessels are commonly processed by embedding in a plastic resin which exhibits considerably more durability than paraffin to allow sectioning with a rotary saw. Several drawbacks are associated with resin embedding as sectioning of resin produces sections that are thicker and as a result less numerous than paraffin and the resin itself hinders the use of many immunohistochemical stains (Rippstein et al., 2006, Malik et al., 1998). A study by Bradshaw and colleagues (Bradshaw et al., 2009) described a method of dissolving human stents by applying a differential voltage across the stented vessel in a weak acid/salt solution which resulted in the metal stent forming ions in solution and thus being removed. Electrolysis is therefore a potential method to circumvent the issues associated with processing stented vessels.

This chapter describes a small pilot study designed to reproduce a mouse model of in-stent stenosis which can then be utilised for further *in vivo* experiments to investigate the role of miRNAs in neointimal formation. The potential of using electrolysis as a means of processing stented vessels is also investigated.

4.2 Aims

- To reproduce a mouse model of in-stent stenosis that can be used for future *in vivo* studies.
- To determine whether electrolysis of stents from mouse vessels is a practical method of processing stented tissue.

4.3 Results

4.3.1 Vessel morphology following stent electrolysis

The stented vessels of C57BL/6 mice were isolated 28 days post-surgery and fixed in 10% formalin. Stents were electrolysed from the surrounding tissue by electrolysis prior to embedding in paraffin. H&E staining was performed on 5 μm sections to assess vessel morphology. A defined neointima that surrounded the stent struts was seen in all vessels that underwent successful electrolysis (~60%) (Figure 4.1). Electrolysis where all stent struts successfully dissolved permitted sectioning by microtome. However, some damage did occur to vessels due to the nature of the electrolysis technique (Figure 4.1). Frequently, stent electrolysis was non-uniform with the outer edge of a stent strut dissolving and leaving the remainder of the strut intact. When this occurred in each strut of a vessel the stent could no longer be hooked on to the expansion spring to continue electrolysis. In these cases loosely attached struts were manually removed with forceps prior to being sectioned.

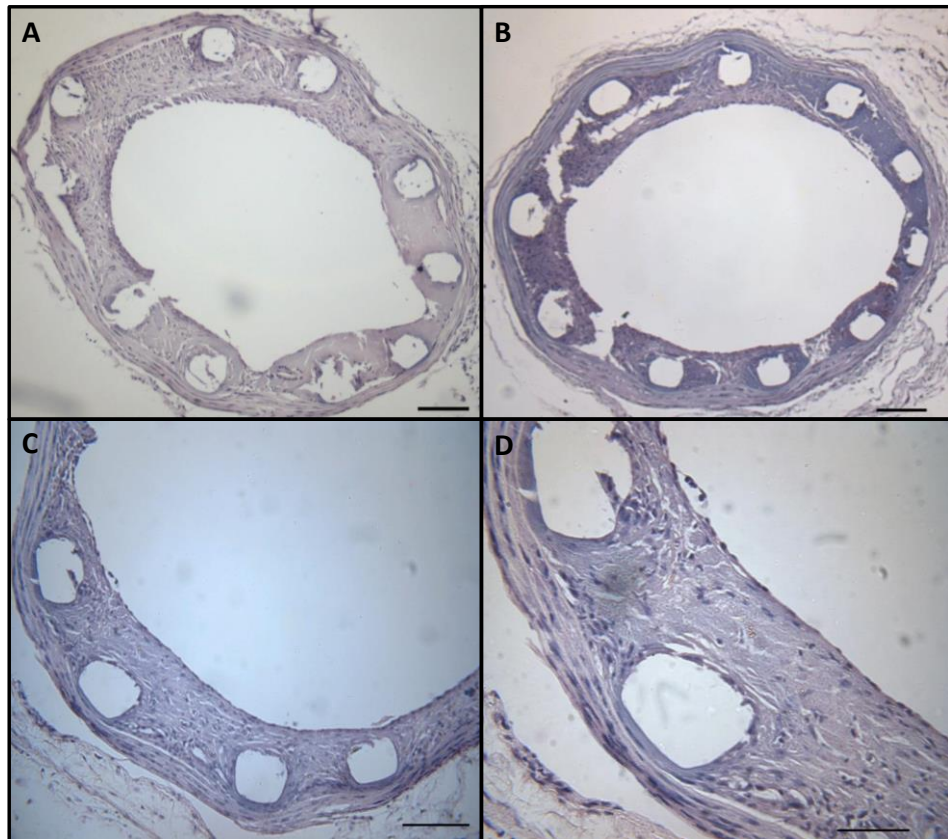


Figure 4.1. Morphology of electrolysed vessels from C57BL/6 mice stained with H&E.

Stented vessels were isolated 28 days post-operative and fixed in 10% formalin. Electrolysis was performed to remove the stent from the surrounding vessel prior to embedding in paraffin and sectioning using a microtome. Sections were stained with H&E to visualise vessel morphology. Representative images are shown at 10X (A-B), 20X (C) and 40X magnification (D). n = 6. Scale bar = 100 μ m (A-C) and 50 μ m (D).

4.3.2 Neointimal formation in C57BL/6 mice 28 day post-stenting

Morphometric measurements were performed on electrolysed sections to quantify the degree of neointimal formation 28 days post-stenting (Table 4.1). Stented sections displayed a defined neointima layer which surrounded the stent struts, with an average neointimal thickness of 96.29 μm and strut depth of 55.98 μm . Neointimal area was approximately 0.19 mm^2 with a lumen area of 0.24 mm^2 and an average percentage stenosis of 37.66%. Injury score was consistent between animals.

Table 4.1. Neointimal measurements from 28 day stented C57BL/6 mice.

Measurement	C57BL/6 mice day 28
Neointimal thickness μm	96.29 \pm 6.08
Strut depth μm	55.98 \pm 6.97
Neointimal area mm^2	0.19 \pm 0.03
Total vessel area mm^2	0.54 \pm 0.02
Medial area mm^2	0.08 \pm 0.01
Lumen area mm^2	0.24 \pm 0.03
Neointimal:medial	1.87 \pm 0.04
% stenosis	37.66 \pm 0.98
Injury Score	0.05 \pm 0.03

Measurements were performed using Image-Pro® Analyzer 7.0 software. n = 6.

4.3.3 Composition of neointima in 28 day stented C57BL/6 mice

In order to determine the cell types comprising the neointima a variety of histological stains for common neointimal components were performed. EVG staining revealed that the neointima of 28 day stented vessels contained a high proportion of collagen and elastin indicating an abundance of ECM (Figure 4.2).

VSMCs migration and proliferation to the intima and ECM production is a major contributor to neointimal formation and in-stent restenosis in humans. Therefore, to determine whether VSMCs were present in the neointima in the mouse stent model immunohistochemistry was performed for α -SMA, a marker of SMCs. DAB staining for α -SMA was seen within the neointima of 28 day stented C57BL/6 mice and was absent in the IgG control sections indicating the presence of VSMCs within the neointima (Figure 4.3). Immunohistochemistry for proliferating cell nuclear antigen (PCNA) which identifies proliferating cells revealed a small number of proliferating cells were present within the neointima of 28 day stented vessels (Figure 4.4 C-D). To gain insight of the inflammatory cell presence in the neointima immunohistochemistry for macrophage marker MAC-2 was performed which detected the presence of macrophages in the neointima of stented vessels (Figure 4.4 A-B).

Immunohistochemistry for CD31, a marker of ECs, was performed to assess whether re-endothelialisation occurred by day 28 following stenting (Figure 4.5). In all sections a thin layer of CD31 staining was that surrounded the lumen was observed indicating an intact EC layer was present.

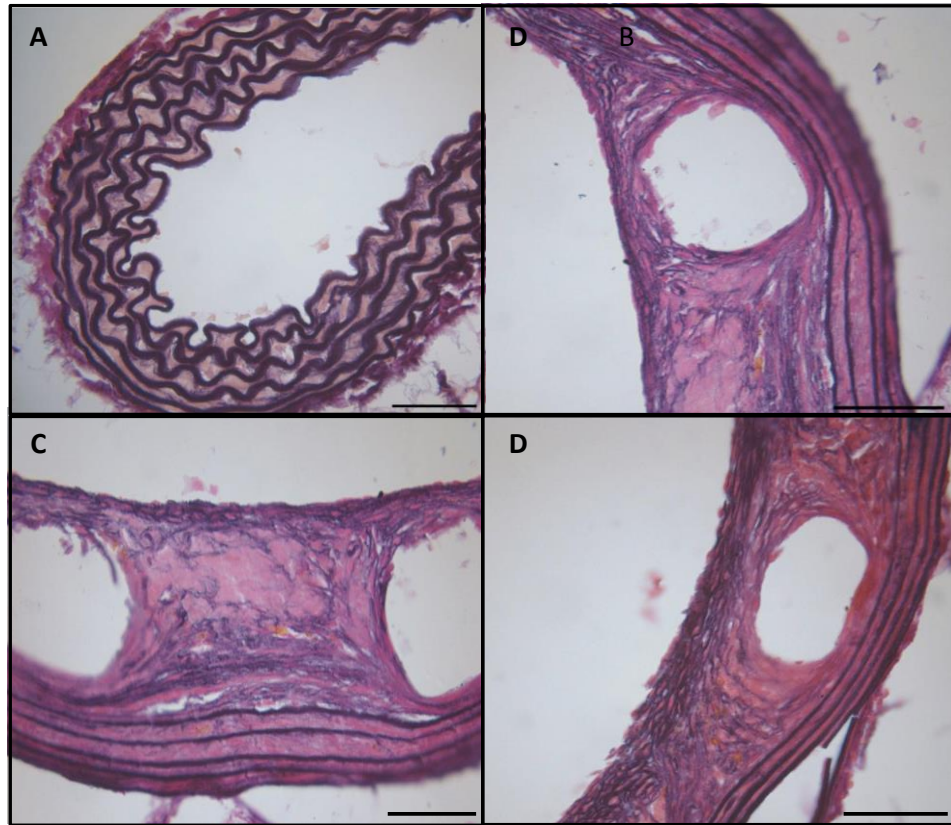


Figure 4.2. EVG staining of electrolysed vessels from C57BL/6 mice.

EVG staining was performed to visualise the elastic lamina and determine the composition of the neointimal layer. Staining revealed a high proportion of elastin (black/purple) and collagen (pink) staining within the neointima. Representative images of control unstented (A) and stented (B-D) aorta. Magnification 40X. n = 6. Scale bar = 50 μ m.

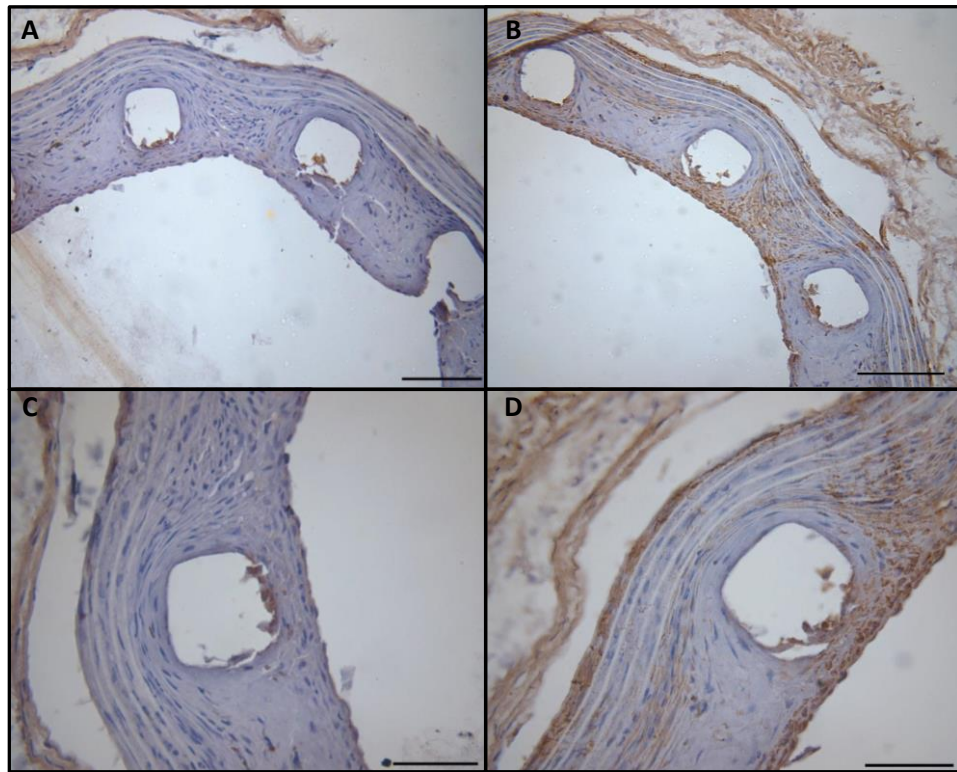


Figure 4.3. α -SMA expression in electrolysed vessels from 28 day stented C57BL/6 mice.

Immunohistochemistry for α -SMA was performed to investigate whether VSMCs formed part of the neointima. α -SMA positive cells are visualised by brown DAB staining. Representative images are shown for IgG control (A and C) and α -SMA (B and D) at 20X and 40X magnification. $n = 6$. Scale bar = 100 μ m (A-B) and 50 μ m (C-D).

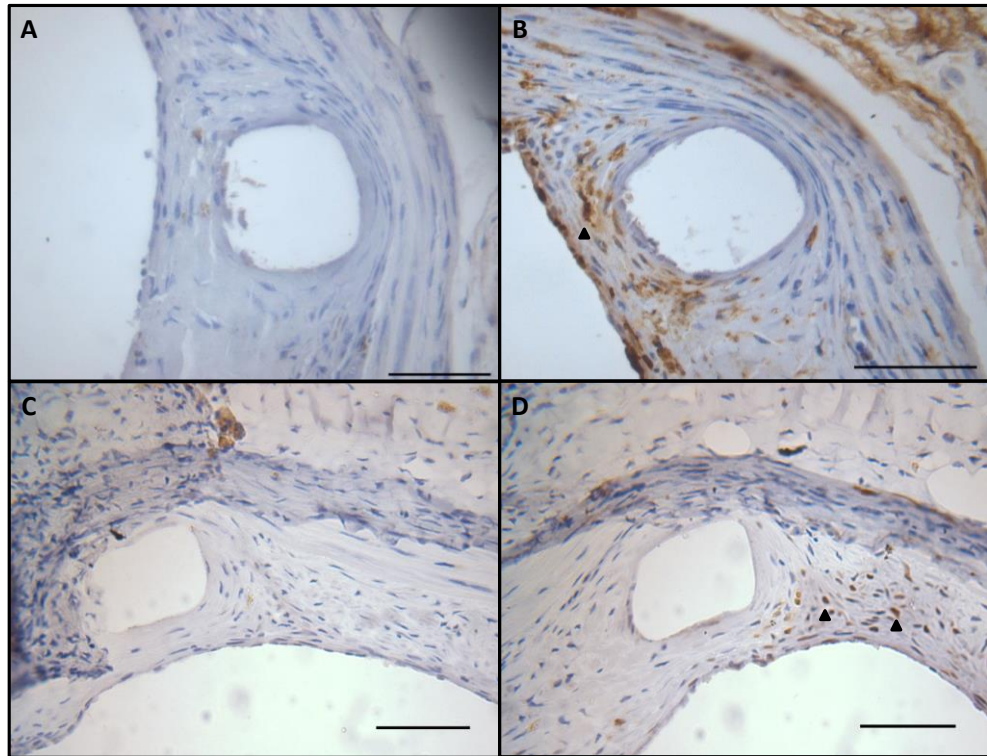


Figure 4.4. MAC-2 and PCNA expression in vessels from 28 day stented C57BL/6 mice
Immunohistochemistry was performed on electrolysed sections for macrophage marker MAC-2 (B) and proliferating cell marker PCNA (arrowheads) (D) and an IgG control (A and C). Positive cells are identified by brown DAB stain. Magnification 40X. n = 6. Scale bar = 50 μ m.

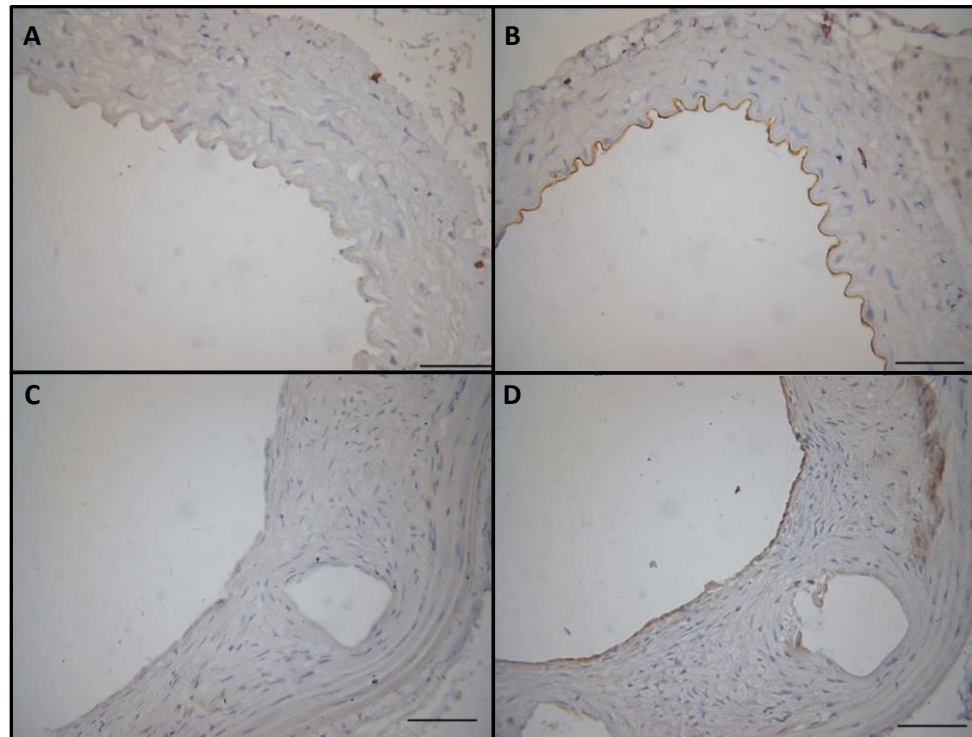


Figure 4.5. CD31 expression in vessels from 28 day stented C57BL/6 mice.

Immunohistochemistry for the EC marker CD31 shown in non-stented control aorta (B) and 28 day stented aorta (D), IgG control (A and C). CD31 staining is visualised by brown DAB (brown) staining. Magnification 40X. n = 6. Scale bar = 50 μ m.

4.4 Discussion

To summarise, this study showed the reproduction of a complex mouse model of in-stent stenosis using the technique originally developed by Ali and colleagues (Ali et al., 2007). BMS were delivered to the thoracic aorta of donor mice and the stented vessels were isolated and interposition grafted into the carotid artery of recipient mice. Stented vessels isolated 28 day post-surgery had a defined neointima surrounding the stent struts which was largely comprised of collagen, elastin and VSMCs. A small number of proliferating cells and macrophages were evident and re-endothelialisation was complete 28 days post-stenting.

Porcine models have been traditionally used to investigate vessel remodelling following stenting as they share structural similarity with the human heart and develop comparable neointimal formation (Schwartz et al., 1992, Miller et al., 1996, Taylor et al., 2001). However, the mouse model of stenting utilised in the present study is advantageous over porcine models, particularly for explorative studies, due to the small size of the animals which enables high throughput and use of genetically modified strains.

Although technically challenging, the model proved highly reproducible and a defined neointimal layer which surrounded the stent struts was observed in all vessels 28 day post stenting. Injury scores were consistent between animals indicating that the degree of injury was comparable between vessels. Stent deployment in the porcine model often leads to fracturing of the internal elastic lamina or medial layers (Schwartz et al., 1992). However, puncture of the internal elastic lamina was rare in the mouse stent model which is most likely due to the elasticity of the mouse aorta versus the muscular coronary arteries of the pig (Lowe et al., 2003).

Proliferation and migration of VSMCs is a pivotal component of neointimal formation (Clowes and Schwartz, 1985, Clowes and Clowes, 1985, Hanke et al., 1990). In the present study α -SMA staining revealed the presence of numerous VSMCs within the neointima of 28 day stented C57BL/6 mice. Furthermore, an abundance of the ECM components collagen and elastin, which are produced by VSMCs (Nikkari et al., 1994, Amento et al., 1991), was also seen within the

neointima, indicating that the mouse model produces a neointima which has a similar composition to that found in porcine models and in clinical restenosis (Lowe et al., 2003). The degree of neointimal formation seen in this study was also comparable with what has been previously reported (Ali et al., 2007), indicating that the model had been successfully reproduced.

Drugs released from DES can result in significant delays and incomplete healing of the endothelium which can lead to late onset in-stent thrombosis (Bavry et al., 2006, Luscher et al., 2007). Re-endothelialisation after injury also appears important in reducing neointimal response with several studies reporting that reduced EC migration and endothelial progenitor cell (EPC) attachment and differentiation is correlated with a greater degree of neointimal formation (Bai et al., 2010, Mayr et al., 2006). It is therefore desirable that any treatment to prevent in-stent restenosis does not delay the re-endothelialisation of vessels. The presence of a defined layer of CD31 positive ECs surrounding the lumen in 28 day stented vessels indicated that re-endothelialisation had occurred by day 28 post-stenting in our model. This is consistent with other models of stenting where re-endothelialisation occurs by day 28 (Joner et al., 2008, Schwartz et al., 2004). EC repopulation in the mouse stent model has been previously shown to occur primarily by proliferation and migration of ECs from the adjacent vasculature and to a lesser extent via EPCs from the bone marrow (Douglas et al., 2012). Our results are in contrast with studies in ApoE KO mice which display impaired re-endothelialisation which is incomplete even at 56 days post-stenting (Douglas et al., 2012), this may be due in part to the reduced number of circulating EPCs in these mice (Xu et al., 2003).

A small number of proliferating cells were detected in the neointima of 28 day stented C57BL/6 mice. This is consistent with previous studies of vascular injury which have detected a high proportion of proliferating cells 7 days after vascular injury which thereafter declines with proliferating cells comprising only around 2% of the neointima by day 28 (Ali et al., 2007, Lindner et al., 1993).

Macrophages play an important role in atherosclerotic plaque formation and progression through the uptake of LDL to form foam cells (Ross, 1993). They also influence plaque remodelling through release of cytokines and growth factors which promote VSMC proliferation and migration (Libby et al., 1992, Assoian et

al., 1987). Furthermore, macrophage presence after vascular injury has been shown to correlate with neointimal lesion size and macrophage inhibition using clodronate liposomes significantly reduces neointimal formation in animal models (Moreno et al., 1996, Danenberg et al., 2002). Consistent with previous reports a small number of inflammatory macrophages were detected in the neointima of 28 day stented mice and tended to be concentrated near the stent struts.

Electrolysis of stents proved challenging due to the small size of the vessels and stent struts often dissolving unevenly. As a result, around 40% of vessels were unusable for morphological analysis. Bradshaw and colleagues (Bradshaw et al., 2009) described similar issues in their study while developing this method. However, the use of human stented vessels in their study meant that undissolved stent struts could be removed manually without causing as much damage as was seen in the delicate mouse vessels. Morphology was more readily conserved in stents that dissolved evenly and these could be embedded in paraffin and cut into thin sections for immunohistochemistry. Further development of this method would be beneficial to optimise the technique and produce more even electrolysis of the stent and negate the need for manual removal of undissolved struts.

Several differences exist between the clinical practice of stenting the mouse model, which are important to consider when interpreting results. Similar to the porcine model the mouse stent model does not involve direct stenting of an atherosclerotic plaque nor does it share the underlying inflammation seen in human atherosclerosis (Ross, 1999). However, potential therapies could be tested in a mouse model of atherosclerosis, such as the ApoE KO mouse (Plump et al., 1992, Piedrahita et al., 1992). ApoE KO mice have elevated blood very-low density lipoprotein (VLDL) and inflammation and start to develop spontaneous atherosclerosis around 6 weeks of age, which can be further exacerbated by high fat feeding (Piedrahita et al., 1992, Plump et al., 1992, Nakashima et al., 1994). These mice have been shown to develop greater neointimal formation than WT mice following stenting without direct stenting of an atherosclerotic plaque (Ali et al., 2007). Another notable difference is that stents are used clinically to press atherosclerotic plaques against the artery wall and therefore restore the lumen to its original diameter. Conversely, the mouse

model involves stretching the vessel wall to a diameter greater than its original size.

The use of donor vessel raises questions about whether engraftment itself may promote neointimal formation to a greater degree than *in situ* stenting. The lumen of a mouse carotid artery is approximately 3-fold smaller than that of the aorta and around 5-fold smaller than the stented aorta (Ali et al., 2007). Therefore blood flow and shear stress may be altered in the model due to the flow of blood from the carotid to the engrafted aorta. This is potentially significant as alterations in shear stress are known to influence atherosclerotic plaque and neointimal formation (Ku et al., 1985, Papafaklis et al., 2009, Sanmartin et al., 2006). Furthermore, an *in situ* model of aortic stenting reported significantly less neointimal formation than what was observed in the present study suggesting that the engraftment process may contribute to neointimal formation (Rodriguez-Menocal et al., 2010). However, engraftment of the uninjured or balloon-catheter injured aorta into the carotid of C57BL/6 mice did not result in any significant neointima formation when compared with control non-engrafted aortas (Ali et al., 2007). This suggests that that majority of neointimal formation seen in our study is due to the mechanical injury of the vessel and presence of the stent.

Despite the differences there are several similarities between the mouse model of in-stent stenosis and the clinical condition in-stent restenosis. Most notably, the mechanical injury to the vessel wall leads formation of a defined neointima comprised largely of VSMCs and ECM (Carter et al., 1994, Ali et al., 2007). This makes the model relevant to investigate the therapeutic benefit of molecules which influence VSMC phenotype.

In summary, 28 day stented C57BL/6 mice had a defined neointimal layer that contained a high proportion of VSMCs and ECM components collagen and elastin. Re-endothelialisation of the vessel had occurred by day 28 which will be important for future studies when determining whether alteration of miRNA levels have a detrimental effect on re-endothelialisation. Finally, electrolysis of stented vessels was a beneficial method as it permitted paraffin embedding and thin sectioning of stented tissue for immunohistochemistry. However the process

was highly variable and refinement of the technique will be required to prevent vessel damage before this method can be used routinely.

5 Analysis of neointimal formation following stenting in miR-143 and miR-145 knockout mice

5.1 Introduction

In vivo studies have shown that expression levels of miR-143 and miR-145 are reduced at sites of vascular injury including mouse models of transverse aortic constriction and carotid artery ligation as well as balloon catheter injury in the rat (Cordes et al., 2009, Elia et al., 2009, Cheng et al., 2009). Furthermore, miR-143 and miR-145 expression levels are also decreased in the vessels of ApoE KO mice, a model of hyperlipidaemia (Elia et al., 2009). Expression levels of these miRNA are further decreased within the vessels of ApoE KO mice following a period of fat feeding, which is known to promote atherosclerotic lesion formation (Piedrahita et al., 1992, Plump et al., 1992). Previous studies have demonstrated that adenovirus-mediated over-expression of miR-143 or miR-145 is sufficient to reduce neointimal formation in the rat carotid balloon-injury model (Elia et al., 2009, Cheng et al., 2009), indicating that loss of miR-143 and miR-145 expression is a contributing factor in neointimal formation.

Mice which are genetically ablated of both miR-143 and miR-145 (miR-143/145 KO) have reduced numbers of contractile and greater number of synthetic VSMCs within their vessels walls (Boettger et al., 2009). *In vitro*, VSMCs isolated from miR-143/145 KO mice show increased migration towards PDGF (Elia et al., 2009). It was also shown that miR-143/145 KO VSMCs have increased propensity to form podosomes, actin rich structures important in cell migration, in response to PDGF (Quintavalle et al., 2010). Furthermore, *in vivo*, accumulations of synthetic VSMCs have been found in the intima of vessels isolated from miR-143/145 KO mice (Elia et al., 2009, Boettger et al., 2009). Neointimal lesions have been identified in the femoral arteries of aged (18 month) miR-143/145 KO mice (Boettger et al., 2009). These lesions contained large amounts of VSMCs, as well as macrophages and collagen I, with the media of the vessel showing thinning (Boettger et al., 2009).

Interestingly, despite the increase in synthetic VSMCs found in miR-143/145 KO mice, virtually no neointimal formation occurred in miR-145 and miR-143/145 KO mice following carotid artery ligation, whilst neointimal formation was significantly reduced in miR-143 KO mice (Xin et al., 2009). This result strongly suggests that miR-143 and miR-145 are important in the triggering or guiding neointimal formation following injury. In the present study miR-143 or miR-145

homozygous KO mice were used to study the individual importance of these miRNA in the context of stenting.

5.2 Aims

- To determine the effect of genetic ablation of miR-143 or miR-145 expression on neointimal formation following stenting.
- To investigate whether miR-143 and miR-145 gene target expression levels are altered in miR-143 or miR-145 KO mice.

5.3 Results

5.3.1 MiRNA expression in miR-143 and miR-145 KO mice

In order to confirm that miR-143 KO and miR-145 KO mice did not express the respective miRNA, RNA was isolated from snap frozen aortas and miRNA expression analysed by Taqman® qRT-PCR. Loss of miR-143 and miR-145 expression was detected in miR-143 KO and miR-145 KO mice respectively, when compared to WT mice (Figure 5.1 A-B). Northern blotting confirmed this result revealing large bands for mature miR-143 and miR-145 in WT mice which were absent in miR-143 and miR-145 KO mice (Figure 5.1 C-D).

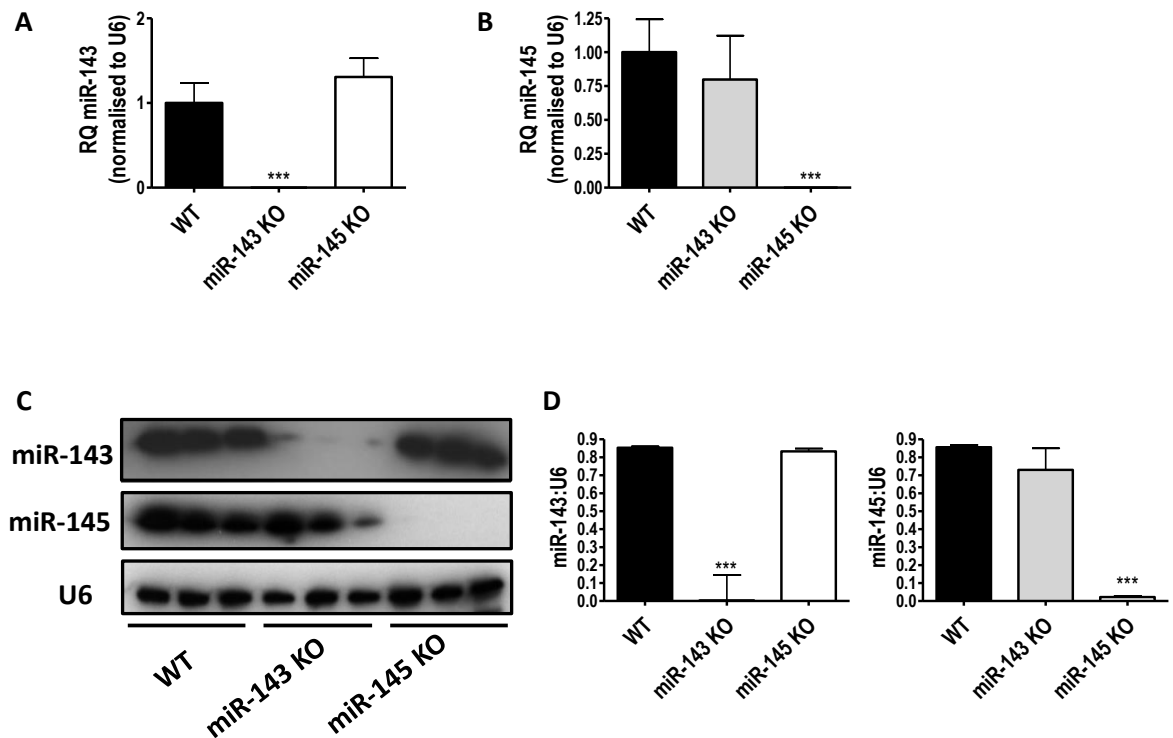


Figure 5.1. MiR-143 and miR-145 expression in mouse aortas.

Aortas were collected at sacrifice from miR-143 KO, miR-145 KO and WT mice and immediately transferred to liquid nitrogen. RNA was isolated and miRNA expression analysed by Taqman® qRT-PCR or northern blotting. Taqman analysis of miR-143 (A) or miR-145 (B). Northern blotting performed using 5 μ g RNA to probe for miR-143, miR-145 or U6 (C) and analysed by densitometry (D). *** $P < 0.001$ vs. WT. $n = 6$ /group.

In order to assess neointimal formation in mice ablated of miR-143 or miR-145 expression, stent surgery was performed on 18 week old miR-143 KO, miR-145

KO and WT mice. Stents were delivered to the thoracic aorta of age matched donor mice and then isolated before being interposition grafted into the carotid artery of recipient mice. Mice were sacrificed 28 day post-operative. Despite the greater body weight seen in miR-143 KO mice at day 0 of the study, body weight was comparable between groups by day 28 (Table 5.1). Formalin fixed stented grafts were embedded in Technovit 8100 resin, sectioned and ground to approximately 7-10 μm and morphometric measurements performed. No significant differences in stent expansion or injury score were present between groups indicating that stent deployment resulted in a consistent injury to the aortic wall (Table 5.1).

Table 5.1. Body weights and injury scores of miRNA KO and WT mice.

	WT	MiR-143 KO	MiR-145 KO
Weight day 0 (g)	25.64 \pm 0.57	28.06 \pm 0.64*	26.62 \pm 0.84
Weight day 28 (g)	27.52 \pm 0.58	28.69 \pm 0.68	28.00 \pm 0.64
Stent Expansion (mm ²)	0.67 \pm 0.01	0.66 \pm 0.03	0.68 \pm 0.03
Injury Score	0.06 \pm 0.05	0.03 \pm 0.03	0.05 \pm 0.03

5.3.2 Neointimal formation in miRNA KO mice

H&E staining was performed on resin embedded stented sections to visualise vessel morphology (Figure 5.2). Morphometric analysis revealed that stented miR-143 KO and miR-145 KO mice displayed significantly less neointimal thickness when compared to WT mice with a mean of 83.09 ± 10.08 , 90.81 ± 7.14 and $121.65 \pm 6.64 \mu\text{m}$ for miR-143 KO, miR-145 KO and WT mice respectively (Figure 5.2 and 5.3A). Strut depth did not significantly differ between groups (Figure 5.3B) however neointimal area was significantly reduced in miR-143 KO when compared to WT mice (0.22 ± 0.03 vs. $0.31 \pm 0.01 \text{ mm}^2$) (Figure 5.3C). Overall percentage stenosis was significantly reduced in both miR-143 KO and miR-145 KO when compared to WT mice (Figure 5.2 and 5.3D). Lumen area was found to be significantly greater in 28 day miR-145 KO mice when compared to WT mice (Figure 5.3E). Total vessel area was reduced in 28 day stented miR-143 KO mice when compared to WT mice (Figure 5.3F) despite no difference in stent

expansion between these groups (Table 5.1). The reduced stenosis seen in miR-143 KO and miR-145 KO mice was not reflected in any change in the neointimal to medial ratio (Figure 5.3G). This was found to be due to reduced medial area in miR-143 KO and miR-145 KO compared with WT mice (Figure 5.3H).

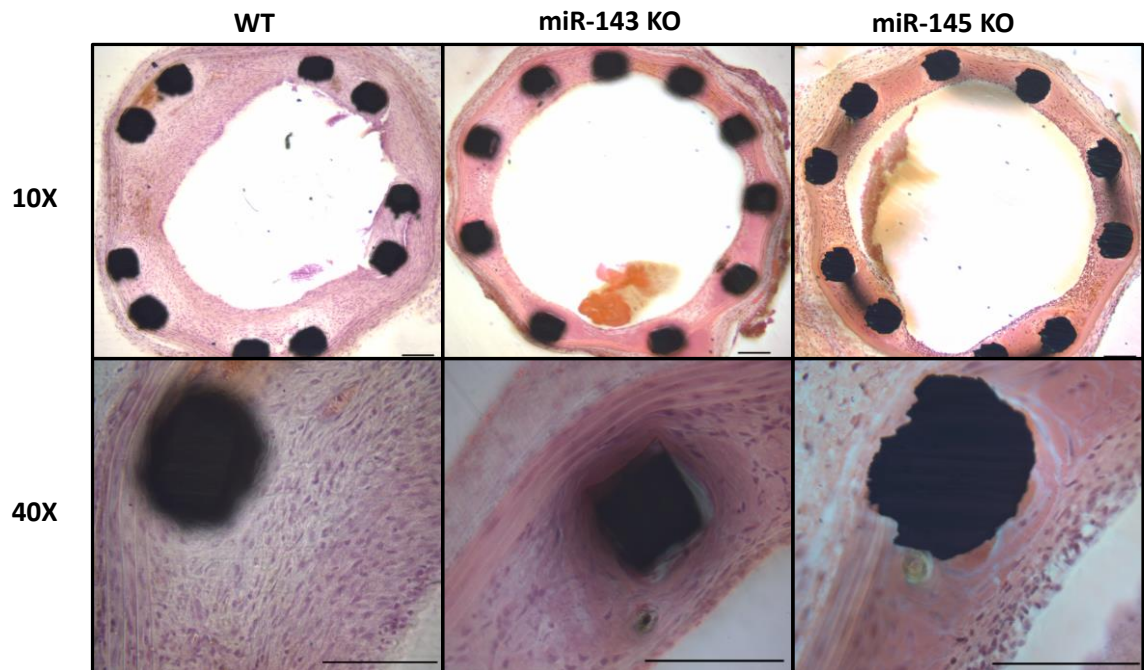


Figure 5.2. H&E staining of 28 day stented vessels from miRNA KO and WT mice.

Representative H&E staining performed on resin embedded sections from stented vessels isolated 28 day post-operative shown at 10X and 40X magnification. Scale bar = 100 μ m.

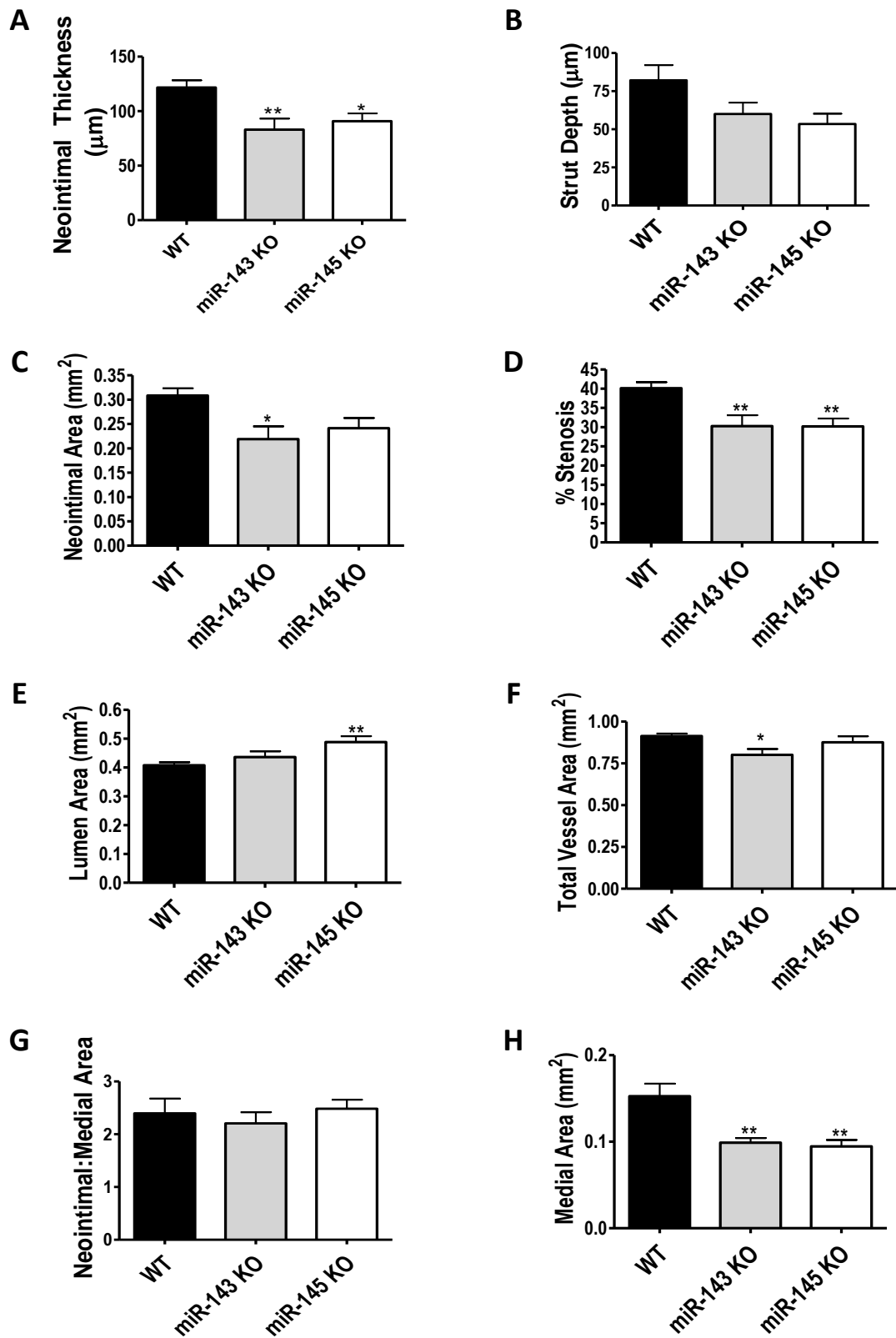


Figure 5.3. Analysis of neointimal formation in 28 day stented miRNA KO and WT mice.

Morphometric analysis was performed on resin embedded sections from 28 day stented mice using Image-Pro® Analyzer 7.0 software. A. Neointimal thickness, B. Strut depth, C. Neointimal area, E. Percentage stenosis, E. Lumen area, F. Total vessel area, G. Neointimal:medial ratio, H. Medial area. *P < 0.05, **P < 0.01 vs. WT. n = 9-13/group.

Mice genetically ablated of both miR-143 and miR-145, or miR-145 alone have been previously reported to have thinner walled aortas than WT mice measured at 8 weeks of age (Xin et al., 2009). In order to assess whether differences in medial wall thickness are observed in 18 week miR-143 KO, miR-145 KO and WT mice prior to stenting, morphometric measurements were performed on thoracic aortas (Figure 5.4). No significant differences in medial thickness or area were detected between groups (Figure 5.4), suggesting that the reduced medial thickness seen in miR-143 KO and miR-145 KO mice following stenting may be due to reduced medial remodelling.

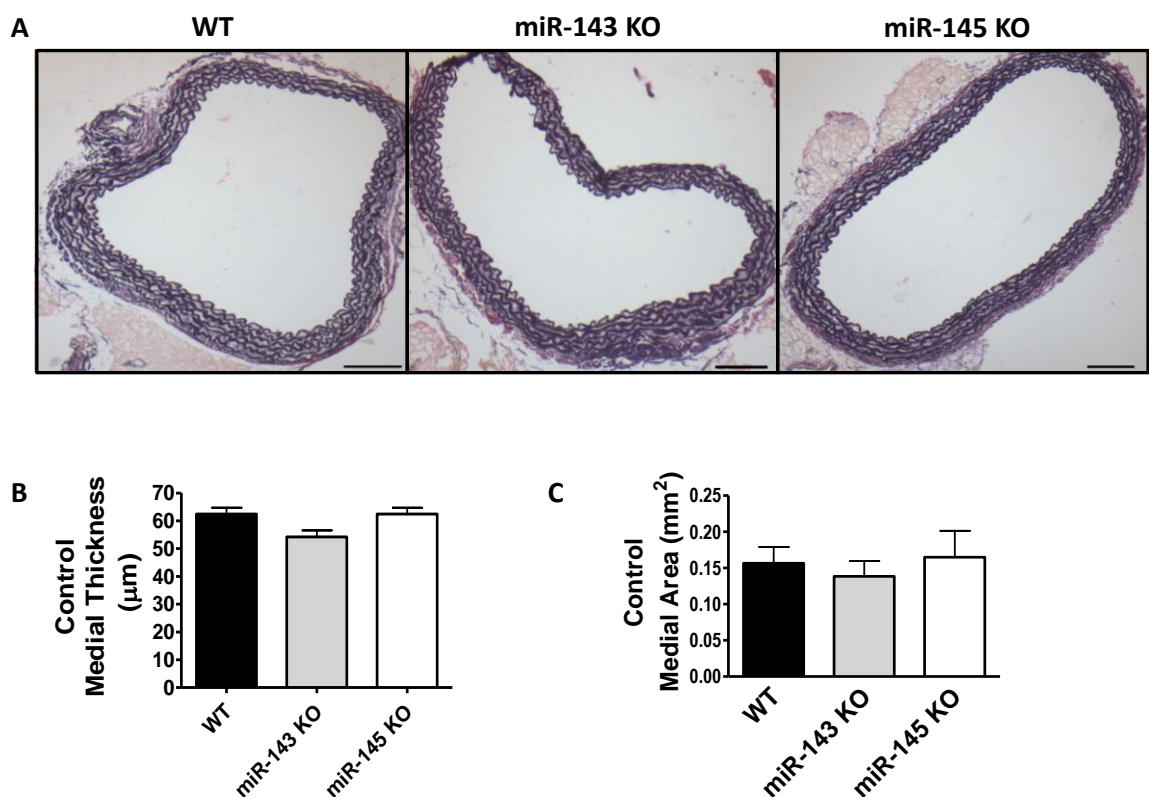


Figure 5.4. Analysis of medial morphometry in control miRNA KO and WT mice.

EVG staining was performed to visualise the elastic lamina of aortas isolated from 18 week old miR-143 KO, miR-145 KO and WT mice. A. Images of EVG stained miR-143 KO, miR-145 KO and WT mice displayed at 10X magnification. B. Mean medial thickness of day 0 aortas. C. Mean medial area of day 0 aortas. Scale bar = 100 µm. n = 6/group.

MiR-143 and miR-145 are the most highly expressed miRNA in the artery wall and have been shown to promote a contractile VSMC phenotype (Ji et al., 2007, Cheng et al., 2009). In order to assess whether genetic ablation of miR-145 or miR-145 alters the presence of VSMCs in the neointima, immunohistochemistry

for SMC marker α -SMA was performed (Figure 5.5). Staining revealed comparable α -SMA expression in the media and neointima of vessels from each group which was not present in the IgG control (Figure 5.5).

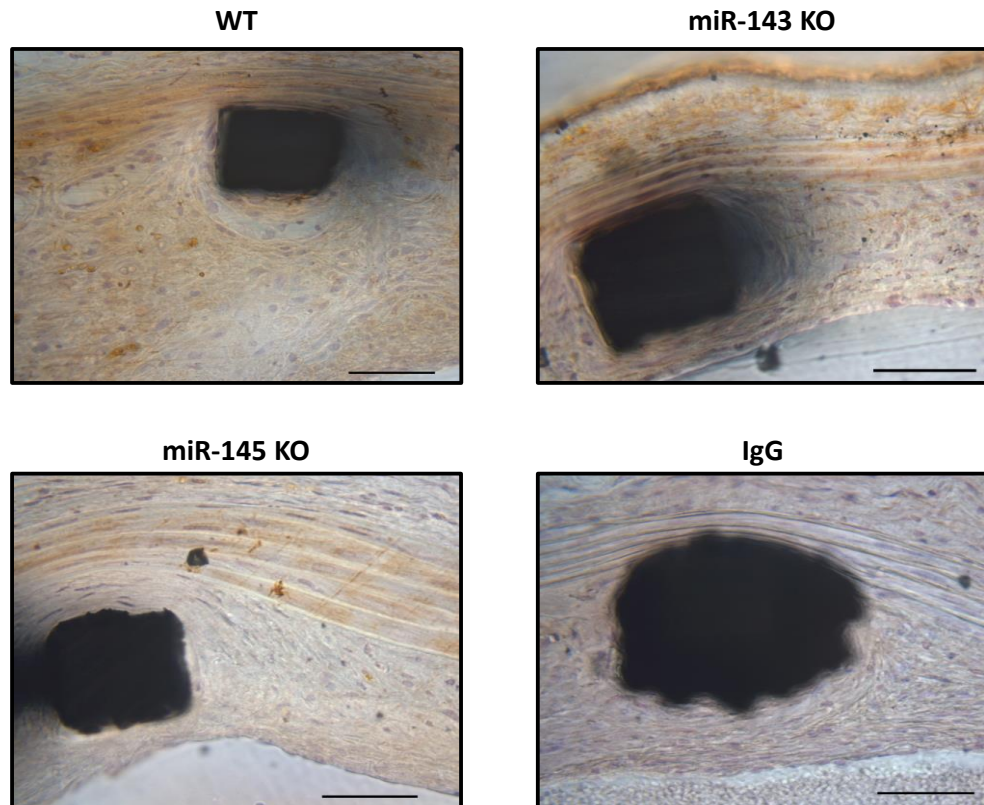


Figure 5.5. α -SMA expression in stented vessels from miRNA KO and WT mice.

Immunohistochemistry probing for α -SMA or control IgG performed on resin embedded sections from 28 day stented miR-143 KO, miR-145 KO and WT mice. Expression is shown by brown DAB staining. 40X magnification. Scale bar = 50 μ m.

5.3.3 MiR-143 and miR-145 target expression in miRNA KO mice

Next the expression of previously identified miR-143 and miR-145 targets KLF4, KLF5 and ELK-1 (Cheng et al., 2009, Xin et al., 2009, Cordes et al., 2009) was analysed in tissue isolated from miR-143 KO, miR-145 KO and WT mice. Taqman® qRT-PCR analysis for target expression in the aorta revealed no significant difference in the expression of KLF4 or ELK-1 between groups (Figure 5.6). KLF5 expression was significantly reduced in miR-143 KO mice compared with control mice (Figure 5.6B).

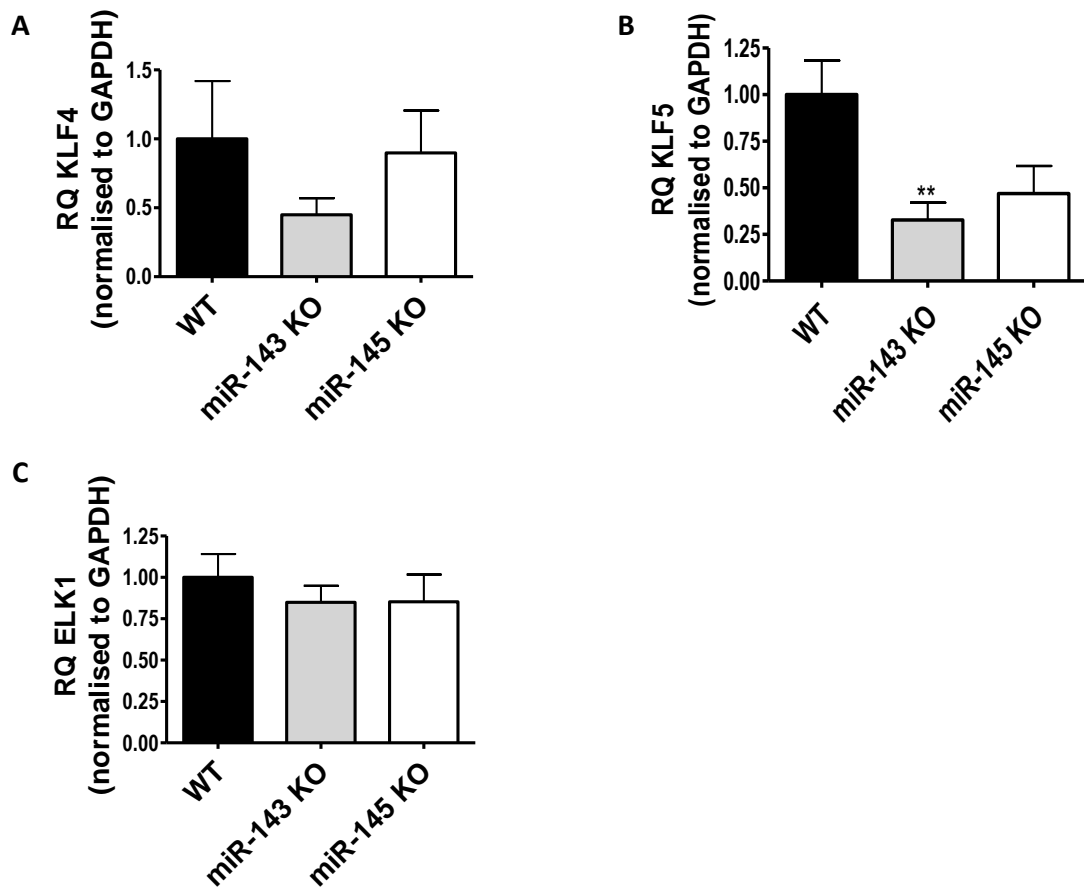


Figure 5.6. MiRNA target expression in the aorta of miR-143 KO, miR-145 KO and WT mice. Taqman® qRT-PCR analysis performed on RNA isolated from snap frozen aortas of miR-143 KO, miR-145 KO and WT mice for KLF4 (A), KLF5 (B) and ELK-1 (C). ** $P < 0.01$ vs. WT. $n = 6$ /group.

To determine whether changes in target expression occurred in other tissues target analysis was also performed on RNA isolated from the heart. MiR-143 and miR-145 expression was, as expected; significantly lower in the hearts of miR-143 KO and miR-145 KO mice when compared to WT mice (Figure 5.7 A-B). However, expression of KLF4, KLF5 or ELK-1, determined by Taqman® qRT-PCR, did not differ significantly between groups (Figure 5.7 C-E). Analysis of KLF5 protein expression, determined by western blot was not significantly different between groups (Figure 5.7F).

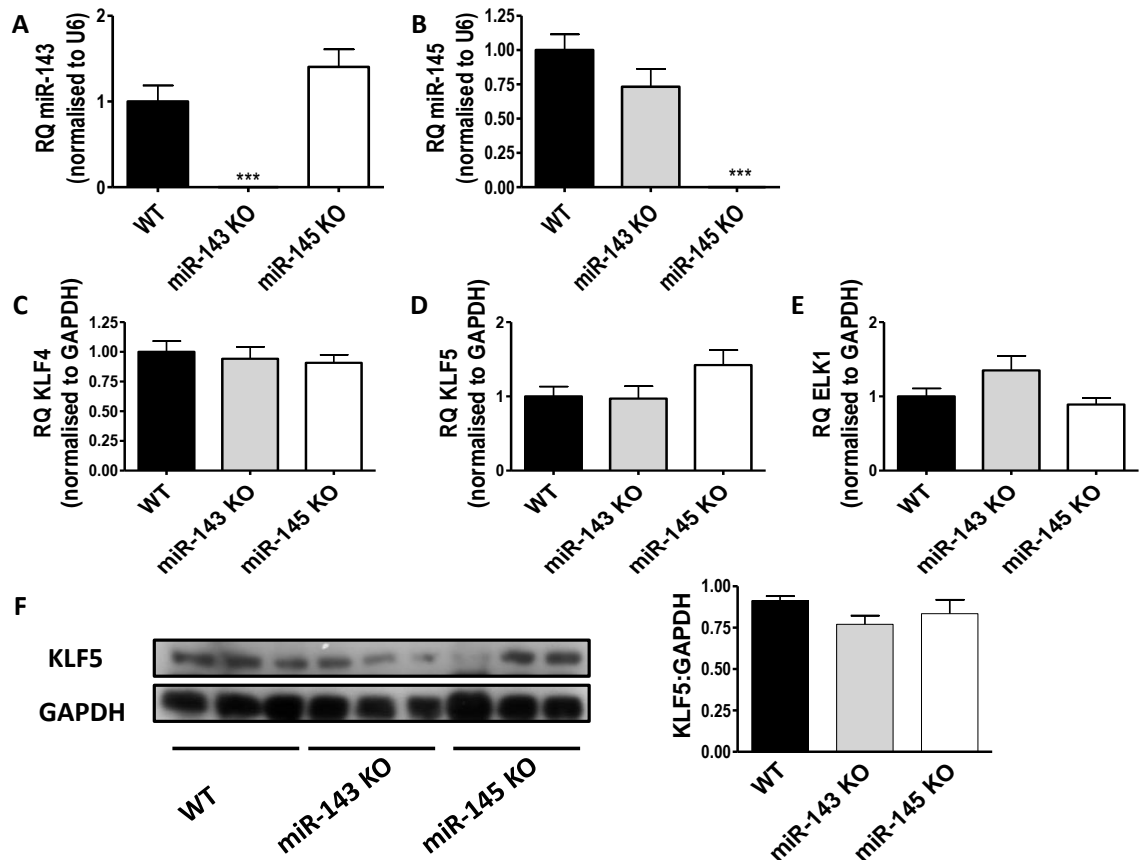


Figure 5.7. MiRNA target expression in the heart of miR-143 KO, miR-145 KO and WT mice. Taqman® qRT-PCR analysis performed on RNA isolated from snap frozen hearts of miR-143 KO, miR-145 KO and WT mice for miRNAs miR-143 (A) and miR-145 (B) and target genes KLF4 (C) KLF5 (D) and ELK-1 (E). (F) Western blot probing for KLF5 or GAPDH (left) and densitometry analysis of western blot (right). *** $P < 0.001$ vs. WT. $n = 6$ /group.

MiR-145 KO mice have been previously shown to have a reduced heart weight and left ventricular mass when compared to WT mice (Xin et al., 2009). To investigate whether this was apparent in our stented mice we measured heart weight following sacrifice at 22 weeks. Neither total heart weight nor right ventricle weight differed significantly between groups (Figure 5.8 A and C) however left ventricle plu0073 septum weight was significantly lower in miR-145 KO mice compared with WT mice (Figure 5.8B).

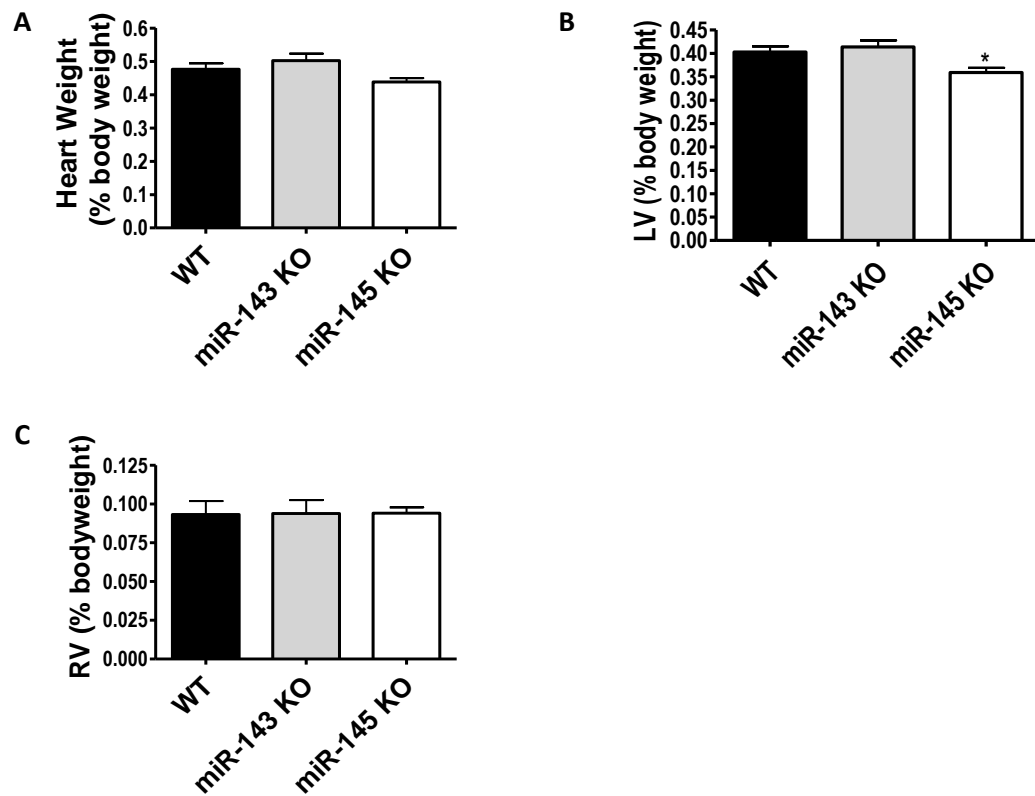


Figure 5.8. Analysis of heart weight indices in miRNA KO and WT mice.

Hearts were perfused at sacrifice with PBS and fixed in 10% formalin overnight before being analysed and displayed as a percentage of bodyweight at sacrifice for A. Whole heart, B. Left ventricle plus septum, C. Right ventricle. n = 12/group.

5.4 Discussion

In this chapter it has been shown that vessel remodelling in response to stenting is reduced by genetic ablation of miR-143 or miR-145. Neointimal thickness and percentage stenosis were significantly less in miR-143 KO and miR-145 KO compared with WT mice. Neointimal area was also reduced in stented vessels from miR-143 KO mice. Furthermore, medial remodelling was reduced in miR-143 KO and miR-145 KO mice. Genetic loss of miR-143 and miR-145 did not result in de-repression of previously identified targets indicating that alternative regulatory mechanisms may be implicated upon loss of miRNA expression.

These results agree, in part, with a previous study where mice genetically ablated of miR-143, miR-145, or both miR-143/145, developed significantly less neointimal formation following carotid artery ligation than WT mice (Xin et al., 2009). Interestingly, in contrast to our model where neointima formation occurred in all mice, miR-145 KO and miR-143/145 KO mice formed virtually no neointima in response to carotid artery ligation (Xin et al., 2009). This may be due to the use of a different vessel or differences in the models. The stent model is driven by EC denudation, mechanical injury to the vessel wall and the presence of a stent, whereas the carotid ligation model is driven by altered blood flow and haemodynamic changes and does not involve mechanical EC denudation (Ali et al., 2007, Kumar and Lindner, 1997). MiR-143/145 KO mice and miR-145 KO mice have been previously shown to have reduced blood pressure as a result of both reduced vascular tone and receptor mediated constriction (Boettger et al., 2009, Xin et al., 2009, Elia et al., 2009). This decrease in blood pressure is likely to have contributed to the altered remodelling in these mice following carotid artery ligation.

MiR-143 and miR-145 expression is not essential for VSMC development per se, however a body of evidence exists to suggest that they are required for the normal VSMC biology. VSMCs isolated from miR-143/145 KO mice show increased proliferative and migratory properties *in vitro* (Elia et al., 2009, Quintavalle et al., 2010). The vessels of miR-143/145 KO mice contain a greater number of synthetic SMCs identified by their increased circularity, reduced numbers of contractile machinery, dense bodies and focal adhesions, and increased numbers of rough E.R, typical of synthetic SMCs (Boettger et al., 2009, Elia et al., 2009).

Furthermore, stress fibers in the aorta of both miR-143/145 KO mice and miR-145 KO mice are less prominent and are disorganised compared with WT mice (Xin et al., 2009). Interestingly, *in vivo* the presence of higher numbers of synthetic and less contractile VSMCs in the vessels of miR-143/145 KO mice is not accompanied by any basal increases in proliferation (Boettger et al., 2009). These studies, together with evidence from the present study that miR-143 or miR-145 ablation reduces neointima formation in mice, suggest the regulatory pathways in VSMCs are likely to be significantly altered by genetic loss of these miRNA. This is perhaps unsurprising when it is considered that a number of signalling molecules are known to utilise miR-143 and miR-145 in their signalling pathways by transcriptional activation (Davis-Dusenbery et al., 2011, Long and Miano, 2011, Xin et al., 2009, Cordes et al., 2009). Loss of endogenous miR-143 and miR-145 expression occurs following vascular injury (Cordes et al., 2009, Elia et al., 2009) and may act as a trigger to promote VSMC proliferation and migration. Genetic KO of these miRNA, could potentially affect the ability of VSMC phenotypic switching to occur which may explain why miR-143 KO and miR-145 KO mice have less neointimal formation.

The present study revealed that medial area of 28 day stented miR-143 KO and miR-145 KO mice was decreased when compared to WT mice. Previous studies have indicated that mice genetically ablated of both miR-143 and miR-145 have thinner walled femoral arteries and to a lesser extent aortas (Boettger et al., 2009, Xin et al., 2009, Elia et al., 2009). This was found to be due to a reduced number of larger, contractile VSMCs and increased numbers of smaller, synthetic VSMCs within the vessel walls of miR-143/145 KO mice, which are attributed to the reduction in wall thickness (Elia et al., 2009, Boettger et al., 2009). Xin and colleagues went on to show that genetic loss of miR-145 alone, but not miR-143 alone led to a reduction in aortic wall thickness (Xin et al., 2009). No quantification was shown in the study to indicate whether miR-145 KO vessels have as great a reduction in wall thickness as miR-143/145 KO mice however we would speculate that miR-143/145 KO mice may display a more severe phenotype due to accumulative effects of loss of both miRNA. Morphometric analysis of non-stented miR-143 KO, miR-145 KO and WT aortas found no difference in basal aortic medial thickness or medial area between the groups. The mice used in our study were however considerably older at the time of

measurements (18 weeks vs. 8 weeks). One explanation for this disparity could be that mice which lack only one of these miRNA and maintain expression of the other may develop compensatory mechanisms to regulate VSMC phenotype by which the reduction in aortic medial thickness in miR-145 KO mice is no longer present by 18 weeks. As basal aortic wall thickness of miR-143 KO mice did not differ from WT mice (Xin et al., 2009) we deduce that the reduced medial area seen in 28 day stented miR-143 and miR-145 KO mice is due to a reduced propensity for medial remodelling following stenting. This observation has also been noted in the carotid artery following ligation (Xin et al., 2009).

Resin embedding of stented grafts was challenging due to the small size of the grafts and their buoyancy within the resin which despite anchorage often resulted in the stent moving from the optimum positioning for sectioning during resin setting. Sectioning of resin embedded sections in itself was also challenging due to the small size of the stent in comparison to the sectioning saw which resulted in only a few sections per stent. Performing immunohistochemistry on resin embedded sections proved problematic and despite several optimisation experiments only proved successful for α -SMA.

Staining for α -SMA was present in sections from all groups indicating the presence of VSMCs within the neointima. α -SMA is a marker protein for SMCs however it is not SMC-specific and is also expressed by myofibroblasts, which can derive from resident cells or the bone marrow following vascular injury (Forte et al., 2010). Studies have indicated that myofibroblasts derived from the adventitia can contribute to neointimal formation following severe vascular injury with dissection of the media (Shi et al., 1996). Myofibroblasts have also been shown to significantly contribute to neointimal formation in the balloon-catheter injured rat carotid without disruption of the media (Siow et al., 2003). However, others disagree with this and state that myofibroblasts contribute only minimally to neointimal formation (De Leon et al., 2001, Maeng et al., 2003). VSMCs have previously been identified as the main cell type present in the neointima following vascular injury and derive from migration and proliferation of activated medial VSMCs (Clowes and Schwartz, 1985, Clowes and Clowes, 1985). However, this does not rule out the possibility that myofibroblasts may contribute to neointimal formation. SM-MHC and smoothelin are not expressed on myofibroblasts and smoothelin expression is thought to be SMC-specific (Forte

et al., 2010) therefore these markers could be utilised in future studies to ensure correct identification of VSMCs in the neointima.

MiR-145 KO mice were found to have reduced left ventricular mass compared with miR-143 KO and WT mice but total heart weight was not decreased as previously reported (Xin et al., 2009). This difference is likely accountable to the difference between methods of measuring heart weight, as a percentage of the total body weight or normalised to tibial length. Although final body weight did not vary significantly between groups fluctuations in body weight in individual mice may have decreased the accuracy of the measurements. Tibial length is constant after maturity and may therefore be preferable to produce more accurate results (Yin et al., 1982).

A previous study showed the upregulation of KLF4 and to a lesser extent KLF5 mRNA in the carotid arteries of miR-143/145 KO mice (Xin et al., 2009). Similarly, in the lung KLF4 expression is increased in miR-145 KO when compared to WT mice (Caruso et al., 2012). The expression of miR-143 and miR-145 targets KLF4, KLF5 and ELK-1 was measured at the mRNA level in both the aorta and heart. Expression of KLF5 was significantly decreased in the aorta of miR-143 KO mice but was not significantly altered within the heart either at the mRNA or protein level. The decrease in KLF5 expression following miR-143 KO is unexpected and may be due to altered regulation of KLF5 expression by other means upon loss of miR-143, possibly by more pronounced negative regulation of KLF5 by miR-145. The unaltered expression of the other targets may be due to compensatory regulation of these targets following loss of miR-143 or miR-145. Changes in target regulation induced by miR-143 or miR-145 KO may however become evident in tissues that are undergoing remodelling, such as the stented vessel itself. One example of this is that miR-145 targets ACE, FSCN1, CTGF and ITGBL1 are expressed at similar levels in the WT and miR-145 KO pulmonary artery at normoxic conditions but are upregulated in the miR-145 KO in hypoxic conditions (Caruso et al., 2012). It is also possible that changes in target expression may be occurring at the protein level and it would be important to assess this in future studies by western blots.

In conclusion, it has been shown that genetic ablation of miR-143 or miR-145 reduces vessel remodelling following stent-induced vascular injury. Further

studies are now needed to define the mechanism and to establish whether this is a result of genetic KO or whether pharmacological knockdown of these miRNA produces similar results.

6 Neointimal formation following AntimiR-mediated knockdown of miR-143 in mice

6.1 Introduction

Loss of local miR-143 and miR-145 expression is often reported following vascular injury and exogenous delivery of these miRNA has been shown to reduce vascular remodelling (Cheng et al., 2009, Elia et al., 2009, Cordes et al., 2009). The results of the study outlined in chapter 5 revealed that genetic KO of miR-143 or miR-145 reduced neointimal formation following stenting in mice. This prompted an investigation into whether pharmacological knockdown of these miRNA produces similar results to genetic KO.

Several methods can be used to decrease miRNA expression *in vivo* including knockdown by antagomiRs or antimiRs or scavenging by miRNA sponges (Ebert and Sharp, 2010, Krutzfeldt et al., 2005, Montgomery et al., 2011). MiRNA sponges are RNAs encoded by transgenes that can be delivered *in vivo* via viruses such as Ads or lentiviruses (Ebert and Sharp, 2010). They encode tandem binding sites for a single or multiple miRNA in their 3' UTR which are bulged at certain sites (usually nucleotides 9-12) to prevent endonucleolytic cleavage by Ago proteins. MiRNA regulation of endogenous targets is competitively inhibited by miRNA binding to complementary regions in sponges thereby resulting in target de-repression (Ebert et al., 2007). AntagomiRs are complementary to the mature miRNA sequence, contain phosphorothioate moieties for enhanced stability and are conjugated to cholesterol by a 2'-O-methyl bond to enhance uptake into tissues, particularly the liver (Krutzfeldt et al., 2005). Use of antagomiRs is gradually being replaced by unconjugated antimiRs, which contain chemical modifications to reduce nuclease degradation and increase melting temperature of the bound duplex thus increasing antimiR stability, these include 2'-O-methoxyethyl and 2'-fluoro modifications (van Rooij and Olson, 2012).

In order to achieve pharmacological knockdown of miR-143 we utilised an unconjugated antimiR that contains a mixture of DNA and LNA bases. LNA bases are structurally based on RNA with the addition of a methylene bridge between the 2' oxygen and the 4' carbon of the ribose ring, which locks the nucleic acid in the 3' endo conformation. This acts to enhance organisation of the backbone and base stacking which increases melting temperature, stability and binding affinity (Braasch and Corey, 2001). AntimiRs also contain phosphorothioate backbone linkages which further stabilise the antimiR by reducing degradation

by nucleases and promote cellular uptake due to their lipophilicity (van Rooij and Olson, 2012, Krutzfeldt et al., 2007). AntimiRs are highly water soluble and delivery by intravenous (IV), SC, or IP routes has been shown to result in comparable knockdown in miRNA expression (Montgomery et al., 2011). Furthermore, antimiRs show enhanced stability and long half-lives within tissues which can lead to robust miRNA inhibition for several weeks after administration (Montgomery et al., 2011). Evidence has suggested that antimiRs containing LNA bases work by forming a high affinity duplex with the miRNA, inhibiting its ability to interact with target mRNA by sequestering rather than degrading the miRNA (Figure 6.1) (Elmen et al., 2008b, Elmen et al., 2008a, Torres et al., 2011). AntimiRs have been shown to effectively inhibit miRNA expression and provide a therapeutic benefit in a number of models including non-human primates (Lanford et al., 2010, Rayner et al., 2011). Delivery of three 10 mg/kg doses of antimiR-122 led to sustained antagonism of miR-122 expression in the liver of African green monkeys and resulted in a dose dependent decrease in serum cholesterol for at least 7 weeks following antimiR-122 delivery (Elmen et al., 2008a). MiR-122 promotes hepatitis C infection in the liver by upregulating the expression of hepatitis C RNA by binding to its 5' non coding region (Lanford et al., 2010). AntimiR-122 has been shown to de-repress a number of miR-122 mRNA targets and significantly reduce viremia in hepatitis infected chimpanzees (Lanford et al., 2010). An antimiR against miR-122 has now been taken forward to clinical trials for treatment of hepatitis C infection (Lindow and Kauppinen, 2012). Target de-repression following delivery of antimiR-33A/33B led to increased expression of target mRNA involved in high density lipoprotein (HDL) biogenesis and fatty acid oxidation resulting in an increase in plasma HDL and decrease in VLDL in African green monkeys (Rayner et al., 2011).

It has been reported that the phenotypic consequence of miRNA knockdown may not become apparent until several weeks following antimiR delivery. For example delivery of antimiR-208a to mice led to rapid knockdown of miR-208a and de-repression of direct target mRNA, however downregulation of indirect targets miR-499 and *Myh7*, of which miR-208a promotes expression, did not occur until several weeks following antimiR-208a delivery (Montgomery et al., 2011). Therefore in the present study mice were pre-dosed with antimiRs to

theoretically allow sufficient time for target modulation/de-repression to occur. The dosing schedule is shown in Figure 6.2.

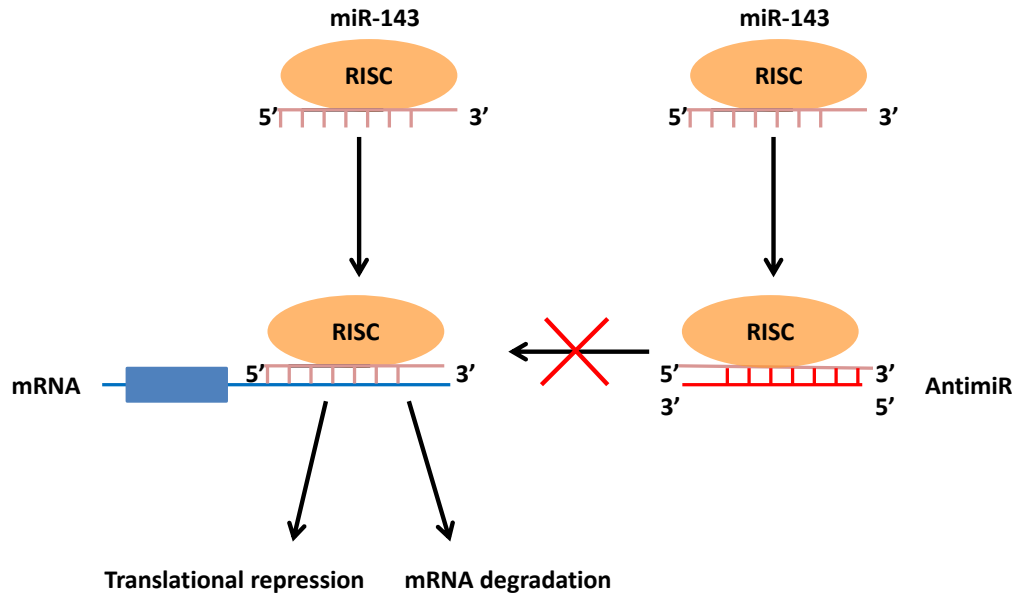


Figure 6.1. Anti-miR mediated inhibition of miRNA.

Anti-miR-143 contains LNA and DNA bases and is complementary to the reverse sequence of miR-143. Following subcutaneous delivery anti-miR-143 is absorbed by cells and binds miR-143 with high affinity. This reduces the proportion of miR-143 within the cell that is bioavailable and thus reduces its ability to bind to target mRNA. As a result de-repression of target mRNA may occur.

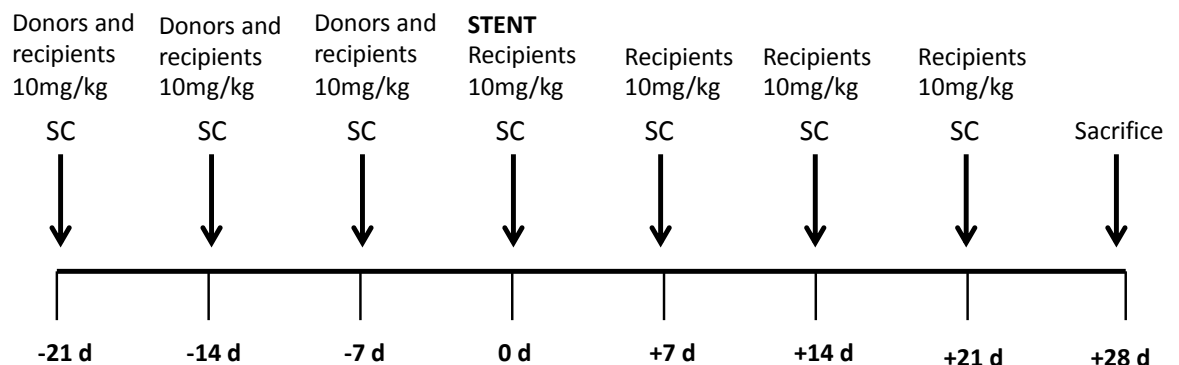


Figure 6.2. Anti-miR study dosing schedule.

C57BL/6 donor and recipient mice received 10 mg/kg SC anti-miR-ctl or anti-miR-143 at 1 week intervals commencing 21 days prior to the surgery and continuing until 1 week prior to sacrifice.

6.2 Aim

- To determine whether antimiR-mediated reduction in miR-143 expression levels leads to altered neointimal formation in mice.

6.3 Results

6.3.1 MiRNA expression levels in tissues of antimiR treated mice

Results described in chapter 5 revealed that both miR-143 KO and miR-145 KO mice displayed significantly less neointimal formation than WT mice in response to stenting, with miR-143 KO mice showing a reduction in the greatest number of measurements. Therefore, in the present study the neointimal formation following antimiR-mediated knockdown of miR-143 was investigated. Both donor and recipient mice were dosed with 10 mg/kg antimiR-143 or antimiR-ctl administered by a once-weekly SC injection on days -21, -14 and -7 in order to establish knockdown of miR-143 within the tissues prior to surgery. Recipient mice received 4 additional 10 mg/kg SC doses of antimiR on day 0, 7, 14 and 21 post-surgery (Figure 6.2).

MiR-143 expression following SC delivery of antimiR-143 was analysed in hearts isolated from donor mice on the day of stent surgery to confirm that miR-143 knockdown had occurred successfully prior to stenting. Due to its use as the donor vessel miR-143 expression could not be measured in the thoracic aorta of donor mice. However, miR-143 expression was analysed in the thoracic aorta of recipient mice at sacrifice to confirm miR-143 knockdown within this tissue. Taqman® qRT-PCR analysis revealed significant loss of miR-143 expression in the heart and aorta following treatment with antimiR-143 but not antimiR-ctl (Figure 6.3 A-B). Northern blotting showed that expression of miR-143 was greater in the aorta than the heart in antimiR-ctl treated mice and that expression was significantly reduced in both tissues by antimiR-143 (Figure 6.3 C-D).

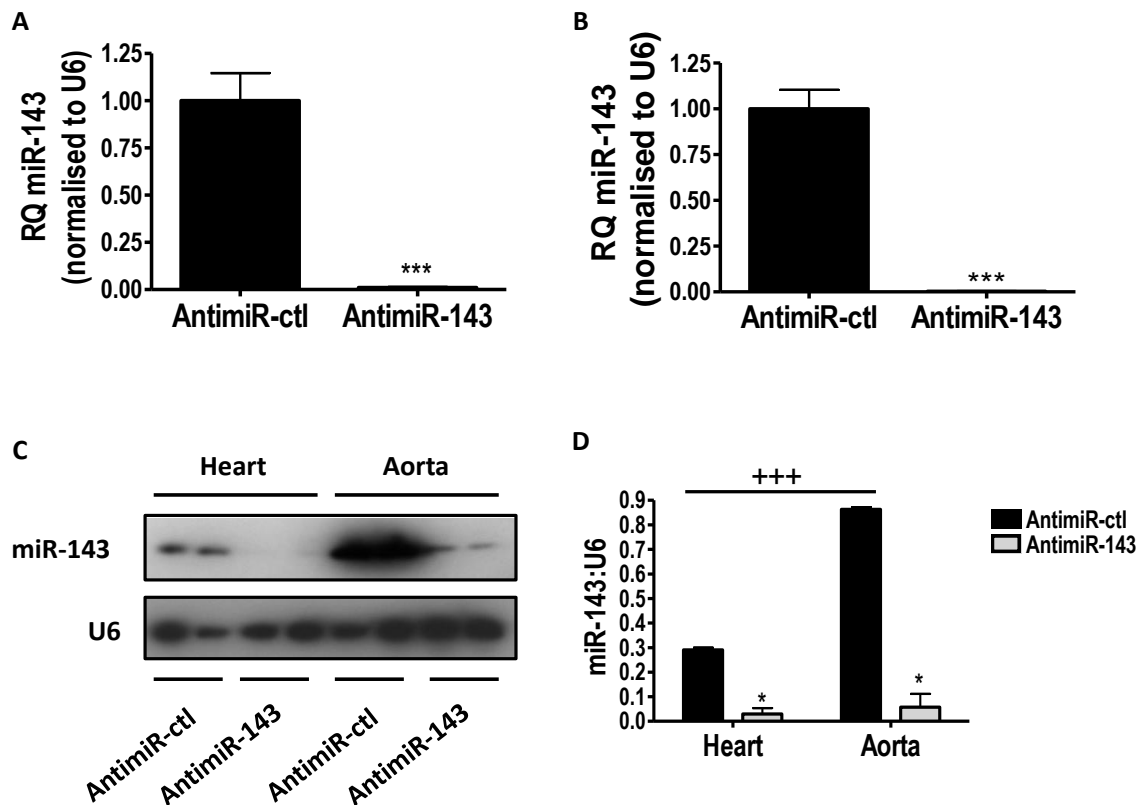


Figure 6.3. Tissue expression of miR-143 following dosing with antimiRs.

Donor C57BL/6 mice received 3 SC 10 mg/kg doses of antimiR-143 or antimiR-ctl at 1 week intervals from - 21 d until - 7 d and hearts were isolated at sacrifice on the day of surgery (0 d). Recipient mice received 7 SC 10 mg/kg doses of antimiR-143 or antimiR-ctl at 1 week intervals beginning at - 21 d until + 21 d and aortas were isolated at sacrifice at + 28 d. MiRNA was isolated and miR-143 expression analysed by Taqman® qRT-PCR in donor hearts (A) or recipient aortas (B) or by northern blotting (C) and densitometry analysis (D). * $P < 0.05$, *** $P < 0.001$ vs. antimiR-ctl. +++ $P < 0.001$ vs. antimiR-ctl heart. $n = 8-12$ /group.

MiR-143 and miR-145 are produced from a bicistronic precursor and are predicted to share a number of common targets despite differences in their seed sequences. They are also known to target different mRNA which are involved in common pathways such as cytoskeletal arrangement (Xin et al., 2009) suggesting that miR-143 and miR-145 may work in unison to contribute to a desired phenotype. We investigated whether knockdown of miR-143 expression by antimiR-143 leads to altered miR-145 expression. Taqman® qRT-PCR analysis revealed that treatment with antimiR-143 significantly reduced miR-145 expression in the heart of donor mice and the aorta of recipient mice when compared to antimiR-ctl (Figure 6.4 A-B). Following treatment with antimiR-143, Taqman® qRT-PCR C_T for miR-145 expression in both the heart and aorta was found to be around 1 C_T higher in mice treated with antimiR-143 compared with antimiR-ctl. In comparison, antimiR-143 increased C_T for miR-143 in the heart

and aorta by 6 C_T and 8 C_T respectively, indicating that antimiR-143 had a much more potent effect on reducing miR-143 expression than miR-145 expression levels. Northern blotting showed that as with miR-143, miR-145 expression was also significantly greater in the aorta than the heart of antimiR-ctl treated mice (Figure 6.4 C-D). However, northern blotting did not reveal any significant decrease in miR-145 expression following treatment with antimiR-143 when compared to antimiR-ctl (Figure 6.4 C-D).

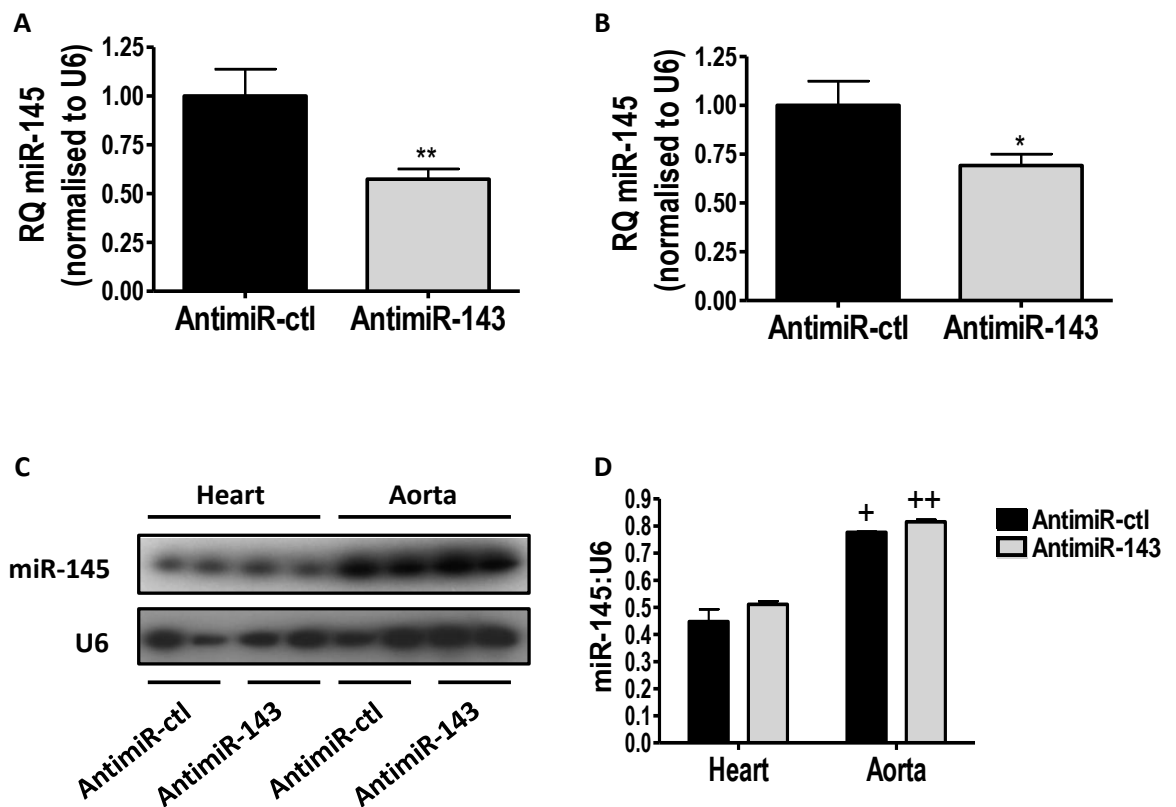


Figure 6.4. Tissue expression of miR-145 following dosing with antimiRs.

Donor C57BL/6 mice received 3 SC 10 mg/kg doses of antimiR-143 or antimiR-ctl at 1 week intervals from -21 d until -7 d and hearts were isolated at sacrifice on the day of surgery (0 d). Recipient mice received 7 SC 10 mg/kg doses of antimiR-143 or antimiR-ctl at 1 week intervals beginning at -21 d until +21 d and aortas were isolated at sacrifice at +28 d. MiRNA was isolated and miR-145 expression analysed by Taqman® qRT-PCR in donor hearts (A) or recipient aortas (B) or by northern blotting (C) and densitometry analysis (D). *P<0.05, **P<0.01 vs. antimiR-ctl. +P<0.05, ++P<0.01 vs. heart. n = 8-12/group.

Neither body weight nor injury score varied significantly between antimiR-ctl and antimiR-145 treated mice over the course of the experiment (Table 6.1).

Table 6.1. Body weights and injury scores of antimiR treated mice.

	AntimiR-ctl	AntimiR-143
Weight (g) 0d	28.92 ± 0.34	29.58 ± 0.36
Weight (g) +7d	28.5 ± 0.22	27.55 ± 0.52
Weight (g) +14d	28.00 ± 0.38	28.75 ± 0.53
Weight (g) +21d	28.13 ± 0.20	29.18 ± 0.56
Weight (g) +28d	28.75 ± 0.37	29.09 ± 0.52
Injury Score	0.05 ± 0.03	0.03 ± 0.02

6.3.2 Analysis of neointimal formation in antimiR treated mice

H&E staining was performed to visualise the stented vessels and morphometric analysis was performed. No significant difference in neointimal thickness, neointimal area, strut depth or percentage stenosis was found in mice treated with antimiR-143 compared with those treated with antimiR-ctl (Figures 6.5 and 6.6) indicating that knockdown of miR-143 expression did not promote neointimal formation in response to stenting. Likewise, no significant differences were found in vessel, medial or lumen area or neointimal to medial ratio between antimiR-143 and antimiR-ctl treated mice (Figure 6.5 and 6.6).

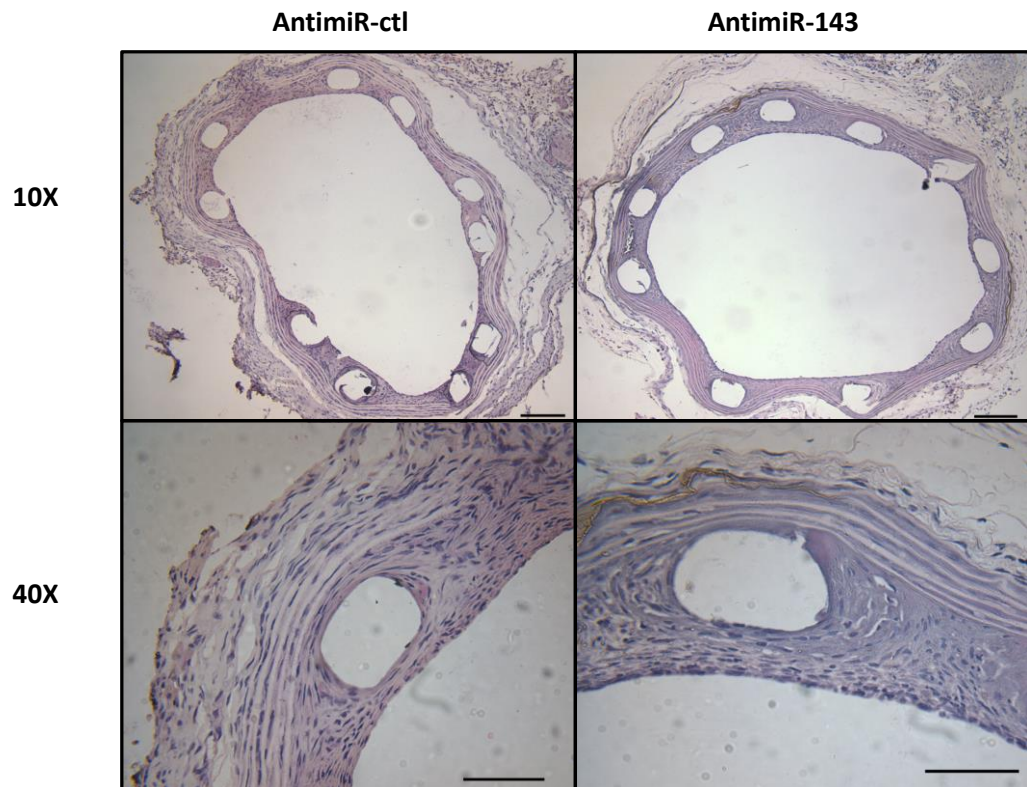


Figure 6.5. H&E staining of stented vessels from antimiR treated mice.

Stented grafts were isolated 28 day post-operative and fixed in 10% formalin before stents were electrolysed and tissue embedded in paraffin wax. H&E staining performed on paraffin embedded sections at 10X and 40X magnification. Scale bar = 100 μ m (top) and 50 μ m (bottom).

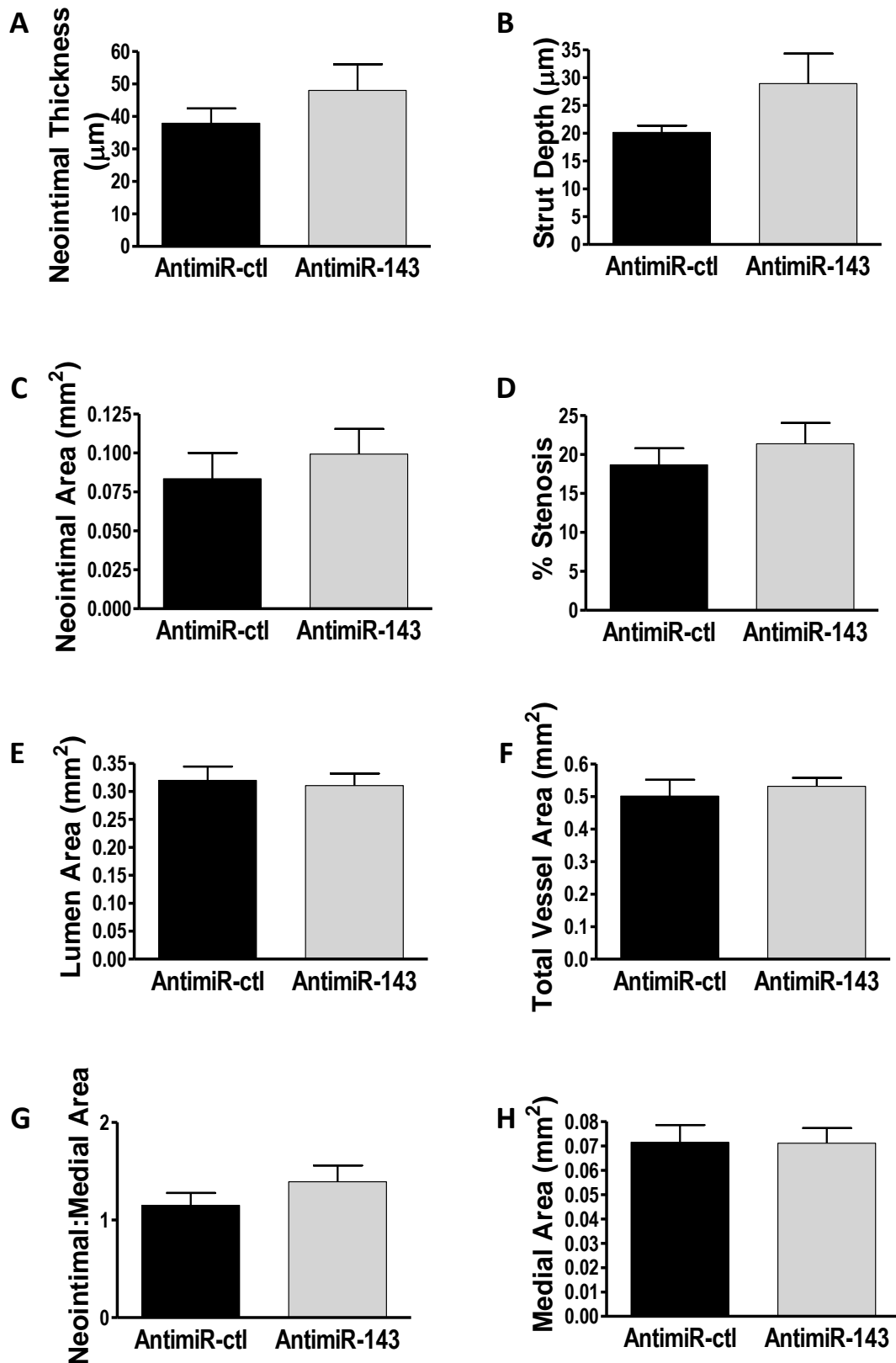


Figure 6.6. Quantification of vessel morphometry in 28 day stented anti-miR treated mice. Morphometric analysis was performed on paraffin embedded sections from 28 day stented mice treated with anti-miR-ctl or anti-miR-143 using Image-Pro® Analyzer 7.0 software. Quantification is shown for A. Neointimal thickness, B. Strut depth, C. Neointimal area, D. Percentage stenosis, E. Lumen area, F. Total vessel area, G. Neointimal:medial ratio, H. Medial area. n = 6-8/group.

6.3.3 Composition of the 28 day neointima in antimiR treated mice

Histological analysis was performed to investigate the composition of the neointima of antimiR-143 and antimiR-ctl treated mice. EVG analysis revealed a large proportion of elastin and was present in the neointimal of both antimiR-ctl and antimiR-143 treated mice (Figure 6.7). Immunohistochemistry for CD31, a marker of ECs showed a complete layer of CD31 positive cells at the luminal edge of the neointima in all sections indicating that re-endothelialisation had occurred by day 28 post-stenting in both antimiR-ctl and antimiR-143 treated mice (Figure 6.8). Similar staining patterns for α -SMA were present in sections from vessels isolated from both antimiR-143 and antimiR-ctl treated mice indicating that treatment with antimiR-143 does not appear to alter the presence of VSMCs within the neointima (Figure 6.9). Both antimiR-ctl and antimiR-143 treated mice contained small numbers of proliferating cells within their neointima 28 day post stenting revealed by staining for PCNA (Figure 6.10). A small number of MAC-2 positive cells were detected in the neointima of approximately 20% of all vessels and did not vary significantly between antimiR-ctl and antimiR-143 treated mice.

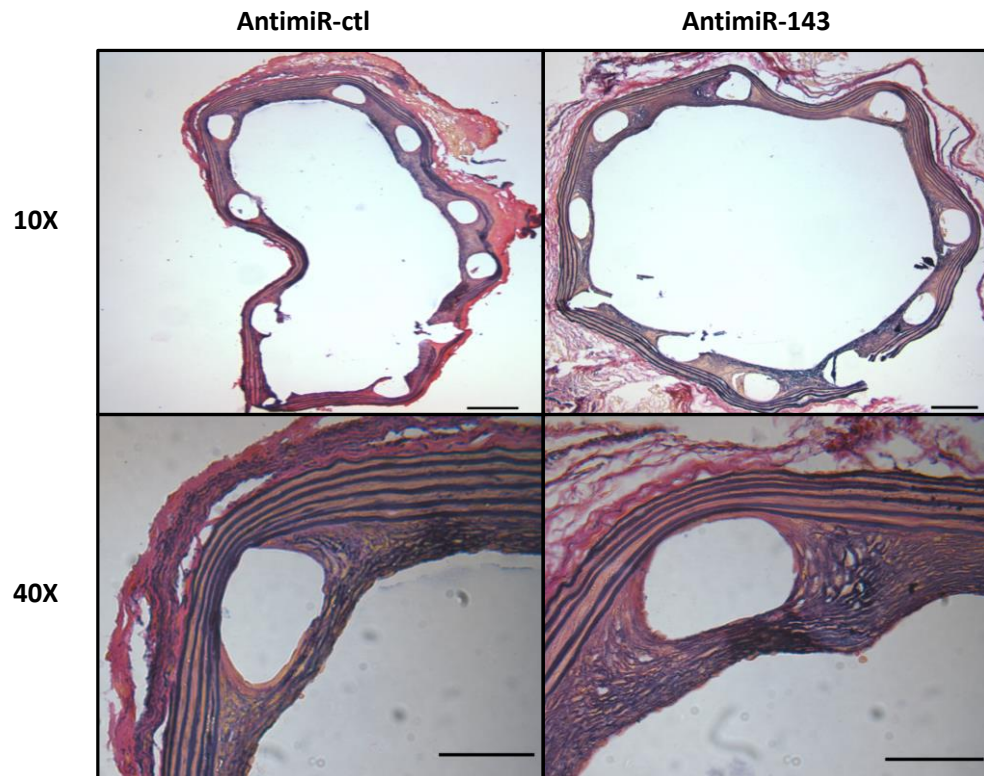


Figure 6.7. EVG staining of 28 day stented vessels from antimiR treated mice.

EVG staining was performed on the electrolysed vessels of antimiR-143 or antimiR-ctl treated C57BL/6 mice 28 d post-stenting to visualise the elastic lamina and determine the composition of the neointimal layer. Representative images showing staining reveal the presence of collagen (pink) and a large proportion of elastin (purple) within the neointima of both antimiR-143 and antimiR-ctl treated mice. Scale bar = 100 μ m (top) 50 μ m (bottom).

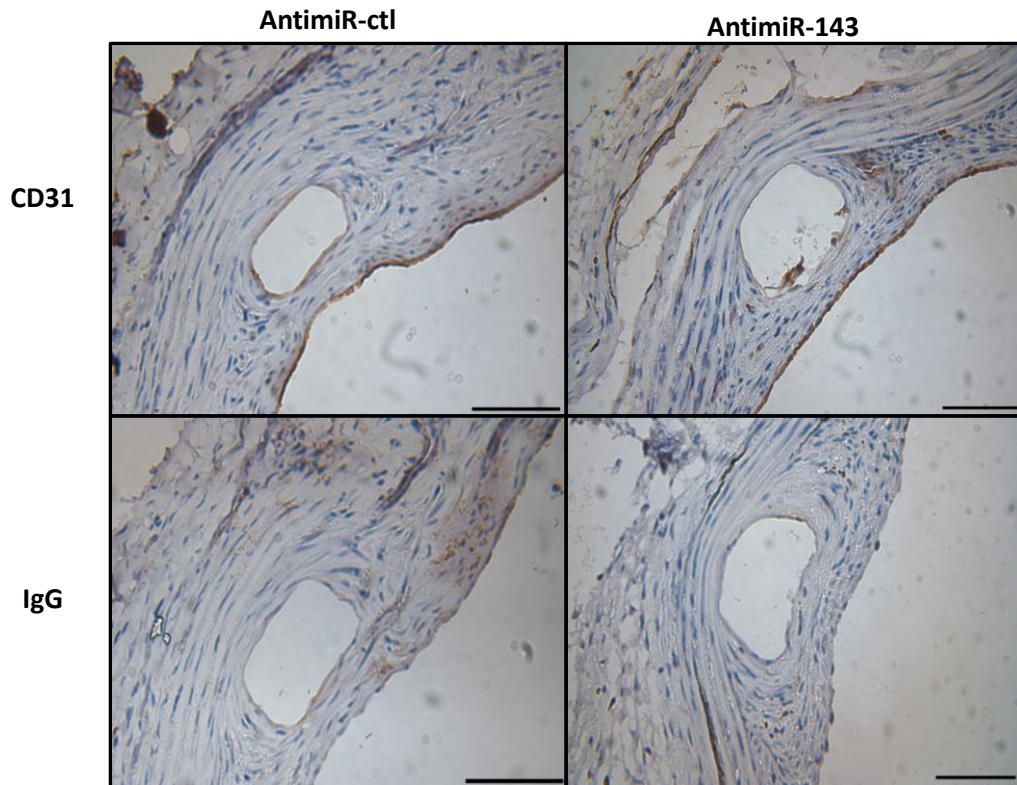


Figure 6.8. CD31 expression in 28 day stented vessels from antimiR treated mice.

Representative images of immunohistochemistry shown by DAB (brown) staining for CD31 or IgG control in vessels isolated from antimiR-ctl and antimiR-143 treated mice. Scale bar = 50 μ m Magnification 40X.

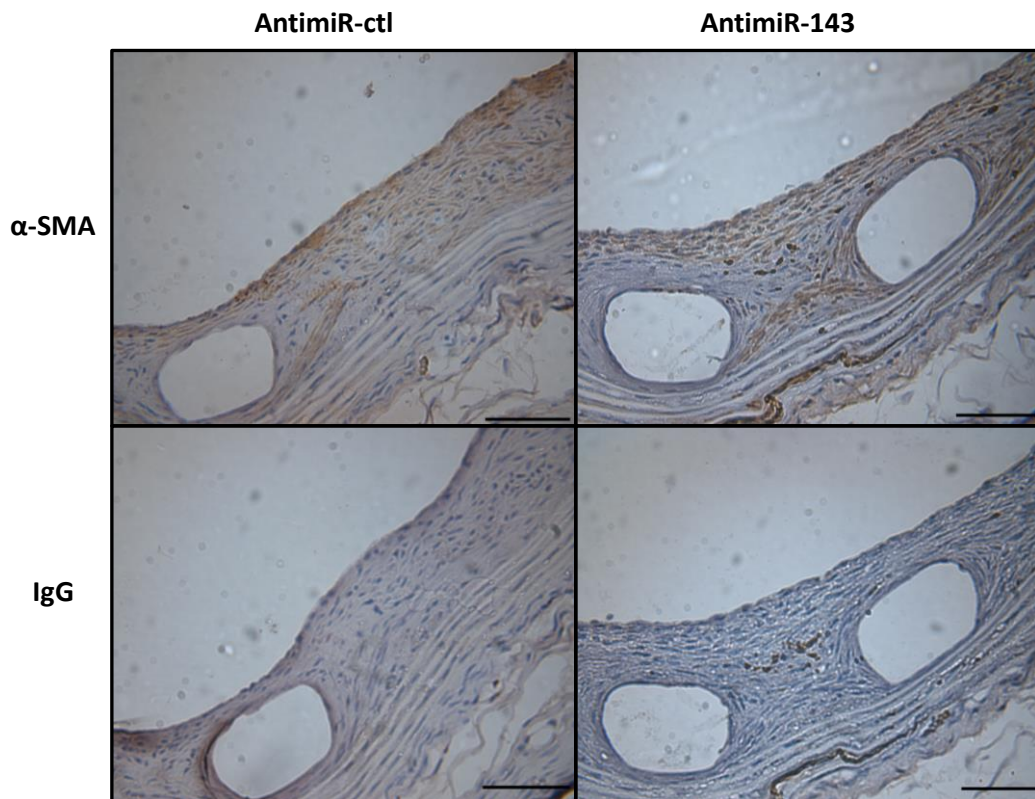


Figure 6.9. α-SMA expression in 28 day stented vessels from antimiR treated mice.

Immunohistochemistry for VSMC marker α-SMA revealed high proportion of α-SMA positive cells in the neointima of 28 day stented antimiR-ctl and antimiR-143 treated mice shown by brown DAB staining which was absent from the IgG control. 40X magnification. Scale bar = 50 μm.

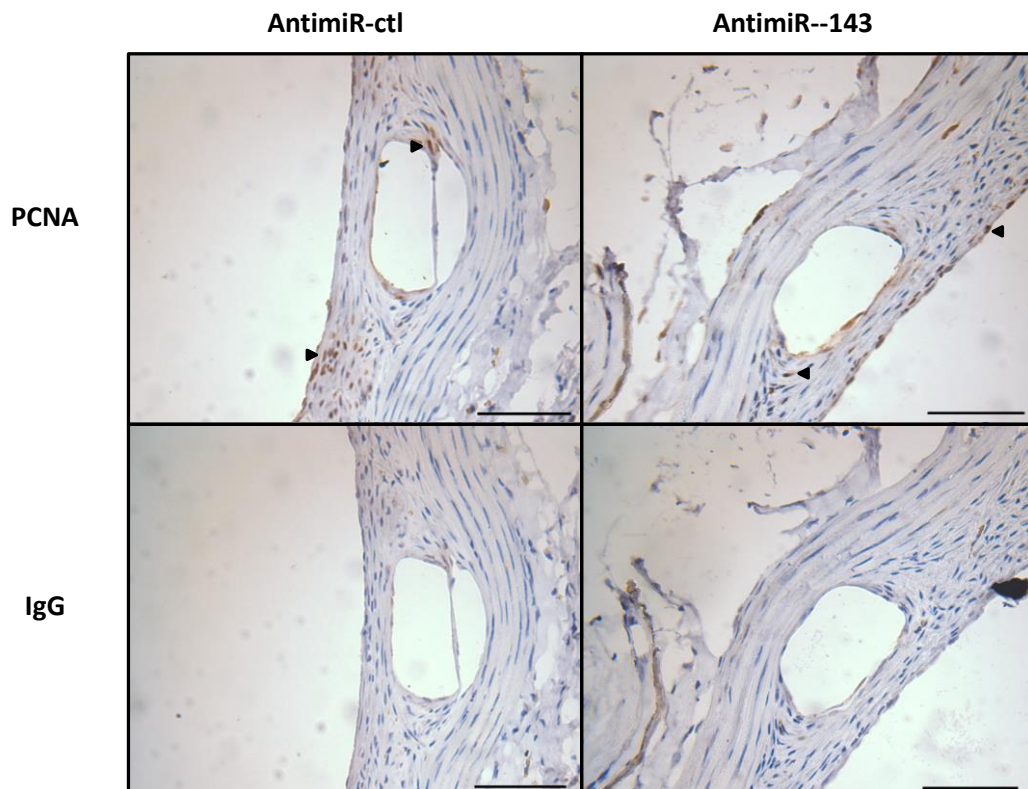


Figure 6.10. PCNA expression in 28 day stented vessels from anti-miR treated mice.

PCNA staining for proliferating cells revealed that a small number of proliferating cells were present in the neointima of both anti-miR-143 and anti-miR-ctl treated mice as shown by DAB staining (arrowheads) for PCNA or (top panel) IgG control (bottom panel). 40X magnification, scale bar = 50 μ m

6.3.4 Target gene expression in tissues from anti-miR treated mice

Following treatment with anti-miR-143 mRNA target expression did not significantly change within the hearts of donor mice (Figure 6.11 A-C). KLF4 expression was significantly decreased in the aorta of recipient mice following treatment with anti-miR-143 however both KLF5 and ELK-1 mRNA expression remained unchanged (Figure 6.11 D-F). To identify whether prolonged treatment (7 doses vs. 3 doses) with anti-miR-143 resulted in altered target mRNA expression, mRNA levels were measured in the hearts of recipient mice, however no significant changes were detected (Figure 6.12 C-E). Interestingly, treatment with anti-miR-143 resulted in a significant increase in miR-145 expression within the heart of recipient mice (Figure 6.12 B). This increase in miR-145 expression within the heart was not present in donor mice which showed reduced miR-145 levels following treatment with anti-miR-143 (Figure 6.4 A).

KLF5 expression was also analysed in the hearts of both donor and recipient mice by western blot to determine whether anti-miR-143 affected target expression at the protein level. No significant difference in KLF5 expression levels were detected western blotting (Figure 6.13).

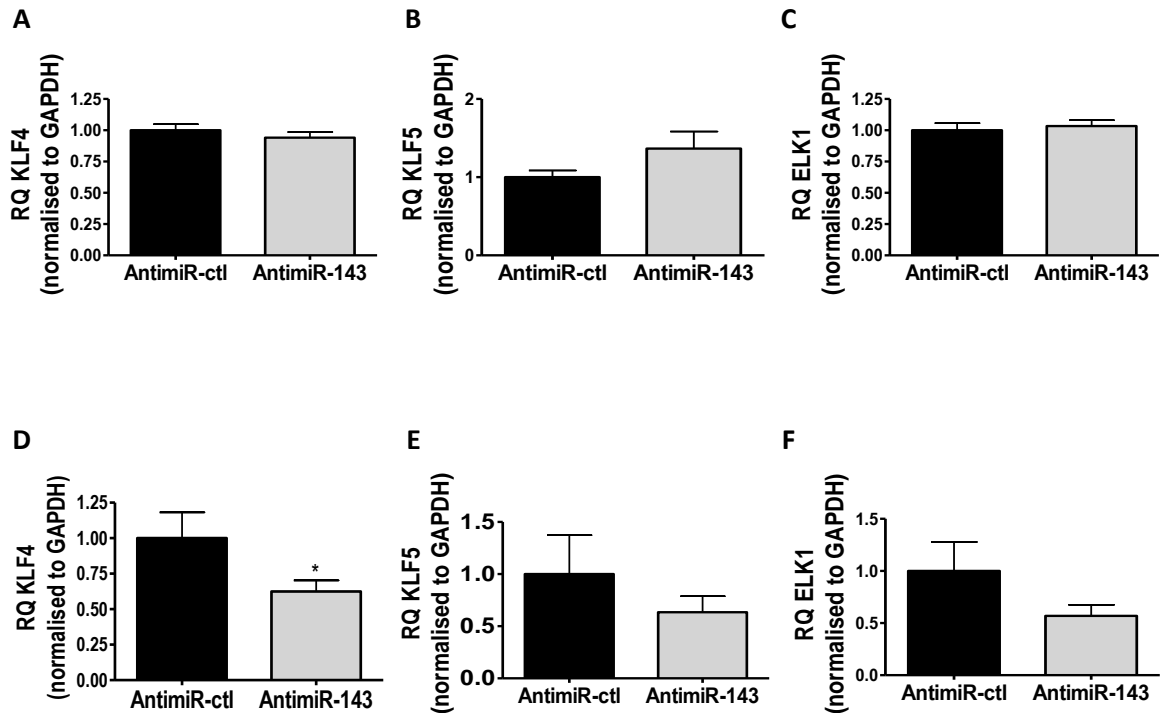


Figure 6.11. Expression of miR-143 target mRNA in the tissues of anti-miR treated mice.

Tissues were isolated on the day of stent surgery (donor hearts) or at sacrifice (recipient aortas) and RNA extracted and expression of target mRNA KLF4, KLF5 or ELK-1 was analysed by Taqman® qRT-PCR in the donor heart (A-C) and the recipient aorta (D-F). *P < 0.05 vs. anti-miR-ctrl. n = 8-12/group.

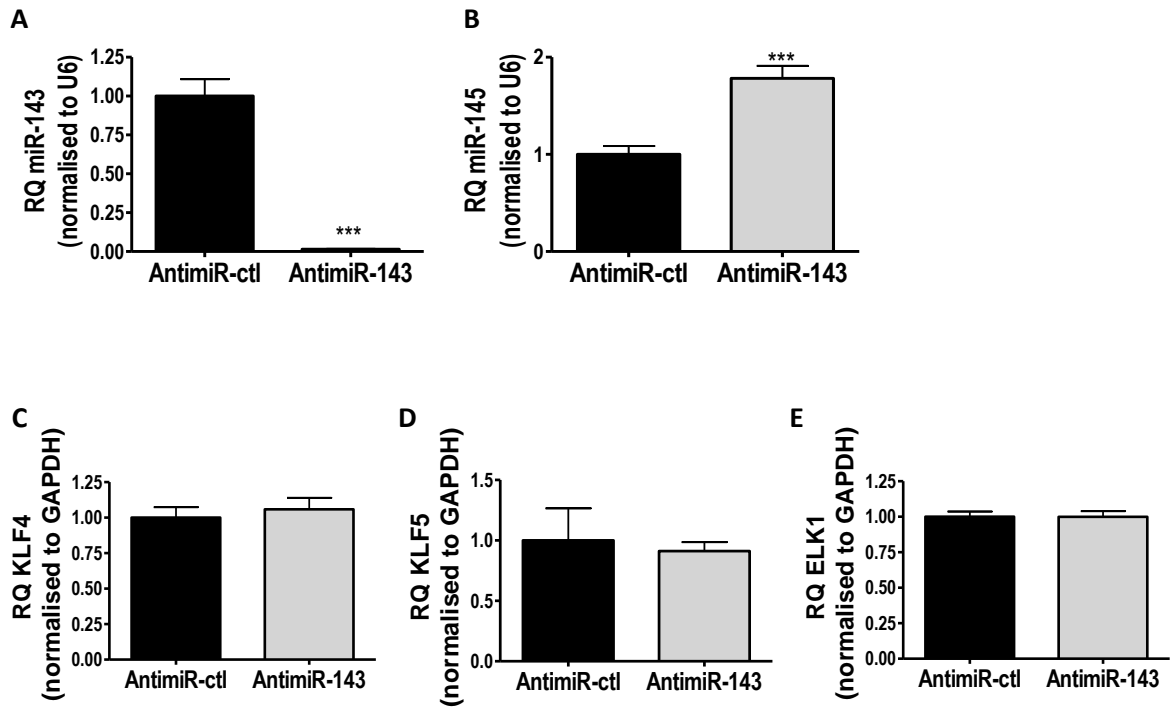


Figure 6.12. Analysis of miRNA and target mRNA expression in the recipient heart.

MiRNA expression was analysed by Taqman® qRT-PCR in the hearts of recipient mice isolated at sacrifice following treatment with 7 doses of 10 mg/kg antimiR-143 or antimiR-ctl delivered at 1 week intervals. Analysis is shown for miR-143 (A) and miR-145 (B). mRNA expression for targets KLF4 (C), KLF5 (D) and ELK-1 (E). *** $P < 0.001$ vs. antimiR-ctl. $n = 8-12$ /group.

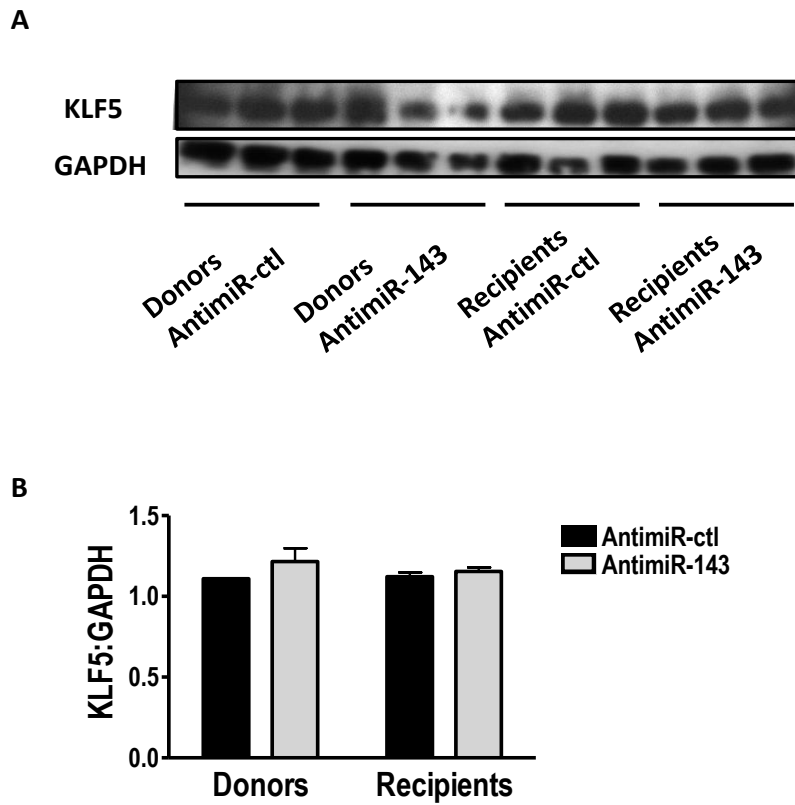


Figure 6.13. Western blot of KLF5 expression in hearts of antimiR treated mice.

Western blots were performed on RNA from the hearts of donor mice or recipient mice isolated at sacrifice following 3 or 7 weekly doses of 10mg/kg antimiR-143 or antimiR-ctl respectively. Blots were probed for KLF5 or GAPDH (A) and analysed by densitometry (B). n = 3/group.

6.4 Discussion

In summary, results from this study revealed that SC delivery of antimiR-143, but not antimiR-ctl resulted in potent knockdown in miR-143 expression within the tissues. Neointimal formation 28 days post-stenting was comparable in mice that received antimiR-ctl and antimiR-143, indicating that pharmacological knockdown of miR-143 expression does not alter neointimal formation in response to aortic stenting in mice.

MiR-143 promotes a contractile VSMC phenotype by repressing mRNA targets which promote proliferation and migration (Cordes et al., 2009, Xin et al., 2009). It has previously been reported that following vascular injury local expression of miR-143 is reduced (Cordes et al., 2009, Elia et al., 2009). Furthermore, adenovirus-mediated delivery of miR-143 to the balloon-injured rat carotid artery results in a significant reduction in neointimal formation (Elia et al., 2009). This indicates that loss of miR-143 expression following vascular injury is a contributing factor in the development of neointima. Additionally, our results detailed in chapter 5 revealed that miR-143 KO mice form less neointima in response to stenting than WT mice. When considered together, these studies suggest that endogenous knockdown of miR-143 levels following vascular injury is necessary for the shift towards a more synthetic VSMC phenotype and that this action is potentially hindered by genetic ablation of miR-143 expression. In the present study, analysis of miRNA expression revealed that antimiR-143 treatment produced a significant knockdown of miR-143 expression levels within the aorta and heart but had no effect on neointimal formation in response to stenting.

Mice treated with antimiR-143, had significantly reduced miR-143 tissue expression levels prior to stenting, whereas mice dosed with antimiR-ctl displayed normal vessel levels of miR-143 expression which, if consistent with previous studies (Cordes et al., 2009, Elia et al., 2009), may have been lost upon vascular injury. AntimiR-mediated knockdown of miR-143 prior to stenting may have mirrored the endogenous process of miR-143 knockdown that occurs following vascular injury (Cordes et al., 2009, Elia et al., 2009). Target de-repression following endogenous or pharmacological knockdown of miR-143 expression levels may be comparable and accordingly the degree of neointimal formation unaffected by antimiR-143.

The possibility of systemic delivery of antimiRs leading to sequestration in cellular compartments such as endosomes has been suggested (van Rooij, 2011), which could lead to reduced bioavailability of antimiRs within cells and hinder their ability to bind miRNA. Addition of LNA/DNA antimiRs to cell lysates has been shown to significantly hinder miRNA detection by northern blot (Torres et al., 2011) which raises the possibility that antimiRs stored in endosomes could be released upon tissue lysis and bind to the target miRNA. Therefore, the genuine degree of miR-143 knockdown induced by antimiR-143 delivery *in vivo* could be less than that detected by methods employed following tissue disruption, including Taqman® qRT-PCR and northern blotting. No consistent upregulation in miR-143 target gene expression was detected in the heart or aorta following antimiR-143 delivery. This may be indicative of antimiR-143 not sufficiently inhibiting miR-143 within the tissues to result in target de-repression and is another potential reason why no difference in the neointimal formation was detected. However, several studies have reported target de-repression following antimiR delivery *in vivo* which have resulted in functional effects (Elmen et al., 2008b, Elmen et al., 2008a) providing evidence that antimiRs do in fact inhibit miRNA expression *in vivo*. For example, antimiR-29b was shown to upregulate the expression of several miR-29b target genes including col1a1 and elastin which resulted in increased fibrosis and reduced abdominal aortic aneurysm progression in 2 different mouse models (Maegdefessel et al., 2012).

The decreased KLF4 expression detected in the aortas of antimiR-143 recipient mice may be due to compensatory increased regulation of this mRNA by miR-145 upon knockdown of miR-143 expression. A number of other possibilities exist as to why target de-repression was not detected following antimiR-143 delivery. MiRNAs have previously been shown to alter mRNA expression for the vast majority of targets (Baek et al., 2008) however this does not rule out that some targets may be regulated at the protein level and western blots could be performed to rule this out. As discussed in chapter 5, de-repression of KLF4, KLF5 or ELK-1 was not detected in miR-143 KO mice and therefore expression of these genes may not be regulated by miR-143 in the tissues analysed. However, it is also possible that de-repression of these targets was not apparent as expression levels were analysed in non-stressed tissues. It has previously been shown that target de-repression may only become apparent following stress such

as hypoxia induced remodelling in the pulmonary artery (Caruso et al., 2012). A drawback of this study was that target expression could not be measured in the stented vessels due to their small size and the demands of histology. AntimiR-29b-dependent increases in target mRNA *col1a1*, *col3a1* and *elastin* were detected at day 14 but not day 7 or 28 following abdominal aortic aneurysm induction by Ang II infusion in ApoE KO mice (Maegdefessel et al., 2012). This indicates that influence of miRNA modulation on a target gene expression can be temporal and is likely to be dependent upon the abundance of the mRNA target during the stage of the remodelling process. It would be important for future studies that target expression is measured in the stented vessel at an appropriate time point during which VSMC proliferation and migration is at a peak. Confirming that target gene de-repression does occur is important to ascertain that antimiR-143 functioned efficiently to inhibit miR-143 expression within the stented aorta and that the detected knockdown in expression is not a processing artefact.

Changes in miRNA and mRNA expression after injury can be both spatial and temporal (Port et al., 2011). Balloon injury to the rat carotid artery induces loss of miR-133 expression by day 2 post-injury when VSMC proliferation is pronounced, however by day 14 post-injury miR-133 levels significantly recover towards levels seen in control animals (Torella et al., 2011). Similar results were seen in the mouse left ventricle following MI where changes in miRNA expression tended to normalise by day 14 post injury (Port et al., 2011). Unpublished findings from our own group have found recovery of miR-143 expression levels towards control levels in the stented porcine coronary artery by day 28 post-injury. It is unknown whether this also occurs in the mouse stent model, however loss of miR-145 expression following balloon injury of the rat carotid is followed by a time dependent recovery of expression (Cheng et al., 2009). Prolonged knockdown of miR-143 over the 28 day post-stenting period did not result in any increase in neointimal formation compared with control mice. This suggests that reduced miR-143 expression is most important in the early stages of vascular injury, possibly by allowing VSMC switching, but is not sufficient to prolong the neointimal formation in itself. Proliferation is greatest 7 days following stenting in the mouse stent model but is minimal by 28 day (Ali et al., 2007). Both antimiR-143 and antimiR-ctl treated mice showed similar

expression of PCNA and α -SMA at day 28 indicating that antimiR-143 treatment did not result in a prolonged increase in proliferation or increased presence of VSMCs within the neointima.

Our results described in chapter 5 showed that genetic KO of miR-143 expression resulted in a significant reduction in neointimal formation compared with WT mice in response to stenting. We hypothesise that the disparity between the results of our genetic KO versus antimiR knockdown of miR-143 is due to altered VSMC signalling following genetic KO. MiR-143 KO mice are viable and display less severe differences in VSMC structure and function than miR-145 KO and miR-143/145 KO mice (Xin et al., 2009, Boettger et al., 2009, Elia et al., 2009). As miR-143 is not essential for VSMC development a large proportion of miR-143 gene regulation may be compensated for by the action of other miRNAs or signalling molecules in its absence. In comparison to miR-143 KO mice antimiR-143 treated mice were fully developed by the time miR-143 loss was induced and as such target de-repression and signalling may be significantly different. MiR-143 and miR-145 are predicted to target a range of genes involved in cytoskeletal arrangement and SRF signalling, and it has been suggested that genetic KO of these miRNA may hinder the ability of VSMCs to alter their phenotype in response to stress (Xin et al., 2009). This is a possible reason for the differences in neointimal formation observed between miR-143 KO and antimiR-143 treated mice.

MiR-145 expression was reduced in both the aorta and heart of recipient mice treated with antimiR-143. This was detectable by Taqman® qRT-PCR but not northern blotting, most probably due to the increased sensitivity of qRT-PCR in detecting small changes in miRNA expression. AntimiR-143 is complimentary to the reverse sequence of miR-143 which shares very little homology with miR-145 and it is therefore unlikely that the decrease in miR-145 expression is due to unspecific binding of antimiR-143. MiR-143 and miR-145 are co-transcribed from a common bicistronic precursor and are transcriptionally activated by signalling molecules including SRF, TGF- β and BMP4 (Cordes et al., 2009, Davis-Dusenbery et al., 2011, Xin et al., 2009). One reason for reduced miR-145 expression could be that loss of miR-143 expression triggers a feedback mechanism whereby transcription of miR-143/145 is reduced. SRF in combination with its cofactor myocardin or MRTF promotes transcription of miR-143/145 by binding to the

CArG box in its regulatory region (Cordes et al., 2009, Xin et al., 2009). Targets of miR-143 and miR-145, ELK-1 and KLF4, have been shown to act as competitive inhibitors of myocardin and MRTF binding to SRF at the CArG box region in contractile genes, significantly reducing transcriptional activation by SRF (Wang et al., 2004, Liu et al., 2005). In the present study ELK-1 expression was not altered at the mRNA level in the heart or aorta of antimiR-143 treated mice however it may only be altered at the protein level as previously reported (Cordes et al., 2009). It is also possible that other targets of miR-143 may act in a similar way as to reduce gene activation by SRF or other signalling molecules which promote miR-143/145 transcription.

Interestingly, in comparison to reduced miR-145 expression seen in donor antimiR-143 treated mice, prolonged miR-143 inhibition in the heart but not the aorta of recipient mice resulted in upregulation in miR-145 expression. MiR-143 and miR-145 are known to regulate gene expression within common pathways and also share a number of targets despite differences in seed sequence (Xin et al., 2009). It is plausible that prolonged loss of miR-143 and target dysregulation could result in a compensatory increase in miR-145 expression within the heart.

As referred to in chapter 5, several issues arose during resin embedding of stented vessels and immunohistochemistry proved challenging. Following several optimisation experiments the success rate of stent electrolysis was improved upon by small adjustments in the technique. In the present study it was decided that electrolysis of stents and paraffin embedding offered more advantages than resin embedding with regards to the number of sections and ability to perform immunohistochemistry. Electrolysis of the stent strut removes the scaffold holding the vessel in position and as such the vessel collapses inward slightly hence the reduced vessel area seen in this study when compared to that of chapter 5.

In the present study the degree of neointimal formation in response to stenting in antimiR-ctl treated mice was found to be considerably less than that of WT mice described in chapter 5. Neointimal formation after vascular injury has been shown to vary significantly between mice of different genetic background, with C57BL/6 mice relatively resistant to neointima formation (Harmon et al., 2000, Kuhel et al., 2002). The transgenic mice used in chapter 5 have a mixed genetic

background (Xin et al., 2009) and thus direct comparisons in neointima formation between these two studies cannot be made and they must be considered separately and compared to their own experimental controls. It was shown in chapter 5 that deployment of the stent by inflation of the balloon catheter to 10 atmospheres pressure resulted in a highly consistent stent expansion. Furthermore injury scores are comparable between the present study and those shown in chapters 4 and 5 indicating that all mice received an equivalent vascular injury. It has previously been shown that C57BL/6J mice develop only a modest neointimal layer following *in situ* stenting of the abdominal aorta with a percentage stenosis of around 20% (Rodriguez-Menocal et al., 2010) which is similar to the present study. Also consistent with the present study was the low presence of macrophages in the model (Rodriguez-Menocal et al., 2010). In contrast, macrophages were detected in all vessels examined in the preliminary study in chapter 4, indicating that these mice had a greater degree of inflammation which may have in turn contributed to development of a more pronounced neointima. Refinement of the procedure may have reduced vessel damage during handling and this together with optimisation of the surgical technique e.g. graft size and position, most likely accounts for the difference in neointima seen between the present study and that described in chapter 4.

To conclude, SC delivery of antimiR-143 resulted in a detectable knockdown of miR-143 expression in both donor and recipient mice. Reduction of miR-143 expression levels by antimiR-143 did not result in any alterations in neointimal formation or composition in response to stenting. This suggests that antimiR-143 may have mimicked the endogenous loss of miR-143 that occurs following vascular injury (Cordes et al., 2009, Elia et al., 2009). Despite reduced miR-143 expression within the tissues no de-repression of miR-143 targets ELK-1, KLF4 or KLF5 was detected. Further studies are required to confirm that target regulation occurs following antimiR-143 treatment to ascertain that miR-143 knockdown did occur *in vivo* and was not detected due to any processing artefacts.

7 General discussion

7.1 General discussion

This thesis contains research outputs that increase current understanding of the role of miR-143 and miR-145 with respect to their regulation of VSMC phenotype. Further we identify for the first time the influence of these miRNA on restenosis following stenting. Using a mouse model we investigated the effect of modulating miR-143 and miR-145 levels on in-stent stenosis and uncovered differences between the effect of genetic and pharmacological knockdown of these miRNA. Genetic KO of miR-143 and miR-145 reduced stenosis following deployment of a metal stent, highlighting the fundamental importance of these miRNA in vessel response to injury.

A common consequence of injury to the vascular wall is activation of VSMCs which causes a shift from a contractile to a synthetic phenotype (Kocher et al., 1991, Orlandi et al., 1994). Synthetic VSMCs show enhanced proliferation and migration which results in vessel remodelling and neointimal formation and is a key component in the development of vascular injury associated diseases including in-stent restenosis and vein graft disease (Schwartz et al., 1992, Cox et al., 1991). DES are currently used to prevent in-stent restenosis, however they are associated with an increased risk of thrombosis due to delayed re-endothelialisation (Joner et al., 2006, Finn et al., 2007). Therefore the development of cell selective therapies is desirable. MiR-143 and miR-145 are enriched in VSMCs and have been shown to regulate VSMC phenotype (Cordes et al., 2009, Elia et al., 2009, Cheng et al., 2009).

Previous reports have indicated that miRNAs can act as a phenotypic switch in VSMCs *in vitro*, for example loss of miR-21 by antagomiR delivery leads to a dose dependent decrease in VSMC proliferation and increase in apoptosis (Ji et al., 2007). Similarly miR-133 overexpression decreases VSMC proliferation whereas knockdown of miR-133 leads to an increased proliferative response (Torella et al., 2011). The studies described in chapter 3 were carried out using primary cells isolated from the human saphenous vein, a vessel often used for CABG (Goldman et al., 2004). These experiments were designed to gain insight into the level of influence miR-143 and miR-145 can exert on VSMC phenotype.

MiRNA mimics and antimiRs were used successfully to increase and knockdown miR-143 and miR-145 expression levels in HSV SMCs and HSV ECs. Modulation of miR-143 or miR-145 alone was insufficient to significantly alter proliferation of HSV SMCs in response to serum. This is in contrast to a study in rat A10 SMC line where an antagomiR against miR-143, but not miR-145, was capable of significantly inducing proliferation (Cordes et al., 2009). MTS proliferation assays were found to be unreliable when used with HSV ECs due to the sensitivity of these cells to transfection and the inability of the assay to account for cell death, thus effect of these miRNA on EC proliferation were inconclusive. Further investigation could not be undertaken due to time constraints however thymidine incorporation experiments such as BrdU assays are a more direct measure of proliferation (Porstmann et al., 1985) and could be performed in future studies to clarify this result. Both miR-143 and miR-145 levels are reduced by PDGF (Quintavalle et al., 2010) and overexpression of these miRNA reduces PDGF induced proliferation and migration in VSMCs (Cordes et al., 2009, Cheng et al., 2009). This would suggest that these miRNAs act as downstream effectors of PDGF-induced but not serum-induced VSMC proliferation. Furthermore knockdown of miR-143 or miR-145 levels alone did not induce VSMC proliferation indicating that additional signalling by PDGF is required to promote proliferation though downregulation of these miRNA.

MiR-143 and miR-145 expression is often downregulated in cancer cells and is associated with reduced migration and metastasis (Lee et al., 2013, Xu et al., 2011). Less is known about the role of miR-143 and miR-145 with regards to SMC migration. VSMCs isolated from miR-143/145 KO mice show increased migration and formation of podosomes, actin rich protrusions involved in cell migration, in response to PDGF (Quintavalle et al., 2010). Several miR-143 and miR-145 target proteins have been identified as regulators of migration including FSCN1 and KLF5 (Quintavalle et al., 2010). To assess whether alteration of miR-143 or miR-145 expression alone is capable of influencing VSMC migration we investigated the response of HSV SMCs and HSV ECs to a well establish scratch assay technique where cells migrate into a wound to replace denuded cells (Liang et al., 2007). PremiRs and antimiRs were used to modulate miRNA levels in these studies as they did not exhibit the toxicity seen with Ads as described in chapter 3. Migration was not affected by overexpression or knockdown of miR-143 or

miR-145 levels in either cell type. As overexpression of miR-143 or miR-145 has been shown to reduce podosome formation induced by PDGF (Quintavalle et al., 2010) it is possible that altered migration could be seen by modulation of miR-143 or miR-145 in a chemotaxis experiment with PDGF such as a boyden chamber assay.

The majority of miRNA targets are regulated at both the mRNA and protein level (Guo et al., 2010). KLF4 and KLF5 have been previously identified as targets of both miR-143 and miR-145 (Cordes et al., 2009, Xin et al., 2009, Cheng et al., 2009, Davis-Dusenbery et al., 2011). Analysis of mRNA in our study supported these findings with KLF4 and KLF5 expression upregulated following delivery of anti-miR-143 to HSV SMCs suggesting that target de-repression had occurred. Following delivery of miR-143 or miR-145 mimics to cells miR-145 was found to exert a more pronounced repression of these mRNA in pulmonary artery SMCs and luciferase vectors that express their 3' UTR (Davis-Dusenbery et al., 2011, Xin et al., 2009). Conversely, our studies in HSV SMCs found that anti-miR-145 delivery did not lead to altered KLF4 or KLF5 expression, indicating that the importance of each miRNA in regulating common targets may vary according to cell type. It is also possible that additional signalling must be activated in order for miR-145 targeting of these mRNA to be seen. AntagomiRs against miR-143 and miR-145 both exert an inhibitory effect on BMP4- or TGF- β -mediated down-regulation of KLF4 expression in pulmonary artery SMCs (Davis-Dusenbery et al., 2011). Furthermore, downregulation of miR-145 levels by PDGF has been shown to lead to de-repression of KLF5 (Cheng et al., 2009). Regulation of KLF4, KLF5 and ELK-1 (Cheng et al., 2009, Cordes et al., 2009) has been reported to only be detectable at protein level however others disagree and have detected changes in mRNA level (Hergenreider et al., 2012, Davis-Dusenbery et al., 2011). Western blots could be carried out in future studies to investigate this.

In contrast to anti-miR-143, delivery of premiR-143 did not alter KLF4 or KLF5 expression. The de-repression of KLF4 and KLF5 evoked by loss of miR-143 expression suggests that under basal conditions miR-143 actively represses these mRNA in HSV SMCs. It is possible that increasing miR-143 levels may result in preferential repression of more highly expressed mRNA targets with greater bioavailability for binding. One study revealed that the availability of miRNA for target binding following delivery of a miRNA mimic is subject to saturation

(Mukherji et al., 2011). This indicates that large increases in miRNA expression seen by qRT-PCR following mimic delivery may not be reflective of the actual amount of miRNA which is incorporated into the RISC and is biologically active.

Significantly, repression or de-repression of mRNA target levels in HSV SMCs by premiRs or antimiRs was not detected for any other previously identified targets tested in the study. Many of these targets were identified in other cell types or by luciferase assay and as such may not be valid targets of miR-143 and miR-145 in HSV SMCs. The development of biotinylated miRNA mimics, offers one approach to identify miR-143 and miR-145 targets in HSV SMCs (Orom and Lund, 2007). These mimics exist as duplexes, structurally similar to the premiR mimics used in chapter 3, but contain a biotin group attached to the 3' sense strand which is selectively chosen for incorporation into the RISC. Following cell lysis miRNAs and bound mRNAs are captured by affinity purification by streptavidin beads and mRNA purified and identified by qRT-PCR or microarray (Orom and Lund, 2007). This method was previously successful in identifying both validated and novel miR-21 targets (Kang et al., 2012). Tandem affinity precipitation target identification (TAP-Tar) increases the specificity of mRNA target purification by using stable cell lines which express tagged AGO proteins (Nonne et al., 2010). Targets are identified from cell lysates first by pulldown of AGO proteins followed by streptavidin bead isolation as described above. This allows identification of biotinylated miRNA in association with the RISC and helps eliminate binding of non-incorporated biotinylated miRNA (Nonne et al., 2010).

Genetic KO studies are often beneficial in identifying the essential roles which a miRNA plays in a biological system. The study described in chapter 5 found that mice genetically ablated of miR-143 or miR-145 develop significantly less neointimal formation in response to stenting than WT mice indicating that these miRNA are essential for normal VSMC response to injury. Similar results were shown in the carotid artery following ligation however, in contrast to our stent model where neointima did form in miR-145 KO mice, ligated mice were shown to develop virtually no neointima (Xin et al., 2009). This is surprising as carotid artery ligation in WT mice produces a substantial neointimal formation far greater than that which develops in WT stented mice (Xin et al., 2009, Ali et al., 2007). The disparities between these two studies are probably due to the underlying differences between these models. Carotid ligation causes cessation

of blood flow through the vessel resulting in reduced vessel diameter a shift in haemodynamic forces that drives neointimal formation (Kumar and Lindner, 1997). MiR-145 KO mice have been reported to have low blood pressure which may have contributed to the lack of neointima seen in the carotid artery ligation model (Xin et al., 2009). This reduction in blood pressure may account for the reduced left ventricular mass index seen in miR-145 KO mice by ourselves and others (Xin et al., 2009). In contrast to the ligation model the stent model is driven by endothelial denudation, vessel stretch and presence of a metal stent (Ali et al., 2007).

Medial remodelling was also reduced following stenting in miR-143 KO and miR-145 KO mice, this was also noted in the carotid artery ligation model (Xin et al., 2009). Several studies have reported reduced medial vessel thickness in miR-143/145 double KO mice (Boettger et al., 2009, Elia et al., 2009) and one report stated that this was also apparent in the aorta of miR-145 but not miR-143 KO mice (Xin et al., 2009). Our own study revealed that aortic wall thickness was comparable between miR-143 KO, miR-145 KO and WT mice. As no quantification was shown in the previous study it is unclear the extent of this vessel reduction in miR-145 KO mice although we would predict it would be less than that seen in miR-143/145 KO (Boettger et al., 2009, Elia et al., 2009) as loss of both miRNA may have accumulative effects. The disparity between our results may be due to our mice being older at the time of measurements, 18 weeks vs. 8 weeks by which point compensatory VSMC regulation, possibly by miR-143 may have led to differences in vessel thickness being rectified.

The results found in chapter 5 added to the body of knowledge on the role of miR-143 and miR-145 by showing how genetic loss of these miRNA affects vessel remodelling in a clinically relevant model which shares many pathological features with human disease (Ali et al., 2007, Carter et al., 1994). Previous studies have shown that restoration of miR-143 or miR-145 expression reduces neointimal formation after injury (Elia et al., 2009, Cheng et al., 2009). MiR-143 and miR-145 are expressed during development and KO mice have been shown to have differences in VSMC phenotype such as disturbed stress fiber formation and increased expression of synthetic machinery (Xin et al., 2009, Cordes et al., 2009). MiR-143 and miR-145 have many predicted targets which are involved in cytoskeletal maintenance and it has been suggested that genetic loss of these

miRNA may affect the ability of VSMC phenotypic switching to occur (Xin et al., 2009). Compensatory regulation of the targets of these miRNA is likely to develop upon genetic loss resulting in altered VSMC signalling which may explain the differences seen between our genetic KO study and previous overexpression studies.

The study performed in chapter 6 is the first carried out, to our knowledge, which assesses the effect of pharmacological-induced loss of miR-143 expression in a vascular injury model. It was shown that SC delivery of an antimiR-143 leads to a potent knockdown of miR-143 expression. Contrary to the results of our genetic KO study which showed reduced neointimal formation in response to loss of miR-143, no significant difference in neointimal formation was detected following antimiR knockdown of miR-143 in mice. There are several possible reasons for this result which suggest the need for further studies. AntimiR-143 treatment may have mimicked the endogenous loss of miR-143 seen after vascular injury (Cordes et al., 2009, Elia et al., 2009, Cheng et al., 2009) and thus may have added no additional affect. Knockdown of miR-145 expression following ligation of the carotid in the rat has been shown to be followed by a time-dependent recover towards control levels (Cheng et al., 2009). As miR-143 is cotranscribed with miR-145 it is probable that miR-143 expression also recovers over time following vascular injury. Pre-treatment of mice resulted in miR-143 loss occurring prior to vascular injury and being sustained throughout the entire study period, indicating that sustained knockdown of this miRNA is not sufficient to further promote neointimal formation. Taken together with overexpression studies this would suggest that low expression of miR-143 is most important during the early stages of vascular injury, perhaps by facilitating the initial highly proliferative and migratory stage.

Another possibility as to why antimiR-143 treatment did not alter neointimal formation in response to stenting is that the antimiRs may not have been processed correctly in the target tissue. It has been shown that antimiRs interfere with miRNA detection methods by binding to miRNAs following cell lysis (Torres et al., 2011). AntimiR-143 could be compartmentalised within cells separate from miR-143 and be release upon tissue lysis, this potential artefact could result in the actual *in vivo* knockdown of the miR-143 being overrepresented. However, several studies using antimiRs of similar structure to

those used in chapter 6 have shown that functional effects occur upon anti-miR delivery *in vivo* providing evidence that true miRNA inhibition does occur (Elmen et al., 2008b, Montgomery et al., 2011, Maegdefessel et al., 2012). Inhibiting endogenous miR-143 bioavailability using a different approach, such as miRNA sponges, is one option to confirm the effect of miR-143 knockdown on neointimal formation. MiRNA sponges encode miRNA target RNA sequences which act to competitively inhibit miRNA repression of endogenous targets (Ebert et al., 2007).

In the simplest model, knockdown of a miRNA would result in an increase in the expression of its target genes. However, as described in chapters 5 and 6, target de-repression was not detectable following genetic KO or anti-miR delivery in mice. Previous studies have revealed that most mRNAs contain multiple binding sites for several different miRNAs within their 3' UTR and thus expression of a given target may be under regulation from multiple miRNAs (Friedman et al., 2009). Fluctuations in target expression that may be induced by modulation of miR-143 or miR-145 expression could potentially be rectified by compensatory increased or decreased repression by other miRNAs.

Under basal conditions miRNAs appear to act to fine-tune target gene expression and single cell studies have indicated that target regulation by miRNAs is both non-linear and subject to thresholds (Mukherji et al., 2011). MiRNAs were shown to only modestly modulate target protein expression when expression of the target mRNA remains above a certain threshold level. However, if target mRNA expression is below the threshold the miRNA will strongly repress the target protein. Increasing the number of complementary binding sites or increasing miRNA expression raises the threshold so that a greater number of target mRNAs are required to meet the threshold (Mukherji et al., 2011). The lack of target de-repression seen following anti-miR-143 delivery could be due to the expression of these target mRNAs being above the threshold and hence subject to only mild regulation by the miR-143. If this were the case then anti-miR knockdown may result in only modest change in target expression, which could be obscured by other compensatory regulation.

It is possible that a tissue may need to be stressed in order for altered target regulation to become apparent. A limitation of the study was that qRT-PCR

analysis of target expression could not be performed on the stented tissue due to the small size and the requirements for histology. It has been previously shown that de-repression may only become apparent following vascular stress such hypoxia, which induces upregulation of miR-145 targets in the lung and pulmonary artery of miR-145 KO mice (Caruso et al., 2012). This could be due to induction of miRNA targets through stress signalling activated upon vascular injury. AntimiR knockdown of miRNA expression in stressed tissue may lead to an exacerbated increase in target expression due to the lack of availability of the miRNA for regulation and the increasing levels of mRNA. Other studies have shown that during vessel remodelling target de-repression by antimiRs occurs in only at certain time points (Maegdefessel et al., 2012) indicating that regulation by antimiRs can be temporal rather than constant. This type of regulation probably depends on the relative abundance of the mRNA target at a specific stage of the remodelling process. It would be important for future studies to assess target de-repression within the stented aorta and at an appropriate time when proliferation and migration are at their peak. Bioinformatics programs offer ways to identify potential miRNA targets by identifying complementary binding sites in the 3' UTR of mRNA. Potential targets could then be confirmed by qRT-PCR. Performing a microarray or proteomic analysis on tissues from antimiR-143 treated mice, in combination with bioinformatics studies is another option to identify targets (Lim et al., 2005, Baek et al., 2008). This would be particularly important as detectable target de-repression is needed to confirm that miR-143 knockdown by antimiR-143 occurs *in vivo* and that the decrease in miR-143 expression detected following tissue lysis is not due to processing artefacts.

Clinically, stenting and CABG are performed in patients that have pre-existing atherosclerosis and thus the effects of hyperlipidaemia and increased inflammation must be considered. To increase the clinical relevance of future studies stenting could be performed in ApoE KO mice (Piedrahita et al., 1992, Plump et al., 1992). These mice have elevated levels of VLDL and increased inflammation and display significantly more neointimal formation than WT mice following stenting (Ali et al., 2007). It would be important to assess whether the therapeutic effect of increased miR-143 and miR-145 expression levels on reducing neointimal formation (Elia et al., 2009) extends to models with

increased pro-inflammatory signalling. Furthermore, delayed EC repopulation is seen in ApoE KO mice (Xu et al., 2003, Douglas et al., 2012) and it would be important to ascertain that overexpression of miR-143 or miR-145 does not have a detrimental effect on EC repopulation as this could have implications for thrombosis.

Results from our genetic KO study support the view that miR-143 and miR-145 expression are essential for normal vessel response to injury. Others have identified that overexpression of these miRNA can reduce remodelling after vascular injury in mouse models (Cheng et al., 2009, Elia et al., 2009, Cordes et al., 2009). Future studies could involve analysis of overexpression of these miRNA in the vessel wall using the adenoviral vectors developed in chapter 3. Further, miRNA transgenes could be re-cloned into a different Ad vector, such as a subgroup B Ad, to improve transgene delivery to the vessel wall (Havenga et al., 2001). Delivery of Ads which express miR-143 or miR-145 has been shown to reduce neointimal formation after balloon-injury to the rat carotid artery (Elia et al., 2009, Cheng et al., 2009). In terms of clinical relevance local delivery of miR-143 or miR-145 to the vessel wall is a preferable therapeutic option as systemic delivery may lead to target repression in non-target tissues which could have functional consequences. Several studies have reported the use of chemistries to attach viruses to metal stents which permit local release to the vessel wall (Johnson et al., 2005, Sharif et al., 2008) providing a possible means of direct miRNA delivery to the site of vascular injury.

In summary, this thesis has presented studies which extend current knowledge of the influence of miR-143 and miR-145 on VSMC phenotype following injury. Modulation of miR-143 or miR-145 levels alone was shown to be insufficient to modify proliferation or migration of human VSMCs. A previous study identified that endogenous loss of miR-143 after injury is important in promoting neointimal formation (Elia et al., 2009). Conversely, we have demonstrated that genetic loss of miR-143 or miR-145 results in reduced neointimal formation in response to stenting, confirming that these miRNA play a fundamental role in modulating VSMC phenotype in response to injury. Further, we have shown that systemic delivery of an anti-miR inhibitor of miR-143 had no effect on neointimal formation despite detecting a sustained reduction in miR-143 expression levels throughout the study duration. This compliments current knowledge of these

miRNA and demonstrates that antimiR-mediated inhibition of miR-143 does not mimic the effects of genetic KO of miR-143 on neointimal formation in response to stenting.

List of References

- ADAM, P. J., REGAN, C. P., HAUTMANN, M. B. & OWENS, G. K. 2000. Positive- and negative-acting Kruppel-like transcription factors bind a transforming growth factor beta control element required for expression of the smooth muscle cell differentiation marker SM22alpha in vivo. *J Biol Chem*, 275, 37798-806.
- ALBINSSON, S., SKOURA, A., YU, J., DILORENZO, A., FERNANDEZ-HERNANDO, C., OFFERMANN, S., MIANO, J. M. & SESSA, W. C. 2011. Smooth muscle miRNAs are critical for post-natal regulation of blood pressure and vascular function. *PLoS One*, 6, e18869.
- ALBINSSON, S., SUAREZ, Y., SKOURA, A., OFFERMANN, S., MIANO, J. M. & SESSA, W. C. 2010. MicroRNAs are necessary for vascular smooth muscle growth, differentiation, and function. *Arterioscler Thromb Vasc Biol*, 30, 1118-26.
- ALI, Z. A., ALP, N. J., LUPTON, H., ARNOLD, N., BANNISTER, T., HU, Y., MUSSA, S., WHEATCROFT, M., GREAVES, D. R., GUNN, J. & CHANNON, K. M. 2007. Increased in-stent stenosis in ApoE knockout mice: insights from a novel mouse model of balloon angioplasty and stenting. *Arterioscler Thromb Vasc Biol*, 27, 833-40.
- AMBROS, V. & HORVITZ, H. R. 1987. The lin-14 locus of *Caenorhabditis elegans* controls the time of expression of specific postembryonic developmental events. *Genes Dev*, 1, 398-414.
- AMENDO, E. P., EHSANI, N., PALMER, H. & LIBBY, P. 1991. Cytokines and growth factors positively and negatively regulate interstitial collagen gene expression in human vascular smooth muscle cells. *Arterioscler Thromb*, 11, 1223-30.
- ARBUSTINI, E., DE SERVI, S., BRAMUCCI, E., PORCU, E., COSTANTE, A. M., GRASSO, M., DIEGOLI, M., FASANI, R., MORBINI, P., ANGOLI, L., BOSCARINI, M., REPETTO, S., DANZI, G., NICCOLI, L., CAMPOLO, L., LUCREZIOTTI, S. & SPECCHIA, G. 1995. Comparison of coronary lesions obtained by directional coronary atherectomy in unstable angina, stable angina, and restenosis after either atherectomy or angioplasty. *Am J Cardiol*, 75, 675-82.
- ASSOIAN, R. K., FLEURDELYS, B. E., STEVENSON, H. C., MILLER, P. J., MADTES, D. K., RAINES, E. W., ROSS, R. & SPORN, M. B. 1987. Expression and secretion of type beta transforming growth factor by activated human macrophages. *Proc Natl Acad Sci U S A*, 84, 6020-4.
- AUERBACH, W. & AUERBACH, R. 1994. Angiogenesis inhibition: a review. *Pharmacol Ther*, 63, 265-311.
- BAEK, D., VILLEN, J., SHIN, C., CAMARGO, F. D., GYGI, S. P. & BARTEL, D. P. 2008. The impact of microRNAs on protein output. *Nature*, 455, 64-71.
- BAI, X., MARGARITI, A., HU, Y. H., SATO, Y., ZENG, L. F., IVETIC, A., HABI, O., MASON, J. C., WANG, X. & XU, Q. B. 2010. Protein Kinase C delta Deficiency Accelerates Neointimal Lesions of Mouse Injured Artery Involving Delayed Reendothelialization and Vasohibin-1 Accumulation. *Arteriosclerosis Thrombosis and Vascular Biology*, 30, 2467-2474.
- BARTEL, D. P. 2009. MicroRNAs: target recognition and regulatory functions. *Cell*, 136, 215-33.

- BASKERVILLE, S. & BARTEL, D. P. 2005. Microarray profiling of microRNAs reveals frequent coexpression with neighboring miRNAs and host genes. *RNA*, 11, 241-7.
- BATTEGAY, E. J., RAINES, E. W., SEIFERT, R. A., BOWEN-POPE, D. F. & ROSS, R. 1990. TGF-beta induces bimodal proliferation of connective tissue cells via complex control of an autocrine PDGF loop. *Cell*, 63, 515-24.
- BAVRY, A. A., KUMBHANI, D. J., HELTON, T. J., BOREK, P. P., MOOD, G. R. & BHATT, D. L. 2006. Late thrombosis of drug-eluting stents: a meta-analysis of randomized clinical trials. *Am J Med*, 119, 1056-61.
- BEITZINGER, M., PETERS, L., ZHU, J. Y., KREMMER, E. & MEISTER, G. 2007. Identification of human microRNA targets from isolated argonaute protein complexes. *RNA Biol*, 4, 76-84.
- BENNETT, M. R., EVAN, G. I. & SCHWARTZ, S. M. 1995. Apoptosis of human vascular smooth muscle cells derived from normal vessels and coronary atherosclerotic plaques. *J Clin Invest*, 95, 2266-74.
- BERGELSON, J. M., CUNNINGHAM, J. A., DROGUETT, G., KURT-JONES, E. A., KRITHIVAS, A., HONG, J. S., HORWITZ, M. S., CROWELL, R. L. & FINBERG, R. W. 1997. Isolation of a common receptor for Coxsackie B viruses and adenoviruses 2 and 5. *Science*, 275, 1320-3.
- BERNSTEIN, E., KIM, S. Y., CARMELL, M. A., MURCHISON, E. P., ALCORN, H., LI, M. Z., MILLS, A. A., ELLEDGE, S. J., ANDERSON, K. V. & HANNON, G. J. 2003. Dicer is essential for mouse development. *Nat Genet*, 35, 215-7.
- BLANK, R. S. & OWENS, G. K. 1990. Platelet-derived growth factor regulates actin isoform expression and growth state in cultured rat aortic smooth muscle cells. *J Cell Physiol*, 142, 635-42.
- BLENKIRON, C., GOLDSTEIN, L. D., THORNE, N. P., SPITERI, I., CHIN, S. F., DUNNING, M. J., BARBOSA-MORAIS, N. L., TESCHENDORFF, A. E., GREEN, A. R., ELLIS, I. O., TAVARE, S., CALDAS, C. & MISKA, E. A. 2007. MicroRNA expression profiling of human breast cancer identifies new markers of tumor subtype. *Genome Biol*, 8, R214.
- BOETTGER, T., BEETZ, N., KOSTIN, S., SCHNEIDER, J., KRUGER, M., HEIN, L. & BRAUN, T. 2009. Acquisition of the contractile phenotype by murine arterial smooth muscle cells depends on the Mir143/145 gene cluster. *J Clin Invest*, 119, 2634-47.
- BOHNSACK, M. T., CZAPLINSKI, K. & GORLICH, D. 2004. Exportin 5 is a RanGTP-dependent dsRNA-binding protein that mediates nuclear export of pre-miRNAs. *RNA*, 10, 185-91.
- BONAUER, A., CARMONA, G., IWASAKI, M., MIONE, M., KOYANAGI, M., FISCHER, A., BURCHFIELD, J., FOX, H., DOEBELE, C., OHTANI, K., CHAVAKIS, E., POTENTE, M., TJWA, M., URBICH, C., ZEIHNER, A. M. & DIMMELER, S. 2009. MicroRNA-92a controls angiogenesis and functional recovery of ischemic tissues in mice. *Science*, 324, 1710-3.
- BORCHERT, G. M., LANIER, W. & DAVIDSON, B. L. 2006. RNA polymerase III transcribes human microRNAs. *Nat Struct Mol Biol*, 13, 1097-101.
- BOSHART, M., WEBER, F., JAHN, G., DORSCH-HASLER, K., FLECKENSTEIN, B. & SCHAFFNER, W. 1985. A very strong enhancer is located upstream of an immediate early gene of human cytomegalovirus. *Cell*, 41, 521-30.
- BOUCHER, J. M., PETERSON, S. M., URS, S., ZHANG, C. & LIAW, L. 2011. The miR-143/145 cluster is a novel transcriptional target of Jagged-1/Notch signaling in vascular smooth muscle cells. *J Biol Chem*, 286, 28312-21.
- BRAASCH, D. A. & COREY, D. R. 2001. Locked nucleic acid (LNA): fine-tuning the recognition of DNA and RNA. *Chem Biol*, 8, 1-7.

- BRADSHAW, S. H., KENNEDY, L., DEXTER, D. F. & VEINOT, J. P. 2009. A practical method to rapidly dissolve metallic stents. *Cardiovasc Pathol*, 18, 127-33.
- BRIGHTWELL, G., POIRIER, V., COLE, E., IVINS, S. & BROWN, K. W. 1997. Serum-dependent and cell cycle-dependent expression from a cytomegalovirus-based mammalian expression vector. *Gene*, 194, 115-23.
- BRITISH HEART FOUNDATION. 2012. *Coronary heart disease statistics. A compendium of health statistics*. [Online]. Available: <http://www.bhf.org.uk/publications/view-publication.aspx?ps=1002097> [Accessed 30.09.13].
- BURKE, A. P., KOLOGIE, F. D., FARB, A., WEBER, D. K., MALCOM, G. T., SMIALEK, J. & VIRMANI, R. 2001. Healed plaque ruptures and sudden coronary death: evidence that subclinical rupture has a role in plaque progression. *Circulation*, 103, 934-40.
- CAI, X., HAGEDORN, C. H. & CULLEN, B. R. 2004. Human microRNAs are processed from capped, polyadenylated transcripts that can also function as mRNAs. *RNA*, 10, 1957-66.
- CAIXETA, A., LEON, M. B., LANSKY, A. J., NIKOLSKY, E., AOKI, J., MOSES, J. W., SCHOFER, J., MORICE, M. C., SCHAMPAERT, E., KIRTANE, A. J., POPMA, J. J., PARISE, H., FAHY, M. & MEHRAN, R. 2009. 5-year clinical outcomes after sirolimus-eluting stent implantation insights from a patient-level pooled analysis of 4 randomized trials comparing sirolimus-eluting stents with bare-metal stents. *J Am Coll Cardiol*, 54, 894-902.
- CAO, L., KONG, L. P., YU, Z. B., HAN, S. P., BAI, Y. F., ZHU, J., HU, X., ZHU, C., ZHU, S. & GUO, X. R. 2012. microRNA expression profiling of the developing mouse heart. *Int J Mol Med*, 30, 1095-104.
- CAPLICE, N. M., ARONEY, C. N., BETT, J. H., CAMERON, J., CAMPBELL, J. H., HOFFMANN, N., MCENIERY, P. T. & WEST, M. J. 1997. Growth factors released into the coronary circulation after vascular injury promote proliferation of human vascular smooth muscle cells in culture. *J Am Coll Cardiol*, 29, 1536-41.
- CARTER, A. J., LAIRD, J. R., FARB, A., KUFS, W., WORTHAM, D. C. & VIRMANI, R. 1994. Morphologic characteristics of lesion formation and time course of smooth muscle cell proliferation in a porcine proliferative restenosis model. *J Am Coll Cardiol*, 24, 1398-405.
- CARUSO, P., DEMPSIE, Y., STEVENS, H. C., MCDONALD, R. A., LONG, L., LU, R., WHITE, K., MAIR, K. M., MCCLURE, J. D., SOUTHWOOD, M., UPTON, P., XIN, M., VAN ROOIJ, E., OLSON, E. N., MORRELL, N. W., MACLEAN, M. R. & BAKER, A. H. 2012. A role for miR-145 in pulmonary arterial hypertension: evidence from mouse models and patient samples. *Circ Res*, 111, 290-300.
- CHAMBERLAIN, J., WHEATCROFT, M., ARNOLD, N., LUPTON, H., CROSSMAN, D. C., GUNN, J. & FRANCIS, S. 2010. A novel mouse model of in situ stenting. *Cardiovasc Res*, 85, 38-44.
- CHAMLEY-CAMPBELL, J., CAMPBELL, G. R. & ROSS, R. 1979. The smooth muscle cell in culture. *Physiol Rev*, 59, 1-61.
- CHEN, J., KITCHEN, C. M., STREB, J. W. & MIANO, J. M. 2002. Myocardin: a component of a molecular switch for smooth muscle differentiation. *J Mol Cell Cardiol*, 34, 1345-56.
- CHEN, J. F., MURCHISON, E. P., TANG, R., CALLIS, T. E., TATSUGUCHI, M., DENG, Z., ROJAS, M., HAMMOND, S. M., SCHNEIDER, M. D., SELZMAN, C. H., MEISSNER, G., PATTERSON, C., HANNON, G. J. & WANG, D. Z. 2008. Targeted deletion of Dicer in the heart leads to dilated cardiomyopathy and heart failure. *Proc Natl Acad Sci U S A*, 105, 2111-6.

- CHENDRIMADA, T. P., GREGORY, R. I., KUMARASWAMY, E., NORMAN, J., COOCH, N., NISHIKURA, K. & SHIEKHATTAR, R. 2005. TRBP recruits the Dicer complex to Ago2 for microRNA processing and gene silencing. *Nature*, 436, 740-4.
- CHENG, Y., LIU, X., YANG, J., LIN, Y., XU, D. Z., LU, Q., DEITCH, E. A., HUO, Y., DELPHIN, E. S. & ZHANG, C. 2009. MicroRNA-145, a novel smooth muscle cell phenotypic marker and modulator, controls vascular neointimal lesion formation. *Circ Res*, 105, 158-66.
- CHIYOMARU, T., ENOKIDA, H., TATARANO, S., KAWAHARA, K., UCHIDA, Y., NISHIYAMA, K., FUJIMURA, L., KIKKAWA, N., SEKI, N. & NAKAGAWA, M. 2010. miR-145 and miR-133a function as tumour suppressors and directly regulate FSCN1 expression in bladder cancer. *Br J Cancer*, 102, 883-91.
- CIFUENTES, D., XUE, H., TAYLOR, D. W., PATNODE, H., MISHIMA, Y., CHELOUFI, S., MA, E., MANE, S., HANNON, G. J., LAWSON, N. D., WOLFE, S. A. & GIRALDEZ, A. J. 2010. A novel miRNA processing pathway independent of Dicer requires Argonaute2 catalytic activity. *Science*, 328, 1694-8.
- CLARKE, M. C., FIGG, N., MAGUIRE, J. J., DAVENPORT, A. P., GODDARD, M., LITTLEWOOD, T. D. & BENNETT, M. R. 2006. Apoptosis of vascular smooth muscle cells induces features of plaque vulnerability in atherosclerosis. *Nat Med*, 12, 1075-80.
- CLOWES, A. W. & CLOWES, M. M. 1985. Kinetics of cellular proliferation after arterial injury. II. Inhibition of smooth muscle growth by heparin. *Lab Invest*, 52, 611-6.
- CLOWES, A. W. & SCHWARTZ, S. M. 1985. Significance of quiescent smooth muscle migration in the injured rat carotid artery. *Circulation Research*, 56, 139-45.
- CORDES, K. R., SHEEHY, N. T., WHITE, M. P., BERRY, E. C., MORTON, S. U., MUTH, A. N., LEE, T. H., MIANO, J. M., IVEY, K. N. & SRIVASTAVA, D. 2009. miR-145 and miR-143 regulate smooth muscle cell fate and plasticity. *Nature*, 460, 705-10.
- COUGHLAN, L., ALBA, R., PARKER, A. L., BRADSHAW, A. C., MCNEISH, I. A., NICKLIN, S. A. & BAKER, A. H. 2010. Tropism-modification strategies for targeted gene delivery using adenoviral vectors. *Viruses*, 2, 2290-355.
- COX, J. L., CHIASSON, D. A. & GOTLIEB, A. I. 1991. Stranger in a strange land: the pathogenesis of saphenous vein graft stenosis with emphasis on structural and functional differences between veins and arteries. *Prog Cardiovasc Dis*, 34, 45-68.
- CUNNINGHAM, K. S. & GOTLIEB, A. I. 2005. The role of shear stress in the pathogenesis of atherosclerosis. *Lab Invest*, 85, 9-23.
- DAEMEN, M. J., LOMBARDI, D. M., BOSMAN, F. T. & SCHWARTZ, S. M. 1991. Angiotensin II induces smooth muscle cell proliferation in the normal and injured rat arterial wall. *Circ Res*, 68, 450-6.
- DANENBERG, H. D., FISHBEIN, I., GAO, J., MONKKONEN, J., REICH, R., GATI, I., MOERMAN, E. & GOLOMB, G. 2002. Macrophage depletion by clodronate-containing liposomes reduces neointimal formation after balloon injury in rats and rabbits. *Circulation*, 106, 599-605.
- DAVIES, M. J., RICHARDSON, P. D., WOOLF, N., KATZ, D. R. & MANN, J. 1993. Risk of thrombosis in human atherosclerotic plaques: role of extracellular lipid, macrophage, and smooth muscle cell content. *Br Heart J*, 69, 377-81.
- DAVIES, M. J. & THOMAS, A. C. 1985. Plaque fissuring--the cause of acute myocardial infarction, sudden ischaemic death, and crescendo angina. *Br Heart J*, 53, 363-73.

- DAVIGNON, J. & GANZ, P. 2004. Role of endothelial dysfunction in atherosclerosis. *Circulation*, 109, III27-32.
- DAVIS-DUSENBERY, B. N., CHAN, M. C., RENO, K. E., WEISMAN, A. S., LAYNE, M. D., LAGNA, G. & HATA, A. 2011. down-regulation of Kruppel-like factor-4 (KLF4) by microRNA-143/145 is critical for modulation of vascular smooth muscle cell phenotype by transforming growth factor-beta and bone morphogenetic protein 4. *J Biol Chem*, 286, 28097-110.
- DAVIS, E., CAIMENT, F., TORDOIR, X., CAVAILLE, J., FERGUSON-SMITH, A., COCKETT, N., GEORGES, M. & CHARLIER, C. 2005. RNAi-mediated allelic trans-interaction at the imprinted Rtl1/Peg11 locus. *Curr Biol*, 15, 743-9.
- DE LEON, H., OLLERENSHAW, J. D., GRIENGLING, K. K. & WILCOX, J. N. 2001. Adventitial cells do not contribute to neointimal mass after balloon angioplasty of the rat common carotid artery. *Circulation*, 104, 1591-3.
- DEANFIELD, J. E., HALCOX, J. P. & RABELINK, T. J. 2007. Endothelial function and dysfunction: testing and clinical relevance. *Circulation*, 115, 1285-95.
- DEATON, R. A., GAN, Q. & OWENS, G. K. 2009. Sp1-dependent activation of KLF4 is required for PDGF-BB-induced phenotypic modulation of smooth muscle. *Am J Physiol Heart Circ Physiol*, 296, H1027-37.
- DEGUCHI, J., NAMBA, T., HAMADA, H., NAKAOKA, T., ABE, J., SATO, O., MIYATA, T., MAKUUCHI, M., KUROKAWA, K. & TAKUWA, Y. 1999. Targeting endogenous platelet-derived growth factor B-chain by adenovirus-mediated gene transfer potently inhibits in vivo smooth muscle proliferation after arterial injury. *Gene Ther*, 6, 956-65.
- DEKKER, R. J., VAN THIENEN, J. V., ROHLENA, J., DE JAGER, S. C., ELDERKAMP, Y. W., SEPPEN, J., DE VRIES, C. J., BIESSEN, E. A., VAN BERKEL, T. J., PANNEKOEK, H. & HORREVOETS, A. J. 2005. Endothelial KLF2 links local arterial shear stress levels to the expression of vascular tone-regulating genes. *Am J Pathol*, 167, 609-18.
- DENLI, A. M., TOPS, B. B., PLASTERK, R. H., KETTING, R. F. & HANNON, G. J. 2004. Processing of primary microRNAs by the Microprocessor complex. *Nature*, 432, 231-5.
- DEWS, M., HOMAYOUNI, A., YU, D., MURPHY, D., SEVIGNANI, C., WENTZEL, E., FURTH, E. E., LEE, W. M., ENDERS, G. H., MENDELL, J. T. & THOMAS-TIKHONENKO, A. 2006. Augmentation of tumor angiogenesis by a Myc-activated microRNA cluster. *Nat Genet*, 38, 1060-5.
- DJEBALI, S., DAVIS, C. A., MERKEL, A., DOBIN, A., LASSMANN, T., MORTAZAVI, A., TANZER, A., LAGARDE, J., LIN, W., SCHLESINGER, F., XUE, C., MARINOV, G. K., KHATUN, J., WILLIAMS, B. A., ZALESKI, C., ROZOWSKY, J., RODER, M., KOKOCINSKI, F., ABDELHAMID, R. F., ALIOTO, T., ANTOSHECHKIN, I., BAER, M. T., BAR, N. S., BATUT, P., BELL, K., BELL, I., CHAKRABORTTY, S., CHEN, X., CHRAST, J., CURADO, J., DERRIEN, T., DRENKOW, J., DUMAIS, E., DUMAIS, J., DUTTAGUPTA, R., FALCONNET, E., FASTUCA, M., FEJES-TOTH, K., FERREIRA, P., FOISSAC, S., FULLWOOD, M. J., GAO, H., GONZALEZ, D., GORDON, A., GUNAWARDENA, H., HOWALD, C., JHA, S., JOHNSON, R., KAPRANOV, P., KING, B., KINGSWOOD, C., LUO, O. J., PARK, E., PERSAUD, K., PREALL, J. B., RIBECA, P., RISK, B., ROBYR, D., SAMMETH, M., SCHAFFER, L., SEE, L. H., SHAHAB, A., SKANCKE, J., SUZUKI, A. M., TAKAHASHI, H., TILGNER, H., TROUT, D., WALTERS, N., WANG, H., WROBEL, J., YU, Y., RUAN, X., HAYASHIZAKI, Y., HARROW, J., GERSTEIN, M., HUBBARD, T., REYMOND, A., ANTONARAKIS, S. E., HANNON, G., GIDDINGS, M. C., RUAN, Y., WOLD, B., CARNINCI, P., GUIGO, R. & GINGERAS, T. R. 2012. Landscape of transcription in human cells. *Nature*, 489, 101-8.

- DOEBELE, C., BONAUER, A., FISCHER, A., SCHOLZ, A., REISS, Y., URBICH, C., HOFMANN, W. K., ZEIHNER, A. M. & DIMMELER, S. 2010. Members of the microRNA-17-92 cluster exhibit a cell-intrinsic antiangiogenic function in endothelial cells. *Blood*, 115, 4944-50.
- DOUGLAS, G., VAN KAMPEN, E., HALE, A. B., MCNEILL, E., PATEL, J., CRABTREE, M. J., ALI, Z., HOERR, R. A., ALP, N. J. & CHANNON, K. M. 2012. Endothelial cell repopulation after stenting determines in-stent neointima formation: effects of bare-metal vs. drug-eluting stents and genetic endothelial cell modification. *European Heart Journal*.
- DU, K. L., IP, H. S., LI, J., CHEN, M., DANDRE, F., YU, W., LU, M. M., OWENS, G. K. & PARMACEK, M. S. 2003. Myocardin is a critical serum response factor cofactor in the transcriptional program regulating smooth muscle cell differentiation. *Mol Cell Biol*, 23, 2425-37.
- EBERT, M. S., NEILSON, J. R. & SHARP, P. A. 2007. MicroRNA sponges: competitive inhibitors of small RNAs in mammalian cells. *Nat Methods*, 4, 721-6.
- EBERT, M. S. & SHARP, P. A. 2010. MicroRNA sponges: progress and possibilities. *RNA*, 16, 2043-50.
- ELIA, L., QUINTAVALLE, M., ZHANG, J., CONTU, R., COSSU, L., LATRONICO, M. V., PETERSON, K. L., INDOLFI, C., CATALUCCI, D., CHEN, J., COURTNEIDGE, S. A. & CONDORELLI, G. 2009. The knockout of miR-143 and -145 alters smooth muscle cell maintenance and vascular homeostasis in mice: correlates with human disease. *Cell Death Differ*, 16, 1590-8.
- ELMEN, J., LINDOW, M., SCHUTZ, S., LAWRENCE, M., PETRI, A., OBAD, S., LINDHOLM, M., HEDTJARN, M., HANSEN, H. F., BERGER, U., GULLANS, S., KEARNEY, P., SARNOW, P., STRAARUP, E. M. & KAUPPINEN, S. 2008a. LNA-mediated microRNA silencing in non-human primates. *Nature*, 452, 896-9.
- ELMEN, J., LINDOW, M., SILAHTAROGLU, A., BAK, M., CHRISTENSEN, M., LINDTHOMSEN, A., HEDTJARN, M., HANSEN, J. B., HANSEN, H. F., STRAARUP, E. M., MCCULLAGH, K., KEARNEY, P. & KAUPPINEN, S. 2008b. Antagonism of microRNA-122 in mice by systemically administered LNA-antimiR leads to up-regulation of a large set of predicted target mRNAs in the liver. *Nucleic Acids Res*, 36, 1153-62.
- EULALIO, A., HUNTZINGER, E., NISHIHARA, T., REHWINKEL, J., FAUSER, M. & IZAUERLALDE, E. 2009. Deadenylation is a widespread effect of miRNA regulation. *RNA*, 15, 21-32.
- EVANS, M. J. & KAUFMAN, M. H. 1981. Establishment in culture of pluripotential cells from mouse embryos. *Nature*, 292, 154-6.
- FALK, E. 1989. Morphologic features of unstable atherothrombotic plaques underlying acute coronary syndromes. *Am J Cardiol*, 63, 114E-120E.
- FALK, E. 1991. Coronary thrombosis: pathogenesis and clinical manifestations. *Am J Cardiol*, 68, 28B-35B.
- FATIGATI, V. & MURPHY, R. A. 1984. Actin and tropomyosin variants in smooth muscles. Dependence on tissue type. *J Biol Chem*, 259, 14383-8.
- FERNS, G. A., RAINES, E. W., SPRUGEL, K. H., MOTANI, A. S., REIDY, M. A. & ROSS, R. 1991. Inhibition of neointimal smooth muscle accumulation after angioplasty by an antibody to PDGF. *Science*, 253, 1129-32.
- FIEDLER, J., JAZBUTYTE, V., KIRCHMAIER, B. C., GUPTA, S. K., LORENZEN, J., HARTMANN, D., GALUPPO, P., KNEITZ, S., PENA, J. T., SOHN-LEE, C., LOYER, X., SOUTSCHEK, J., BRAND, T., TUSCHL, T., HEINEKE, J., MARTIN, U., SCHULTE-MERKER, S., ERTL, G., ENGELHARDT, S., BAUERSACHS, J. & THUM, T. 2011. MicroRNA-24 regulates vascularity after myocardial infarction. *Circulation*, 124, 720-30.

- FINN, A. V., JONER, M., NAKAZAWA, G., KOLODZIE, F., NEWELL, J., JOHN, M. C., GOLD, H. K. & VIRMANI, R. 2007. Pathological correlates of late drug-eluting stent thrombosis: strut coverage as a marker of endothelialization. *Circulation*, 115, 2435-41.
- FISCHMAN, D. L., LEON, M. B., BAIM, D. S., SCHATZ, R. A., SAVAGE, M. P., PENN, I., DETRE, K., VELTRI, L., RICCI, D., NOBUYOSHI, M. & ET AL. 1994. A randomized comparison of coronary-stent placement and balloon angioplasty in the treatment of coronary artery disease. Stent Restenosis Study Investigators. *N Engl J Med*, 331, 496-501.
- FORTE, A., DELLA CORTE, A., DE FEO, M., CERASUOLO, F. & CIPOLLARO, M. 2010. Role of myofibroblasts in vascular remodelling: focus on restenosis and aneurysm. *Cardiovasc Res*, 88, 395-405.
- FRANK, F., SONENBERG, N. & NAGAR, B. 2010. Structural basis for 5'-nucleotide base-specific recognition of guide RNA by human AGO2. *Nature*, 465, 818-22.
- FRIEDMAN, R. C., FARH, K. K. H., BURGE, C. B. & BARTEL, D. P. 2009. Most mammalian mRNAs are conserved targets of microRNAs. *Genome Research*, 19, 92-105.
- FURCHGOTT, R. F. & ZAWADZKI, J. V. 1980. The obligatory role of endothelial cells in the relaxation of arterial smooth muscle by acetylcholine. *Nature*, 288, 373-6.
- GAGGAR, A., SHAYAKHMETOV, D. M. & LIEBER, A. 2003. CD46 is a cellular receptor for group B adenoviruses. *Nat Med*, 9, 1408-12.
- GALIS, Z. S., SUKHOVA, G. K., LARK, M. W. & LIBBY, P. 1994. Increased expression of matrix metalloproteinases and matrix degrading activity in vulnerable regions of human atherosclerotic plaques. *J Clin Invest*, 94, 2493-503.
- GENG, Y. J. & LIBBY, P. 1995. Evidence for apoptosis in advanced human atheroma. Colocalization with interleukin-1 beta-converting enzyme. *Am J Pathol*, 147, 251-66.
- GENG, Y. J., WU, Q., MUSZYNSKI, M., HANSSON, G. K. & LIBBY, P. 1996. Apoptosis of vascular smooth muscle cells induced by in vitro stimulation with interferon-gamma, tumor necrosis factor-alpha, and interleukin-1 beta. *Arterioscler Thromb Vasc Biol*, 16, 19-27.
- GEORGE, S. J., WAN, S., HU, J., MACDONALD, R., JOHNSON, J. L. & BAKER, A. H. 2011. Sustained reduction of vein graft neointima formation by ex vivo TIMP-3 gene therapy. *Circulation*, 124, S135-42.
- GIMONA, M., KAVERINA, I., RESCH, G. P., VIGNAL, E. & BURGSTALLER, G. 2003. Calponin repeats regulate actin filament stability and formation of podosomes in smooth muscle cells. *Mol Biol Cell*, 14, 2482-91.
- GIRALDEZ, A. J., MISHIMA, Y., RIHEL, J., GROCOCK, R. J., VAN DONGEN, S., INOUE, K., ENRIGHT, A. J. & SCHIER, A. F. 2006. Zebrafish MiR-430 promotes deadenylation and clearance of maternal mRNAs. *Science*, 312, 75-9.
- GO, A. S., MOZAFFARIAN, D., ROGER, V. L., BENJAMIN, E. J., BERRY, J. D., BORDEN, W. B., BRAVATA, D. M., DAI, S., FORD, E. S., FOX, C. S., FRANCO, S., FULLERTON, H. J., GILLESPIE, C., HAILPERN, S. M., HEIT, J. A., HOWARD, V. J., HUFFMAN, M. D., KISSELA, B. M., KITTNER, S. J., LACKLAND, D. T., LICHTMAN, J. H., LISABETH, L. D., MAGID, D., MARCUS, G. M., MARELLI, A., MATCHAR, D. B., MCGUIRE, D. K., MOHLER, E. R., MOY, C. S., MUSSOLINO, M. E., NICHOL, G., PAYNTER, N. P., SCHREINER, P. J., SORLIE, P. D., STEIN, J., TURAN, T. N., VIRANI, S. S., WONG, N. D., WOO, D. & TURNER, M. B. 2013. Heart disease and stroke statistics--2013

- update: a report from the American Heart Association. *Circulation*, 127, e6-e245.
- GOLDMAN, S., ZADINA, K., MORITZ, T., OVITT, T., SETHI, G., COPELAND, J. G., THOTTAPURATHU, L., KRASNICKA, B., ELLIS, N., ANDERSON, R. J. & HENDERSON, W. 2004. Long-term patency of saphenous vein and left internal mammary artery grafts after coronary artery bypass surgery: results from a Department of Veterans Affairs Cooperative Study. *J Am Coll Cardiol*, 44, 2149-56.
- GREGORY, P. A., BERT, A. G., PATERSON, E. L., BARRY, S. C., TSYKIN, A., FARSHID, G., VADAS, M. A., KHEW-GOODALL, Y. & GOODALL, G. J. 2008. The miR-200 family and miR-205 regulate epithelial to mesenchymal transition by targeting ZEB1 and SIP1. *Nat Cell Biol*, 10, 593-601.
- GREGORY, R. I., YAN, K. P., AMUTHAN, G., CHENDRIMADA, T., DORATOTAJ, B., COOCH, N. & SHIEKHATTAR, R. 2004. The Microprocessor complex mediates the genesis of microRNAs. *Nature*, 432, 235-40.
- GRIMSON, A., FARH, K. K., JOHNSTON, W. K., GARRETT-ENGELE, P., LIM, L. P. & BARTEL, D. P. 2007. MicroRNA targeting specificity in mammals: determinants beyond seed pairing. *Mol Cell*, 27, 91-105.
- GUO, H., INGOLIA, N. T., WEISSMAN, J. S. & BARTEL, D. P. 2010. Mammalian microRNAs predominantly act to decrease target mRNA levels. *Nature*, 466, 835-40.
- HAASE, A. D., JASKIEWICZ, L., ZHANG, H., LAINE, S., SACK, R., GATIGNOL, A. & FILIPOWICZ, W. 2005. TRBP, a regulator of cellular PKR and HIV-1 virus expression, interacts with Dicer and functions in RNA silencing. *EMBO Rep*, 6, 961-7.
- HAN, C. I., CAMPBELL, G. R. & CAMPBELL, J. H. 2001. Circulating bone marrow cells can contribute to neointimal formation. *J Vasc Res*, 38, 113-9.
- HAN, J., LEE, Y., YEOM, K. H., KIM, Y. K., JIN, H. & KIM, V. N. 2004. The Drosha-DGCR8 complex in primary microRNA processing. *Genes Dev*, 18, 3016-27.
- HAN, J., LEE, Y., YEOM, K. H., NAM, J. W., HEO, I., RHEE, J. K., SOHN, S. Y., CHO, Y., ZHANG, B. T. & KIM, V. N. 2006. Molecular basis for the recognition of primary microRNAs by the Drosha-DGCR8 complex. *Cell*, 125, 887-901.
- HANKE, H., STROHSCHNEIDER, T., OBERHOFF, M., BETZ, E. & KARSCH, K. R. 1990. Time course of smooth muscle cell proliferation in the intima and media of arteries following experimental angioplasty. *Circulation Research*, 67, 651-9.
- HARMON, K. J., COUPER, L. L. & LINDNER, V. 2000. Strain-dependent vascular remodeling phenotypes in inbred mice. *Am J Pathol*, 156, 1741-8.
- HARRIS, T. A., YAMAKUCHI, M., FERLITO, M., MENDELL, J. T. & LOWENSTEIN, C. J. 2008. MicroRNA-126 regulates endothelial expression of vascular cell adhesion molecule 1. *Proc Natl Acad Sci U S A*, 105, 1516-21.
- HAUTMANN, M. B., MADSEN, C. S. & OWENS, G. K. 1997. A transforming growth factor beta (TGFbeta) control element drives TGFbeta-induced stimulation of smooth muscle alpha-actin gene expression in concert with two CArG elements. *J Biol Chem*, 272, 10948-56.
- HAVENGA, M. J., LEMCKERT, A. A., GRIMBERGEN, J. M., VOGELS, R., HUISMAN, L. G., VALERIO, D., BOUT, A. & QUAX, P. H. 2001. Improved adenovirus vectors for infection of cardiovascular tissues. *J Virol*, 75, 3335-42.
- HENDRICKSON, D. G., HOGAN, D. J., MCCULLOUGH, H. L., MYERS, J. W., HERSCHLAG, D., FERRELL, J. E. & BROWN, P. O. 2009. Concordant regulation of translation and mRNA abundance for hundreds of targets of a human microRNA. *PLoS Biol*, 7, e1000238.

- HENDRIX, J. A., WAMHOFF, B. R., MCDONALD, O. G., SINHA, S., YOSHIDA, T. & OWENS, G. K. 2005. 5' CARg degeneracy in smooth muscle alpha-actin is required for injury-induced gene suppression in vivo. *J Clin Invest*, 115, 418-27.
- HERGENREIDER, E., HEYDT, S., TREGUER, K., BOETTGER, T., HORREVOETS, A. J., ZEIHNER, A. M., SCHEFFER, M. P., FRANGAKIS, A. S., YIN, X., MAYR, M., BRAUN, T., URBICH, C., BOON, R. A. & DIMMELER, S. 2012. Atheroprotective communication between endothelial cells and smooth muscle cells through miRNAs. *Nat Cell Biol*, 14, 249-56.
- HERMILLER, J. B., TENAGLIA, A. N., KISSLO, K. B., PHILLIPS, H. R., BASHORE, T. M., STACK, R. S. & DAVIDSON, C. J. 1993. In vivo validation of compensatory enlargement of atherosclerotic coronary arteries. *Am J Cardiol*, 71, 665-8.
- HOLYCROSS, B. J., BLANK, R. S., THOMPSON, M. M., PEACH, M. J. & OWENS, G. K. 1992. Platelet-derived growth factor-BB-induced suppression of smooth muscle cell differentiation. *Circ Res*, 71, 1525-32.
- HOSHINO, Y., KURABAYASHI, M., KANDA, T., HASEGAWA, A., SAKAMOTO, H., OKAMOTO, E., KOWASE, K., WATANABE, N., MANABE, I., SUZUKI, T., NAKANO, A., TAKASE, S., WILCOX, J. N. & NAGAI, R. 2000. Regulated expression of the BTEB2 transcription factor in vascular smooth muscle cells: analysis of developmental and pathological expression profiles shows implications as a predictive factor for restenosis. *Circulation*, 102, 2528-34.
- HOUBAVIY, H. B., MURRAY, M. F. & SHARP, P. A. 2003. Embryonic stem cell-specific MicroRNAs. *Dev Cell*, 5, 351-8.
- HOUSE, S. J. & SINGER, H. A. 2008. CaMKII-delta isoform regulation of neointima formation after vascular injury. *Arterioscler Thromb Vasc Biol*, 28, 441-7.
- HTAY, T. & LIU, M. W. 2005. Drug-eluting stent: a review and update. *Vasc Health Risk Manag*, 1, 263-76.
- HUGHES, S. E., CROSSMAN, D. & HALL, P. A. 1993. Expression of basic and acidic fibroblast growth factors and their receptor in normal and atherosclerotic human arteries. *Cardiovasc Res*, 27, 1214-9.
- HUMPHREYS, D. T., WESTMAN, B. J., MARTIN, D. I. & PREISS, T. 2005. MicroRNAs control translation initiation by inhibiting eukaryotic initiation factor 4E/cap and poly(A) tail function. *Proc Natl Acad Sci U S A*, 102, 16961-6.
- HUTVAGNER, G., MCLACHLAN, J., PASQUINELLI, A. E., BALINT, E., TUSCHL, T. & ZAMORE, P. D. 2001. A cellular function for the RNA-interference enzyme Dicer in the maturation of the let-7 small temporal RNA. *Science*, 293, 834-8.
- IGNARRO, L. J., BUGA, G. M., WOOD, K. S., BYRNS, R. E. & CHAUDHURI, G. 1987. Endothelium-derived relaxing factor produced and released from artery and vein is nitric oxide. *Proc Natl Acad Sci U S A*, 84, 9265-9.
- IHGSC 2004. Finishing the euchromatic sequence of the human genome. *Nature*, 431, 931-45.
- ISNER, J. M., KEARNEY, M., BORTMAN, S. & PASSERI, J. 1995. Apoptosis in human atherosclerosis and restenosis. *Circulation*, 91, 2703-11.
- JAFFE, E. A., NACHMAN, R. L., BECKER, C. G. & MINICK, C. R. 1973. Culture of human endothelial cells derived from umbilical veins. Identification by morphologic and immunologic criteria. *J Clin Invest*, 52, 2745-56.
- JAWIEN, A., BOWEN-POPE, D. F., LINDNER, V., SCHWARTZ, S. M. & CLOWES, A. W. 1992. Platelet-derived growth factor promotes smooth muscle migration and intimal thickening in a rat model of balloon angioplasty. *J Clin Invest*, 89, 507-11.

- JI, R., CHENG, Y., YUE, J., YANG, J., LIU, X., CHEN, H., DEAN, D. B. & ZHANG, C. 2007. MicroRNA expression signature and antisense-mediated depletion reveal an essential role of MicroRNA in vascular neointimal lesion formation. *Circ Res*, 100, 1579-88.
- JOHNSON, T. W., WU, Y. X., HERDEG, C., BAUMBACH, A., NEWBY, A. C., KARSCH, K. R. & OBERHOFF, M. 2005. Stent-based delivery of tissue inhibitor of metalloproteinase-3 adenovirus inhibits neointimal formation in porcine coronary arteries. *Arterioscler Thromb Vasc Biol*, 25, 754-9.
- JONER, M., FINN, A. V., FARB, A., MONT, E. K., KOLODGIE, F. D., LADICH, E., KUTYS, R., SKORIJA, K., GOLD, H. K. & VIRMANI, R. 2006. Pathology of drug-eluting stents in humans: delayed healing and late thrombotic risk. *J Am Coll Cardiol*, 48, 193-202.
- JONER, M., NAKAZAWA, G., FINN, A. V., QUEE, S. C., COLEMAN, L., ACAMPADO, E., WILSON, P. S., SKORIJA, K., CHENG, Q., XU, X., GOLD, H. K., KOLODGIE, F. D. & VIRMANI, R. 2008. Endothelial cell recovery between comparator polymer-based drug-eluting stents. *Journal of the American College of Cardiology*, 52, 333-42.
- JOPLING, C. L., YI, M., LANCASTER, A. M., LEMON, S. M. & SARNOW, P. 2005. Modulation of hepatitis C virus RNA abundance by a liver-specific MicroRNA. *Science*, 309, 1577-81.
- KANELLOPOULOU, C., MULJO, S. A., KUNG, A. L., GANESAN, S., DRAPKIN, R., JENUWEIN, T., LIVINGSTON, D. M. & RAJEWSKY, K. 2005. Dicer-deficient mouse embryonic stem cells are defective in differentiation and centromeric silencing. *Genes Dev*, 19, 489-501.
- KANG, H., DAVIS-DUSENBERY, B. N., NGUYEN, P. H., LAL, A., LIEBERMAN, J., VAN AELST, L., LAGNA, G. & HATA, A. 2012. Bone morphogenetic protein 4 promotes vascular smooth muscle contractility by activating microRNA-21 (miR-21), which down-regulates expression of family of dedicator of cytokinesis (DOCK) proteins. *J Biol Chem*, 287, 3976-86.
- KANO, M., SEKI, N., KIKKAWA, N., FUJIMURA, L., HOSHINO, I., AKUTSU, Y., CHIYOMARU, T., ENOKIDA, H., NAKAGAWA, M. & MATSUBARA, H. 2010. miR-145, miR-133a and miR-133b: Tumor-suppressive miRNAs target FSCN1 in esophageal squamous cell carcinoma. *Int J Cancer*, 127, 2804-14.
- KHVOROVA, A., REYNOLDS, A. & JAYASENA, S. D. 2003. Functional siRNAs and miRNAs exhibit strand bias. *Cell*, 115, 209-16.
- KIEMENEIJ, F., SERRUYS, P. W., MACAYA, C., RUTSCH, W., HEYNDRIKX, G., ALBERTSSON, P., FAJADET, J., LEGRAND, V., MATERNE, P., BELARDI, J., SIGWART, U., COLOMBO, A., GOY, J. J., DISCO, C. M. & MOREL, M. A. 2001. Continued benefit of coronary stenting versus balloon angioplasty: five-year clinical follow-up of Benestent-I trial. *J Am Coll Cardiol*, 37, 1598-603.
- KIM, Y. K. & KIM, V. N. 2007. Processing of intronic microRNAs. *EMBO J*, 26, 775-83.
- KOCHER, O., GABBIANI, F., GABBIANI, G., REIDY, M. A., COKAY, M. S., PETERS, H. & HUTTNER, I. 1991. Phenotypic features of smooth muscle cells during the evolution of experimental carotid artery intimal thickening. Biochemical and morphologic studies. *Lab Invest*, 65, 459-70.
- KOCHER, O., SKALLI, O., BLOOM, W. S. & GABBIANI, G. 1984. Cytoskeleton of rat aortic smooth muscle cells. Normal conditions and experimental intimal thickening. *Lab Invest*, 50, 645-52.
- KOTANI, M., FUKUDA, N., ANDO, H., HU, W. Y., KUNIMOTO, S., SAITO, S. & KANMATSUSE, K. 2003. Chimeric DNA-RNA hammerhead ribozyme

- targeting PDGF A-chain mRNA specifically inhibits neointima formation in rat carotid artery after balloon injury. *Cardiovasc Res*, 57, 265-76.
- KOVANEN, P. T., KAARTINEN, M. & PAAVONEN, T. 1995. Infiltrates of activated mast cells at the site of coronary atheromatous erosion or rupture in myocardial infarction. *Circulation*, 92, 1084-8.
- KOYAMA, N., KOSHIKAWA, T., MORISAKI, N., SAITO, Y. & YOSHIDA, S. 1990. Bifunctional effects of transforming growth factor-beta on migration of cultured rat aortic smooth muscle cells. *Biochem Biophys Res Commun*, 169, 725-9.
- KRICHEVSKY, A. M., KING, K. S., DONAHUE, C. P., KHRAPKO, K. & KOSIK, K. S. 2003. A microRNA array reveals extensive regulation of microRNAs during brain development. *RNA*, 9, 1274-81.
- KRUTZFELDT, J., KUWAJIMA, S., BRAICH, R., RAJEEV, K. G., PENA, J., TUSCHL, T., MANOHARAN, M. & STOFFEL, M. 2007. Specificity, duplex degradation and subcellular localization of antagomirs. *Nucleic Acids Res*, 35, 2885-92.
- KRUTZFELDT, J., RAJEWSKY, N., BRAICH, R., RAJEEV, K. G., TUSCHL, T., MANOHARAN, M. & STOFFEL, M. 2005. Silencing of microRNAs in vivo with 'antagomirs'. *Nature*, 438, 685-9.
- KU, D. N., GIDDENS, D. P., ZARINS, C. K. & GLAGOV, S. 1985. Pulsatile flow and atherosclerosis in the human carotid bifurcation. Positive correlation between plaque location and low oscillating shear stress. *Arteriosclerosis*, 5, 293-302.
- KUEHBACHER, A., URBICH, C., ZEIHNER, A. M. & DIMMELER, S. 2007. Role of Dicer and Drosha for endothelial microRNA expression and angiogenesis. *Circ Res*, 101, 59-68.
- KUHEL, D. G., ZHU, B., WITTE, D. P. & HUI, D. Y. 2002. Distinction in genetic determinants for injury-induced neointimal hyperplasia and diet-induced atherosclerosis in inbred mice. *Arterioscler Thromb Vasc Biol*, 22, 955-60.
- KUMAR, A. & LINDNER, V. 1997. Remodeling with neointima formation in the mouse carotid artery after cessation of blood flow. *Arterioscler Thromb Vasc Biol*, 17, 2238-44.
- KUMAR, M. S., ERKELAND, S. J., PESTER, R. E., CHEN, C. Y., EBERT, M. S., SHARP, P. A. & JACKS, T. 2008. Suppression of non-small cell lung tumor development by the let-7 microRNA family. *Proc Natl Acad Sci U S A*, 105, 3903-8.
- KUMARSWAMY, R., VOLKMANN, I., JAZBUTYTE, V., DANGWAL, S., PARK, D. H. & THUM, T. 2012. Transforming growth factor-beta-induced endothelial-to-mesenchymal transition is partly mediated by microRNA-21. *Arterioscler Thromb Vasc Biol*, 32, 361-9.
- KURO-O, M., NAGAI, R., NAKAHARA, K., KATOH, H., TSAI, R. C., TSUCHIMUCHI, H., YAZAKI, Y., OHKUBO, A. & TAKAKU, F. 1991. cDNA cloning of a myosin heavy chain isoform in embryonic smooth muscle and its expression during vascular development and in arteriosclerosis. *J Biol Chem*, 266, 3768-73.
- KWAK, P. B. & TOMARI, Y. 2012. The N domain of Argonaute drives duplex unwinding during RISC assembly. *Nat Struct Mol Biol*, 19, 145-51.
- LAGOS-QUINTANA, M., RAUHUT, R., LENDECKEL, W. & TUSCHL, T. 2001. Identification of novel genes coding for small expressed RNAs. *Science*, 294, 853-8.
- LANDTHALER, M., YALCIN, A. & TUSCHL, T. 2004. The human DiGeorge syndrome critical region gene 8 and its D. melanogaster homolog are required for miRNA biogenesis. *Curr Biol*, 14, 2162-7.
- LANFORD, R. E., HILDEBRANDT-ERIKSEN, E. S., PETRI, A., PERSSON, R., LINDOW, M., MUNK, M. E., KAUPPINEN, S. & ORUM, H. 2010. Therapeutic silencing

- of microRNA-122 in primates with chronic hepatitis C virus infection. *Science*, 327, 198-201.
- LAU, N. C., LIM, L. P., WEINSTEIN, E. G. & BARTEL, D. P. 2001. An abundant class of tiny RNAs with probable regulatory roles in *Caenorhabditis elegans*. *Science*, 294, 858-62.
- LEE, H. K., BIER, A., CAZACU, S., FINNISS, S., XIANG, C., TWITO, H., POISSON, L. M., MIKKELSEN, T., SLAVIN, S., JACOBY, E., YALON, M., TOREN, A., REMPEL, S. A. & BRODIE, C. 2013. MicroRNA-145 is downregulated in glial tumors and regulates glioma cell migration by targeting connective tissue growth factor. *PLoS One*, 8, e54652.
- LEE, R. C., FEINBAUM, R. L. & AMBROS, V. 1993. The *C. elegans* heterochronic gene *lin-4* encodes small RNAs with antisense complementarity to *lin-14*. *Cell*, 75, 843-54.
- LEE, Y., AHN, C., HAN, J., CHOI, H., KIM, J., YIM, J., LEE, J., PROVOST, P., RADMARK, O., KIM, S. & KIM, V. N. 2003. The nuclear RNase III Drosha initiates microRNA processing. *Nature*, 425, 415-9.
- LEE, Y., HUR, I., PARK, S. Y., KIM, Y. K., SUH, M. R. & KIM, V. N. 2006. The role of PACT in the RNA silencing pathway. *EMBO J*, 25, 522-32.
- LEE, Y., JEON, K., LEE, J. T., KIM, S. & KIM, V. N. 2002. MicroRNA maturation: stepwise processing and subcellular localization. *EMBO J*, 21, 4663-70.
- LEE, Y., KIM, M., HAN, J., YEOM, K. H., LEE, S., BAEK, S. H. & KIM, V. N. 2004. MicroRNA genes are transcribed by RNA polymerase II. *EMBO J*, 23, 4051-60.
- LENDON, C. L., DAVIES, M. J., BORN, G. V. & RICHARDSON, P. D. 1991. Atherosclerotic plaque caps are locally weakened when macrophages density is increased. *Atherosclerosis*, 87, 87-90.
- LEWIS, B. P., SHIH, I. H., JONES-RHOADES, M. W., BARTEL, D. P. & BURGE, C. B. 2003. Prediction of mammalian microRNA targets. *Cell*, 115, 787-98.
- LI, L., LIU, Z., MERCER, B., OVERBEEK, P. & OLSON, E. N. 1997. Evidence for serum response factor-mediated regulatory networks governing SM22alpha transcription in smooth, skeletal, and cardiac muscle cells. *Dev Biol*, 187, 311-21.
- LI, S., WANG, D. Z., WANG, Z., RICHARDSON, J. A. & OLSON, E. N. 2003. The serum response factor coactivator myocardin is required for vascular smooth muscle development. *Proc Natl Acad Sci U S A*, 100, 9366-70.
- LIANG, C. C., PARK, A. Y. & GUAN, J. L. 2007. In vitro scratch assay: a convenient and inexpensive method for analysis of cell migration in vitro. *Nat Protoc*, 2, 329-33.
- LIBBY, P., SCHWARTZ, D., BROGI, E., TANAKA, H. & CLINTON, S. K. 1992. A cascade model for restenosis. A special case of atherosclerosis progression. *Circulation*, 86, 1147-52.
- LIM, L. P., LAU, N. C., GARRETT-ENGELE, P., GRIMSON, A., SCHELTER, J. M., CASTLE, J., BARTEL, D. P., LINSLEY, P. S. & JOHNSON, J. M. 2005. Microarray analysis shows that some microRNAs downregulate large numbers of target mRNAs. *Nature*, 433, 769-73.
- LINDER, S. & AEPFELBACHER, M. 2003. Podosomes: adhesion hot-spots of invasive cells. *Trends Cell Biol*, 13, 376-85.
- LINDNER, V., FINGERLE, J. & REIDY, M. A. 1993. Mouse model of arterial injury. *Circ Res*, 73, 792-6.
- LINDNER, V. & REIDY, M. A. 1991. Proliferation of smooth muscle cells after vascular injury is inhibited by an antibody against basic fibroblast growth factor. *Proc Natl Acad Sci U S A*, 88, 3739-43.

- LINDOW, M. & KAUPPINEN, S. 2012. Discovering the first microRNA-targeted drug. *J Cell Biol*, 199, 407-12.
- LIU, J., CARMELL, M. A., RIVAS, F. V., MARSDEN, C. G., THOMSON, J. M., SONG, J. J., HAMMOND, S. M., JOSHUA-TOR, L. & HANNON, G. J. 2004. Argonaute2 is the catalytic engine of mammalian RNAi. *Science*, 305, 1437-41.
- LIU, N., BEZPROZVANNAYA, S., WILLIAMS, A. H., QI, X., RICHARDSON, J. A., BASSEL-DUBY, R. & OLSON, E. N. 2008. microRNA-133a regulates cardiomyocyte proliferation and suppresses smooth muscle gene expression in the heart. *Genes Dev*, 22, 3242-54.
- LIU, X., CHENG, Y., ZHANG, S., LIN, Y., YANG, J. & ZHANG, C. 2009. A necessary role of miR-221 and miR-222 in vascular smooth muscle cell proliferation and neointimal hyperplasia. *Circ Res*, 104, 476-87.
- LIU, Y., SINHA, S., MCDONALD, O. G., SHANG, Y., HOOFNAGLE, M. H. & OWENS, G. K. 2005. Kruppel-like factor 4 abrogates myocardin-induced activation of smooth muscle gene expression. *J Biol Chem*, 280, 9719-27.
- LONG, X., BELL, R. D., GERTHOFFER, W. T., ZLOKOVIC, B. V. & MIANO, J. M. 2008. Myocardin is sufficient for a smooth muscle-like contractile phenotype. *Arterioscler Thromb Vasc Biol*, 28, 1505-10.
- LONG, X. & MIANO, J. M. 2011. Transforming growth factor-beta1 (TGF-beta1) utilizes distinct pathways for the transcriptional activation of microRNA 143/145 in human coronary artery smooth muscle cells. *J Biol Chem*, 286, 30119-29.
- LOVREN, F., PAN, Y., QUAN, A., SINGH, K. K., SHUKLA, P. C., GUPTA, N., STEER, B. M., INGRAM, A. J., GUPTA, M., AL-OMRAN, M., TEOH, H., MARSDEN, P. A. & VERMA, S. 2012. MicroRNA-145 targeted therapy reduces atherosclerosis. *Circulation*, 126, S81-90.
- LOWE, H. C., SCHWARTZ, R. S., MAC NEILL, B. D., JANG, I. K., HAYASE, M., ROGERS, C. & OESTERLE, S. N. 2003. The porcine coronary model of in-stent restenosis: current status in the era of drug-eluting stents. *Catheter Cardiovasc Interv*, 60, 515-23.
- LOWENSTEIN, P. R., SHERING, I. A. F., BAIN, D., CASTRO, M. G., AND WILKINSON, G. W. G. 1996. *How to examine the interactions between adenoviral mediated gene transfer and different indentified target brain cell types in vitro*, In *Towards Gene Therapy for Neurological Disorders* Chichester, UK.
- LU, J., GETZ, G., MISKA, E. A., ALVAREZ-SAAVEDRA, E., LAMB, J., PECK, D., SWEET-CORDERO, A., EBERT, B. L., MAK, R. H., FERRANDO, A. A., DOWNING, J. R., JACKS, T., HORVITZ, H. R. & GOLUB, T. R. 2005. MicroRNA expression profiles classify human cancers. *Nature*, 435, 834-8.
- LUCIANO, D. J., MIRSKY, H., VENDETTI, N. J. & MAAS, S. 2004. RNA editing of a miRNA precursor. *RNA*, 10, 1174-7.
- LUDMER, P. L., SELWYN, A. P., SHOOK, T. L., WAYNE, R. R., MUDGE, G. H., ALEXANDER, R. W. & GANZ, P. 1986. Paradoxical vasoconstriction induced by acetylcholine in atherosclerotic coronary arteries. *N Engl J Med*, 315, 1046-51.
- LUND, E., LIU, M., HARTLEY, R. S., SHEETS, M. D. & DAHLBERG, J. E. 2009. Deadenylation of maternal mRNAs mediated by miR-427 in *Xenopus laevis* embryos. *RNA*, 15, 2351-63.
- LUSCHER, T. F., STEFFEL, J., EBERLI, F. R., JONER, M., NAKAZAWA, G., TANNER, F. C. & VIRMANI, R. 2007. Drug-eluting stent and coronary thrombosis - Biological mechanisms and clinical implications. *Circulation*, 115, 1051-1058.

- MA, J. B., YE, K. & PATEL, D. J. 2004. Structural basis for overhang-specific small interfering RNA recognition by the PAZ domain. *Nature*, 429, 318-22.
- MACHLIN, E. S., SARNOW, P. & SAGAN, S. M. 2011. Masking the 5' terminal nucleotides of the hepatitis C virus genome by an unconventional microRNA-target RNA complex. *Proc Natl Acad Sci U S A*, 108, 3193-8.
- MACK, C. P. & OWENS, G. K. 1999. Regulation of smooth muscle alpha-actin expression in vivo is dependent on CArG elements within the 5' and first intron promoter regions. *Circ Res*, 84, 852-61.
- MACRAE, I. J., MA, E., ZHOU, M., ROBINSON, C. V. & DOUDNA, J. A. 2008. In vitro reconstitution of the human RISC-loading complex. *Proc Natl Acad Sci U S A*, 105, 512-7.
- MACRAE, I. J., ZHOU, K., LI, F., REPIC, A., BROOKS, A. N., CANDE, W. Z., ADAMS, P. D. & DOUDNA, J. A. 2006. Structural basis for double-stranded RNA processing by Dicer. *Science*, 311, 195-8.
- MAEGDEFESSEL, L., AZUMA, J., TOH, R., MERK, D. R., DENG, A., CHIN, J. T., RAAZ, U., SCHOELMERICH, A. M., RAIESDANA, A., LEEPER, N. J., MCCONNELL, M. V., DALMAN, R. L., SPIN, J. M. & TSAO, P. S. 2012. Inhibition of microRNA-29b reduces murine abdominal aortic aneurysm development. *J Clin Invest*, 122, 497-506.
- MAENG, M., MERTZ, H., NIELSEN, S., VAN EYS, G. J., RASMUSSEN, K. & ESPERSEN, G. T. 2003. Adventitial myofibroblasts play no major role in neointima formation after angioplasty. *Scand Cardiovasc J*, 37, 34-42.
- MAJESKY, M. W., LINDNER, V., TWARDZIK, D. R., SCHWARTZ, S. M. & REIDY, M. A. 1991. Production of transforming growth factor beta 1 during repair of arterial injury. *J Clin Invest*, 88, 904-10.
- MALIK, N., GUNN, J., HOLT, C. M., SHEPHERD, L., FRANCIS, S. E., NEWMAN, C. M., CROSSMAN, D. C. & CUMBERLAND, D. C. 1998. Intravascular stents: a new technique for tissue processing for histology, immunohistochemistry, and transmission electron microscopy. *Heart*, 80, 509-16.
- MANABE, I. & OWENS, G. K. 2001. CArG elements control smooth muscle subtype-specific expression of smooth muscle myosin in vivo. *J Clin Invest*, 107, 823-34.
- MANDERSON, J. A., MOSSE, P. R., SAFSTROM, J. A., YOUNG, S. B. & CAMPBELL, G. R. 1989. Balloon catheter injury to rabbit carotid artery. I. Changes in smooth muscle phenotype. *Arteriosclerosis*, 9, 289-98.
- MANN, J. & DAVIES, M. J. 1999. Mechanisms of progression in native coronary artery disease: role of healed plaque disruption. *Heart*, 82, 265-8.
- MARON, D. J., FAZIO, S. & LINTON, M. F. 2000. Current perspectives on statins. *Circulation*, 101, 207-13.
- MARTIN, G. R. 1981. Isolation of a pluripotent cell line from early mouse embryos cultured in medium conditioned by teratocarcinoma stem cells. *Proc Natl Acad Sci U S A*, 78, 7634-8.
- MAYORGA, M. E. & PENN, M. S. 2012. miR-145 is differentially regulated by TGF-beta1 and ischaemia and targets Disabled-2 expression and wnt/beta-catenin activity. *J Cell Mol Med*, 16, 1106-13.
- MAYR, U., ZOU, Y. P., ZHANG, Z. Y., DIETRICH, H., HU, Y. H. & XU, Q. B. 2006. Accelerated arteriosclerosis of vein grafts in inducible NO synthase(-/-) mice is related to decreased endothelial progenitor cell repair. *Circulation Research*, 98, 412-420.
- MCCAFFREY, T. A., CONSIGLI, S., DU, B., FALCONE, D. J., SANBORN, T. A., SPOKOJNY, A. M. & BUSH, H. L., JR. 1995. Decreased type II/type I TGF-beta receptor ratio in cells derived from human atherosclerotic lesions.

- Conversion from an antiproliferative to profibrotic response to TGF-beta1. *J Clin Invest*, 96, 2667-75.
- MCFADDEN, E. P., STABILE, E., REGAR, E., CHENEAU, E., ONG, A. T., KINNAIRD, T., SUDDATH, W. O., WEISSMAN, N. J., TORGUSON, R., KENT, K. M., PICHARD, A. D., SATLER, L. F., WAKSMAN, R. & SERRUYS, P. W. 2004. Late thrombosis in drug-eluting coronary stents after discontinuation of antiplatelet therapy. *Lancet*, 364, 1519-21.
- MEISTER, G., LANDTHALER, M., PATKANIOWSKA, A., DORSETT, Y., TENG, G. & TUSCHL, T. 2004. Human Argonaute2 mediates RNA cleavage targeted by miRNAs and siRNAs. *Mol Cell*, 15, 185-97.
- MERCER, T. R., DINGER, M. E. & MATTICK, J. S. 2009. Long non-coding RNAs: insights into functions. *Nat Rev Genet*, 10, 155-9.
- MIANO, J. M., LONG, X. & FUJIWARA, K. 2007. Serum response factor: master regulator of the actin cytoskeleton and contractile apparatus. *Am J Physiol Cell Physiol*, 292, C70-81.
- MII, S., WARE, J. A. & KENT, K. C. 1993. Transforming growth factor-beta inhibits human vascular smooth muscle cell growth and migration. *Surgery*, 114, 464-70.
- MILLER, D. D., KARIM, M. A., EDWARDS, W. D. & SCHWARTZ, R. S. 1996. Relationship of vascular thrombosis and inflammatory leukocyte infiltration to neointimal growth following porcine coronary artery stent placement. *Atherosclerosis*, 124, 145-55.
- MINENO, J., OKAMOTO, S., ANDO, T., SATO, M., CHONO, H., IZU, H., TAKAYAMA, M., ASADA, K., MIROCHNITCHENKO, O., INOUE, M. & KATO, I. 2006. The expression profile of microRNAs in mouse embryos. *Nucleic Acids Res*, 34, 1765-71.
- MOHR, F. W., MORICE, M. C., KAPPETEIN, A. P., FELDMAN, T. E., STAHL, E., COLOMBO, A., MACK, M. J., HOLMES, D. R., JR., MOREL, M. A., VAN DYCK, N., HOULE, V. M., DAWKINS, K. D. & SERRUYS, P. W. 2013. Coronary artery bypass graft surgery versus percutaneous coronary intervention in patients with three-vessel disease and left main coronary disease: 5-year follow-up of the randomised, clinical SYNTAX trial. *Lancet*, 381, 629-38.
- MONTEYS, A. M., SPENGLER, R. M., WAN, J., TECEDOR, L., LENNOX, K. A., XING, Y. & DAVIDSON, B. L. 2010. Structure and activity of putative intronic miRNA promoters. *RNA*, 16, 495-505.
- MONTGOMERY, R. L., HULLINGER, T. G., SEMUS, H. M., DICKINSON, B. A., SETO, A. G., LYNCH, J. M., STACK, C., LATIMER, P. A., OLSON, E. N. & VAN ROOIJ, E. 2011. Therapeutic inhibition of miR-208a improves cardiac function and survival during heart failure. *Circulation*, 124, 1537-47.
- MORENO, P. R., BERNARDI, V. H., LOPEZ-CUELLAR, J., NEWELL, J. B., MCMELLON, C., GOLD, H. K., PALACIOS, I. F., FUSTER, V. & FALLON, J. T. 1996. Macrophage infiltration predicts restenosis after coronary intervention in patients with unstable angina. *Circulation*, 94, 3098-102.
- MORENO, R., FERNANDEZ, C., HERNANDEZ, R., ALFONSO, F., ANGIOLILLO, D. J., SABATE, M., ESCANED, J., BANUELOS, C., FERNANDEZ-ORTIZ, A. & MACAYA, C. 2005. Drug-eluting stent thrombosis - Results from a pooled analysis including 10 randomized studies. *Journal of the American College of Cardiology*, 45, 954-959.
- MUKHERJI, S., EBERT, M. S., ZHENG, G. X., TSANG, J. S., SHARP, P. A. & VAN OUDENAARDEN, A. 2011. MicroRNAs can generate thresholds in target gene expression. *Nat Genet*, 43, 854-9.

- MURCHISON, E. P., PARTRIDGE, J. F., TAM, O. H., CHELOUFI, S. & HANNON, G. J. 2005. Characterization of Dicer-deficient murine embryonic stem cells. *Proc Natl Acad Sci U S A*, 102, 12135-40.
- NABEL, E. G., SHUM, L., POMPILI, V. J., YANG, Z. Y., SAN, H., SHU, H. B., LIPTAY, S., GOLD, L., GORDON, D., DERYNCK, R. & ET AL. 1993. Direct transfer of transforming growth factor beta 1 gene into arteries stimulates fibrocellular hyperplasia. *Proc Natl Acad Sci U S A*, 90, 10759-63.
- NAGA PRASAD, S. V., DUAN, Z. H., GUPTA, M. K., SURAMPUDI, V. S., VOLINIA, S., CALIN, G. A., LIU, C. G., KOTWAL, A., MORAVEC, C. S., STARLING, R. C., PEREZ, D. M., SEN, S., WU, Q., PLOW, E. F., CROCE, C. M. & KARNIK, S. 2009. Unique microRNA profile in end-stage heart failure indicates alterations in specific cardiovascular signaling networks. *J Biol Chem*, 284, 27487-99.
- NAKASHIMA, Y., PLUMP, A. S., RAINES, E. W., BRESLOW, J. L. & ROSS, R. 1994. ApoE-deficient mice develop lesions of all phases of atherosclerosis throughout the arterial tree. *Arterioscler Thromb*, 14, 133-40.
- NEMENOFF, R. A., HORITA, H., OSTRIKER, A. C., FURGESON, S. B., SIMPSON, P. A., VANPUTTEN, V., CROSSNO, J., OFFERMANN, S. & WEISER-EVANS, M. C. 2011. SDF-1alpha induction in mature smooth muscle cells by inactivation of PTEN is a critical mediator of exacerbated injury-induced neointima formation. *Arterioscler Thromb Vasc Biol*, 31, 1300-8.
- NIKKARI, S. T., JARVELAINEN, H. T., WIGHT, T. N., FERGUSON, M. & CLOWES, A. W. 1994. Smooth muscle cell expression of extracellular matrix genes after arterial injury. *Am J Pathol*, 144, 1348-56.
- NIKOL, S., ISNER, J. M., PICKERING, J. G., KEARNEY, M., LECLERC, G. & WEIR, L. 1992. Expression of transforming growth factor-beta 1 is increased in human vascular restenosis lesions. *J Clin Invest*, 90, 1582-92.
- NISHIOKA, T., LUO, H., EIGLER, N. L., BERGLUND, H., KIM, C. J. & SIEGEL, R. J. 1996. Contribution of inadequate compensatory enlargement to development of human coronary artery stenosis: an in vivo intravascular ultrasound study. *J Am Coll Cardiol*, 27, 1571-6.
- NONNE, N., AMEYAR-ZAZOUA, M., SOUIDI, M. & HAREL-BELLAN, A. 2010. Tandem affinity purification of miRNA target mRNAs (TAP-Tar). *Nucleic Acids Res*, 38, e20.
- NOTTROTT, S., SIMARD, M. J. & RICHTER, J. D. 2006. Human let-7a miRNA blocks protein production on actively translating polyribosomes. *Nat Struct Mol Biol*, 13, 1108-14.
- OLSEN, P. H. & AMBROS, V. 1999. The lin-4 regulatory RNA controls developmental timing in *Caenorhabditis elegans* by blocking LIN-14 protein synthesis after the initiation of translation. *Dev Biol*, 216, 671-80.
- OLSON, N. E., CHAO, S., LINDNER, V. & REIDY, M. A. 1992. Intimal smooth muscle cell proliferation after balloon catheter injury. The role of basic fibroblast growth factor. *Am J Pathol*, 140, 1017-23.
- ORLANDI, A., EHRLICH, H. P., ROPRAZ, P., SPAGNOLI, L. G. & GABBIANI, G. 1994. Rat aortic smooth muscle cells isolated from different layers and at different times after endothelial denudation show distinct biological features in vitro. *Arterioscler Thromb*, 14, 982-9.
- OROM, U. A. & LUND, A. H. 2007. Isolation of microRNA targets using biotinylated synthetic microRNAs. *Methods*, 43, 162-5.
- OWENS, G. K., KUMAR, M. S. & WAMHOFF, B. R. 2004. Molecular regulation of vascular smooth muscle cell differentiation in development and disease. *Physiol Rev*, 84, 767-801.

- PALMER, R. M., FERRIGE, A. G. & MONCADA, S. 1987. Nitric oxide release accounts for the biological activity of endothelium-derived relaxing factor. *Nature*, 327, 524-6.
- PAPAFAKLIS, M. I., BOURANTAS, C. V., THEODORAKIS, P. E., KATSOURAS, C. S., FOTIADIS, D. I. & MICHALIS, L. K. 2009. Relationship of shear stress with in-stent restenosis: bare metal stenting and the effect of brachytherapy. *Int J Cardiol*, 134, 25-32.
- PARKER, A. L., WHITE, K. M., LAVERY, C. A., CUSTERS, J., WADDINGTON, S. N. & BAKER, A. H. 2013. Pseudotyping the adenovirus serotype 5 capsid with both the fibre and penton of serotype 35 enhances vascular smooth muscle cell transduction. *Gene Ther*.
- PASTERKAMP, G., WENSING, P. J., POST, M. J., HILLEN, B., MALI, W. P. & BORST, C. 1995. Paradoxical arterial wall shrinkage may contribute to luminal narrowing of human atherosclerotic femoral arteries. *Circulation*, 91, 1444-9.
- PETERSEN, C. P., BORDELEAU, M. E., PELLETIER, J. & SHARP, P. A. 2006. Short RNAs repress translation after initiation in mammalian cells. *Mol Cell*, 21, 533-42.
- PFISTERER, M., BRUNNER-LA ROCCA, H. P., BUSER, P. T., RICKENBACHER, P., HUNZIKER, P., MUELLER, C., JEGER, R., BADER, F., OSSWALD, S. & KAISER, C. 2006. Late clinical events after clopidogrel discontinuation may limit the benefit of drug-eluting stents: an observational study of drug-eluting versus bare-metal stents. *J Am Coll Cardiol*, 48, 2584-91.
- PIAO, X., ZHANG, X., WU, L. & BELASCO, J. G. 2010. CCR4-NOT deadenylates mRNA associated with RNA-induced silencing complexes in human cells. *Mol Cell Biol*, 30, 1486-94.
- PIEDRAHITA, J. A., ZHANG, S. H., HAGAMAN, J. R., OLIVER, P. M. & MAEDA, N. 1992. Generation of mice carrying a mutant apolipoprotein E gene inactivated by gene targeting in embryonic stem cells. *Proc Natl Acad Sci U S A*, 89, 4471-5.
- PILLAI, R. S., BHATTACHARYYA, S. N., ARTUS, C. G., ZOLLER, T., COUGOT, N., BASYUK, E., BERTRAND, E. & FILIPOWICZ, W. 2005. Inhibition of translational initiation by Let-7 MicroRNA in human cells. *Science*, 309, 1573-6.
- PLUMP, A. S., SMITH, J. D., HAYEK, T., AALTO-SETALA, K., WALSH, A., VERSTUYFT, J. G., RUBIN, E. M. & BRESLOW, J. L. 1992. Severe hypercholesterolemia and atherosclerosis in apolipoprotein E-deficient mice created by homologous recombination in ES cells. *Cell*, 71, 343-53.
- POLISENO, L., TUCCOLI, A., MARIANI, L., EVANGELISTA, M., CITTI, L., WOODS, K., MERCATANTI, A., HAMMOND, S. & RAINALDI, G. 2006. MicroRNAs modulate the angiogenic properties of HUVECs. *Blood*, 108, 3068-71.
- PORSTMANN, T., TERNYNCK, T. & AVRAMEAS, S. 1985. Quantitation of 5-bromo-2-deoxyuridine incorporation into DNA: an enzyme immunoassay for the assessment of the lymphoid cell proliferative response. *J Immunol Methods*, 82, 169-79.
- PORT, J. D., WALKER, L. A., POLK, J., NUNLEY, K., BUTTRICK, P. M. & SUCHAROV, C. C. 2011. Temporal expression of miRNAs and mRNAs in a mouse model of myocardial infarction. *Physiol Genomics*, 43, 1087-95.
- QUINTAVALLE, M., ELIA, L., CONDORELLI, G. & COURTNEIDGE, S. A. 2010. MicroRNA control of podosome formation in vascular smooth muscle cells in vivo and in vitro. *J Cell Biol*, 189, 13-22.
- RAINES, E. W. & ROSS, R. 1993. Smooth muscle cells and the pathogenesis of the lesions of atherosclerosis. *Br Heart J*, 69, S30-7.

- RAMALINGAM, P., PALANICHAMY, J. K., SINGH, A., DAS, P., BHAGAT, M., KASSAB, M. A., SINHA, S. & CHATTOPADHYAY, P. 2014. Biogenesis of intronic miRNAs located in clusters by independent transcription and alternative splicing. *RNA*, 20, 76-87.
- RAO, P. K., TOYAMA, Y., CHIANG, H. R., GUPTA, S., BAUER, M., MEDVID, R., REINHARDT, F., LIAO, R., KRIEGER, M., JAENISCH, R., LODISH, H. F. & BLELLOCH, R. 2009. Loss of cardiac microRNA-mediated regulation leads to dilated cardiomyopathy and heart failure. *Circ Res*, 105, 585-94.
- RAPPOLEE, D. A., MARK, D., BANDA, M. J. & WERB, Z. 1988. Wound macrophages express TGF-alpha and other growth factors in vivo: analysis by mRNA phenotyping. *Science*, 241, 708-12.
- RAYNER, K. J., ESAU, C. C., HUSSAIN, F. N., MCDANIEL, A. L., MARSHALL, S. M., VAN GILS, J. M., RAY, T. D., SHEEDY, F. J., GOEDEKE, L., LIU, X., KHATSENKO, O. G., KAIMAL, V., LEES, C. J., FERNANDEZ-HERNANDO, C., FISHER, E. A., TEMEL, R. E. & MOORE, K. J. 2011. Inhibition of miR-33a/b in non-human primates raises plasma HDL and lowers VLDL triglycerides. *Nature*, 478, 404-7.
- REDDY, K. B. & HOWE, P. H. 1993. Transforming growth factor beta 1-mediated inhibition of smooth muscle cell proliferation is associated with a late G1 cell cycle arrest. *J Cell Physiol*, 156, 48-55.
- REHWINKEL, J., BEHM-ANSMANT, I., GATFIELD, D. & IZAURRALDE, E. 2005. A crucial role for GW182 and the DCP1:DCP2 decapping complex in miRNA-mediated gene silencing. *RNA*, 11, 1640-7.
- RHOADES, M. W., REINHART, B. J., LIM, L. P., BURGE, C. B., BARTEL, B. & BARTEL, D. P. 2002. Prediction of plant microRNA targets. *Cell*, 110, 513-20.
- RIPPSTEIN, P., BLACK, M. K., BOIVIN, M., VEINOT, J. P., MA, X., CHEN, Y. X., HUMAN, P., ZILLA, P. & O'BRIEN, E. R. 2006. Comparison of processing and sectioning methodologies for arteries containing metallic stents. *J Histochem Cytochem*, 54, 673-81.
- RO, S., PARK, C., YOUNG, D., SANDERS, K. M. & YAN, W. 2007. Tissue-dependent paired expression of miRNAs. *Nucleic Acids Res*, 35, 5944-53.
- RODRIGUEZ-MENOCAL, L., WEI, Y., PHAM, S. M., ST-PIERRE, M., LI, S., WEBSTER, K., GOLDSCHMIDT-CLERMONT, P. & VAZQUEZ-PADRON, R. I. 2010. A novel mouse model of in-stent restenosis. *Atherosclerosis*, 209, 359-66.
- ROSS, R. 1993. The pathogenesis of atherosclerosis: a perspective for the 1990s. *Nature*, 362, 801-9.
- ROSS, R. 1999. Atherosclerosis--an inflammatory disease. *N Engl J Med*, 340, 115-26.
- ROSS, R., MASUDA, J., RAINES, E. W., GOWN, A. M., KATSUDA, S., SASAHARA, M., MALDEN, L. T., MASUKO, H. & SATO, H. 1990. Localization of PDGF-B protein in macrophages in all phases of atherogenesis. *Science*, 248, 1009-12.
- RUBARTELLI, P., VERNA, E., NICCOLI, L., GIACHERO, C., ZIMARINO, M., BERNARDI, G., VASSANELLI, C., CAMPOLO, L. & MARTUSCELLI, E. 2003. Coronary stent implantation is superior to balloon angioplasty for chronic coronary occlusions: six-year clinical follow-up of the GISSOC trial. *J Am Coll Cardiol*, 41, 1488-92.
- RUVKUN, G. & GIUSTO, J. 1989. The *Caenorhabditis elegans* heterochronic gene *lin-14* encodes a nuclear protein that forms a temporal developmental switch. *Nature*, 338, 313-9.
- SABATEL, C., MALVAUX, L., BOVY, N., DEROANNE, C., LAMBERT, V., GONZALEZ, M. L., COLIGE, A., RAKIC, J. M., NOEL, A., MARTIAL, J. A. & STRUMAN, I.

2011. MicroRNA-21 exhibits antiangiogenic function by targeting RhoB expression in endothelial cells. *PLoS One*, 6, e16979.
- SAINI, H. K., GRIFFITHS-JONES, S. & ENRIGHT, A. J. 2007. Genomic analysis of human microRNA transcripts. *Proc Natl Acad Sci U S A*, 104, 17719-24.
- SAKAMOTO, H., SAKAMAKI, T., KANDA, T., HOSHINO, Y., SAWADA, Y., SATO, M., SATO, H., OYAMA, Y., NAKANO, A., TAKASE, S., HASEGAWA, A., NAGAI, R. & KURABAYASHI, M. 2003. Smooth muscle cell outgrowth from coronary atherectomy specimens in vitro is associated with less time to restenosis and expression of a key Transcription factor KLF5/BTEB2. *Cardiology*, 100, 80-5.
- SANMARTIN, M., GOICOLEA, J., GARCIA, C., GARCIA, J., CRESPO, A., RODRIGUEZ, J. & GOICOLEA, J. M. 2006. [Influence of shear stress on in-stent restenosis: in vivo study using 3D reconstruction and computational fluid dynamics]. *Rev Esp Cardiol*, 59, 20-7.
- SATA, M., SAIURA, A., KUNISATO, A., TOJO, A., OKADA, S., TOKUHISA, T., HIRAI, H., MAKUUCHI, M., HIRATA, Y. & NAGAI, R. 2002. Hematopoietic stem cells differentiate into vascular cells that participate in the pathogenesis of atherosclerosis. *Nat Med*, 8, 403-9.
- SAUER, B. 1998. Inducible gene targeting in mice using the Cre/lox system. *Methods*, 14, 381-92.
- SCHAMPAERT, E., MOSES, J. W., SCHOFFER, J., SCHLUTER, M., GERSHLICK, A. H., COHEN, E. A., PALISAITIS, D. A., BREITHARDT, G., DONOHUE, D. J., WANG, H., POPMA, J. J., KUNTZ, R. E., LEON, M. B. & INVESTIGATORS, S. E.-C.-S. 2006. Sirolimus-eluting stents at two years: A pooled analysis of SIRIUS, E-SIRIUS, and C-SIRIUS with emphasis on late revascularizations and stent thromboses. *American Journal of Cardiology*, 98, 36-41.
- SCHMITTGEN, T. D. & LIVAK, K. J. 2008. Analyzing real-time PCR data by the comparative C(T) method. *Nat Protoc*, 3, 1101-8.
- SCHOENHAGEN, P., ZIADA, K. M., KAPADIA, S. R., CROWE, T. D., NISSEN, S. E. & TUZCU, E. M. 2000. Extent and direction of arterial remodeling in stable versus unstable coronary syndromes : an intravascular ultrasound study. *Circulation*, 101, 598-603.
- SCHWARTZ, R. S., CHRONOS, N. A. & VIRMANI, R. 2004. Preclinical restenosis models and drug-eluting stents: still important, still much to learn. *Journal of the American College of Cardiology*, 44, 1373-85.
- SCHWARTZ, R. S., HUBER, K. C., MURPHY, J. G., EDWARDS, W. D., CAMRUD, A. R., VLIETSTRA, R. E. & HOLMES, D. R. 1992. Restenosis and the proportional neointimal response to coronary artery injury: results in a porcine model. *J Am Coll Cardiol*, 19, 267-74.
- SCHWARTZ, S. M., STEMERMAN, M. B. & BENDITT, E. P. 1975. The aortic intima. II. Repair of the aortic lining after mechanical denudation. *Am J Pathol*, 81, 15-42.
- SCHWARZ, D. S., HUTVAGNER, G., DU, T., XU, Z., ARONIN, N. & ZAMORE, P. D. 2003. Asymmetry in the assembly of the RNAi enzyme complex. *Cell*, 115, 199-208.
- SEIFERT, R. A., SCHWARTZ, S. M. & BOWEN-POPE, D. F. 1984. Developmentally regulated production of platelet-derived growth factor-like molecules. *Nature*, 311, 669-71.
- SELBACH, M., SCHWANHAUSSER, B., THIERFELDER, N., FANG, Z., KHANIN, R. & RAJEWSKY, N. 2008. Widespread changes in protein synthesis induced by microRNAs. *Nature*, 455, 58-63.
- SERRUYS, P. W., DE JAEGERE, P., KIEMENEIJ, F., MACAYA, C., RUTSCH, W., HEYNDRIKX, G., EMANUELSSON, H., MARCO, J., LEGRAND, V., MATERNE,

- P. & ET AL. 1994. A comparison of balloon-expandable-stent implantation with balloon angioplasty in patients with coronary artery disease. Benestent Study Group. *N Engl J Med*, 331, 489-95.
- SERRUYS, P. W., MORICE, M. C., KAPPETEIN, A. P., COLOMBO, A., HOLMES, D. R., MACK, M. J., STAHL, E., FELDMAN, T. E., VAN DEN BRAND, M., BASS, E. J., VAN DYCK, N., LEADLEY, K., DAWKINS, K. D. & MOHR, F. W. 2009. Percutaneous coronary intervention versus coronary-artery bypass grafting for severe coronary artery disease. *N Engl J Med*, 360, 961-72.
- SHAH, P. K., FALK, E., BADIMON, J. J., FERNANDEZ-ORTIZ, A., MAILHAC, A., VILLAREAL-LEVY, G., FALLON, J. T., REGNSTROM, J. & FUSTER, V. 1995. Human monocyte-derived macrophages induce collagen breakdown in fibrous caps of atherosclerotic plaques. Potential role of matrix-degrading metalloproteinases and implications for plaque rupture. *Circulation*, 92, 1565-9.
- SHANAHAN, C. M. & WEISSBERG, P. L. 1998. Smooth muscle cell heterogeneity: patterns of gene expression in vascular smooth muscle cells in vitro and in vivo. *Arterioscler Thromb Vasc Biol*, 18, 333-8.
- SHARIF, F., HYNES, S. O., COONEY, R., HOWARD, L., MCMAHON, J., DALY, K., CROWLEY, J., BARRY, F. & O'BRIEN, T. 2008. Gene-eluting stents: adenovirus-mediated delivery of eNOS to the blood vessel wall accelerates re-endothelialization and inhibits restenosis. *Mol Ther*, 16, 1674-80.
- SHI, Y., O'BRIEN, J. E., FARD, A., MANNION, J. D., WANG, D. & ZALEWSKI, A. 1996. Adventitial myofibroblasts contribute to neointimal formation in injured porcine coronary arteries. *Circulation*, 94, 1655-64.
- SHINDO, T., MANABE, I., FUKUSHIMA, Y., TOBE, K., AIZAWA, K., MIYAMOTO, S., KAWAI-KOWASE, K., MORIYAMA, N., IMAI, Y., KAWAKAMI, H., NISHIMATSU, H., ISHIKAWA, T., SUZUKI, T., MORITA, H., MAEMURA, K., SATA, M., HIRATA, Y., KOMUKAI, M., KAGECHIKA, H., KADOWAKI, T., KURABAYASHI, M. & NAGAI, R. 2002. Kruppel-like zinc-finger transcription factor KLF5/BTEB2 is a target for angiotensin II signaling and an essential regulator of cardiovascular remodeling. *Nat Med*, 8, 856-63.
- SIGWART, U., PUEL, J., MIRKOVITCH, V., JOFFRE, F. & KAPPENBERGER, L. 1987. Intravascular stents to prevent occlusion and restenosis after transluminal angioplasty. *N Engl J Med*, 316, 701-6.
- SIOW, R. C., MALLAWAARACHCHI, C. M. & WEISSBERG, P. L. 2003. Migration of adventitial myofibroblasts following vascular balloon injury: insights from in vivo gene transfer to rat carotid arteries. *Cardiovasc Res*, 59, 212-21.
- SMITH, J. D., BRYANT, S. R., COUPER, L. L., VARY, C. P., GOTWALS, P. J., KOTELIANSKY, V. E. & LINDNER, V. 1999. Soluble transforming growth factor-beta type II receptor inhibits negative remodeling, fibroblast transdifferentiation, and intimal lesion formation but not endothelial growth. *Circ Res*, 84, 1212-22.
- SONG, J. J., LIU, J., TOLIA, N. H., SCHNEIDERMAN, J., SMITH, S. K., MARTIENSSEN, R. A., HANNON, G. J. & JOSHUA-TOR, L. 2003. The crystal structure of the Argonaute2 PAZ domain reveals an RNA binding motif in RNAi effector complexes. *Nat Struct Biol*, 10, 1026-32.
- SONG, J. J., SMITH, S. K., HANNON, G. J. & JOSHUA-TOR, L. 2004. Crystal structure of Argonaute and its implications for RISC slicer activity. *Science*, 305, 1434-7.
- SOUTHGATE, K. & NEWBY, A. C. 1990. Serum-induced proliferation of rabbit aortic smooth muscle cells from the contractile state is inhibited by 8-Br-cAMP but not 8-Br-cGMP. *Atherosclerosis*, 82, 113-23.

- STEINBERG, D. 1997. Low density lipoprotein oxidation and its pathobiological significance. *J Biol Chem*, 272, 20963-6.
- STONE, G. W., LANSKY, A. J., POCOCK, S. J., GERSH, B. J., DANGAS, G., WONG, S. C., WITZENBICHLER, B., GUAGLIUMI, G., PERUGA, J. Z., BRODIE, B. R., DUDEK, D., MOCKEL, M., OCHALA, A., KELLOCK, A., PARISE, H. & MEHRAN, R. 2009. Paclitaxel-eluting stents versus bare-metal stents in acute myocardial infarction. *N Engl J Med*, 360, 1946-59.
- STOUFFER, G. A. & OWENS, G. K. 1994. TGF-beta promotes proliferation of cultured SMC via both PDGF-AA-dependent and PDGF-AA-independent mechanisms. *J Clin Invest*, 93, 2048-55.
- SUAREZ, Y., FERNANDEZ-HERNANDO, C., POBER, J. S. & SESSA, W. C. 2007. Dicer dependent microRNAs regulate gene expression and functions in human endothelial cells. *Circ Res*, 100, 1164-73.
- SUAREZ, Y., FERNANDEZ-HERNANDO, C., YU, J., GERBER, S. A., HARRISON, K. D., POBER, J. S., IRUELA-ARISPE, M. L., MERKENSCHLAGER, M. & SESSA, W. C. 2008. Dicer-dependent endothelial microRNAs are necessary for postnatal angiogenesis. *Proc Natl Acad Sci U S A*, 105, 14082-7.
- SUCHAROV, C., BRISTOW, M. R. & PORT, J. D. 2008. miRNA expression in the failing human heart: functional correlates. *J Mol Cell Cardiol*, 45, 185-92.
- SUH, M. R., LEE, Y., KIM, J. Y., KIM, S. K., MOON, S. H., LEE, J. Y., CHA, K. Y., CHUNG, H. M., YOON, H. S., MOON, S. Y., KIM, V. N. & KIM, K. S. 2004. Human embryonic stem cells express a unique set of microRNAs. *Dev Biol*, 270, 488-98.
- SUN, S. G., ZHENG, B., HAN, M., FANG, X. M., LI, H. X., MIAO, S. B., SU, M., HAN, Y., SHI, H. J. & WEN, J. K. 2011. miR-146a and Kruppel-like factor 4 form a feedback loop to participate in vascular smooth muscle cell proliferation. *EMBO Rep*, 12, 56-62.
- SUZUKI, T., SAWAKI, D., AIZAWA, K., MUNEMASA, Y., MATSUMURA, T., ISHIDA, J. & NAGAI, R. 2009. Kruppel-like factor 5 shows proliferation-specific roles in vascular remodeling, direct stimulation of cell growth, and inhibition of apoptosis. *J Biol Chem*, 284, 9549-57.
- TAKAHASHI, K., TANABE, K., OHNUKI, M., NARITA, M., ICHISAKA, T., TOMODA, K. & YAMANAKA, S. 2007. Induction of pluripotent stem cells from adult human fibroblasts by defined factors. *Cell*, 131, 861-72.
- TANG, R. H., ZHENG, X. L., CALLIS, T. E., STANSFIELD, W. E., HE, J., BALDWIN, A. S., WANG, D. Z. & SELZMAN, C. H. 2008. Myocardin inhibits cellular proliferation by inhibiting NF-kappaB(p65)-dependent cell cycle progression. *Proc Natl Acad Sci U S A*, 105, 3362-7.
- TANG, Z., WANG, A., YUAN, F., YAN, Z., LIU, B., CHU, J. S., HELMS, J. A. & LI, S. 2012. Differentiation of multipotent vascular stem cells contributes to vascular diseases. *Nat Commun*, 3, 875.
- TAYLOR, A. J., GORMAN, P. D., KENWOOD, B., HUDAK, C., TASHKO, G. & VIRMANI, R. 2001. A comparison of four stent designs on arterial injury, cellular proliferation, neointima formation, and arterial dimensions in an experimental porcine model. *Catheter Cardiovasc Interv*, 53, 420-5.
- TORELLA, D., IACONETTI, C., CATALUCCI, D., ELLISON, G. M., LEONE, A., WARING, C. D., BOCHICCHIO, A., VICINANZA, C., AQUILA, I., CURCIO, A., CONDORELLI, G. & INDOLFI, C. 2011. MicroRNA-133 controls vascular smooth muscle cell phenotypic switch in vitro and vascular remodeling in vivo. *Circ Res*, 109, 880-93.
- TORRES, A. G., FABANI, M. M., VIGORITO, E. & GAIT, M. J. 2011. MicroRNA fate upon targeting with anti-miRNA oligonucleotides as revealed by an

- improved Northern-blot-based method for miRNA detection. *RNA*, 17, 933-43.
- VAN DER WAL, A. C. & BECKER, A. E. 1999. Atherosclerotic plaque rupture--pathologic basis of plaque stability and instability. *Cardiovasc Res*, 41, 334-44.
- VAN DER WAL, A. C., BECKER, A. E., KOCH, K. T., PIEK, J. J., TEELING, P., VAN DER LOOS, C. M. & DAVID, G. K. 1996. Clinically stable angina pectoris is not necessarily associated with histologically stable atherosclerotic plaques. *Heart*, 76, 312-6.
- VAN DER WAL, A. C., BECKER, A. E., VAN DER LOOS, C. M. & DAS, P. K. 1994. Site of intimal rupture or erosion of thrombosed coronary atherosclerotic plaques is characterized by an inflammatory process irrespective of the dominant plaque morphology. *Circulation*, 89, 36-44.
- VAN ROOIJ, E. 2011. The art of microRNA research. *Circ Res*, 108, 219-34.
- VAN ROOIJ, E. & OLSON, E. N. 2012. MicroRNA therapeutics for cardiovascular disease: opportunities and obstacles. *Nat Rev Drug Discov*, 11, 860-72.
- VAN ROOIJ, E., SUTHERLAND, L. B., LIU, N., WILLIAMS, A. H., MCANALLY, J., GERARD, R. D., RICHARDSON, J. A. & OLSON, E. N. 2006. A signature pattern of stress-responsive microRNAs that can evoke cardiac hypertrophy and heart failure. *Proc Natl Acad Sci U S A*, 103, 18255-60.
- VARNAVA, A. M., MILLS, P. G. & DAVIES, M. J. 2002. Relationship between coronary artery remodeling and plaque vulnerability. *Circulation*, 105, 939-43.
- VAUGHAN, C. J., GOTTO, A. M., JR. & BASSON, C. T. 2000. The evolving role of statins in the management of atherosclerosis. *J Am Coll Cardiol*, 35, 1-10.
- VON SEGGERN, D. J., KEHLER, J., ENDO, R. I. & NEMEROW, G. R. 1998. Complementation of a fibre mutant adenovirus by packaging cell lines stably expressing the adenovirus type 5 fibre protein. *J Gen Virol*, 79 (Pt 6), 1461-8.
- WALKER, L. N., BOWEN-POPE, D. F., ROSS, R. & REIDY, M. A. 1986. Production of platelet-derived growth factor-like molecules by cultured arterial smooth muscle cells accompanies proliferation after arterial injury. *Proc Natl Acad Sci U S A*, 83, 7311-5.
- WANG, C., HAN, M., ZHAO, X. M. & WEN, J. K. 2008a. Kruppel-like factor 4 is required for the expression of vascular smooth muscle cell differentiation marker genes induced by all-trans retinoic acid. *J Biochem*, 144, 313-21.
- WANG, D. Z., LI, S., HOCKEMEYER, D., SUTHERLAND, L., WANG, Z., SCHRATT, G., RICHARDSON, J. A., NORDHEIM, A. & OLSON, E. N. 2002. Potentiation of serum response factor activity by a family of myocardin-related transcription factors. *Proc Natl Acad Sci U S A*, 99, 14855-60.
- WANG, S., AURORA, A. B., JOHNSON, B. A., QI, X., MCANALLY, J., HILL, J. A., RICHARDSON, J. A., BASSEL-DUBY, R. & OLSON, E. N. 2008b. The endothelial-specific microRNA miR-126 governs vascular integrity and angiogenesis. *Dev Cell*, 15, 261-71.
- WANG, Z., WANG, D. Z., HOCKEMEYER, D., MCANALLY, J., NORDHEIM, A. & OLSON, E. N. 2004. Myocardin and ternary complex factors compete for SRF to control smooth muscle gene expression. *Nature*, 428, 185-9.
- WASSMANN, S., WASSMANN, K., JUNG, A., VELTEN, M., KNUEFERMANN, P., PETOUMENOS, V., BECHER, U., WERNER, C., MUELLER, C. & NICKENIG, G. 2007. Induction of p53 by GSK3 is essential for inhibition of proliferation of vascular smooth muscle cells. *J Mol Cell Cardiol*, 43, 301-7.
- WATANABE, N., KURABAYASHI, M., SHIMOMURA, Y., KAWAI-KOWASE, K., HOSHINO, Y., MANABE, I., WATANABE, M., AIKAWA, M., KURO-O, M.,

- SUZUKI, T., YAZAKI, Y. & NAGAI, R. 1999. BTEB2, a Kruppel-like transcription factor, regulates expression of the SMemb/Nonmuscle myosin heavy chain B (SMemb/NMHC-B) gene. *Circ Res*, 85, 182-91.
- WIENHOLDS, E., KLOOSTERMAN, W. P., MISKA, E., ALVAREZ-SAAVEDRA, E., BEREZIKOV, E., DE BRUIJN, E., HORVITZ, H. R., KAUPPINEN, S. & PLASTERK, R. H. 2005. MicroRNA expression in zebrafish embryonic development. *Science*, 309, 310-1.
- WIGHTMAN, B., HA, I. & RUVKUN, G. 1993. Posttranscriptional regulation of the heterochronic gene *lin-14* by *lin-4* mediates temporal pattern formation in *C. elegans*. *Cell*, 75, 855-62.
- WOLF, Y. G., RASMUSSEN, L. M. & RUOSLAHTI, E. 1994. Antibodies against transforming growth factor-beta 1 suppress intimal hyperplasia in a rat model. *J Clin Invest*, 93, 1172-8.
- WORLD HEALTH ORGANIZATION. 2013. *Cardiovascular diseases (CVDs) Fact sheet N° 317*. [Online]. Available: <http://www.who.int/mediacentre/factsheets/fs317/en/index.html> [Accessed 30.09.13].
- WU, L., FAN, J. & BELASCO, J. G. 2006. MicroRNAs direct rapid deadenylation of mRNA. *Proc Natl Acad Sci U S A*, 103, 4034-9.
- XIN, M., SMALL, E. M., SUTHERLAND, L. B., QI, X., MCANALLY, J., PLATO, C. F., RICHARDSON, J. A., BASSEL-DUBY, R. & OLSON, E. N. 2009. MicroRNAs miR-143 and miR-145 modulate cytoskeletal dynamics and responsiveness of smooth muscle cells to injury. *Genes Dev*, 23, 2166-78.
- XU, B., NIU, X., ZHANG, X., TAO, J., WU, D., WANG, Z., LI, P., ZHANG, W., WU, H., FENG, N., HUA, L. & WANG, X. 2011. miR-143 decreases prostate cancer cells proliferation and migration and enhances their sensitivity to docetaxel through suppression of KRAS. *Mol Cell Biochem*, 350, 207-13.
- XU, Q., ZHANG, Z., DAVISON, F. & HU, Y. 2003. Circulating progenitor cells regenerate endothelium of vein graft atherosclerosis, which is diminished in ApoE-deficient mice. *Circulation Research*, 93, e76-86.
- YANG, J. S., MAURIN, T., ROBINE, N., RASMUSSEN, K. D., JEFFREY, K. L., CHANDWANI, R., PAPAPETROU, E. P., SADELAIN, M., O'CARROLL, D. & LAI, E. C. 2010. Conserved vertebrate mir-451 provides a platform for Dicer-independent, Ago2-mediated microRNA biogenesis. *Proc Natl Acad Sci U S A*, 107, 15163-8.
- YANG, W., CHENDRIMADA, T. P., WANG, Q., HIGUCHI, M., SEEBURG, P. H., SHIEKHATTAR, R. & NISHIKURA, K. 2006. Modulation of microRNA processing and expression through RNA editing by ADAR deaminases. *Nat Struct Mol Biol*, 13, 13-21.
- YANG, X., DU, W. W., LI, H., LIU, F., KHORSHIDI, A., RUTNAM, Z. J. & YANG, B. B. 2013. Both mature miR-17-5p and passenger strand miR-17-3p target TIMP3 and induce prostate tumor growth and invasion. *Nucleic Acids Res*, 41, 9688-704.
- YEKTA, S., SHIH, I. H. & BARTEL, D. P. 2004. MicroRNA-directed cleavage of HOXB8 mRNA. *Science*, 304, 594-6.
- YI, R., QIN, Y., MACARA, I. G. & CULLEN, B. R. 2003. Exportin-5 mediates the nuclear export of pre-microRNAs and short hairpin RNAs. *Genes Dev*, 17, 3011-6.
- YIN, F. C., SPURGEON, H. A., RAKUSAN, K., WEISFELDT, M. L. & LAKATTA, E. G. 1982. Use of tibial length to quantify cardiac hypertrophy: application in the aging rat. *Am J Physiol*, 243, H941-7.
- YOSHIDA, T., KAESTNER, K. H. & OWENS, G. K. 2008. Conditional deletion of Kruppel-like factor 4 delays downregulation of smooth muscle cell

- differentiation markers but accelerates neointimal formation following vascular injury. *Circ Res*, 102, 1548-57.
- YOSHIDA, T., SINHA, S., DANDRE, F., WAMHOFF, B. R., HOOFNAGLE, M. H., KREMER, B. E., WANG, D. Z., OLSON, E. N. & OWENS, G. K. 2003. Myocardin is a key regulator of CArG-dependent transcription of multiple smooth muscle marker genes. *Circ Res*, 92, 856-64.
- ZAMAN, A. G., HELFT, G., WORTHLEY, S. G. & BADIMON, J. J. 2000. The role of plaque rupture and thrombosis in coronary artery disease. *Atherosclerosis*, 149, 251-66.
- ZENG, Y., YI, R. & CULLEN, B. R. 2003. MicroRNAs and small interfering RNAs can inhibit mRNA expression by similar mechanisms. *Proc Natl Acad Sci U S A*, 100, 9779-84.
- ZHANG, B., PAN, X., COBB, G. P. & ANDERSON, T. A. 2007. microRNAs as oncogenes and tumor suppressors. *Dev Biol*, 302, 1-12.
- ZHANG, H., KOLB, F. A., BRONDANI, V., BILLY, E. & FILIPOWICZ, W. 2002. Human Dicer preferentially cleaves dsRNAs at their termini without a requirement for ATP. *EMBO J*, 21, 5875-85.
- ZHANG, Y., YANG, P., SUN, T., LI, D., XU, X., RUI, Y., LI, C., CHONG, M., IBRAHIM, T., MERCATALI, L., AMADORI, D., LU, X., XIE, D., LI, Q. J. & WANG, X. F. 2013. miR-126 and miR-126* repress recruitment of mesenchymal stem cells and inflammatory monocytes to inhibit breast cancer metastasis. *Nat Cell Biol*, 15, 284-94.
- ZHAO, Y., RANSOM, J. F., LI, A., VEDANTHAM, V., VON DREHLE, M., MUTH, A. N., TSUCHIHASHI, T., MCMANUS, M. T., SCHWARTZ, R. J. & SRIVASTAVA, D. 2007. Dysregulation of cardiogenesis, cardiac conduction, and cell cycle in mice lacking miRNA-1-2. *Cell*, 129, 303-17.
- ZHAO, Y., SAMAL, E. & SRIVASTAVA, D. 2005. Serum response factor regulates a muscle-specific microRNA that targets Hand2 during cardiogenesis. *Nature*, 436, 214-20.
- ZHU, N., ZHANG, D., CHEN, S., LIU, X., LIN, L., HUANG, X., GUO, Z., LIU, J., WANG, Y., YUAN, W. & QIN, Y. 2011. Endothelial enriched microRNAs regulate angiotensin II-induced endothelial inflammation and migration. *Atherosclerosis*, 215, 286-93.